



THE HONG KONG
POLYTECHNIC UNIVERSITY

香港理工大學

Pao Yue-kong Library

包玉剛圖書館

Copyright Undertaking

This thesis is protected by copyright, with all rights reserved.

By reading and using the thesis, the reader understands and agrees to the following terms:

1. The reader will abide by the rules and legal ordinances governing copyright regarding the use of the thesis.
2. The reader will use the thesis for the purpose of research or private study only and not for distribution or further reproduction or any other purpose.
3. The reader agrees to indemnify and hold the University harmless from and against any loss, damage, cost, liability or expenses arising from copyright infringement or unauthorized usage.

IMPORTANT

If you have reasons to believe that any materials in this thesis are deemed not suitable to be distributed in this form, or a copyright owner having difficulty with the material being included in our database, please contact lbsys@polyu.edu.hk providing details. The Library will look into your claim and consider taking remedial action upon receipt of the written requests.

Department of Building Services Engineering

The Hong Kong Polytechnic University

**Pedestrian level wind and thermal environment
around buildings – Wind tunnel investigations**

Xia Qian

**A thesis submitted in partial fulfilment of the requirements for the Degree
of Doctor of Philosophy**

April, 2014

Certificate of Originality

I hereby declare that this thesis represents my own work and that, to the best of my knowledge and belief, it reproduces no material previously published or written, nor material that has been accepted for the award of any other degree or diploma, except where due acknowledgement has been made in the text.

Xia Qian

Department of Building Services Engineering

The Hong Kong Polytechnic University

Hong Kong SAR, China

March, 2014

Abstract

Constructing a new building will always affect the microclimate at the building and its surrounding area. This can lead to low airflow or poor outdoor ventilation around the building blocks, which can negatively influence indoor air quality, pollutant dispersion in the surroundings, and airborne transmission of infectious diseases. Conversely, high wind speeds can also be encountered in densely built up areas that can introduce discomfort or danger. The air flow patterns at pedestrian level around buildings, particularly high-rise buildings, are generally complicated. And there are insufficient studies focusing on the pedestrian-level wind environment for different building designs, especially those with optimizations. One of the design options for optimizations, which is called lift-up design has been proposed in this work. Three tall building configurations, a singular building (SB), a row of buildings (RB) and a row of building with podium (PB) were selected from a systematic study by Tsang et al (2012) that resulted in the lowest wind speed zones. Buildings with a lift-up design may have a number of impacts on the pedestrian-level wind and pollutant dispersion environment. A 3.5m lift-up in prototype scale was added to each of the three configurations producing three lift-up designs for comparison. Scale models of the designs were studied in the wind tunnel to ascertain the lift-up design influence on airflow and ventilation around the buildings. Undesirable areas of low wind speed leading to poor air ventilation and discomfort due to strong wind conditions at the other extreme are both identified in the results, and their practical implications are discussed.

In this series of study, wind direction is normal to the building façade. For the building configurations without the lift-up design, the wind hits the windward façade of the building and a downwash flow is generated. This downwash results in a backflow in front of the building at pedestrian level. When the two opposing windward and backflows encounter

each other, a low wind speed zone is created at the upstream of buildings. For the buildings with lift-up designs, the low or poor ventilation situation of the upstream near-field has been improved due to a 3.5m lift-up area underneath of these buildings. This is because part of the downwash and the approaching wind can flow through the lift-up area of the buildings where there is reduced blocking of flow. Consequently less backflow wind and approaching wind meets in front of the building at the pedestrian level.

This study also focuses on the pedestrian-level pollutant dispersion from an upstream or downstream line source representing vehicular emission from a line of stopped buses. Pollutant dispersions from the respective line sources upstream and downstream were compared, and the practical implications to the wind and thermal comfort and pollutant dispersions are discussed. Lift-up design in general results in higher pollutant concentrations when upstream line source is implemented. Even higher pollutant concentrations are found when downstream line source is used. Building geometry and sizes can affect the pollutant dispersion dramatically. Larger building results in lower pollutant concentrations, and vice versa. Lift-up design for podium building is the most effective building type studied to reduce the normalized pollutant concentration when the pollutant source is located downstream side of the building.

Because the 3.5m lift-up height is much lower than the building height, the 3.5m lift-up design has not much effect on the upper part of the building. Consequently, this study only emphasized on the lower part of the building. The surface pressure, which potentially affects cross the ventilation potential at the lower part of the building for different building configurations has been evaluated. It has been discovered that the lift-up design can all increase the cross ventilation potential for SB, RB and PB. But the RB with lift-up design has the highest ventilation potential among the three building configurations.

Thermal sensation of SB, RB and PB with and without the lift-up design has also been investigated. Two predictive formulas from Cheng et al's (2010) study have been utilized to analyse the thermal sensation and overall comfort, which is based on PET. Summer and winter have been considered for this research work respectively. In summer, only positive thermal sensation is found for the pedestrians for singular building with and without the lift-up design for all the zones. For a row of buildings and podium building, there are negative thermal sensation values for some zones. Lift-up design is the most effectively improve the thermal environment for pedestrians for singular building and a slab of building among three building types. This design can improve the downstream thermal environment for a row of buildings. But it is not so useful for podium building at all. In winter, all the zones for singular building, a row of buildings and podium building are all under negative thermal environment. But due to the cold environment in winter, lift-up design does not benefit the pedestrians significantly. In practice, architects or engineers can use singular building or a slab of buildings with lift-up design to achieve better mean wind speed and thermal comfort if these aspects are the aspects they need to consider in the architectural design. If pollution is the aspect that architects or engineers need to considered, it would be better to have a large scale building such as a podium building and locating the pollutant source downstream when the lift-up design is used to reduce the pollutant effect. But for the real situation inside the street canyon, it is suggested to conduct a simulation first, such as CFD simulations, as there are so many combinations of street canyons and cities.

Publications arising from the thesis

Journal Papers

- **Xia, Qian**, Niu, Jianlei & Liu, Xiaoping. 2012. Dispersion of air pollutants around buildings: A review of past studies and the methodologies. *Journal of Indoor and Built Environment*,
- **Xia, Qian**, Liu, Xiaoping, Niu, Jianlei & Kenny Kwok. 2014. Effects of building lift-up design on pedestrian wind environment. *Journal of Wind Engineering and Industrial Aerodynamics* (under review).
- **Xia Qian**, Liu, Xiaoping, Niu, Jianlei & Kenny Kwok. 2014. Wind tunnel study of the pedestrian wind environment and pollutant dispersion around buildings with lift-up design, *Journal of Atmospheric Environment* (Manuscript).

Conference Paper

- **Xia, Qian**, Niu, Jianlei & Liu, Xiaoping. A review of investigating airflows around buildings. Third International Postgraduate Conference on Infrastructure and Environment, 11-12 July 2011, Hong Kong, China
- **Xia, Qian**, Niu, Jianlei & Liu, Xiaoping. Reviewing pollutant dispersion around buildings. The 7th International Symposium on Heating, Ventilation and Air Conditioning, November 6-9, Shanghai, China
- **Xia, Qian**, Niu, Jianlei & Liu, Xiaoping. Airflow around buildings: Effects on pedestrian wind environment by implementing building lift-up design. Proceedings of the International Conference on Environmental Pollution and Remediation, July 15-17, 2013. Toronto, Ontario, Canada.

- **Xia, Qian,** Liu, Xiaoping, Niu, Jianlei & Kenny Kwok. Effects of building lift-up design on pedestrian level wind environment. 16th Australasian Wind Engineering Society Workshop, July 18-19, 2013. Brisbane, Australia.
- **Xia, Qian,** Liu, Xiaoping, Niu, Jianlei & Kenny Kwok. Effects of building lift-up design on pedestrian level wind environment. The Eighth Asia-Pacific Conference on Engineering, December 10-14, 2013, Chennai, India.
- **Xia, Qian,** Liu, Xiaoping, Niu, Jianlei & Kenny Kwok. Effects of building lift-up design on pedestrian gust wind environment. *Indoor Air*, July 7-12, 2014, Hong Kong, China (accepted).
- **Xia, Qian,** Liu, Xiaoping, Niu, Jianlei & Kenny Kwok. Effects of building lift-up design on pedestrian pollutant dispersion. *Indoor Air*, July 7-12, 2014, Hong Kong, China (accepted).

Acknowledgements

I wish to thank the following people for their assistance during this research work.

Acknowledgements go towards my chief supervisor Prof. Niu Jianlei, for his supervision, thoughtful consideration, invaluable guidance, constructive comments, advice and encouragement throughout this study. It is a great honour to join in his research team, and learn how to carry out research work from him.

I would like to thank my Co-supervisor, Dr Mak Cheuk-ming, for his kind help and comments during my Ph.D study.

I would like to express my deep gratitude to Prof. K.C.S. Kwok for his extensive help, comments, references, recommendations, all the meetings and communications from the beginning of the wind tunnel experiment for experiment design and data analysis. I would also like to thank Dr. Issac Shum and his technical team of CLP Wind tunnel, Hong Kong University of Science and Technology in preparing the scaled models and assisting the wind tunnel tests.

Hong Kong Polytechnic University for the research funding during my research studies here.

Finally but most importantly, I would like to thank my dearest parents, my husband and my coming daughter, Mia Cheung. Without your accompany, endless love, encouragement and support through the course of this research work, this could not be possible.

Table of Contents

Certificate of Originality	ii
Abstract.....	iii
Acknowledgements.....	viii
Table of Contents	ix
Lists of Figures	xiii
List of Tables	xvii
Chapter One: Introduction.....	1
1.1 Introduction	1
1.2 Statement of the Problem and Scope of This Study	3
1.3 Objectives of the Current Research Work.....	5
1.4 Structure of the Dissertation.....	6
Chapter Two: Literature review of air flow and air pollutant dispersion around buildings.....	10
2.1 Introduction	10
2.2 On-site measurements	13
2.2.1 Full scale measurement	13
2.2.2 Physically-scaled model on-site measurements.....	20
2.3 Wind/water Tunnel Physically-scaled measurements.....	22
2.3.1 Wind tunnel measurements	22
2.3.2 Water tunnel measurements	34
2.4 Numerical experiments/simulations.....	37
2.4.1 Direct Numerical Simulation (DNS).....	37
2.4.2 Reynold-averaged Navier-Stokes numerical simulations (RANS) and Large eddy simulation (LES).....	39
2.5 Discussions.....	53
2.6 Summary.....	56

Chapter Three: Research Methodology.....	58
3.1 Introduction.....	58
3.2 Wind Tunnel Modelling Requirements	59
3.3 The CLP Power Wind/Wave Tunnel	63
3.4 Approaching Wind Profile.....	64
3.5 Measurement Instruments.....	69
3.5.1 Pressure measurements.....	69
3.5.2 Wind speed measurement.....	72
3.5.3 Pollutant dispersion Measurements	81
3.6 Summary.....	88
Chapter Four: Effects of natural ventilation potential by using the lift-up design	89
4.1 Introduction.....	89
4.2 Methodology.....	91
4.3 Results and Discussions.....	92
4.3.1 Singular building with and without lift-up design.....	92
4.3.2 A row of buildings with and without lift-up design	105
4.3.3 Podium building with and without lift-up design.....	120
4.4 Summary.....	129
Chapter Five: Effects of building lift-up design on pedestrian wind environment	132
5.1 Introduction.....	132
5.2 Research Methodologies	134
5.3 Results and Discussion.....	134
5.3.1 Pedestrian mean wind conditions	135
5.3.2 Pedestrian comfort under strong wind conditions.....	145
5.4 Summary.....	153
Chapter Six: Thermal Sensation of different building configurations with and without lift-up design under different weather conditions	155

6.1 Introduction:.....	155
6.2 Research Methodology	157
6.3 Results and Discussion	161
6.3.1 Thermal sensation under summer conditions	161
6.3.2 Thermal sensation under winter conditions.....	167
6.4 Conclusion	173
Chapter Seven: Wind tunnel study of the pedestrian wind environment and pollutant dispersion in building lift-up design	177
7.1 Introduction	177
7.2 Experimental setup.....	181
7.2.1 The atmospheric boundary layer wind tunnel	181
7.2.2 Measurement techniques	181
7.3 Results and discussions.....	182
7.3.1 Distribution of mean wind speed.....	183
7.3.2 Distribution of pollutant distribution with lift-up design and line source upstream of building	188
7.3.3 Distribution of pollutant distribution with lift-up design and line source downstream of building	195
7.4 Summary	201
Chapter Eight: Concluding Remarks and Recommendations	205
8.1 Conclusions.....	205
8.1.1 Surface pressure distribution and natural ventilation potentials.....	205
8.1.2 Pedestrian wind environment	206
8.1.3 Pedestrian thermal comfort.....	208
8.1.4 Pedestrian pollutant dispersion.....	209
8.2 Recommendations for the Further Studies.....	210
Appendices	212

References 222

Lists of Figures

Figure 1-1(a). HSBC building in Hong Kong, (b): ground floor is fully open to the streets.....	4
Figure 2-1. On-site investigation of cross-contamination of two adjacent rooms with tracer gases (Niu & Tung, 2008).....	16
Figure 2-2. Three flow regimes with different building-height-to-street-width ratios H/W (Lucas et al. 1967).....	19
Figure 2-3. Building arrangements (Chavez et al. 2011).....	28
Figure 2-4. Experimental configuration for the street canyon (Klein & Plate, 1999).....	32
Figure 2-5. Plan view of Amoy Garden (Yu et al. 2004).	41
Figure 2-6. Layout of non-uniform street canyon, in top view (a) and side view (b).....	49
Figure 3-1. Plan view of WWTF	64
Figure 3-2. Wind tunnel setup for wind profile	66
Figure 3-3. Profiles of mean wind speed and turbulence intensity	67
Figure 3-4. Isometric of podium building.....	67
Figure 3-5: Plan view of pressure measurement of singular building	70
Figure 3-6. Front view of pressure measurement of singular building.....	71
Figure 3-7. Plan view of pressure measurement of singular building with lift-up design.....	71
Figure 3-8. Front view of pressure measurement of singular building with lift-up.....	72
Figure 3-9. Irwin Probes Distribution for singular building with and without lift-up design .	73
Figure 3-10. Dimensions of the designed Irwin Sensor (mm): $d = 1.6$, $d_i = 0.8$, $h = 10$, $D = 5$, $H = 5.5$	74
Figure 3-11. Wind speed vs $\sqrt{\Delta P}$ calibration of stochastic selections of Irwin Sensors	80
Figure 3-12. Cross section of individual trace gas injector	84
Figure 3-13. Cross section of 255 tubes along the line source	84
Figure 3-14. Capping brass bar design over the top of the line source.....	85
Figure 3-15. Pressure distribution for podium buildings with or without lift-up design when line source lined upstream	86
Figure 3-16. Pressure distribution for podium buildings with or without lift-up design when line source lined downstream.....	87
Figure 4-1. Plan of pressure measurement locations for singular building with and without lift-up design	93
Figure 4-2. Pressure contours diagram for facade A-B for singular building with and without lift-up design	94
Figure 4-3. Pressure contours diagram for facade B-C for singular building with and without lift-up design	95
Figure 4-4. Pressure contours diagram for facade C-D for singular building with and without lift-up design	96
Figure 4-5. Pressure difference distribution for singular building for different floors.....	98
Figure 4-6. Pressure difference distribution for singular building with Lift-up Design for different floors	99
Figure 4-7 Pressure differences for different floors of singular building with and without lift-up design	103

Figure 4-8. Plan of pressure measurement for a row of buildings with and without lift-up design	105
Figure 4-9. Pressure contour diagram for RB1 for a row of buildings with and without lift-up design	107
Figure 4-10. Pressure contours diagrams for RB2 for a row of buildings with and without lift-up design	108
Figure 4-11. Pressure difference distribution for RB1 for different floors.....	111
Figure 4-12. Pressure difference distribution for RB1 with lift-up design for different floors	111
Figure 4-13. Pressure difference distribution for RB2 for different floors.....	112
Figure 4-14. Pressure difference distribution for RB2 with lift-up design for different floors	112
Figure 4-15. Pressure differences for different floors of RB1 with and without lift-up design	116
Figure 4-16. Pressure differences for different floors of RB2 with and without lift-up design	119
Figure 4-17. Plan view of pressure coefficient distribution for PB	120
Figure 4-18. Pressure contour diagram for facade A-B for podium building with and without lift-up design	121
Figure 4-19. Pressure contour diagram for facade B-C for singular building with and without lift-up design	122
Figure 4-20. Pressure contour diagram for facade C-D for singular building with and without lift-up design	123
Figure 4-21. Pressure difference distribution for podium building for different floors.....	124
Figure 4-22. Pressure difference distribution for podium building with lift-up design for different floors	124
Figure 4-23. Pressure differences for different floors of podium building with and without lift-up design	129
Figure. 5-1. Distribution of the normalized mean wind speed with and without lift-up design for different building configurations.....	136
Figure. 5-2. Eight different zones for pedestrian wind speed measurement.....	140
Figure. 5-3. Normalized wind speed distribution for different zones for different building configurations	142
Figure 5-4a). The two measurement points underneath the singular building	143
Figure. 5-5b). Normalized mean wind speeds at the two points beneath the singular building with lift-up design	144
Figure. 5-6a). Measurement points underneath podium building.....	144
Figure. 5-7b). Normalized mean wind speed beneath podium building with lift-up design .	145
Figure 5-8. Distribution of the normalized GEM wind speed with and without lift-up design for different building configurations.....	148
Figure 5-9. Gust velocity distribution in different zones for different building configurations	151

Figure 5-10. Normalized gust wind speed distribution underneath different building configurations	152
Figure 6-1: Contour diagram of SB, RB and PB with and without lift-up design under summer climatic conditions	162
Figure. 6-3. Eight different zones for pedestrian wind speed measurement.....	163
Figure 6-4. Thermal sensation distribution of different zone of different building configurations with and without lift-up design under summer conditions	167
Figure 6-2: Contour diagram of SB, RB and PB with and without lift-up design under winter climatic conditions	169
Figure 6-5. Thermal sensation distribution of different zone of singular building with and without lift-up design under winter conditions.....	173
Figure 7-1. Isometric of Singular Building, A Row of Buildings, Podium Building with Lift-up Design	181
Figure 7-2. Eight different zones for pedestrian wind speed with upstream or downstream line source	184
Figure 7-3. Normalized wind speed distribution for different building configurations with or without lift-up design.....	188
Figure 7-4. Different zonal distributions for pedestrian pollutant measurement with upstream line source for different building configurations	190
Figure 7-5. Concentration distribution for upstream line source for different building configurations with or without lift-up design	195
Figure 7-6. Different zonal distributions for pedestrian pollutant measurement with downstream line source for different building configurations.....	197
Figure 7-7. Concentration distribution for downstream line source for different building configurations with and without lift-up design.....	201
Figure 3-1. Plan view of pressure measurement of a row of buildings	212
Figure 3-2. Front view of pressure measurement of a row of buildings.....	212
Figure 3-3. Plan view of pressure measurement of a row of buildings with lift-up design...	213
Figure 3-4. Front view of pressure measurement of a row of buildings with lift-up design	213
Figure 3-5. Plan view of pressure measurement of a row of buildings with podium	214
Figure 3-6. Front view of pressure measurement of a row of buildings with podium	214
Figure 3-7. Plan view of pressure measurement of a row of buildings with podium and lift-up design	215
Figure 3-8. Front view of pressure measurement of a row of buildings with podium and lift-up design.....	215
Figure 3-9. Irwin Probes Distribution for a row of buildings with and without lift-up design	216
Figure 3-10. Irwin Probes Distribution for podium building with or without lift-up design.	217
Figure 3-11. Pressure distribution for a row of buildings with or without lift-up design when line source lined upstream	218
Figure 3-12. Pressure distribution for a row of buildings with or without lift-up design when line source lined downstream.....	219

Figure 3-13. Pressure distribution for podium buildings with or without lift-up design when line source lined upstream	220
Figure 3-14. Pressure distribution for podium buildings with or without lift-up design when line source lined downstream.....	221

List of Tables

Table 2-1. Wind tunnel test of pollutant dispersion around an isolated building.....	25
Table 2-2. Wind tunnel test of pollutant dispersion of building array.....	30
Table 2-3. Water channel test of pollutant dispersion of building array	36
Table 2-4. DNS simulation of pollutant dispersion around an obstacle and in street canyons	38
Table 2-5. RANS and LES simulations of pollutant dispersion around an obstacle/isolated building.....	44
Table 2-6. RANS and LES simulations of pollutant dispersion in building arrays.....	46
Table 3-1. Dimensions of building setups	67
Table 6-1: Different levels of thermal sensation.....	158
Table 6-2: 2013 weather data from Hong Kong Observatory	159

Chapter One: Introduction

1.1 Introduction

Living in Hong Kong is living in one of the most densely populated cities in the world. Although high density living can efficiently utilise land and public transport, and optimally use other infrastructure and public utilities, this also can led to some adverse effects, for instance, congested building designs and urban environment. Due to the limited availability of the land in Hong Kong, urban renewal projects have become one of the most important topics throughout Hong Kong. Most of these modern buildings are not only high-rise buildings, but also located inside the densely packed old districts. Therefore, it normally imposes the effects of altering the surrounding wind environments. Residents nearby always complain the tall and bulky buildings obstructs winds from penetrating the downstream urban fabric and result in poor natural air ventilations.

The utilisation of wind tunnels to investigate the effects of wind near the earth's surface started more than a century ago when a scientist named Irminger located a model house in a small wind tunnel for wind pressure measurement. Many attempts have been made to develop useful laboratory representations of the highly variable atmospheric winds. Early researchers used wind tunnels to simulate steady wind flow situations. In the last thirty years, reasonable laboratory simulation of "atmospheric boundary layer" (ABL) flow was discovered. The nature of winds inside the atmosphere began to be investigated from 1950s. Due to the increased demand and concern for human health, serious attempts to control air pollution, and the development of

research capabilities have resulted in ever more studies on pollutant transportation within the building environment since the 1970s (Cermak, 1975).

To solve the problem of providing scientific proof of insufficient wind penetrating the downstream urban fabric and resulting poor natural air ventilation due to tall and bulky structures, the Planning Department of The Government of the Hong Kong Special Administrative Region has introduced Air Ventilation Assessment (AVA) to predict the urban wind environment by means of physical or computational methods. The main purpose is to find out whether a new development would significantly affect the natural ventilation of the surrounding environment by wind speed measurements. It is also a means of determining the low wind speed areas after a building has been built in an existing urban area. This is vital for assessing the proposed development at a particular location. But the measured results from each test are unique for a particular built environment and topography and concerns are mainly focused on the low wind speed areas. High wind speeds on the other hand can adversely affect the pedestrian comfort and restrict leisure activities as well.

Additionally, Hong Kong belongs to a sub-tropical climate, tending towards temperate for nearly half of a year. From early May until early November, much of the population uses air conditioning systems to cool down their living and working spaces to achieve a comfortable indoor environment. This implies that people in Hong Kong relies on air conditioning more than six months in a year, or even longer in public areas such as shopping malls and public transport. Therefore, thermal comfort of pedestrians has become more and more important in people's everyday life. Furthermore, private cars and public transport play a great role in any residences' life in the world. The interesting aspect for Hong Kong is that many drivers keep the engine

running when their vehicles are stopped in urban areas, partially due to the driver wanting to maintain the cool and comfortable driving environment during the hot summers. This not only has side effects on the environment and energy, but also the vehicular pollutant emissions can endanger the health of pedestrians. There are more than 100 types of harmful substances in vehicular exhausts, such as tiny suspended particles (particulate matter), carbon monoxide (CO), nitrogen oxides (NO_x), sulphur dioxide (SO_x), hydrocarbons (HC), formaldehyde, benzene, lead etc. In recent years, emissions from vehicle exhaust have become one of the major urban air pollutions due to the dramatic growth of vehicle population despite significant improvements in fuel and engine technology (Vardoulakis et al., 2003).

1.2 Statement of the Problem and Scope of This Study

After the outbreak of the severe acute respiratory syndrome (SARS) epidemic in 2003 and the recent bouts of Influenza H1N1 (Swine flu), awareness of wind environment and pollutant dispersion has been raised, especially in those environments with significant alterations by new buildings constructions where either poor ventilation or strong wind concerns have been reported from the communities. This presented work furthers the work of Tsang et al. (2012). Based on Tsang et al's (2012) work, three different types of building configurations giving the lowest wind speed zone had been selected for further investigation. A common design of void ground floor in Hong Kong called "lift-up design" has been added to each of the building configurations. In order to have a better illustration, some examples are giving below in Figure 1-1.



a)



b)



c)

Figure 1-1(a). HSBC building in Hong Kong, (b): ground floor is fully open to the streets.

c) The podium floor at HKPolyU are devoid of rooms, which provides a well-connected campus

The presented study focuses on the study of wind speed distribution, transport and diffusion of vehicular pollutants at the pedestrian level around singular building (SB), a row of buildings (RB) and podium building (PB). The main goal is to gain a better understanding of how vehicular upstream and downstream pollutant source disperse with the ambient airflow at the nearby pedestrian-level. The region of influence, the dispersion route under different location of vehicular source, the wind speed distribution and the surface pressure of lower floors for singular building, a row of buildings and podium building with and without the lift-up design are investigated during this study. Meanwhile, the thermal sensation distributions at the pedestrian

level for different building configurations with and without the lift-up have also been estimated. The obtained results have been compared in order to attain whether lift-up design affects all the environmental aspects mentioned earlier.

The scope of research defined above involves a variety of disciplines and areas. Basically, only one complementary method, physical modelling in a wind tunnel has been employed to study the mechanisms of vehicular pollutant transmission at the pedestrian level when the source is located upstream or downstream of a building. Meanwhile, the ventilation potential at the lower level of the building, low wind speed zone, high wind speed zone and thermal at the pedestrian level has also been evaluated. Most importantly, it is for analysing how useful employing the lift-up design is for all these aspects.

1.3 Objectives of the Current Research Work

The overall aim of this research work is to evaluate the risks of poor vehicular dispersion and, low wind speed distribution caused by the low wind speed, as well as discomfort caused by extremely high wind speed at the pedestrian level. The internal natural ventilation potential at the lower floor of the different building configurations has also been studied by analyzing surface pressure differences between the windward and leeward façade.

The detailed aims for this dissertation have been listed below.

- 1) To investigate the ventilation potential of singular building, a row of buildings and podium building with lift-up design and to determine whether lift-up design can improve cross ventilation.

- 2) To study the pedestrian level wind environment around three kinds of building configurations with and without lift-up designs and to assess the potential improvement of low wind speed zone at the pedestrian level by lift-up design and to discover the discomfort zone at the pedestrian level of these different building types and to examine whether the lift-up design can exacerbate the discomfort area.
- 3) To examine the pedestrian-level thermal comfort environment around singular building, a row of buildings and podium building configurations with and without lift-up design under summer and winter climatic conditions and to assess the potential improvement of thermally discomfort area at the pedestrian level by lift-up design during summer and winter season.
- 4) To conclude the benefits and drawbacks of utilising the lift-up design on the thermal sensation at different seasons and how to make the building designs to be more efficient for providing a neutrally thermal conditions for the pedestrians and to provide recommendations which are prudent to urban designers, architects, engineers and even urban policy makers for improving the urban environment relating to the aims listed above.
- 5) To learn the significance of the lift-up design on pollutant dispersion around these three tall building configurations with upstream and downstream pollutant emission sources.

1.4 Structure of the Dissertation

This dissertation consists of eight chapters that involve the introduction of the thesis, a literature review of the past investigations done by other researchers that are related to the current research work, physical modelling analysis of natural ventilation potential of lower floor levels of singular

building, a row of buildings and podium building with and without lift-up design, experimental study of building lift-up design on pedestrian wind environment and pollution dispersion. The contents in each chapter are summarized as following:

Chapter 1 introduces the background and motivation of current research and overall view of this dissertation is also provided.

Chapter 2 extensively reviews and discusses with the main emphasis on the airflow and dispersion around buildings. The airflow and pollutant dispersion at the pedestrian level has been emphasised here. Most of the previous work in this field is introduced here and the significance of the current study is also discussed in this section.

Chapter 3 describes the research methodologies in this section. Only one well-established and experimental research approach, wind tunnel is introduced. The differences based on different study purpose are discussed, ranging from pressure measurement, to a large scale of wind speed measurement and pollutant dispersion measurement. Equipment for each different measurement has been described in details in this section. The detailed considerations about experiment design and arrangement are also given.

Chapter 4 reports the first stage of wind tunnel studies. A 1:200 scale singular building, a row of buildings and podium building with and without lift-up design was constructed to illustrate the basic features of pressure under wind effect for singular building, a row of buildings and podium building with and without lift-up design. Pressure distributions at the lower level of different building configurations have been given in this chapter and natural ventilation potential of different floors of various building types has also been given. Meanwhile, the significance of lift-

up design for different building configurations for improving or exacerbating the natural ventilation potential has been analysed and discussed.

Chapter 5 presents the second stage of wind tunnel investigations. The 1:200 scale building model is also used for this chapter. 2m in prototype scale of pedestrian-level wind speed measurement was conducted inside the wind tunnel. Meanwhile, the contour diagrams for mean wind speed and gust wind speed for different building configuration with and without lift-up design have been described respectively. Low wind speed zone and discomfort areas caused by insufficient wind-induced natural ventilation and excessive high wind at the relevant areas. Different areas of the overall measurement zone have been discussed individually. Therefore, some suggestions for urban planners, engineers or architects are given here in regarding to how and where to locate the relevant facilities. And the importance of implementing lift-up design for different building types has been concluded.

Chapter 6 used the mean measured wind speed data from chapter 5 in the second stage of the wind tunnel experiment to analyse the thermal comfort environment of different building configurations with and without the lift-up design under summer and winter climatic conditions. Thermal contour diagrams of each different building configuration have been described and the thermal sensation distributions at different zones for the mean wind speed measurement area have been discussed in details. How significant of lift-up design in thermal environment at the pedestrian level has been concluded in this chapter.

Chapter 7 describes the third and final stage of wind tunnel. The detailed concentration distribution at the pedestrian level 2m in prototype for different building types with upstream and downstream line source is also been given in this chapter. The pollutant dispersion for different location has been compared between the building configuration with and without the lift-up design. For this comparison, mean wind speed distribution has also been taken into consideration. A summary whether lift-up design is useful for singular building, a row of buildings and podium building for pollutant dispersion when line source is located upstream or downstream has been given.

Chapter 8 gives a general conclusion drawn from the present work, and states the limitations of this research work as well as the suggestions for future researches.

Chapter Two: Literature review of air flow and air pollutant dispersion around buildings

2.1 Introduction

People spend more than 90% of their time indoors (Li et al. 2007), especially in the urban area. Long-term exposure to poor indoor air quality (IAQ) can cause various health problems, exacerbated as Sick Building Syndrome (SBS), which can lead to morbidity, disability, disease or even death (ASHRAE Handbook, 2009). More than 2 million people, mainly women and children, die annually due to the deadly mixture of pollutants resulting from the burning of biomass, especially when cooking indoors in developing countries (Sundell, 2004). In developed countries, the use of synthetic building materials has increased in building insulations, internal furnishing and craft materials. Consequently, many contaminant sources are being introduced into the indoor working and living environment, releasing volatile organic compounds (VOCs). Some VOCs cause eye, nose and throat irritation, and others damage liver, kidney and central nervous systems. VOC levels indoors are normally 2 to 5 times higher than outdoors, but significantly higher VOCs level can occur after the immediate use of materials. Consequently, buildings have become sources of contamination and are often more polluted than their surroundings (Spengler & Chen, 2000).

Meanwhile, pollutant dispersion in urban areas has become another issue of public concern, particularly in those densely populated cities. Pollutants might affect pedestrians directly and occupants inside the building indirectly. Exhaust gases from rooftop vents (Li and Stathopoulos,

1997), stacks and other sources around a building (Cowan et al, 1997; Hefny & Ooka, 2009; Higson et al. 1996; Mavroidis et al. 1999) can all lead to air quality problems depending on wind conditions and released chemical quantities, resulting in intake air to the building or surrounding buildings containing high concentrations of toxic and odorous chemicals. The flow adjacent to the lee face of a building is more or less upward; and in the building wake there exists a reversed flow in the lower part. When a pollutant source is located within the recirculating wake, high concentrations may accumulate. In building arrays, plumes are normally 2 to 4 times wider than in the open terrain (Macdonald et al. 1998). Building shapes and the arrangement of obstacles in the array determine pollutant dispersions in the near-wake region (Mavroidis & Griffiths, 2001). When the buildings are very tall, greater influence on lateral flow and concentration of the plume is exhibited.

After the Severe Acute Respiratory Syndrome (SARS) outbreak in 2003, airborne transmission is suspected to be the major route leading to large scale outbreaks in high-density residential environments (Yu et al. 2004; Niu & Tung, 2007). The airborne spread concept was first introduced by Wells (Wells, 1934; Wells, 1955) and Riley and O' Grady (1961) to culminate in the well-known Wells-Riley equation (Riley et al. 1978) for evaluating the effects of ventilation, filtration and other physical processes on the transmission of airborne diseases. With respect to vertical cross-floor air contamination, second hand tobacco smoke and fish-cooking fumes from lower floors are two most obvious examples. Mavroidis et al. (2003) initially proved that the pollutant air could be entrained and mixed vertically up to the top of a building. Buoyancy driven upward air convection could carry airborne fine droplets upwards. Therefore, this vertical contaminant flow can bring potential health problems to the adjacent occupants upstairs, especially in high-rise buildings. Cluster of SARS cases occurred in a number of large high-rise

residential blocks, and there appeared to be upward spread patterns i.e. - upper floor residents were affected by those on the lower floors. Also DNA strands of the SARS Corona-Virus have been found within window sill and floors deposits on the upper floors of an index patient (Niu & Tung, 2007). These blocks have rectangular plan layouts and operable windows flush with a flat-façade. When doors are shut and a window functions as both inlet and outlet, these flats become single-side ventilated. The air flowing from the lower floors rises up along the façade due to buoyancy effect and can directly flow into the adjacent upper floors.

It can generally be concluded that airflow around building blocks influence indoor air quality, pollutant dispersion in the surroundings, and airborne transmission of infectious diseases. To address these practical concerns, researchers worldwide have adopted a number of techniques and methods in their investigations.

Pedestrian wind environment is particularly interesting for researchers to investigate the air flow and pollutant dispersion at the pedestrian level. The effects of wind force on pedestrians have been a concern since it was realized that tall buildings could greatly accelerate the wind at grade (Soligo et al. 1998). The air flow at the pedestrian level can cause insufficient air flow for the pedestrians. So that the pollutant from the traffic and industrial manufacturer etc can all accumulate at these areas. Consequently, occupants at the lower level of the residential or office building can be affected. For those fully exposed to this environment are even worse, such as pedestrians, shop keepers etc. On the other hand, too strong wind at the pedestrian can cause unpleasant, discomfort and dangerous for the pedestrian. Pedestrians can hardly walk, blown off etc. In some of extreme cases, it can also impact on human safety, particularly for those areas having typhoon season. Therefore, evaluating the wind environment is an indispensable element

in the design of buildings (Yamada et al. 1996). Wind comfort and wind safety for pedestrians are an important requirements in urban areas. May city authorities request studies of pedestrian wind comfort and wind safety for new buildings and new urban areas. These investigations include combining statistical meteorological data, aerodynamic information and criteria for wind comfort and wind safety (Metje et al. 2008; Stathopoulos, 2006; Durgin, 1997; Sanz-Andres & Cuerva, 2006). Detailed aerodynamic information can be attained by using wind tunnel experimentation, on-site measurements and Computational Fluid Dynamics (CFD) modeling (Blocken et al. 2012). Therefore, some alternatives have also been studied by other researchers. More discussion will be provided in the later section.

The purpose of this article is to review the current state of knowledge of each technique and available software for measuring air quality in single building block and among building arrays, which means on-site measurements, reduced-scale wind/water tunnel experiments and Computational fluid dynamics (CFD) numerical simulations. What has been carried out in the field of pollutant dispersions around buildings will be summarized to shed light on the research gaps in air pollutant dispersions around buildings.

2.2 On-site measurements

On-site measurements have been classified into two categories namely, full scale measurements, and physical scaled measurements.

2.2.1 Full scale measurement

Full scale measurement means testing flow and concentration around a single building, or between a prototype-sized building array, under real atmospheric conditions.

2.2.1.1 An isolated low rise building

Drivas and Shair (1974) released Sulfur hexafluoride (SF_6) as an instantaneous point source in the wake region, on the roof, and inside a three-story building to explore the air flow and dispersion pattern within the wake. Tracer gas was detected by electron-capture gas chromatography. The wind velocity and direction over the building and 18 m above ground level were measured using an anemometer. The wake region of the building was discovered to be well-mixed in all three dimensions and the characteristic exponential dilution time was approximately 1 min. Santos et al. (2005) conducted field experiments to examine the fluctuating time-series of concentration on the wall and to ascertain the influence of atmospheric stability and building dimensions of a complex building. The experiments occurred at atmospheric conditions from stable to unstable for both west and south wind directions. 14 photo ionization detectors (PIDs) on the wall and 2 on the roof had been used to detect the tracer gas (propylene) with a time interval of 1/50s. It was demonstrated that concentration levels on the external walls except for the windward one was greatly affected by the atmospheric stability conditions, and the concentration values could be highly influenced - by the ratio between the building width and height. Mavroidis et al. (1999; 2000; 2007) released a dual source of ammonia and propane, at normal and 45° to the mean wind direction upwind of a single cubic building, and deployed a Flame Ionization Detector (FID) co-located with a Ultra-Violet Ion Collector (UVIC) to measure the concentration levels. The atmospheric stability conditions ranged from very stable to very unstable. The purpose of their study (Mavroidis et al. 1999) was to discover the potential influence of atmospheric stability conditions on the dispersion behavior of entrainment and detrainment in the wake region of an obstacle. It was found that the concentration in the recirculation region decayed exponentially and the decay duration (it is the time that the tracer

gas is fully detrained at the wake) was longer in stable atmospheric conditions due to lower wind speeds and higher concentrations in the wake region of the cube. Mavroidis et al. (2007) summarized both the mean concentration and the concentration fluctuation statistics in the vicinity of an isolated building. Concentration fluctuation results showed that intermittency values increased as the source was displaced from the centerline. Sudden peaks could occur when a source was displaced further away from the centerline where gas entrainment was intermittent. The research also revealed that a dual source/receptor system technique was useful for providing data for statistical analysis and modeling. The agreement between the experimental measurements and numerical results was good, and it was observed that a single ammonia experiment could produce concentrations 30% higher in mean value and 70% higher in fluctuating component at the wake than those for propane (2007).

2.2.1.2 High-rise building

On-site measurements have been reported by Niu and Tung (2008) to study the potential inter-floor virus-spreading mechanisms through open windows. When the wind speed is small (define small/low e.g. $\leq 2\text{m/s}$), the buoyancy force is dominant, especially for those densely built-up districts with buildings over 30 storeys. The actual airflow around the buildings, particularly at lower floors, is much lower due to the surrounding obstructions. For a multi-family building in a sub-urban private residential area, with 3-storey and 15 residential units on each floor, a dual tracer gas of carbon dioxide (CO_2) and SF_6 was released simultaneously to examine the quantity of exhaust air coming out of the window of the lower floor that re-enters the open-window in the upper floor. CO_2 was used for examining the ventilation rate. SF_6 was used as a tracer of indoor pollutant originating from the lower floor and also to quantify the air change rate of the lower room. It was discovered that air in the upstairs room contained up to 7% of the air from the

downstairs room. The work proved that windows flush with a flat façade can be a major route for vertical spread of pathogen-containing aerosols in high-rise buildings (**Figure 2-1**).

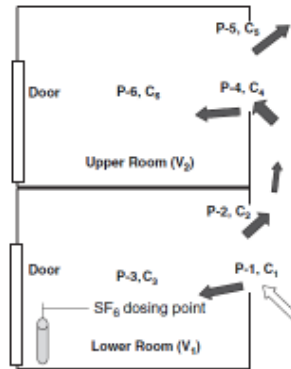


Figure 2-1. On-site investigation of cross-contamination of two adjacent rooms with tracer gases (Niu & Tung, 2008).

2.2.1.3 Building Arrays

In the early days, many researchers (Lucas et al. 1967; Moor & Paper, 1967; Lucas & Paper, 1967; Hamilton, 1967; Hino, 1968; Bullock & Lewis, 1968; Bringfelt, 1968; Barynin & Wilson, 1972) employed full-scale on-site measurements for examining the pollutant dispersion from power stations (Lucas et al. 1967; Moor & Paper, 1967; Lucas & Paper, 1967; Hamilton, 1967; Hino, 1968; Barynin & Wilson, 1972), urban traffic (Bullock & Lewis, 1968; Drivas & Shair, 1974; Drivas & Shair, 1974; Karra et al. 2011; Nakamura & Oke, 1988), industrial complexes (Barynin & Wilson, 1972) and laboratories (Karra et al. 2011). Lucas et al. (1967) performed a field measurement of surface sulfur dioxide (SO₂) concentration at distances of 1 km to 12 km downwind of a 360MW Tilbury Power Station within a sector of $\pm 30^\circ$ of a single wind direction and a lidar device based on a ruby laser to measure the height of the plume. Twenty-two SO₂ recorders were used to collect 3-min air samples for ground level SO₂ concentration

measurements (Lucas et al. 1967). Munro and Casella anemometers were employed for measuring wind speeds above and below 2m/s respectively (Lucas et al. 1967). Lucas et al. (1967) concluded that the plume rise could reach 1000m or more horizontally and turbulence decreased above a height of 100m generally. Increased chimney height did not necessarily produce increased plume rise (Hamilton, 1967). Similarly, Barynin and Wilson (1972) employed fast-response flame-photometric detector for recording the concentration of sulfur compounds in air 5km downwind of West Burton Power Station on a rooftop of Imperial College, London. The rapidly fluctuating concentration dramatically influenced the human response, though it could be quickly reduced by adaptation. Hino (1968) carried out field experiments on atmospheric diffusion of smoke from high stacks of power stations. Cobalt sulfate particles and Freon-12 gas as tracers were released into the stack, and a total number of 48 air sampling points were located at distances 3 to 15 km from the sources and within 45° of the wind direction to investigate dispersion (Hino, 1968). Drivas and Shair (1974) released 66.5kg of SF₆ in Anaheim over 45 minutes at noon time, and collected the air samples by electron-capture gas chromatography in five communities downwind of Anaheim throughout the afternoon. They concluded that SF₆ appeared to be an ideal tracer for studying transport and dispersion of pollutants over urban areas. It was also used to simulate a quasi-instantaneous line source of vehicle exhausts, with its concentrations being detected 0.4 to 3.2km downwind of the motorway at ground level (Drivas & Shair, 1974). The data from this field observation was used to validate the Gaussian plume model and various forms of the semi-empirical diffusion equation (Drivas & Shair, 1974). A field work regarding traffic pollutant dispersion within a non-symmetrical canyon with an off-centre traffic lane in the city of Nicosia, Cyprus was investigated under oblique and parallel winds for approximately a month (Karra et al, 2011). The tracer gas carbon monoxide (CO) was

emitted at different locations and recorded for eight hours per day at several locations along both sides of the street, at heights of 1.5m and 2.5m from the ground (Karra et al, 2011). ICOM monitors were used for CO measurements and CO concentration was higher at 1.5m than 2.5m. Thus, pollutant concentrations are expected to be higher at pedestrian level than rooftop level. High levels were also measured in the middle of the street canyon. Concentration levels remained similar for both side of the street but consistently 10% higher on the North side during a parallel wind direction, but much higher concentration levels were observed when the wind direction was oblique (Karra et al, 2011).

A street canyon generally refers to a relatively narrow street formed between buildings that line up continuously along both sides. It has a distinct climate where micro-scale meteorological processes dominate (Nakamura & Oke, 1988) where air ventilation and pollutant removal occur solely through the roof level. The flow pattern inside a street canyon depends on its geometry, especially the building-height (H) to street-width (W) ratio. The flow field between widely spaced buildings ($H/W < 0.3$) do not interact, resulting in the isolated roughness flow (IRF) regime. At closer spacing ($0.3 < H/W < 0.7$) the wake behind the upwind building is disturbed by the recirculation created in front of the windward building, which is the wake interference flow (WIF) regime. Reduced spacing ($H/W > 0.7$) results in the skimming flow (SF) regime. The IRF, WIF and SF airflow regimes are shown in Fig.2. Wilson and Lamb (1994) performed a field experiment to examine and refine a minimum dilution model within buildings cluster in a university campus. Hourly average air samples were collected at 44 building roof locations to examine SF6 tracer gas dispersion from six uncapped fume hood exhaust vents. It was found that the model predictions agreed well with measured maximum concentrations over the 5-270m

range of exhaust to receptor distances, and that the hourly averaged dilution was strongly influenced by upwind building generated turbulence.

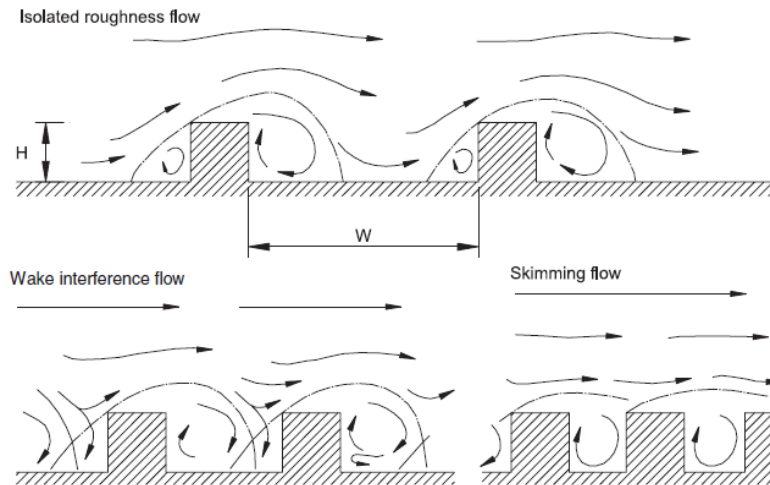


Figure 2-2. Three flow regimes with different building-height-to-street-width ratios H/W (Lucas et al. 1967).

In Davidson et al.'s (1995) study, flow visualization and gas concentration measurement were conducted to investigate plume dispersion below the building array height and along the array. Certain mean concentration statistics did not change materially as the plume passed through the obstacle array, which included the form of the cross-sectional profiles, the decay along the centre line and the lateral growth with downstream distance. However, a 40-50% increase of the mean vertical extent of the plume had been detected. Due to the magnitude of the building arrays, it is difficult and cost prohibitive to perform the tracer gas measurements as many samplers and receptors are needed. Probably partly because of this reason, on-site tracer gas measurements for building arrays are scarce.

In terms of pedestrian wind environment is concerned, Metje et al. (2008) investigated the complex relationship between physical and psychological parameters on human comfort levels. A site on the University of Birmingham, UK campus had been chosen for investigation. The meteorological data were collected by completing questionnaire including demography and clothing values and from a portable MiniMet Automatic Weather Station from Skype Instruments Ltd. This equipment consisted of internal sensors measuring the air temperature and humidity and separate three-cup anemometer, wind vane and a pyranometer for relative humidity (RH), air temperature, wind speed, wind direction and direct solar radiation. Blocken et al. (2004) presented the assessment of wind climate and particularly the study had been performed to modify the wind climate in the passages of the Silvertop Towers which is a comprehensive redevelopment project for three high-rise residential buildings in the city of Antwerp, Belgium. The assessment was carried out by using CFD numerical modelling. As expected, the pedestrian wind climate was highly unacceptable. An automatic control system was designed and used to modify the wind climate in the passages. The actuators of the system were sliding doors that were mounted at both ends of the passage. The opening and closing of the doors was control by a decision algorithm based on local wind measurements. If the threshold wind speed in the passage was exceeded, at least one door would be closed. The passages were approximately opened for about 50 to 70% of the time.

2.2.2 Physically-scaled model on-site measurements

Some researchers use physical scaled models placed under real atmospheric and environmental conditions. In this review, it is termed ‘physical scaled model on-site measurements’ and is an alternative to the expensive full-scaled measurement, especially in urban areas with obstacle groups. However, this method may suffer from inherent similarity problems since the wind speed

of the scaled-down model should be lower than the full-scale model, with limited literature available.

2.2.2.1 An isolated building

Mavroidis et al. (2003) studied the plume entrainment behaviors from longitudinal, lateral and vertical source locations using physical scaled models for isolated obstacles in the field. A dual-gas with ammonia and propane was released continuously $2.0H$ upwind of two buildings; a building with a height $H = 1.15\text{m}$ and diameter $D = 1.15\text{m}$, and another taller building with $H = 2.3\text{m}$ at a nominal scale of $1/10$ and $1/20$ respectively. The results of the tracer gas demonstrated that taller obstacles resulted in reduced ground level concentrations.

2.2.2.2 Building arrays

Higson et al. (1996) used $1/3$ to $1/10$ scaled model buildings, in flat terrain under stable to slightly unstable atmospheric conditions. The pollutant source was placed upstream of the building and concentrations measured using a 1s response time detector. The purpose of the work is to compare the mean concentrations, standard deviation, intermittency and concentration fluctuations, obtained using the physical scale model on-site measurement and wind tunnel respectively. It was found that turbulence intensity obtained in a wind tunnel occurred at a smaller scale. Macdonald et al. (1998; 1997) released a tracer gas of pure-grade propylene (C_3H_6) upwind of a $1/10$ scale cubic building arrays in the field. UVIC detectors were deployed to measure the propylene concentrations. Ultrasonic anemometers were placed at $1H$ height and 6 to $10H$ upwind of the arrays for measuring the mean and fluctuating velocity. Illustrations showed concentrations were much higher than rooftop ones in the front rows of the array, possibly due to the horseshoe vortex system around front row buildings. A higher lateral

concentration profile could be found closer to the source. Macdonald et al. (1997) observed that a greater initial dispersion plume was found when releases were located inside the array instead of upwind of the array. Mavroidis et al. (2001) also examined pollutant dispersion within building arrays of $S/H = 1.5$ (where S is the space between two consecutive array elements) at a scale between $1/10$ and $1/20$ in the field. A dual-gas using ammonia and propane had been released constantly $2.0H$ upwind of the obstacle at a height of $0.5H$. The ammonia could be moved along three coordinate directions from the obstacle but the propane remained in the same position. The results suggested that mixing and dispersion were enhanced within the array.

2.3 Wind/water Tunnel Physically-scaled measurements

Achieving steady weather conditions for on-site measurements is challenging. A physically-scaled measurement in a simulated, controlled environment can help overcome this, by reducing the geometrical scale of a given domain and adjusting the reference parameters to reproduce data under the original full-scale conditions. It has been proved especially useful in CFD model development (Baker & Hargreaves, 2001) Wind tunnel and water channel are two types of physical scaled facilities in studying airflow around buildings.

2.3.1 Wind tunnel measurements

Scaled building models may be used as objects in a wind tunnel. Three monitoring techniques are often used in a wind tunnel experiment: flow visualization for revealing the possible flow patterns, tracer dispersion quantifying concentrations at receptor locations, and Laser Doppler Anemometry (LDA) for studying the flow in detail. Also, although pressure distribution may not be the target for air quality studies, it is important for estimating air-infiltration in envelopes and is also used for validating numerical results. Conversely, although a wind tunnel might have

scaling difficulties, it can help to effectively approximate real atmospheric conditions in urban streets and investigate micro-scale pollutant dispersion around a building.

For most wind tunnel experiments, the mean wind speed profile of the atmospheric boundary layer could be expressed as a power law function (Eq. 1.) or a logarithmic law function (Eq.2.2):

$$U(z) = U_H(z/H)^\alpha \quad (2.1)$$

where U is mean velocity (m/s) at the reference height H (m), and α is the power law exponent, which varies with different terrains.

$$U(z)/U_H = \ln(z/H)/\kappa \quad (2.2)$$

where κ = von Karman's constant (= 0.4).

The turbulence level of the approaching wind is often controlled according to turbulence intensity, which is defined as.

$$I = u' / U \quad (2.3)$$

where u' is the root-mean-square of the turbulent velocity fluctuations (m/s), U is the mean velocity (Reynolds averaged) (m/s).

$$u' = [1/3(u_x'^2 + u_y'^2 + u_z'^2)]^{0.5} = (k/3)^{0.5} \quad (2.4)$$

$$U = (U_x^2 + U_y^2 + U_z^2)^{0.5} \quad (2.5)$$

where k is the turbulent energy, U_x , U_y and U_z are mean velocity components.

In analyzing pollutant dispersion based on tracer gas testing, the mean concentration could be normalized in the dimensionless form:

$$K = 10^{-6}CUH^2/Q \quad (2.6)$$

where C is the measured concentration (ppm), U is the mean wind speed (m/s) at building model height H (m), and Q is the volumetric flow rate of the tracer gas (cm^3/s).

2.3.1.1 An isolated building

To study the pollutant dispersion of an isolated building, tracer gas can be released at different locations around a building in the wind tunnel. Table 2-1 summarizes these studies which in general aim at revealing characteristics of ventilation exhaust dispersion around a single building of various shapes and orientations. Flow pattern and pollutant dispersion around an isolated building were studied using different tracer gases and air flow equipment inside the wind tunnel. Different tracer gases were also released either point source or line source from different locations relative to the singular obstacle. The purpose of these investigations is to offer more information about phenomena and critical parameters of flow field and plume dispersion around an isolated building; and to provide some future design guidelines for a singular obstacle

Table 2-1. Wind tunnel test of pollutant dispersion around an isolated building

Concerns addressed	Pollutant Dispersion	Tracer Gas		Air Flow Measurement	Conclusion
		Release	Monitoring		
To illustrate a method of studying a necessary and adequate height (Robins & Castro, 1977) and to describe flue gas dispersion from chimneys and stacks (Leutheusse & Motycka, 1978).	Exhaust gas from the stacks (Robins & Castro, 1977) and a chimney (Robins & Castro, 1977; Leutheusse & Motycka, 1978).	Smoke was produced by a paraffin oil-fog generator. 10,000ppm methane (Robins & Castro, 1977) and an oil aerosol (Leutheusse & Motycka, 1978) were emitted as the effluent.	Smoke was visualized by a Graflex camera. A FID was continuously used for concentration measurements (Robins & Castro, 1977). The simultaneous effluent concentration at selected points was measured by a photo-electric light-scattering probe (Leutheusse & Motycka, 1978).	A Thermo-Systems anemometer system measured both mean velocity and turbulence intensity (Robins & Castro, 1977). Disk-type air speed indicator was used for indicating air velocity as low as 0.25m/s (Leutheusse & Motycka, 1978).	The stack should be high enough such that air quality standards would not be exceeded (Robins & Castro, 1977). The measured data of dispersion over flat terrain agreed well with that from the theoretical ones, but not with mildly complex topography (Leutheusse & Motycka, 1978).
To study the velocity and turbulence (Robins & Castro, 1977) and plume above a surface mounted cube (Puttock, 1979).	Exhaust gas in the surface and from a stack (Robins & Castro, 1977; Puttock, 1979).	A mixture of helium and propane was released of the cube and from a stack (Robins & Castro, 1977; Puttock, 1979).	The mean concentration was measured by a flame-ionisation technique simultaneously from up to 32 points (Robins & Castro, 1977; Puttock, 1979).	Velocity and turbulence were taken with pitot tubes, hot wires and pulse hot wires (Robins & Castro, 1977; Puttock, 1979).	The concentration field beyond about two cube heights from the source could be adequately described by the use of effective source height concepts (Puttock, 1979).

Table 2-1 (Continued)

Concerns addressed	Pollutant Dispersion	Tracer Gas		Air Flow Measurement	Conclusion
		Release	Monitoring		
To study the air flow patterns, concentration dispersion on and around a cube (Ogawa et al. 1983; Saathoof et al. 1995; Yassin et al. 2005); the effect of model scale and concentration (Yassin et al. 2005).	Exhaust gas from the roof (Ogawa et al. 1983; Saathoof et al. 1995; Yassin et al. 2005) and stacks (Yassin et al. 2005).	SF6 as tracer gas emitted from center of cube roof (Ogawa et al. 1983; Saathoof et al. 1995; Yassin et al. 2005) and a 0.25m diameter stack with a height of 3m (Yassin et al. 2005).	Concentrations were taken for five wind angles between 0° to 45° and four upwind roughnesses from smooth to rough (Ogawa et al. 1983), by a movable probe and a varian gas chromatograph of models (Saathoof et al. 1995), by a photoacoustic multi-gas monitor (Yassin et al. 2005).	A two-colour Laser Doppler anemometer (LDA) (u and w) (Ogawa et al. 1983), hot-wire anemometers (u, v and w) (Ogawa et al. 1983; Saathoof et al. 1995; Yassin et al. 2005), an ultrasonic anemometer and a 3D LDA (Yassin et al. 2005)	Smooth surface and $\theta=0^\circ$ generated reverse flow at source and high concentrations at leading edge; but even higher rooftop values by rough surface (Ogawa et al. 1983), which were overvalued by wind tunnel (Ogawa et al. 1983). Leeward concentrations did not affect much by model scale (Yassin et al. 2005).
To evaluate the flow (Leitl et al. 1997; Mirzai et al. 1994) downwind concentrations (Huber 1991; Huber 1989), concentration near (Leitl et al. 1997) or at a plane behind a building (Mirzai et al. 1994).	Emitted from the windward (Huber 1991; Huber 1989), roof, upwind (Leitl et al. 1997) and downwind (Mirzai et al. 1994)	Emitting Ethane upwind (Huber 1991; Huber 1989), SF6 on the roof, upwind and downwind (Leitl et al. 1997), Helium leeward (Mirzai et al. 1994).	It was measured by a FID (Huber 1991; Huber 1989) at different speeds, buildings size (Huber 1991), angles from -30° to 60° and W/H ratios from 2 to 22 (Huber 1989); by a leak detector at angles from 0° to 180° at different height [50]; by a modified 'T.S.I.' probe at angles from -10° to 0° of a cube (Mirzai et al. 1994).	X-array hot-wire probe with constant-temperature anemometer (Huber 1991; Huber 1989) and hot-wire anemometers (Leitl et al. 1997; Mirzai et al. 1994)	Greater concentrations near the building generated than downward side (Huber 1991). The largest plume was the lateral one from a source near the center of the building (Huber 1989). Higher discrepancies for ground sources than situations with roof sources were found (Leitl et al. 1997).

Table 2-1 (Continued)

Concerns addressed	Pollutant Dispersion	Tracer Gas		Air Flow Measurement	Conclusion
		Release	Monitoring		
To study using bipolar space for dispersion charging (Boreham 1986), concentration trends (Huber & Arya, 1989; Huber, 1988), behavior of a cloud (Krogstad & Pettersen, 1986).	Emitted from floor level, midway along the upwind (Huber & Arya, 1989; Huber, 1988).	Generating oil droplet fog at floor level (Boreham 1986) and introducing propane from a hemisphere midway along the upwind (Huber, 1988).	It was measured by ion detector in the near, intermediate and far wake region of a building at 1/12 scaled atmospheric boundary layer. An aspirating hot wire probe at 5cm height tested the mean concentration ((Krogstad & Pettersen, 1986).	A pitot tube (Boreham 1986), a camera (Boreham 1986; Huber & Arya, 1989; Huber, 1988) and hot-wire anemometers (Krogstad & Pettersen, 1986)	Video image could analyse smoke (Huber & Arya, 1989). The frequencies near the wake center were 0.1-0.3 times V/H ratio (Huber, 1988). Wilder model resulted in higher surface concentrations (Krogstad & Pettersen, 1986).
To study pollutant dispersion on the near field of three different building configurations indicating in Fig. 3 (Chavez et al. 2011).	Emitted from a stack with equivalent heights of 1m (Chavez et al. 2011).	A mixture of SF ₆ and nitrogen with a concentration of 10ppm was released from the stack on the top of B1 building (Chavez et al. 2011).	A gas chromatograph (GC) was taken for valuing the gas concentrations that collected by applying the syringe samplers up to an averaging time of 1 min in the wind tunnel (Chavez et al. 2011).	Hot-wire anemometers (Chavez et al. 2011)	The calculation by ASHRAE 2007 offers much lower dilutions than those attained from the wind tunnel experiment (Chavez et al. 2011).

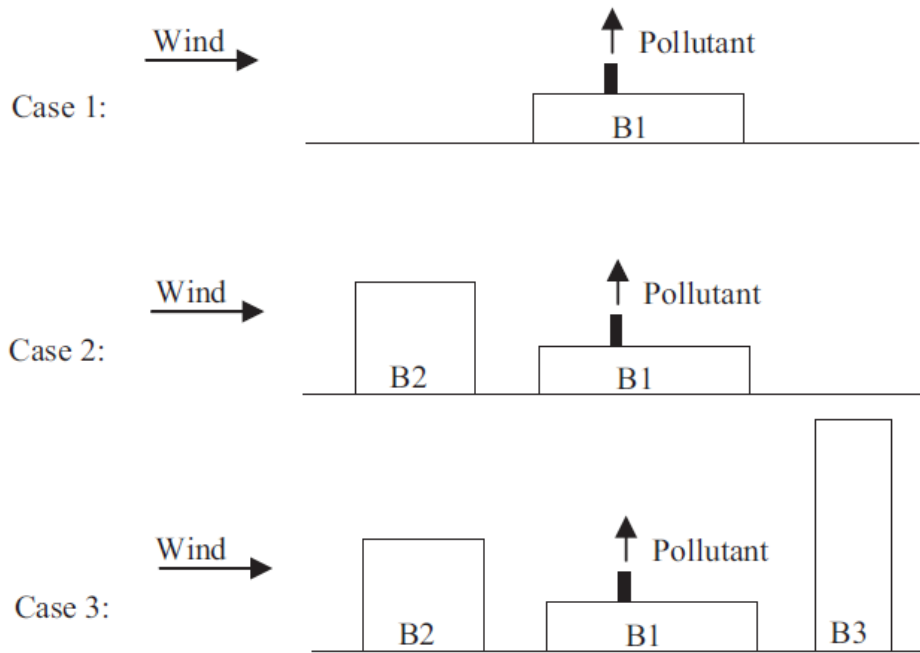


Figure 2-3. Building arrangements (Chavez et al. 2011)

2.3.1.2 High-rise building

In high-rise residential buildings, each household has individual vent exhausts. In comparison, the vertical and horizontal cross contaminant between different floors of an isolated high-rise building has not been widely researched as indicated by the only relevant paper found in this review by Liu et al. (2010). They adopted a 1:30 scale model to represent a 10-story typical Hong Kong residential building in a 4m (high) x 5m (wide) x 41m (long) wind tunnel to examine the cross-contamination phenomenon in the re-entrance spaces. Tracer gas was continuously released at a constant flow rate matching the exhausted room air at the 3rd, 6th and 9th floors. The measured concentrations in the re-entrance spaces revealed that the pollutant released at the three floors spread upwards and downwards differently. Combined with the pressure distribution at the wall surfaces, possible horizontal pollutant spread was also analyzed.

2.3.1.3 Building array

A number of wind tunnel studies of pollutant dispersion phenomena around building arrays and in street canyons are summarized in Table 2-2. These studies used various tracer gases and air flow equipment to investigate pollutant dispersion around urban arrays inside the wind tunnel. Different tracer gases were released either point source or line source from upwind, ground level, rooftop or within the building arrays. The purpose of these investigations is to offer more information about phenomena and critical parameters of flow field and plume dispersion inside the building array; and to provide some future design guidelines for densely populated areas.

Table 2-2. Wind tunnel test of pollutant dispersion of building array

Concerns addressed	Pollutant Dispersion	Tracer Gas		Air Flow Measurement	Conclusion
		Release	Monitoring		
To study flow field, plume dispersion around buildings (Macdonald et al. 1998; Davidson et al. 1996; Yee et al. 2006), the effect of near-field dispersion for downstream buildings (Hajra & Stathopoulos, 2012). The scaling effects (Yee et al. 2006) and the W/H ratio for a fixed obstacle density (Macdonald et al. 1998) had also been tested.	Near-field plume dispersion around urban buildings (Macdonald et al. 1998; Davidson et al. 1996; Yee et al. 2006; Hajra & Stathopoulos, 2012)	Releasing Ethane (Davidson et al. 1996), Methane (Macdonald et al. 1998) upwind of the building array; pure Ethylene upwind and within the building array (Yee et al. 2006); SF ₆ and nitrogen from rooftop stacks 1, 3 or 5m height and M range from 1 to 3 (Hajra & Stathopoulos, 2012).	A few of Flame Ionization Detectors (FIDs) had been utilized for obtaining plume internal structure and mean concentration (Macdonald et al. 1998; Yee et al. 2006). Another FID was for the background concentration (Macdonald et al. 1998). Horizontal and vertical FIDs were used (Yee et al. 2006). A syringe sample was used for collecting samples. A VARIAN 3400 Gas Chromatograph (GC) was applied for estimating the concentration from the syringe samples (Hajra & Stathopoulos, 2012).	An x-array hot-wire (Davidson et al. 1996), a pulsed-wire anemometer (Davidson et al. 1996), a type JBJ pulsed-wire anemometer (Macdonald et al. 1998) and crossed hot-wire coupled with a digital vane anemometer (Yee et al. 2006), Cobra Probe (Hajra & Stathopoulos, 2012)	The mean concentration was a Gaussian form (Macdonald et al. 1998; Davidson et al. 1996). Its fluctuation was decreased by the small-scale and high-strength turbulence (Davidson et al. 1996). 2 to 3 times larger lateral and vertical spreads of plume but lower peak values from wind tunnel (Yee et al. 2006). The height and across wind dimension of the downstream building and the spacing between buildings are critical in plume dispersion (Hajra & Stathopoulos, 2012).
A two-dimensional street canyon (Fig. 4.) with different parameters was studied (Huang et al. 2007; Klein & Plate, 1999).	Vehicle emissions (Huang et al. 2007; Klein & Plate, 1999)	Emitting SF ₆ in lines of 35m (Huang et al. 2007) and 85m (Klein & Plate, 1999) away from building I and B respectively.	Concentrations were measured by a leak detector for wind directions 0 ^o , 15 ^o , 30 ^o , 45 ^o , 60 ^o and 90 ^o (Huang et al. 2007; Klein & Plate, 1999).	Hot-wire Anemometer (Huang et al. 2007; Klein & Plate, 1999).	Roof shape affected the incanyon vortex dynamics and orientation (Huang et al. 2007; Klein & Plate, 1999). Maximum concentrations depended on the sampling location.

Table 2-2 (Continued)

Concerns addressed	Pollutant Dispersion	Tracer Gas		Air Flow Measurement	Conclusion
		Release	Monitoring		
To study properties of building wakes and wind, impact of dispersion of material (Halitsky et al. 1977).	Reactor emission (Halitsky et al. 1977)	The tracer was emitted near the ground of the northeast side of buildings (Halitsky et al. 1977).	Concentration were measured downwind of the reactor containment structure at the EBR-II complex (Halitsky et al. 1977).	Hot-wire Anemometer (Halitsky et al. 1977)	The wake dimensions are inversely proportional to the atmospheric turbulence intensity in the respective directions (Halitsky et al. 1977).
To study 2D plumes in stable conditions (Robins & Castro, 2001) and the impact of tree on ventilation and dispersion (Gromke & Ruck, 2007; Gromke & Ruck, 2009).	Transport dispersion (Robins & Castro, 2001; Gromke & Ruck, 2007; Gromke & Ruck, 2009)	A nominal 3% by volume of propane in CO ₂ (Robins & Castro, 2001), The line SF ₆ source at ground level (Gromke & Ruck, 2007; Gromke & Ruck, 2009).	Flow visualization and FID (Robins & Castro, 2001), electron capture detection (ECD) (Gromke & Ruck, 2007; Gromke & Ruck, 2009).	Fibre-optic and LDA with Dantec burst spectrum signal (Robins & Castro, 2001), Laser Doppler velocimetry (LDV) (Gromke & Ruck, 2007; Gromke & Ruck, 2009).	Entrainment speed will not over-predict plume dilution rate (Robins & Castro, 2001). The air exchange between street cantons and the ambience could be decreased by the tree planting (Gromke & Ruck, 2007; Gromke & Ruck, 2009).
To provide design guidelines for densely populated areas for improving urban ventilation (Bady et al. 2009).	Vehicular emissions (Bady et al. 2009)	Ethylene and synthetic air emitted from four ground level sources (Bady et al. 2009).	FID (Bady et al. 2009)	Thermal-type purified Germanium probes (GeZ-200m, Tohnic) (Bady et al. 2009)	Building layouts and wind directions are important for ventilation aspects. Larger building gaps tend to induce more wind to the canyon (Bady et al. 2009).

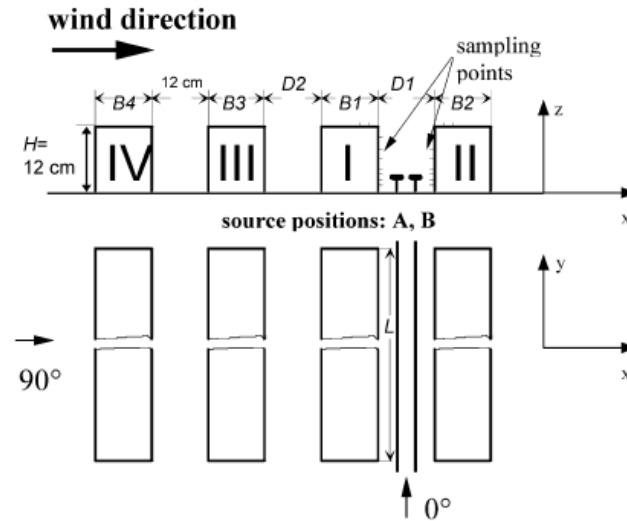


Figure 2-4. Experimental configuration for the street canyon (Klein & Plate, 1999)

Some papers reported the comparison between field measurements and physical scaled measurements. Bachlin et al. (1991) and Yassin et al. (2005) showed quite consistent agreement of results under neutral conditions for model and prototype in properly scaled conditions. Sommers et al. (1980) found that overcritical Reynolds numbers by the wind tunnel test agreed well with the field data. Aubrun and Leitl (2004) also confirmed a good agreement between field and wind tunnel data under neutral conditions, so the unsteady properties of a dispersion process could be produced if the unsteady turbulent behavior of the atmospheric boundary layer in wind tunnel was properly modeled. However, disagreements were also identified by some researchers. Mavroidis et al. (2003) showed that the plume was more dispersed in the field attributable to additional atmospheric wind meander. The research also revealed that centerline concentrations were higher and the effect of lateral source displacement more apparent in the wind tunnel. Similar findings indicated that field concentration fluctuation intensities were generally greater than those measured in the wind tunnel, except in the near-wake region (Higson et al. 1996) Macdonald et al. (1998) also agreed that more scattered results could be obtained from field

measurements. Ogawa et al. (1983) found that the maximum ground level concentrations from the field and wind tunnel measurements were in reasonable agreement, but the wind tunnel model tended to overestimate the concentration on the roof. Conversely, under-predictions were found by Lateb et al. (2010) for wind tunnel experiments, particularly along the centre region of the roof and leeward of the tower. It was also summarized that wind tunnel measurements overestimated pollutant concentrations around the roof stack but underestimated concentrations elsewhere. The cause of these discrepancies may be due to lower Reynolds number in the wind tunnel and larger variations in the meteorological conditions in the field tests, for instance, wind velocity, direction and temperature. Yassin et al.'s (2005) is an ideal example where the wind velocity and direction varied hourly during daytime field measurements.

Most of the pedestrian-level wind environment works were conducted inside the wind tunnel. A convenient method to evaluate the pedestrian-level wind environment around buildings has been developed to yield a visual representation of the wind condition near the ground. A model is located at a heated floor and immersed in a flow. Infrared thermography has been utilized for measuring the temperature distribution on the wind tunnel floor surface. A thermal image can be displayed afterwards. Yamada et al. (1996) studied the relationship between the surface temperature and the wind speed. A simple empirical formula was derived in the regions where wind speeds increase, i.e. $U \geq 1.0$. But it is difficult to present a description in the regions where wind speeds decrease. It generally overestimates the mean wind speed in the region where mean wind speed is low but turbulence is great. Sasaki et al. (1997) combined the thermography technique and the knowledge-based system to give a more reasonable evaluation of the pedestrian-level wind environment. An allowable error was found when the system predicted the higher-speed regions around the two buildings. But this system is still limited to simple

arrangements. To and Lam (1995) investigated wind environment around the base of a row of identical tall buildings through wind tunnel experiments. Wind speeds and angles at the pedestrian level were obtained with a split-fibre probe side-by-side arrangement of buildings to enable us to evaluate the wind environment with two different pedestrian-level wind descriptors. When the wind direction was perpendicular to the row, significant flow channelling is observed, which suppressed the formation of large-scale vertical structures separated from the building's upwind corners at the base. Strong sheltering was discovered for the downwind building and separation of horseshoe-type vortices from their bases were suppressed when wind blew in the direction along the row of buildings. Metje et al. (2008) investigated the complex relationship between physical and psychological parameters on human comfort levels. Also a total 30 different test candidates were tested in the wind tunnel for give different combination of wind speed and air temperature for 15 min. They were standing in the wind tunnel and were told not to cover up their hands by putting them in their pockets. A clear relationship between air temperature, the wind speed and the human comfort level was determined. While the solar radiation and relative humidity did not show a strong relationship on the human comfort level.

2.3.2 Water tunnel measurements

Although wind tunnels have been more widely used for studying pollutant dispersion than water tunnels, the same principles and considerations can be employed for both methods. The major potential advantage of water tunnel over wind tunnel is its relative ease of simulating buoyancy effects. Salt bath modeling is a technique that uses water infused with varying salt solution concentrations to replicate thermal buoyancy in a full scale structure. Yet, dimensional analysis is still needed to maintain consistency between the model and prototype. Providing a similar atmospheric boundary layer in water is still a challenge, particularly with regards to maintaining

geometric similarity, viscosity and density. **Table 2-3** summarizes a number of water tunnel based studies. These studies utilized the density differences between the salt water and water along with a coloured tracer to simulate plume dispersions within a building array. Pollutant dispersion and flow visualization in the near-field and the peak-to-mean concentrations of the upwind stagnant location of a building array were investigated. The feasibility of the buoyancy effect of plume dispersion in a water channel was also evaluated.

Table 2-3. Water channel test of pollutant dispersion of building array

Concerns addressed	Pollutant Dispersion	Measurement apparatus	Flow Measurement	Conclusion
<p>To assess the feasibility of plume dispersion in a water channel (Cheah et al, 1983). Vertical and crosswind profiles of mean, variance, intermittency and conditional intensity of non-zero fluctuations were studied (Contini & Robins, 2004). Pollutant dispersion in the near- field in a building array was reported (Yee et al. 2006).</p>	<p>Releasing saline (Cheah et al, 1983) and sodium fluorescein dye tracer (Yee et al. 2006) at ground level in a stably rough surface atmospheric boundary layer.</p>	<p>The concentration was measured simultaneously at multi-points by the laser-induced fluorescence (LIF) technique of a 1/205 scale model under neutrally stratified atmospheric boundary layer with a working section of 0.9m high x 1.5m wide x 10m long (Yee et al. 2006).</p>	<p>A pitot tube (Cheah et al, 1983), a fibre-optic Laser Doppler velocimeter (LDV) powered by an argon-ion laser (Contini & Robins, 2004) and a Laser-Doppler anemometer in backscatter mode with a 16mV He-Ne laser (Yee et al. 2006) measured mean velocity; single sensor and X-array, cylindrical fibre film probes with a two channel DISA 55M Series anemometer tested turbulent velocity (Cheah et al, 1983).</p>	<p>Mean, fluctuating (Cheah et al, 1983) and maximum mean concentration (Yee et al. 2006); concentration fluctuation intensity (Yee et al. 2006) and its decay (Yee et al. 2006; Contini & Robins, 2004) could be accurately measured. Even with increasing downwind distance, the lateral and vertical plume could be reproduced well by water channel (Contini & Robins, 2004). But it overestimated fraction of non-zero concentration periods near the edges of the plume (Contini & Robins, 2004).</p>
<p>To study buoyant plume sources (Contini & Robins, 2006) and two identical buoyant plumes (Bara et al. 1992). Peak-to-mean concentrations of ground level point sources at the upwind stagnant position of a large building array were determined (Hinds, 1969).</p>	<p>Buoyant emissions were emitted at the top of a salted water tank (Contini & Robins, 2006). The fluorescent pigment, zinc sulfide as the atmospheric tracer emitted into a dry cleaning solvent, trichloroethane (Hinds, 1969).</p>	<p>Both quantitative plume visualizations and point concentration detection with a colorimeter system in a water towing-tank had been deployed (Contini & Robins, 2006; Bara et al. 1992). A Self-Orienting Real Time Sampler (SORTS) and a Real Time Sampler (RTS) were applied for measured time history concentration. The SORTS was located at a point on the centerline. There were 14 samplers at 30m and 10 samplers at 50 and 100m from the center of the building (Hinds, 1969).</p>		<p>The extra-rise of twin plume could be as large as 30% (Contini & Robins, 2006). The asymmetry reduced during plume development, the concentration becomes similar to that of a single plume with a double-vortex structure (Bara et al. 1992). No difference between peak-to-mean ratios measured in unobstructed and obstructed flow (Hinds, 1969).</p>

2.4 Numerical experiments/simulations

Since the 1960s, the CFD technique has been applied to analyze fluid flow, heat transfer and associated phenomena e.g. chemical reactions. The increasing popularity of numerical simulation software, attributable to increased computational power, becomes a major tool for designers when analyzing complex fluid flow and thermal systems. In this review, we focus on its application in airflow and pollutant dispersion around buildings.

2.4.1 Direct Numerical Simulation (DNS)

By DNS it is meant that the Navier-Stokes equations are numerically solved directly without the use of turbulence models. It captures the mean flow and all relevant scales of turbulent motions, so extremely fine grids are required in consideration of the small eddies. It appears that some essential flow features such as the vortex behind a building is best captured by the DNS method. However, it is not amenable to use DNS in engineering applications due to the prohibitive computational time and memory requirements. Consequently, data from reliable DNS studies is scarce (Yakhot et al. 2006). **Table 2-4** summarizes studies of DNS modelling for external flows (Yakhot et al. 2006; Rossi & Iaccarino; Coceal et al. 2006; Versteeg & Malalasekera, 2007; Launder & Spalding, 1974). DNS was utilized for testing airflow pattern, heat transfer, chemical species transportation and urban air pollution in different locations of a singular building or building array. The mean flow structure and turbulence intensities were both analyzed. The aim of these investigations is to prove DNS's potential as a tool in air pollutant dispersion in urban areas.

Table 2-4. DNS simulation of pollutant dispersion around an obstacle and in street canyons

Practical concerns addressed	Conclusion
<p>To examine the potentiality of using DNS for testing urban air pollution due to chemical and biological dispersion around a cube (Aberdi & Omidyeganeh, 2008). To predict airflow pattern, heat transfer and chemical species transportation in the indoor environment (Chen & Srebric, 2002).</p> <p>To report the negative turbulence could be generated in front of the cube and large-scale anisotropic flows of the reverse energy transport from small to large scale (Yakhot et al. 2006). To study dispersion in the wake of a cube as a step towards the analysis of bio-agent release in urban environments (Rossi & Iaccarino). To investigate dependence between building array, mean flow structure and turbulence statistics (Coceal et al. 2006).</p>	<p>Generally, the concentration patterns from DNS agreed well with the experiment (Aberdi & Omidyeganeh, 2008; Chen & Srebric, 2002); the low turbulence in the wake of the cube from DNS, RANS and lab also agreed well (Rossi & Iaccarino). Although the primary results based on big simplifications were reasonable, pollutant dispersion around a cube had not been evaluated completely (Aberdi & Omidyeganeh, 2008). The Kolmogorov length scale was around 0.01 to 0.001m for air flow, which meant the grid number needed in a DNS was in a range of 10^{15} to 10^{18} even for a small room. So applying for DNS simulation is not very practical (Chen & Srebric, 2002). But DNS was able to evaluate the wake region of a square obstacle under very sensitive inflow conditions. RANS was unable to predict the streamwise turbulence flux (Rossi & Iaccarino). 3D simulation was necessary for building array issue and urban canopy models or LES at lower resolutions were recommended (Rossi & Iaccarino). An abnormal normal-to-the-wall velocity distribution was found near the cube front façade (Yakhot et al. 2006).</p>

2.4.2 Reynold-averaged Navier-Stokes numerical simulations (RANS) and Large eddy simulation (LES)

RANS are the “oldest” approach to turbulence modeling, which employs an integral approach for the whole turbulence spectrum so that turbulence modeling assumptions are required. This approach requires more modest computational requirements compared to DNS, reasonable results are achieved. Thus, they have been the mainstay of engineering flow calculations over the last three decades (Tominaga & Stathopoulos, 2009). The attention of RANS models is focused on the mean flow and the effect of turbulence on mean flow properties. Prior to the application of numerical methods the N-S equations were time-averaged. Extra terms, appearing in the time-averaged flow equations due to interactions between various turbulent fluctuations, are modeled with different approximations. The most common RANS turbulence models are classified on the basis of the number of additional transport equations that need solving along with the RANS flow equations. Reynolds-stress models (RSM) which have seven extra transport equations are superior to the eddy-viscosity models, as it does not use the Bousinessq approximation. However, penalties occur in terms of model complexity, computing time and numeric algorithm stability. Therefore, the most widely used are two equation eddy-viscosity turbulence models. These are generally suitable for modeling air flow when secondary recirculation is not the main interest. The three main types of RANS models are the standard $k - \varepsilon$ models, the RNG $k - \varepsilon$ models and the Realizable $k - \varepsilon$ model are three main types of RANS models. The most popular model is the standard $k - \varepsilon$ model developed by Launder and Spalding (1974). However, Tominaga and Stathopoulos (2009) pointed out that the standard $k - \varepsilon$ model provides “insufficient” results for the concentration field around a cubic building due to poor reproducibility of the basic flow structure, such as the reverse flow on the roof. The best tested turbulence model is the RNG

$k - \varepsilon$ model. Mahjoub et al. (2003) also proved that, among the three first order $k - \varepsilon$ models, only the RNG $k - \varepsilon$ model could provide good results in the exit region and in the trailing zone of a jet, although they rendered identical results in the upstream and far downstream regions of a jet. Hence, the RNG $k - \varepsilon$ model has been widely used recently (Yakhot et al. 1992). Recent works indicated that these models seem to be very promising in describing complex processes (Canepa & Rodi, 1997); while some authors (e.g. (Lakehal & Rodi, 1997)) highlighted difficulties in downwash simulation by $k - \varepsilon$ models.

Yu et al. (2004) used $k - \varepsilon$ model predictions to interpret the spatial transmission pattern of a large scale SARS outbreak in a private high-rise estate involving 7 blocks and infecting 300 residents. As illustrated in Figure 2-5. Plan view of Amoy Garden (Yu et al. 2004)., epidemiological evidence demonstrated that the index patient, who resided briefly on the 16th floor in Block E, infected residents in this block and adjacent blocks. CFD and multi-zone modeling were applied to illustrate that buoyancy and wind driven airflow could have caused the airborne spread of the pathogen-laden respiratory aerosols. More residents living on the middle floors of the nearby blocks downstream of the index apartment were affected than those living in buildings upstream of the index apartment, while fewer households of the Dc and Da units of the nearby blocks were infected. In this application, the $k - \varepsilon$ model predictions played a qualitative role in understanding the airborne disease transmission.

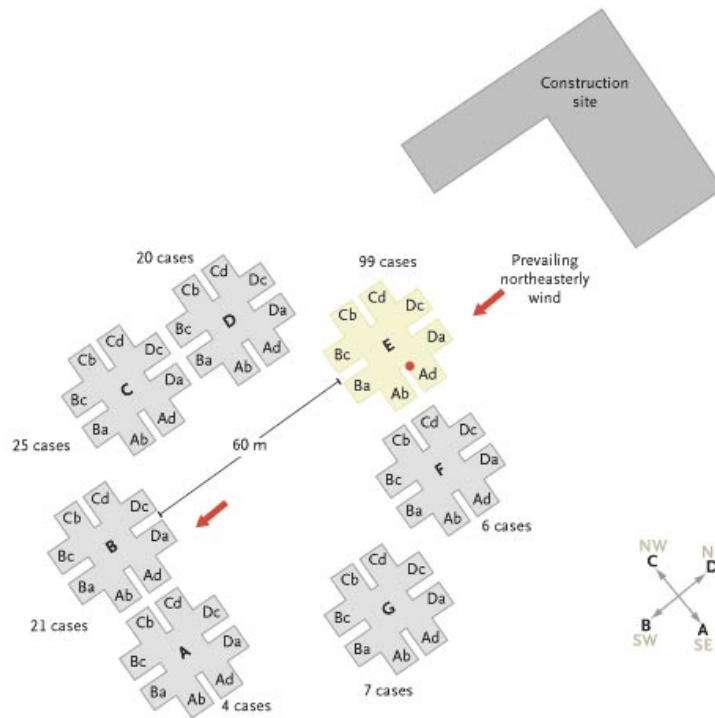


Figure 2-5. Plan view of Amoy Garden (Yu et al. 2004).

$k-\varepsilon$ model is another commonly used method for researchers to carry out their study on pedestrian-level wind environment. Tominaga et al. (2008) introduces guidelines that are proposed by the Working Group of the Architectural Institute of Japan (AIJ). These involves a lot of wind tunnel experiments, field measurements and computations by using high Reynolds number (Re) RANS models to investigate the influence of many types of computational conditions for various flow fields. Yoshie et al. (2007) discusses the influences of different simulation conditions based on CFD data, and the problems in CFD prediction of the pedestrian wind environment around the buildings and the present status as well. Yoshie et al. (2007) concluded that the accuracy of the weak wind regions behind the buildings is ungratified by CFD modelling. This might because RANS models are impossible to produce the vortex shedding. But for the strong wind region, the prediction accuracy was fairly high. For single building models, the CFD results were showed prediction accuracy was about 10% with experimental

data in the strong wind region. But simulated wind velocity was lower than the experimental one in the wake region. The reattachment length was longer in the computational analysis. For the urban block model, standard k- ϵ model showed a better accuracy than the modified k- ϵ model. Blocken et al. (2012) presented a general simulation and decision framework for the evaluation of pedestrian wind comfort and wind safety in urban areas by using CFD. One of the case studies is based on the campus of Eindhoven University of Technology. The 3D steady Reynolds-average Navier-Stokes equations with the realisable k- ϵ model on an extensive high-resolution grid based on grid-convergence analysis was solved to produce the turbulence wind flow pattern over the campus terrain. The simulation results have been compared with the long-term and short-term on-site measurements. The overall average deviation between simulated and measured wind speed is considered a good agreement. Part of the deviations is caused by the deficiencies of steady RANS modelling and by the large wind speed gradients at many of the measurement positions. He and Song (1999) introduced some practical examples of the CFD model applications to environmental wind evaluation. Mochida et al. (2008) examining pedestrian-level wind environment for reproducing the aerodynamics effects based on k- ϵ model. The numerical results had compared with the values from the field measurements. Hu and Yoshie (2013) evaluated the effects of building arrangements (including building coverage ratio, building array and building height variation) on average ventilation efficiency in newly-built residential areas at pedestrian-level by utilizing the standard k- ϵ model. A reference urban model was designed based on a typical residential area in Shanghai. A large spatially-averaged wind speed ratio and a low visitation frequency induced a low spatially-averaged normalized concentration were the relationship found.

LES is an intermediate form of turbulence calculations which tracks the behaviors of the larger eddies. The premise of LES is to simulate the large-scale turbulent motions and approximate the small-scale motions through modeling. The effects on the resolved flow (mean flow plus large eddies) due to the smallest, unresolved eddies are included by means of a so-called sub-grid scale model. The success of the LES stems from the fact that the main contribution to turbulent transport comes from the large-eddy motion. In the meantime, because small-scale turbulence is modeled, LES requires considerably less computational resources and time than DNS. The key to successfully predicting airflow by the LES is to accurately represent the unresolved sub-grid-scale (SGS) motion. As computing power increases, LES becomes widely used. Table 5 and 6 summarize applications of RANS and LES in airflows around an isolated building, around high-rise buildings and in building arrays. RANS and LES were both applied for evaluating the factors like stack height, pollutant exhaust velocity, city breathability, pollutant removal, pedestrian ventilation, pollutant dilution, buoyancy effects, uneven building arrangements, etc. for both an obstacle and a building array under stable and unstable conditions. Various pollutant sources were located at ground level to the rooftop and from upstream to downstream of the building. Both turbulence models were compared to procure capability and identify advantages and disadvantages. Meanwhile, the numerical results from both models were compared with experimental measurements.

Table 2-5. RANS and LES simulations of pollutant dispersion around an obstacle/isolated building

Practical Concerns And Purposes	Turbulence models	Pollutant sources and flow conditions	Conclusion
<p>To quantify the fraction of the plume (Brzoska et al. 1997), to value the influence of stack height and pollutant exhaust velocity on the concentration distribution in neighbourhood of the emitting building (Lateb et al, 2011), urban air pollutant dispersion (Blocken et al. 2008; 5], to compare with wind tunnel results (Kang et al. 2008), to study city breathability and pollutant removal within urban-like geometries (Buccolieri & Sabatino, 2010) and to simulate the effect on the pedestrian ventilation and pollutant dilution with different building height, aspect ratios and street lengths under the high-rise square arrays (Hang et al. 2012).</p>	<p>Standard $k-\epsilon$ (Brzoska et al. 1997; Blocken et al. 2008; Kang et al. 2008; Buccolieri & Sabatino, 2010; Hang et al. 2012), strain/vorticity modified (Brzoska et al. 1997), realizable $k-\epsilon$ (Lateb et al, 2011) and RNG $k-\epsilon$ (Hang et al. 2012) turbulence models</p>	<p>Source released from a stack within a recirculation area behind a building Lakehal & Rodi, 1997; Brzoska et al. 1997), or from the stack (Li & Stathopoulos, 1997), rooftop (Brzoska et al. 1997; Li & Stathopoulos, 1997) and ground level (Li & Stathopoulos, 1997). Uniform Carbon Monoxide near the ground of the entire street due to vehicular motions was released from 0m to 2m at full scale (Hang et al. 2012).</p>	<p>Numerical results were satisfactory at the far downwind area but less satisfactory near the wall and in the wake (Li & Stathopoulos, 1997). Rooftop dispersions were reasonable, but vertical side was overvalued and lateral side was undervalued (Lateb et al, 2011). Better steep gradients were provided by finite element method than finite difference method especially when employing multi-node elements (Lakehal & Rodi, 1997). The leeward wall of the emitting building is optimum for fresh-air intake due to its lowest concentration for all stack heights and momentum ratios (Brzoska et al. 1997). Larger and stronger recirculation zones and the reversed flow within the domain for a very compact city. So larger pollutant and maximum local mean age of air was found within more compact cities (Buccolieri & Sabatino, 2010). Larger building height variations induce better pedestrian ventilation. Reducing aspect ratios or increasing street lengths may also enhance pollutant dilution for arrays with uniform heights (Hang et al. 2012).</p>
<p>To estimate the effects of buoyancy on the air flow and dispersion in the near-wake region (Olvera et al. 2008), Gao et al. (2008) studied the possibility of virus-laden aerosols transmission in high-rise residential buildings.</p>	<p>RNG $k-\epsilon$ turbulence model (Olvera et al. 2008; Gao et al. 2008)</p>	<p>Emitting a buoyant and four non-buoyant sources in the near-wake (Olvera et al. 2008); particle expiration droplet residues at a lower floor (Gao et al. 2008).</p>	<p>The size and shape of the cavity region, the flow and concentration were affected by plume buoyancy. But a greater fraction of plume could be captured with buoyant sources (Olvera et al. 2008). Roughly 7.5% of the exhaust air transported into the upper room on a windless day through open windows and the infection risks were estimated Gao et al. 2008).</p>

Table 2-5 (Continued)

Practical Concerns And Purposes	Turbulence models	Pollutant sources and flow conditions	Conclusion
To evaluate numerical method for reproducing controlled and non-controlled experiment of dispersion in the wake of a cube by comparing the results from wind tunnel [73].	Realizable $k - \varepsilon$ turbulence model [73]	Rooftop source [73]	Numerical method overvalued the pollutant at the roof, undervalued along the roof center, at the leeward and in the wake and incorrectly simulated the upper half between two buildings, resulting in an insufficiently vertically elevated plume [73].
To evaluate the capability of Kato and Launder $k - \varepsilon$ models and RSM model by examining dispersion (Delaunary et al. 1997).	Kato & Launder $k - \varepsilon$, RSM model (Delaunary et al. 1997).	Sources were released from six chimneys (Delaunary et al. 1997).	The modified model could predict pollutant dispersions on the roof and faces of the rectangular building despite some deficiencies (Delaunary et al. 1997).
Studying the flow and dispersion around a cubic building (Sada & Sato, 2000; 2002; Calhoun et al, 2004; Tominaga & Stathopoulos, 2009; 2010), evaluate various $k - \varepsilon$ model (Tominaga & Stathopoulos, 2009), comparing LES, wind tunnel (Sada & Sato, 2000; Sada & Sato, 2002) and field data (Calhoun et al, 2004) for testing the accuracy, the discrepancy (Tominaga & Stathopoulos, 2010), and obtaining insight (Calhoun et al, 2004) of LES.	The standard, the RNG, Kato & Launder, the Realizable $k - \varepsilon$ model (Tominaga & Stathopoulos, 2009), LES (Sada & Sato, 2000; 2002; Calhoun et al, 2004; Tominaga & Stathopoulos, 2009; 2010), and puff method (Sada & Sato, 2000; 2002).	Source emitted from an elevated position and windward (Sada & Sato, 2000; 2002), upstream (Calhoun et al, 2004) and rooftop (Tominaga & Stathopoulos, 2009; 2010) of the building.	LES could give better insights for horizontal concentration diffusion and instantaneous concentration fluctuations (Calhoun et al, 2004; Tominaga & Stathopoulos, 2009). 25 times more computational resources, higher-resolution boundary and initial conditions should be given by field experiment for fully using LES (Tominaga & Stathopoulos, 2010). All the $k - \varepsilon$ models poorly predicted the concentration distribution of the side and leeward surfaces. The concentrations were less diffusive than those of the experiment (Tominaga & Stathopoulos, 2009).
To study pollutant dispersion on the near field region of three different building configurations indicating in Fig. 3 (Chavez et al. 2011).	Realizable $k - \varepsilon$ model with different Sc_t (Chavez et al. 2011)	Rooftop source (Chavez et al. 2011)	Variation of Sc_t is less influenced on assessing pollutant dispersion in the presence of adjacent buildings. But it impacted the pollutant transportation dramatically for the isolated building shape (Chavez et al. 2011).

Table 2-6. RANS and LES simulations of pollutant dispersion in building arrays

Practical Concerns and Investigation Purposes	Turbulence model	Pollutant sources and flow conditions	Conclusion
<p>Flow and pollutant from motor vehicles dispersion within an urban street canyon were studied (Chan et al. 2002; Kim & Baik, 2004; Chang & Meroney, 2003; Sagrado et al. 2002; Tsai & Chen, 2004; Meroney et al. 1999; Gromke et al. 2008), especially nitrogen oxides and hydrocarbons. Simulation and experimental results with different source strengths, wind speed and street canyon shapes were compared (Chan et al. 2002). The impacts of ambient wind direction on flow and pollutant dispersion (Kim & Baik, 2004) at height of upstream and downstream (Chang & Meroney, 2003) were studied. To present bluff body effect on flow and pollutant dispersions in an urban place with different street aspect ratios under open-country and urban atmospheric conditions (Chang & Meroney, 2003).</p>	<p>RNG (Chan et al. 2002; Kim & Baik, 2004; Sagrado et al. 2002), Realizable (Chan et al. 2002; Chang & Meroney, 2003), Standard $k-\epsilon$ turbulence model and RSM (Tsai & Chen, 2004; Meroney et al. 1999)</p>	<p>Continuous sources 0.15m above the ground (Kim & Baik, 2004) and in the middle (Chang & Meroney, 2003; Sagrado et al. 2002); west to east aligned traffic line sources (Sagrado et al. 2002) along the canyon (Meroney et al. 1999; Gromke et al. 2008)</p>	<p>The simulated results were generally similar to the experimental data (Chan et al. 2002; Kim & Baik, 2004; Chang & Meroney, 2003; Tsai & Chen, 2004). When street aspect ratio was 0.5, plume could be directed to the downwind. The flow field could be perturbed by individual buildings when W/H became over 5 (Chang & Meroney, 2003). Only 0.8% error was found between the realizable $k-\epsilon$ model and DNS simulation for pollution values. But RNG $k-\epsilon$ model was the optimum turbulence model coupled with this 2D street canyon (Chan et al. 2002). RSM models could provide more realistic results than other RANS models (Meroney et al. 1999; Gromke et al. 2008), but the concentrations on the leeward wall were over-predicted by more than one order of magnitude (Meroney et al. 1999).</p>
<p>To predict the concentrations on a cluster of buildings due to exhaust from the stack on the building roofs (Banks et al. 2003).</p>	<p>Standard $k-\epsilon$ turbulence model (Banks et al. 2003)</p>	<p>Release from a short stack on the buildings' roof (Banks et al. 2003).</p>	<p>CFD overestimated by 5 to 10 times by the peak concentration downstream of the stack compared with experimental results. But the predictions on the downstream ground level were quite accurate (Banks et al. 2003).</p>
<p>To evaluate the feasibility and capability of TWIST by examining wind environment and urban dispersion downtown Montreal region (Stathopoulos & Baskaran, 1996).</p>	<p>Standard $k-\epsilon$ turbulence model (Stathopoulos & Baskaran, 1996)</p>	<p>A line source in the middle (Stathopoulos & Baskaran, 1996)</p>	<p>Mean wind conditions agreed well for most locations between computed and experimental results. Modelling small scale, AND influence of fluctuating wind components, inputting specific topographical and building forms were still difficult (Stathopoulos & Baskaran, 1996).</p>

Table 2-6 (Continued)

Practical Concerns and Investigation Purposes	Turbulence model	Pollutant sources and flow conditions	Conclusion
To study flow and reactive pollutant dispersion a street canyon with various street-bottom heating intensity from incoming solar radiation (Lakehal & Rodi, 1997).	RANS with the re-normalization group $k-\varepsilon$ model (Lakehal & Rodi, 1997).	NO and NO ₂ emission from automobiles and background O ₃ (Lakehal & Rodi, 1997)	The street-bottom heating intensity impacts the flow patterns, the time series of the street canyon-averaged pollutant concentration and fluctuating pattern (Lakehal & Rodi, 1997).
To confirm the accuracy and discrepancy of LES (Tominaga & Stathopoulos, 2011) and other RANS models (Gromke et al, 2008) in modeling pollutant dispersion in a street canyon by comparison with wind tunnel (Tominaga & Stathopoulos, 2011; Gallagher et al, 2011).	Standard $k-\varepsilon$, RSM (Gromke et al, 2008), RNG (Meroney et al, 1999), LES model (Meroney et al, 1999; Gromke et al, 2008)	A point source (Meroney et al, 1999) and traffic line sources (Gromke et al, 2008) released at the centre of the street canyon	RSM performed better than standard $k-\varepsilon$ model apart from the centerline of the walls (Gromke et al, 2008). LES can study the transient mixing process inside the street canyon (Gromke et al, 2008). It also could provide better results of the distribution of mean concentration and the horizontal diffusion of concentration than RANS model (Meroney et al, 1999). In general, numerical results agreed well with experimental data (Meroney et al, 1999; Gromke et al, 2008).
To establish the effectiveness of parked cars in urban street canyons as passive controls on pedestrian personal pollutant exposure (Salim et al, 2011).	LES (Salim et al, 2011)	CO ₂ discharged at ground level with flow rate 1×10^{-5} kg/s (Salim et al, 2011).	Parallel parked cars provided the best air quality on footpath among three setups. Wind speed and direction did not improve the pollutant reduction much (Salim et al, 2011).
Xie and Castro (2009) studied the sensitivity to wind direction, inflow condition and source location in the intersection road in London.	LES (Xie & Castro, 2009)	A line source upstream of the major intersection (Xie & Castro, 2009)	Approximately full-scale resolution of one meter could predict the flow, mean dispersion and concentration fluctuations reasonably (Xie & Castro, 2009).
To propose a practicable, simplified uneven street canyon model and to evaluate effects of uneven building arrangement on air flow and pollutant dispersion in uniform and non-uniform street canyon in Fig. 6. (Zhang et al. 2011).	LES (Zhang et al. 2011)	A vehicle emission line source located at the centre of the canyon (Zhang et al. 2011).	The results presented that concentrations in the non-uniform street canyons are lower than those in the uniform one at the pedestrian level. So pollutant dispersions and human health in the urban area can be improved by uneven building layouts (Zhang et al. 2011).

Table 2-6 (Continued)

Practical Concerns and Investigation Purposes	Turbulence model	Pollutant sources and flow conditions	Conclusion
To predict the capability of LES for unsteady flows (Gu et al. 2011).	LES (Gu et al. 2011)	Vertical line sources placed within the urban canopy (Gu et al. 2011).	The simulated LES mean, lateral and vertical contaminants were similar to wind tunnel measurements (Gu et al. 2011).
Flow and urban air contaminant dispersion within an urban street canyon (Letzel et al, 2008; Walton et al, 2002; Walton & Cheng, 2002; Cai et al. 2008; Shi et al, 2008) and neighborhood scale (Cai et al. 2008) have been studied. Feasibility and reliability of LES for testing turbulent flow and dispersion inside a group of buildings (Shi et al, 2008); unsteady flows and alleviating discrepancies between CFD and wind tunnel methods were examined (Shi et al, 2008)	LES (Letzel et al, 2008; Walton et al, 2002; Walton & Cheng, 2002; Cai et al. 2008; Shi et al, 2008)	Intermittent source top of the middle part of (Letzel et al, 2008; Walton et al, 2002) and in front of (Cai et al. 2008) the street canyon; a line of constant rate along the street (Shi et al, 2008).	Due to the intrinsically unsteady and highly intermittent diffusion process of LES model (Shi et al, 2008), it could offer more accurate turbulent statistics of the flow than RANS model (Walton & Cheng, 2002; Cai et al. 2008), especially giving higher turbulence intensities, turbulence kinetic energy, better mixing and dispersion results (Cai et al. 2008).
Urban air dispersion and urban turbulence characteristics in a street canyon and neighborhood scale had been explored (Laatar et al. 2002).	The parallelized LES model PALM (Laatar et al. 2002)	Vertical line sources placed within the urban canopy (Laatar et al. 2002).	No underestimation of the intermittency of turbulent flow in quasi-2D geometries for the time-averaging process in LES or the RANS approach due to the steady canyon vortex. But some features may only be resolved at very high resolution even by using 3D LES (Laatar et al. 2002).
To study the influence of different sensible heat flux of a surface on a plume dispersion in an urban convective boundary layer (UCBL) (Cai, 2000).	LES (Cai, 2000)	Different points in the center of the built-up area (Cai, 2000).	Surface concentration was generally higher and the pollutant was less dispersed in the vertical direction, when the point source was located above the central line across the park areas (Cai, 2000).

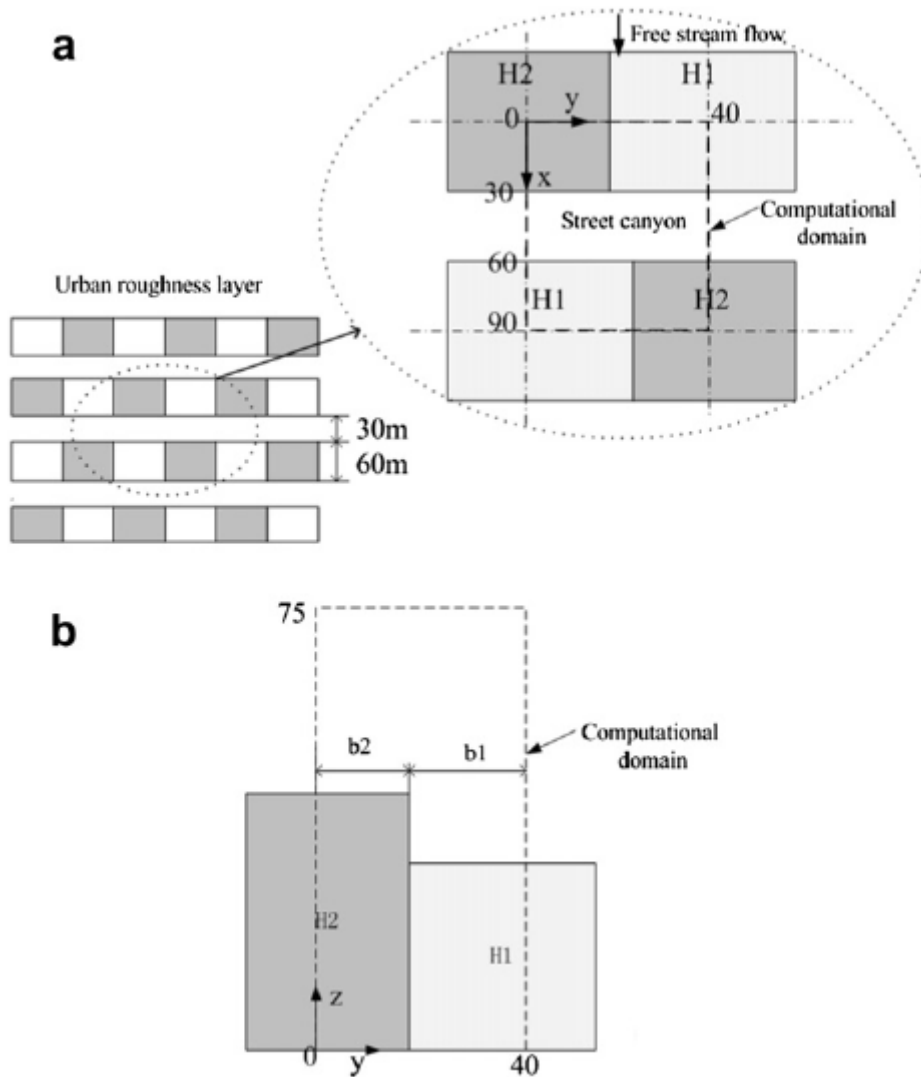


Figure 2-6. Layout of non-uniform street canyon, in top view (a) and side view (b).

The area depicted with dashed lines is the computational domain. Deep grey areas indicate the high buildings. H_1 and H_2 are the heights of the high building and low building, respectively. b_1 and b_2 are the lengths of the low and high buildings occupied in the computational domain, respectively (Zhang et al. 2011).

From the above reviews about airflow studies around isolated buildings, high-rise buildings and building arrays, it is not hard to discover that RANS and LES are the most commonly investigated models. When both the LES and turbulent transport models are available in CFD code, the latter can be very appealing for environment design (Rossi & Iaccarino) due to

significantly reduced computing time and increased simulating accuracy. RANS modeling might be inappropriate for some cases due to the averaging procedure used. The standard $k-\varepsilon$ model in general strongly depends on the Schmidt number (Sc_t), whose optimum value is case-dependent and a priori unknown (Gousseau et al. 2011). Johnson and Hunter (1998) found that a $k-\varepsilon$ model predicted larger concentration gradients in the wake region than those in wind tunnel experiments. Consequently, the $k-\varepsilon$ model underestimated turbulent diffusion and turbulence intensities in the wake. However, Gao et al. (2008) revealed that RNG $k-\varepsilon$ models were unable to examine the turbulent fluctuations and instantaneous air exchanges through openings, especially for wind-driven single-side natural ventilation. Meroney et al. (1999) also concluded that over-predicted surface concentrations downwind of the sources emitted in the vicinity of bluff bodies could be obtained from $k-\varepsilon$ models (since RANS $k-\varepsilon$ models cannot produce the intermittent nature of bluff-body flow). Tominaga et al. (2008) compared computational fluid dynamics (CFD) results using various revised $k-\varepsilon$ models and large eddy simulation (LES) applied to flow around a high-rise building model. The results showed that $k-\varepsilon$ model could not reproduce the reverse flow on the roof, which was corrected by revised $k-\varepsilon$ models. But modified $k-\varepsilon$ models overestimated the reattachment length behind the building, which could be improved by LES. It also revealed that -the LES with inflow turbulence showed generally good agreement with experimental results. The wind effects on a tall steel building was numerical evaluated by Huang et al. (2007) and illustrated it is necessary to correctly simulate both the incident wind velocity profile and turbulence intensity profile in CFD computations for successful predicting wind effects on tall buildings. Yoshie et al. (2011) observed that the RANS model overestimated the size of the recirculation zone and could not reproduce vortex shedding phenomena. Compared to experimental data, stronger reverse flow near the ground and the rising flow along the rear surface of the building were shown. LES without inflow turbulence also

overestimated the horseshoe vortex in front of the building and the recirculation zone, but underestimated the lateral gas dispersion. This could be significantly improved with LES with inflow turbulence. Gousseau et al. (2011) reported the results between the standard $k - \varepsilon$ simulations and wind tunnel measurements for southwest wind direction which agreed well but larger dispersions for west wind direction. Comparatively speaking, LES was better in both cases. Generally, LES produces higher exchanged fluxes compared to RANS (2011). A good agreement was also found between LES simulation and the wind tunnel measurement in respect of mean concentration, fluctuation intensity, peak concentration values, the windward length of a cavity region behind the building, the measured mean velocity and turbulent intensity (Aubrun & Leitl, 2004). Compared to the RANS standard $k - \varepsilon$ model, no additional parameter input is required to solve the dispersion equation for LES with dynamic Smagorinsky subgrid-scale model (Gousseau et al. 2011). Moonen et al. (2011) suggested that LES is capable of obtaining the counter-gradient mechanism that governs turbulent mass transfer for the pollutant sources emitted from a stack place in the wake of an isolated building, but only in the streamwise direction. Correct parameterization of the turbulent fluxes via Sc_t is required for providing a fairly accurate concentration field when the pollutant source is placed outside of detachment regions. In the case of discharge pollutant source on the rooftop vent, LES can give better accuracy as it considers the influence of the building on the dispersion process, particularly in separation regions on the roof and in the wake of the building. Unfortunately for this case, modification of Sc_t cannot compensate for deficiencies of the flow-field. Zhang et al. (2011) studied the induced effects of real-time boundary wind condition on air flow and pollutant dispersion inside and above an urban street canyon with LES. The measured time series of boundary wind conditions were used as input. The findings showed that the steady boundary wind condition underestimated the real-time air flow turbulence inside and above the street canyon.

Therefore, real-time boundary conditions can reproduce much better condition for pollutant dispersion. The effects of uneven building layout on air flow and pollutant dispersion were also simulated by LES (Zhang et al. 2011). Pollutant dispersions and human health in the urban area can be improved by uneven building layouts (Zhang et al. 2011). So et al. (2005) also revealed that flow regime and pollution pattern demarcations strongly depend on the canyon geometry and Reynolds number. In Salim et al.'s (2011) research, steady-state Reynolds-averaged Navier–Stokes (RANS) turbulence closure models, the standard k – ϵ and Reynolds Stress Model (RSM), and Large Eddy Simulation (LES) coupled with the advection–diffusion method for species transport were used for examining the pollutant dispersion within a street canyon of $W/H=1$. The results provided that RSM performed better than standard k – ϵ turbulent model except the centreline of the canyon walls. But LES could more accurately predict the concentration distribution due to its capability of capturing the unsteady and intermittent fluctuations of the flow field, even for the horizontal diffusion of concentration (Tominaga & Stathopoulos, 2011). Therefore, it could resolve the transient mixing process within the street canyon. This can be concluded as one of the major advantages of LES. LES also can generate detailed information on the turbulence structure. Conversely, without inflow turbulence, LES could produce too much vortex shedding behind the building, overestimating the pollutant fluctuation in the lateral direction in the wake region. Besides, owing to large computational resource demands of the LES technique, it is regarded mainly as a research tool rather than a practical way to engineering applications (Yakhot et al. 2006). However, with rapid advances of computing power, LES modeling will be a realistic option in the near future.

2.5 Discussions

Theoretically speaking, field measurements should be the most accurate method as it captures the real physical phenomena in nature, but using and interpreting this method could also be problematic due to the properties of the atmospheric boundary layer. Also the set-ups for these experiments are very time-consuming and expensive. Laboratory-scale physical modeling had the advantage of fully controllable upwind boundary conditions for airflow and building geometries to generate some statistically reproducible results. The flexibility of the set-up enables researchers to carry out some systematic and parametric studies but drawbacks are still exist. Firstly of all, physical-scale modeling is expensive to build, operate and maintain, and secondly, accuracy of physical-scaled modeling is another concern. Overestimation of pollutant levels along the centre region of the roof and leeward façade of the building has been found although improper model scaling may be the cause. This is because dynamic similarity requires ideal scaling for accurate results, but unsteady atmospheric conditions are difficult to simulate in wind tunnel experiments. Therefore, with few exceptions, wind tunnels simulate only neutral stability conditions. The effects of model scale are another concern for laboratory-scale physical simulation. Smaller Reynolds Number (Re) and more vortices were observed in the laboratory-scale environment than the real environment (Yang & Shao, 2008; Eliasson et al. 2006, Li et al. 2008). Therefore, laboratory-scale models may fail to simulate real wind flow and pollutant dispersion as the multi-vortices could confine pollutant dispersions (Zhang et al. 2011). In the street canyon, large vertical gradient concentrations could be produced by the multi-vortex (Li et al. 2008). As far as field measurements and CFD predictions are concerned, although on-site measurement could offer the exact dynamic conditions, the conditions are difficult to control and record. Although LES is capable of handling flow unsteadiness and intermittency of the flow, it still overestimates reattachment lengths behind the building. LES simulation times could also be

several time that of the RANS model. Theoretically, these problems can be solved using DNS but would require too fine a mesh and excessive computing capacity to simulate very small eddies. As a result, RANS models are currently the most prevalent and limitations accounted for during results analyses.

Generally speaking, the mean concentration and pollutant dispersion patterns have been widely investigated, especially under stable atmospheric conditions. In contrast, few relevant measurements and simulations have occurred with respect to concentration fluctuation, particularly for unsteady atmospheric conditions. Researchers had been involved into these areas (Coceal et al. 2007; Gousseau et al. 2012; Khalighi et al. 2001; Heschl et al. 2010), but in practice there is still a great need to predict complex phenomena like separation and reattachment, unsteady vortex shedding and bimodal behavior, high turbulence, large-scale turbulent structures as well as curved shear layers. This is mainly due to the heterogeneity of urban areas and the inherent complexity of turbulent flows, even for relatively simple geometries. Also concentration fluctuations in unsteady environments are particularly important for odorant, flammable or highly toxic gases as they are related to odour perception, combustion and acute health effects. Historically, numerous field measurements in different cities were conducted, but owing to a lack of basic understanding of turbulent flow characteristics over building clusters, data interpretation is often unclear. Due to the popularity of urban air quality research, increasingly more research regarding turbulent processes at the street level were conducted, but mainly on small spatial and time scales. Applications depending on flow dynamics such as pollutant dispersions may require much more detailed unsteady flow studies. Horizontal pollutant dispersion phenomena have been extensively tested for isolated buildings and building arrays, but the investigation of vertical pollutant dispersion of high-rise buildings and street canyon is still rare, especially for

buoyancy driven natural ventilation. Furthermore, practical solutions of how to avoid vertical and horizontal pollutant dispersion in high-rise building, building arrays and street canyons are not yet readily available and required further studied.

In terms of pedestrian-level wind environment is concerned, most of the studied were conducted by either wind tunnel experiment or k- ϵ model for a row of buildings or building arrays. Although there are some works done by the on-site measurement, quantity of work is quite limited. The remaining pedestrian-level wind studies were focusing on the wind criteria and wind safety code analyzing. Willemsen and Wisse (2007) described a code for assessing wind comfort and wind danger in the built environment in the Netherlands. The code prescribed a software package to calculate the statistics of the reference wind speed at a height of 60m, which included the most up-to-date data from meteorological station the Netherlands. Wu and Kriksic (2012) presented an integrated approach towards different aspects of pedestrian outdoor comfort conditions. The methodologies for microclimate assessment and strategies for master planners and building designers to create wind and comfort conditions that are more responsive to the local climate had been described. This will encourage pedestrians to walk, bike or take public transit as opposed to driving personal vehicles. Koss (2006) compared different wind comfort criteria presently used at European wind engineering institutions. The differences and similarities were identified. Criteria based on hourly mean wind speed allowed for identifying relationships between different comfort approaches and was used to propose a more general formulation. But criteria using gust wind speeds were more complex in design and application. Stathopoulos (2006) outlined an approach towards the establishment of an overall comfort index taking into account, in addition to wind speed, the temperature and relative humidity in the area. But interestingly,

there is none of work has conducted any research on pedestrian-level wind environment or pollutant dispersion for buildings with any interesting feature.

2.6 Summary

This review shows that the airflow, pollutant dispersion and infection spread risks in an isolated building and building arrays have been studied by means of field measurements, physical scaled measurements and numerical simulations. This review also reveals the research had done on the pedestrian-level wind environment by utilizing the experimental or numerical methods. Studies show physical scale modeling can be more controllable in terms of stable airflow boundary conditions, but its accuracy is compromised due to limitations in simulating the real atmospheric boundary layer in terms of turbulence characteristics. The physical scale model on-site measurement, having similar problems as wind tunnel tests, can over-predict the pollutant concentrations along the roof center and at leeward façade.

Theoretically speaking, DNS can provide the most accurate results because of the consideration of small eddies, but due to its large computational requirements, it is impractical to use for airflow problems around buildings. The LES can solve the unsteadiness and intermittency of flow separation, but over-predicts the lateral pollutant concentration in the wake region of a building. The RANS models, being the most commonly used, currently shows obvious deficiencies in predicting the separation at a building roof and the wake flow at the leeward of a building.

Despite the practical concerns to be resolved, recent studies have revealed many phenomena about an isolated building or groups of buildings, horizontal contaminant dispersion and the effects on the horizontal neighborhood. Few have focused on the vertical contaminant dispersion, especially with high-rise buildings. Moreover, studies of strong upward air motion dominated by buoyancy effects due to solar radiation under low wind conditions remains

scarce. Hence, combined buoyancy effects and wind forces should be considered. As this phenomenon would be difficult to investigate in wind tunnel tests, the increasing computing power favors LES models which are perceived to play a greater role in the future.

In terms of pedestrian-level wind environment is concerned, most of the works were focusing on the air flow or wind comfort criteria for some simple geometry. But very few studies had conducted a systematic research on air flow and pollutant dispersion for buildings with interesting features, such as lift-up design.

Chapter Three: Research Methodology

3.1 Introduction

The experimental and analytical methods used in this research to accomplish the goals outline in Chapter 1 are briefly and generally described in this chapter. The experimental component of this work was achieved through wind tunnel testing. The analytical components of this work consisted of applying statistical techniques to interpret experimental data; estimating and comparing wind velocity distribution and traffic pollutant dispersion at pedestrian level among different building configurations by using international codes, standards, and guide publications. It can be divided into two main categories. Firstly, aimed at those building configurations reported by Tsang et al. (2012) which provided the lowest wind speed, the wind velocity distribution and pollutant dispersion have both been researched at the pedestrian level for a singular building (SB), a row of buildings (RB) and a row of buildings with podium (PB). Next, a 3.5m lift-up design was added underneath each building configuration. The pedestrian wind distribution and pedestrian pollutant distribution for each configuration was studied whether any benefits were available for using the lift-up design.

In this chapter, a number of issues have been described.

- 1) Fundamental information involving modelling requirements are presented.
- 2) The wind tunnel facilities and the simulation of approaching wind used throughout this study.
- 3) The experimental details for this study are also provided, such as building sizes etc.
- 4) Introduction to the instrumentation for pedestrian-level wind environment simulations in wind tunnels, including calibration and characterizations techniques.

5) Instrumentation for pedestrian-level pollutant dispersion in wind tunnel studies and equipment setup.

6) Selection of suitable analysis methods for both wind speed and pollutant dispersion.

Detailed information is also presented.

3.2 Wind Tunnel Modelling Requirements

Wind tunnel modelling is a type of physical scale modelling method. The so-called physical scaled modelling is to reduce the geometrical scale of a given flow domain and model size; meanwhile the reference parameters such as flow velocity etc. can be adjusted to reproduce the full scale size flow correctly. In order to simulate accurately the dynamics of the flow in the physical model, similarity criteria are required for the non-dimensional coefficients between the physical model and the atmosphere. Cermak (1975) summarized all the requirements which are listed below.

- Undistorted scaling of geometry
- Equal Rossby Number

$$Ro = \frac{\text{Inertial forces}}{\text{Coriolis forces}} = \frac{V}{Lf} \quad (3.1)$$

Where,

V = Horizontal velocity scale;

L = Length scale;

f = Coriolis parameter.

The earth's rotation effects should be simulated for obtaining the Rossby Number.

- Equal Gross Richardson Number

$$R_i = \frac{g}{T_0} \frac{\left(\frac{\partial \theta}{\partial z}\right)}{\left(\frac{\partial V}{\partial z}\right)^2} \quad (3.2)$$

Where,

g = Gravitational acceleration;

T_0 = Reference temperature;

θ = Potential temperature.

The Richardson Number is a representation of buoyant forces and inertial forces.

- Equal Reynolds Number

$$Re = \frac{\text{Convective inertial forces}}{\text{Viscous forces}} = \frac{Vl}{\nu} \quad (3.3)$$

Where,

V = Characteristic velocity;

l = Length scale;

ν = Kinematic viscosity.

- Equal Prandtl Number

$$Pr = \frac{\text{Kinematic viscosity}}{\text{Thermal diffusivity}} = \frac{\nu}{\alpha} \quad (3.4)$$

This only involves the properties of the fluid.

- Equal Eckert Number

$$Ec = \frac{\text{Heat generated by friction}}{\text{Heat compression}} = \frac{v^2}{\Delta T C_p} \quad (3.5)$$

Where,

C_p = The constant-pressure specific heat of the flow;

ΔT = A characteristic temperature difference of the flow.

In reality, it is impossible to satisfy all the requirements simultaneously. Only the most significant aspects of each application should be chosen under the specific model conditions. Thus, parameters with low relevant importance can be. From the above similarity requirements summarized by Cermak (1975), the significances of each parameter will be discussed in the following paragraph.

A scaled model with all lengths equally scaled in three dimensions will meet geometric similarity. Therefore, accurate model making is particularly important to satisfy the geometric similarity requirement. With regards to the Rossby Number, it represents the ratio of acceleration to Coriolis acceleration due to the rotation of the earth. However, there is no rotation inside the wind tunnel, so the Rossby number is infinite. The rotation of the earth influences the upper layer of the atmosphere in nature. In this current research, the wind distribution and pollutant dispersion at the pedestrian level will be studied. Consequently, this number is negligible. The Richardson Number can also be relaxed as the presented experiments are conducted at room temperature, thus atmospheric stratification effects are negligible. Besides the target fluid in both the physical model and the prototype is air, so Prandtl number similarity is automatically matched in the experiment. Moreover, the velocities in these experiments are much smaller than the speed of sound and the flow is incompressible, so the Eckert number can be neglected.

Reynolds number (Re) is defined as the ratio of convective inertial forces to viscous forces. It is impossible to have strict Re equality. This is because scale reduction of 1:100 to 1:1000 can result in the model's Re to be two to three orders of magnitude smaller than those in the atmosphere. But flows around bluff bodies with sharp edges, such as buildings, are commonly insensitive to Reynolds number. Above a certain Re threshold a flow becomes turbulent and the gross structure of the turbulence becomes similar over a wide range of Re. Modelling of plumes interacting with structures and simulations for measurement locations in the middle to far wake region ($x > 1H$ downwind) may only require $Re = U_H H / \nu > 3,000$ if a truly turbulent exhaust plume exists (Meroney 2004). AWES Quality Assurance Manual suggested that a proper Re should base on the minimum building width and on the reference wind speed at the top of the model, of 5×10^4 , or above.

Therefore, the scaled model flow in the current study will be dynamically similar to the full-scale case if the Re is larger than 5×10^4 . Similar geometry and the approaching wind profile should be matched in the wind tunnel and in prototype. The overall dimensions of the target building model should be as accurate within 2%. Extra care should be taken at edges as it governs separation and reattachment. Architectural details should be included if their full dimension is 1 metre or greater. The similarity flow-characteristics require the following flow features:

- Distribution of mean and turbulent velocities
- A zero longitudinal pressure gradient
- Distribution of mean and fluctuating temperature
- Equality of the ratio H_2/H_1 if the flow is layered

The last two criteria can be neglected as there is no buoyancy effect on the flow pattern and pollutant dispersion. A combination of turbulence generating spires, a barrier at the entrance of the wind tunnel, and roughness elements along the wind tunnel floor upstream of the model can help to achieve the targeted wind characteristics. The mean speed and turbulence intensity in the approaching wind should be obtained within 10% error of the target values. Adjusting the wind tunnel roof height to make the flow non-accelerating as it is in outdoor atmosphere will provide a zero longitudinal pressure gradient. Meanwhile, the blockage ratio is another important parameter to demonstrate the constraining effect of the wind tunnel wall that leads to flow patterns that are not truly representative of the prototype. It is defined as a ratio of the projected area of the near field simulation to the wind tunnel cross-section area. It should be less than 10% to minimize the significance of the blockage correction (AWES-QAM-1-2001). The height of the building models should not exceed half the wind tunnel height.

3.3 The CLP Power Wind/Wave Tunnel

The experiments were undertaken in the CLP Power Wind/Wave Tunnel (WWT) at The Hong Kong University of Science and Technology. Although in the real conditions, the flows and pollutant transport in the atmospheric boundary layer is rarely uniform in temperature, an isothermal wind tunnel is utilized here as it is very difficult to simulate the temperature differences inside the wind tunnel. The CLP Power Wind/Wave Tunnel Facility has a closed circuit subsonic boundary layer wind tunnel with two parallel test sections (high-speed and large cross-section) for civil/structural engineering and environmental engineering applications. The high-speed test section is 29.2m long, 3m wide and 2m high. The maximum free stream wind speed is approximately 28m/s. The low-speed section which has a larger cross-section is 40m long, 5m wide and 4m high. The maximum free stream wind speed is

approximately 10m/s. The wind tunnel can be converted from close circuit to open circuit by opening the purge doors in the return leg connecting the low and high-speed sections. This is to prevent pollutants accumulating in the tunnel during the pollutant dispersion experiments.

A plan view of the wind tunnel is given in **Figure 3-1**.

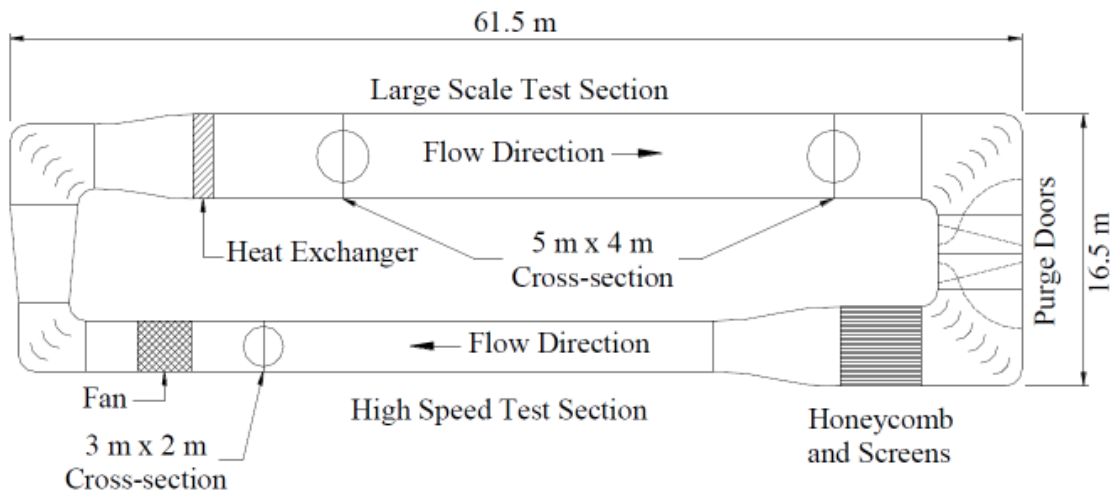


Figure 3-1. Plan view of WWTF

In the current research, the experiments were carried out in the high-speed test section which is operated by an integrated computer for adjusting fan speed and a number of roughness elements. The roughness elements are used to induce different categories of turbulent boundary layers.

3.4 Approaching Wind Profile

The velocity profile of the atmospheric boundary layer in the wind tunnel can be described by a logarithmic law or a power law function.

- Logarithmic Law Function

$$U(z)/U_H = \ln(z/H)1/\kappa \quad (3.6)$$

Where

κ = von Karman's constant (which is equal to 0.4).

- Power Law Function

$$U(z) = U(H) \left(\frac{z}{H}\right)^\alpha \quad (3.7)$$

Where

$U(z)$ = mean velocity at z level above the ground;

$U(H)$ = mean velocity at the height of the building model;

z = distance above the ground;

H = the model height;

α = the power law exponent.

A series of spires and roughness elements were placed at the entrance of the test section to create a fully developed turbulent boundary layer flow, which was used as the approaching flow. Therefore, in this study, a power law exponent of 0.2 was adopted for the approaching turbulent wind flow to simulate a suburban boundary condition which is in accordance with Terrain Category 2 stipulated in Australian/New Zealand Standard (2002). The wind profiles of these experiments are indicated in Figure 3-3. This was carried out in the high-speed section of wind tunnel where most of the pneumatically operated roughness elements are controlled by computers to form the turbulent boundary layer flow. The mean wind velocity profile was given by wind velocity ratio that is defined as U/U_r to satisfy the boundary conditions similarity criteria. It was normalized by the appropriate characteristic velocity U_r which is approximately 10m/s at 150m in prototype scale above ground and measured by a hotwire anemometer. The target and measured velocity (U) and turbulence intensity (TI)

profile were shown in Figure 3-4. The measured U and TI are within 5% difference of the design U and TI.



Figure 3-2. Wind tunnel setup for wind profile

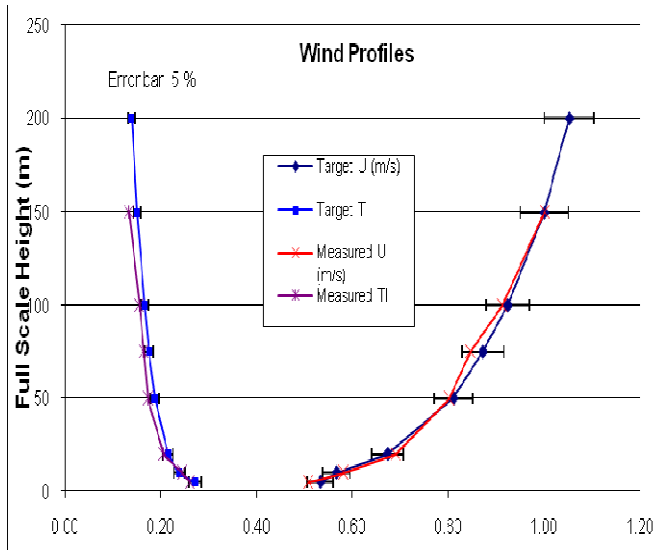


Figure 3-3. Profiles of mean wind speed and turbulence intensity

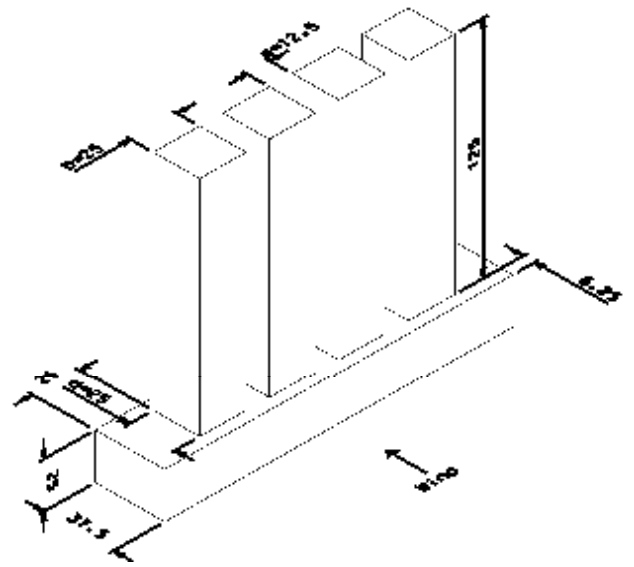


Figure 3-4. Isometric of podium building

Table 3-1. Dimensions of building setups

Building Type ¹	Building Height (h) (m)	Building Width(b) (m)	Building Depth(d) (m)	Spacing(s) (m)	Podium included	Lift-up height (h) (m)	Central Core Size (m)	Total height (m)
SB	50	75	25	N/A	N/A	N/A	N/A	50
Lifted_SB	50	75	25	N/A	N/A	3.5	8x8	53.5
RB	125	25	25	12.5	N/A	N/A	N	125
Lifted_RB	125	25	25	12.5	N/A	3.5	16x16	128.5
PB	125	25	25	12.5	187.5 (b) x37.5 (d)	N/A	N/A	150
Lifted_PB	125	25	25	12.5	187.5 (b) x37.5 (d)	3.5	16x16	153.5

¹ - SB: singular building; RB: a row of buildings; PB: a row of building with podium

Three different building configurations from Tsang et al's (2012) study were chosen for this study. The three building types were selected for producing the lowest wind speed areas. The prototype sizes of all building configurations were summarized in Table 3-1 and an isometric diagram of a podium building is shown in Figure 3-4, to illustrate the building configuration. The building models were constructed at a scale of 1 to 200. During this study, the test wind direction was normal to the building face and perpendicular to the row of buildings. For wind tunnel modelling of flow, a variety of scaling requirements between scale model and prototype should be satisfied to represent the prototype scale properly (Snyder, 1979, Cermak, 1975). Dimensional groups between prototype and model scale should be consisted. But fortunately, a number of dimensionless parameters can be neglected due to their low relative importance when simulating air flow around buildings, while Reynolds number (Re) independence is required in terms of the normalized Navier-Stokes equation. The Reynolds number (Re) is a measure of inertial forces to viscous force. When the Reynolds number is sufficiently large, air flow is effectively independent of Re , without considering thermal effects. Reynolds number is normally large when air flow over bluff bodies with sharp corners. AWES Quality Assurance Manual suggested that the minimum Reynolds number should be 5×10^4 based on the building width and reference wind speed at the top of the model. For this study, Re even for singular building configurations with and without lift-up is 8.2×10^4 , which is much higher than the threshold value AWES Quality Assurance Manual recommends. Which is unsurprising since the singular building is the smallest and shortest building among the three building configurations. Conversely, Re for a row of buildings and podium building with and without the lift-up design is far above the minimum threshold value AWES suggested. On the other hand, geometric scaling ratio (L) is another important parameter for simulating pedestrian-level wind when using a scaled down model. It is defined as ratios of model integral scale of longitudinal turbulence $(xLu)_m$ to prototype integral scale

of longitudinal turbulence $(xLu)_p$. L should be up to 3 without significantly affecting measurements (Surry 1982). Accuracy of building model is another additional important aspect, especially for the physical size, building surface details. Within 2% error is acceptable for the overall dimension of the target building model. Architectural details should be inclusive if the prototype dimension is one metre or above. Last but not least, the blockage ratio is significant for producing acceptable pedestrian level wind by using physical mode. The blockage ratio is the projected area of the building models to the wind tunnel cross-section area. Less than 10% is satisfied by all building configurations in the experiment to minimize the constraining effect of wind tunnel walls and the building height should not exceed half of the wind tunnel height. The tallest building configuration studied is the podium building with lift-up design. The building's height occupied only 38% of the wind tunnel height.

3.5 Measurement Instruments

3.5.1 Pressure measurements

For the pressure measurements, only the lower parts of the buildings have been investigated. As the lift-up height is only 3.5m in prototype, which is quite short compared to the overall height of the building. Therefore, the influence of lift-up design might not affect so obvious to the higher floors of the building. Consequently, in this research, how much change does the lift-up design bring to the lower part of the buildings has been investigated. As the lift-up height is only 3.5m, it is quite short compared to overall building height. Consequently, the lift-up might not have much influences on the higher part of the buildings. Therefore, 7 floors had been studied for the singular building with and without the lift-up design and podium building with and without the lift-up design, but only 6 floors had been studied for a row of buildings with and without the lift-up design.

In total, there were 273 pressure measurement points for singular building with and without the lift-up design. For a row of building with and without the lift-up design, there were 432 pressure measurement points. There were 371 pressure measurement points for podium building with and without the lift-up design.

In order to better demonstrate how these pressure measurement points are distributed on the building façade, pressure measurement points for singular building with and without the lift-up design have been given below in Figure 3-5 and Figure 3-6. The remaining plan and front views for other cases are given in Appendix 1.

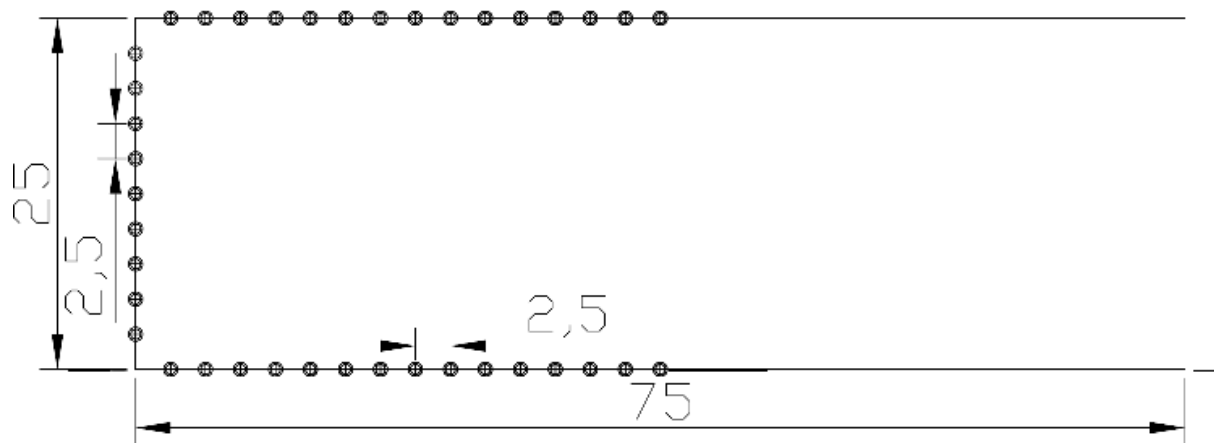


Figure 3-5: Plan view of pressure measurement of singular building

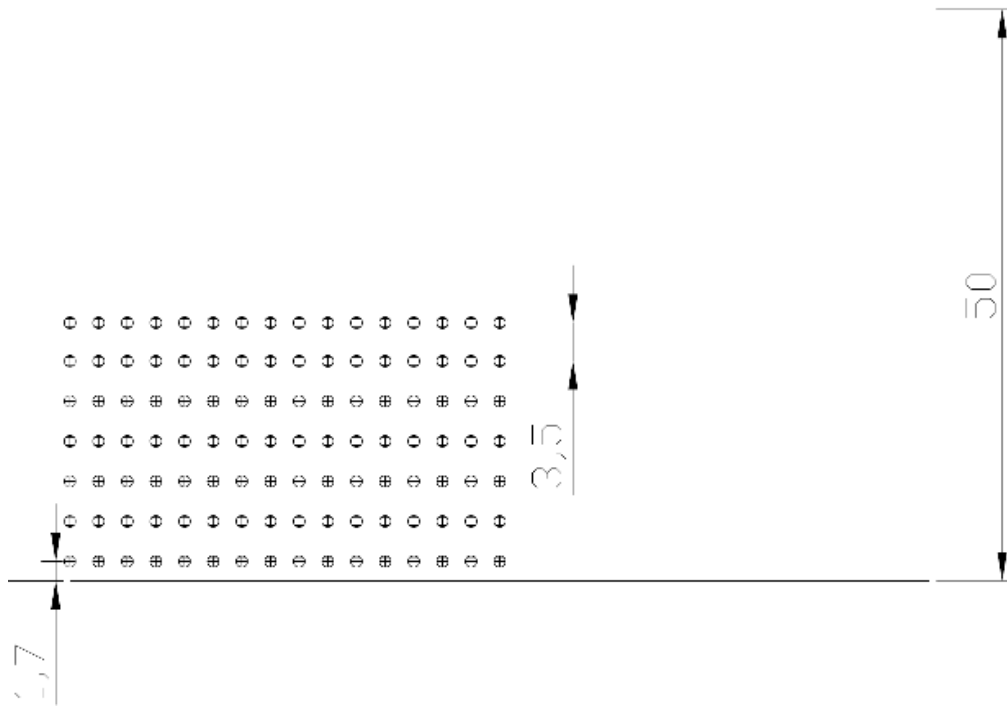


Figure 3-6. Front view of pressure measurement of singular building

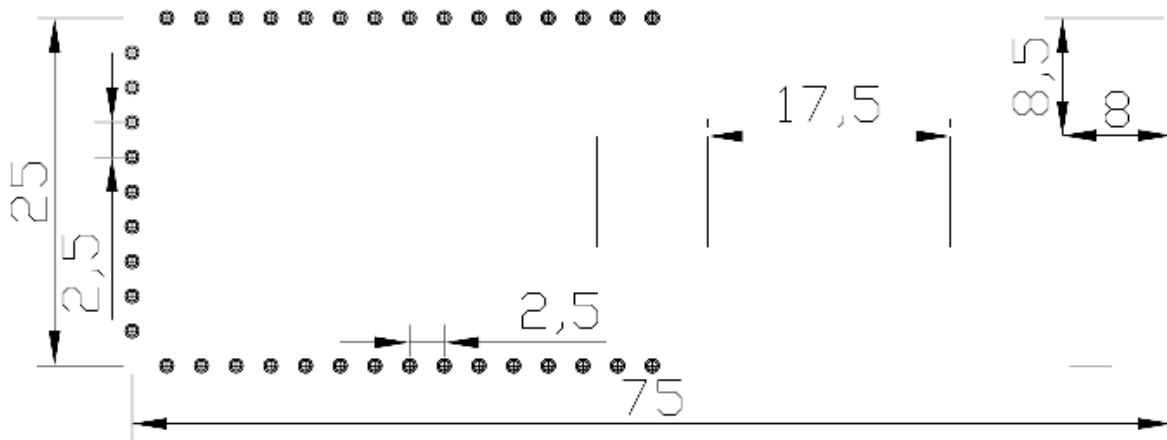


Figure 3-7. Plan view of pressure measurement of singular building with lift-up design

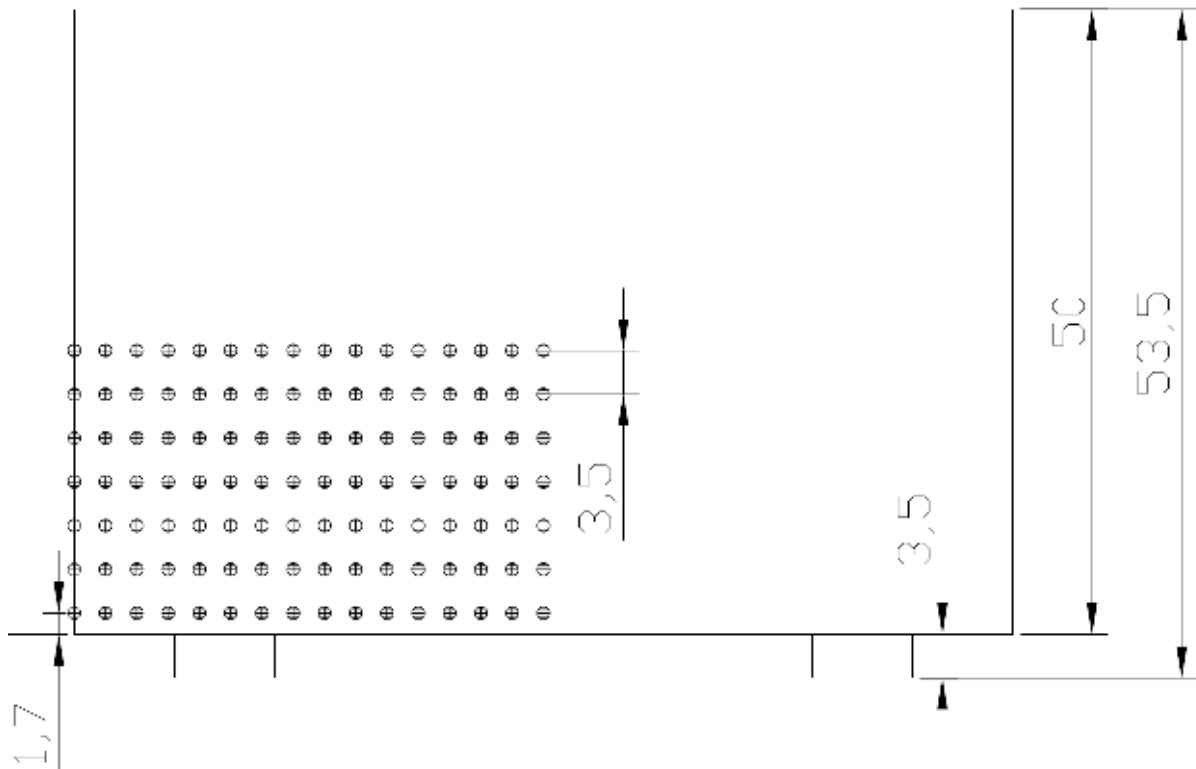


Figure 3-8. Front view of pressure measurement of singular building with lift-up

3.5.1.1 Pressure measurement system

The main control unit can manipulate and record the data sent from 32 Easterline miniature ESP-16HD electronic differential pressure transducers. Each transducer has 16 measurement channels that are connected to a common reference which is atmospheric pressure. Fluctuating pressure signals for each channel can be measured at a sampling frequency of up to 1200Hz. In total, the system can handle a maximum of 512 channels or 512 pressure holes.

3.5.2 Wind speed measurement

3.5.2.1 The Irwin Sensor

Over 200 Irwin Probes (Irwin, 1981) have been used for measuring pedestrian wind speeds in this experiment. All the sensors were installed at a height of 2m in full scale or 10mm in physical scale. The measurement area extends to 1.5d upstream, 2.5d laterally and 15d

downstream from the building (refer to Table 3-1 for definition of d). The sensor distributions for the singular building with and without lift-up design are given in Figure 3-9. The remaining sensor distributions for the other building configurations are given in Appendix 1. The spacing between sensors is 12.5m in prototype size when within 100m of the building. Where the distance is further than 100m, the spacing between sensors was 25m. By assuming the air flow is symmetrical about the building's centreline, measurement points are only required on one half of the buildings.

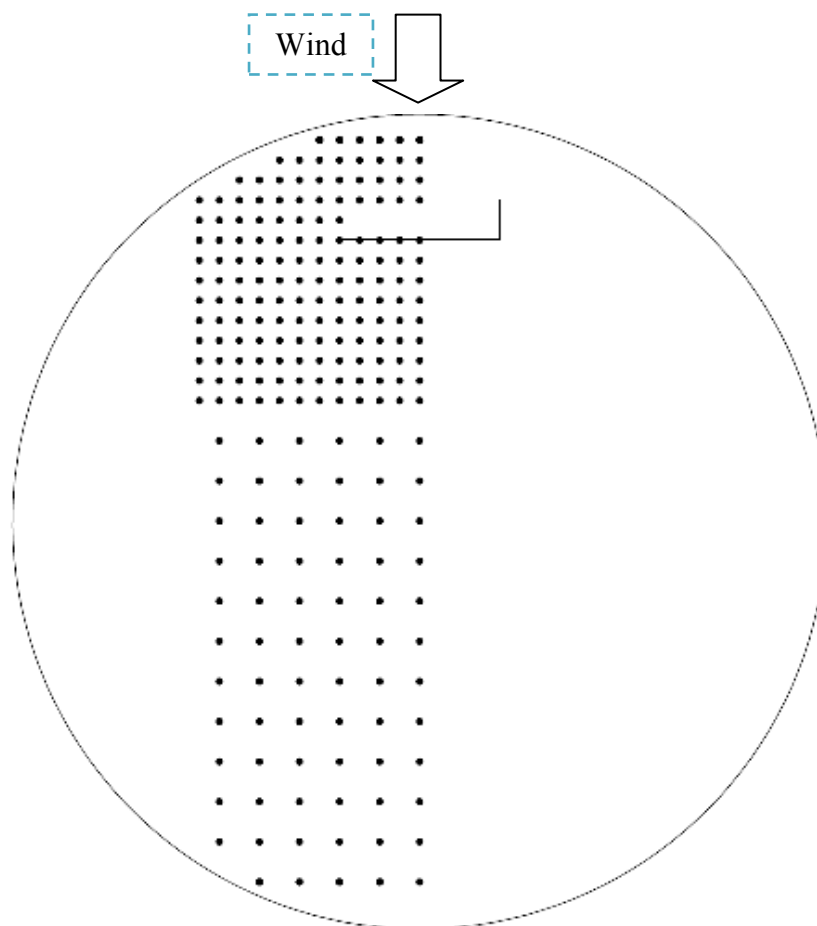


Figure 3-9. Irwin Probes Distribution for singular building with and without lift-up design

The Irwin probe for measuring wind speed at pedestrian level was first proposed by Irwin (1981) due to its simplicity and omni-directional pressure measurement. A number of wind tunnel studies (Wu and Stathopoulos, 1994, Soligo et al., 1998) conducted in the past have

found satisfaction in using this equipment for practical applications in wind tunnel environments. The benefit of using this sensor compared to hotwire anemometer and cobra probe is due to its tiny sizes so that a large number can be installed and data collected without affecting the wind flow significantly (Wu and Stathopoulos, 1994). This type of probe is axisymmetric about its vertical axis and consists of a sensor tube that protrudes above the model surface to a desired height and is mounted into the model surface as shown in **Figure 3-10**. The measured pressure difference between the sensor hole and the top of the sensor tube allows the wind speed at that height above the ground to be calculated. The modified Irwin probe used by Tsang et al. (2012) has been utilized for this investigation. The modified sensor has a protruding copper tube height of 10mm which is equivalent to 2m pedestrian height in the 1:200 scale building models. Irwin probes and the pressure transducer measurement system were connected by single lengths of PVC tubing at 650mm long.

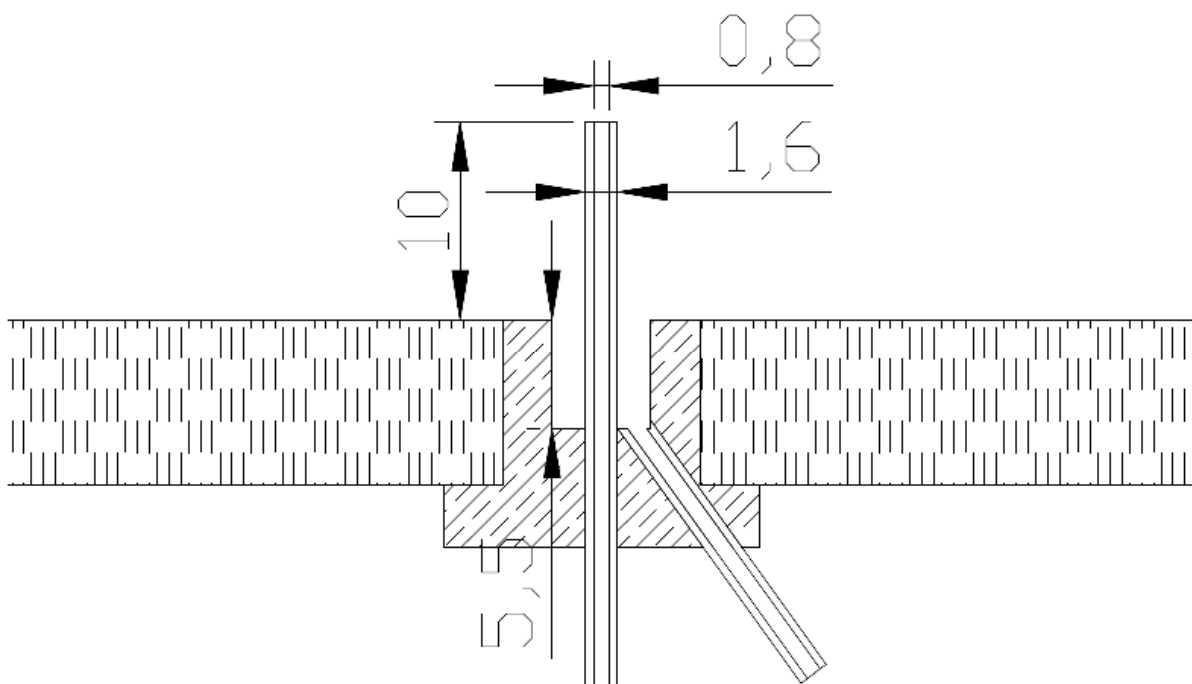


Figure 3-10. Dimensions of the designed Irwin Sensor (mm): $d = 1.6$, $d_i = 0.8$, $h = 10$, $D = 5$,

$$H = 5.5.$$

3.5.2.2 The Irwin Sensor Operation Theory

In a turbulent boundary layer, the wind speed profile very close to a flat surface should obey the universal law below. This law is applicable for the laminar sublayer and log-law region.

$$U = u_{\tau} f_1(u_{\tau} z / \nu) \quad (3.8)$$

Where

U = the wind speed;

u_{τ} = the skin friction velocity;

z = the distance from the surface;

ν = the kinematic viscosity air;

f_1 = a universal function.

With regards to the pressure distribution over each Irwin Sensor, it should also obey a universal law. The pressure difference Δp between two points of every Irwin Sensor should follow:

$$(\Delta p h^2) / (\rho \nu^2) = f_2(u_{\tau} h / \nu) \quad (3.9)$$

Where,

h = the sensor height;

ρ = the air density;

f_2 = a universal function.

The formula between wind speed and pressure difference at the sensor height can be derived equation (3.8) beneath by applying equation (3.6) and equation (3.7).

$$(\Delta p h^2)/(\rho v^2) = f_3(Uh/v) \quad (3.10)$$

Where,

f_3 = a universal function.

Based on all this theory, Irwin carried out numerous experiments on Irwin Sensors to acquire an empirical formula between the wind speed and pressure difference by deploying hotwire anemometer for wind speed measurement close to the Irwin Sensor.

$$U \frac{h}{v} = A + B \frac{h}{v} \sqrt{\frac{\Delta p}{\rho}} \quad (3.11)$$

Where,

U = the instantaneous wind speed at top of the sensor;

A, B = constants.

Equation (11) can be simplified as beneath form.

$$U = \alpha + \beta \sqrt{\Delta p} \quad (3.12)$$

Once sensor height, the sensor dimensions and surrounding conditions are fixed, constants α and β can be obtained by calibrating the sensor against a hotwire anemometer.

3.5.2.3 Pressure measurement system

From the previous section, it is already mentioned that the wind speed measurement by the Irwin Sensor is based on pressure measurements from the top and base points. Consequently, a pressure measurement system was used to record pressure signals in this experiment. The main control unit can manipulate and record the data sent from 32 Easterline miniature ESP-16HD electronic differential pressure transducers. Each transducer has 16 measurement

channels that are connected to a common reference which is atmospheric pressure. Fluctuating pressure signal for each channel can be measured at sampling frequency up to 1200Hz. Each Irwin Sensor demands two channels for measuring the pressure difference between the top and the base point. In total, the system can manage a maximum of 512 channels or 256 Irwin Sensors.

3.5.2.4 Correction of distortion effects caused by tubing system in fluctuation pressure

The Irwin probe's frequency response is controlled by both characteristics of the pressure transducer and the tubing connecting the pressure transducer and the probe. The recording capability of pressure transducer used for this investigation can reach up to 1000Hz sampling frequency. Pedestrian level wind environment studies are satisfactory with much lower frequencies for measurement. Consequently, only the tubing system should be considered for the tests. In the current research, a single length of tubing configuration was employed. However, one-section tubing system always induces distortion effects in fluctuating results. So distortion effects induced by one-section PVC tubing system for simultaneous pressure should be corrected.

In order to provide time history pressures, measuring the pressures via lengths of tubing connecting the pressure taps to a scanivalve that contains a pressure transducer is a common and economical practice. The pressure measurements at various locations can be obtained in sequence by this type of approach. But it introduces distortion of the pressure fluctuations which depends on the tube length and diameter of the scanivalve internal passageways and the transducer internal volume. Distortion can typically be minimised by either keeping the tube length and transducer internal volume as small as possible or to insert a restrictor in the tube to allow great lengths that can be utilized. However, in the current research work, a digital method of correcting fluctuating pressure distortion effect on both amplitude and

phase by using the inverse of the tubing system transfer function has been utilised. Simply recording the distorted signal and digitally correcting the signals of the distortion effects of the pressure measuring system are required for this method. Irwin et al. (1979) also examined the effectiveness of the application of the inversed transfer function (ITF) method of a given tubing system in practice. The advantages of this approach are that longer tube lengths and a higher frequency response can be achieved. The undistorted fluctuating pressure at the pressure tap $P_0(t)$ can be written as

$$P_0(t) = \sum_{n=-\infty}^{\infty} (A_n \exp(in\omega t)) \quad (3.13)$$

Where A_n are complex Fourier coefficients of the desired pressure $P_0(t)$ and $i = \sqrt{-1}$.

Similarly, the measured pressure $P_1(t)$ at the pressure transducer can be written as

$$P_1(t) = \sum_{n=-\infty}^{\infty} (B_n \exp(in\omega t)) \quad (3.14)$$

Where B_n are complex Fourier coefficients of the measured pressure $P_1(t)$.

$$T_n = B_n/A_n \quad (3.15)$$

Where T_n is the tubing system transfer function. Assuming the transfer function T_n is known and B_n can be obtained from Eqn. [3.14], therefore, A_n can be calculated from Eqn. [3.15]. Eventually, $P_0(t)$ can be computed from Eqn. [3.13]. This method is called Fast Fourier Transform techniques. It is feasible and can correct both the amplitude and the phase.

3.5.2.5 Wind Speed Calibration of Irwin Sensor

Wind speed calibration constants for Irwin Probe were calculated by comparing the wind speed reading between an Irwin Probe and a Hotwire anemometer. The anemometer is considered accurate for determining wind speed measurements higher than 3m/s. The Irwin probe that has been used in the studies is identical in size to those used for Tsang et al's (2012) research. The sensor height is 10mm for both studies. In order to ensure the Irwin

probe readings are analogous with Tsang et al's (2012) study, wind speed calibrations were carried out. In the calibration process, the wind environment was similar to Tsang et al's (2012) study. However Tsang et al's (2012) tests were accomplished almost 3 to 4 years ago. Therefore, some of the internal conditions for wind tunnel in the current study are not exactly the same as Tsang et al's (2012) experiment, even when the same 0.2 power law exponent of suburban boundary condition for the approaching turbulent wind flow was applied. The detailed boundary condition of this study is given in Section 3.4. Furthermore, the external atmospheric conditions might not be the same for these two experiments which could cause differences between the wind environments.

The calibrations were performed by installing a hotwire anemometer and an Irwin probe together inside the wind tunnel test section, at a same height of 10mm above the floor of the wind tunnel. Different wind speeds and turbulence intensities were given for drawing the relationship between pressure differences and wind speed. During this process, various wind speeds were generated by adjusting the fan from 1m/s to 4.5m/s with interval 0.5m/s; and turbulence intensities were created by setting a 300mm tall fence from 1m to 10m from the instrument at the upstream area. The reason of doing these is to produce the different wind environment. The constants derived from equation (1) are presented below:

$$\alpha = 0.01, \quad \beta = 1.82$$

The constants determined by Tsang et al. (2012) are $\alpha = 0.01$, $\beta = 1.66$ for the same design of the Irwin Sensors. The difference between the Tsang et al (2012)'s and current calibrations is approximately 8% which is an acceptable value. The calibration results are shown below in **Figure 3-11**.

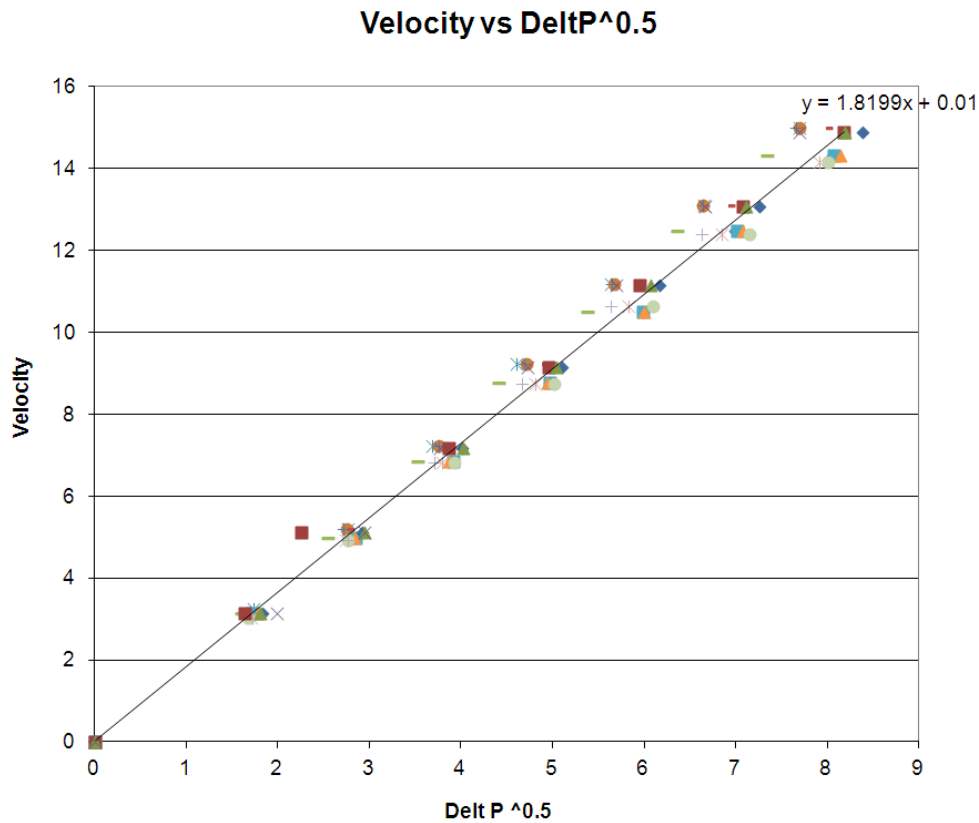


Figure 3-11. Wind speed vs $\sqrt{\Delta P}$ calibration of stochastic selections of Irwin Sensors

3.5.2.6 Mean wind speed distribution

The mean wind speeds at pedestrian level were normalized by the reference mean wind speed (\bar{U}_r) of the approach flow at $z = 150\text{m}$ in prototype scale. The normalized mean wind speeds range from 0.0 to 1.0. As the mean wind speed distribution was used to allocate the low wind speed areas for air ventilation proposes, threshold wind speed was set be around 1 to 2m/s, which corresponds to the minimum noticeable wind speed for human. Using Hong Kong as an example, the mean wind speed at 150m is approximately 5 to 6m/s for 50% probability of occurrence. Consequently, the minimum noticeable normalized mean wind speed (\bar{U}/\bar{U}_r) is about 0.3. As a result, areas with the \bar{U}/\bar{U}_r lower than 0.3, were defined as low wind speed zone. Correspondingly, the areas with \bar{U}/\bar{U}_r higher than 0.3, were considered to be reasonably well ventilated.

3.5.2.6 Gust wind speed distribution

The gust wind speeds at pedestrian level were normalized by the reference mean wind speed ($\overline{U_r}$) of the approach flow at $z = 150\text{m}$ in prototype scale. This was utilized to illustrate the discomfort areas caused by strong winds. So a threshold discomfort wind speed was set at 10m/s for a probability of exceedance of 5%. The corresponding $U_g/\overline{U_r}$ is approximately 0.8. Therefore, areas with $U_g/\overline{U_r}$ higher than 0.8, were defined as discomfort zones. Correspondingly, areas with $U_g/\overline{U_r}$ lower than 0.8, were considered to be reasonably comfortable for human activities. For simplicity and accuracy, the multiple extremes method was used to analysis the gust wind speed in this study. The sampling time is required to be more than 5 hours (full scale). The sample was divided evenly so that the divided samples can be regarded as multiple one-hour samples in repeated identical experiments. The gust wind speed was calculated by averaging the peaks from these one-hour samples.

3.5.3 Pollutant dispersion Measurements

For the traffic pollutant concentration wind tunnel experiment, SF₆ was used as the tracer gas. SF₆ is an inorganic, colourless, odourless, and non-flammable greenhouse gas. There are three experimental methods of releasing tracer gas:

- 1) Decay/growth,
- 2) Constant concentration
- 3) Constant injection (ASHRAE Handbook-Fundamentals, 2009).

The constant injection method, in which the tracer gas is released at a constant rate, was applied in the experiment. The mixture of 10% pure SF₆ and 90% compressed air gas were mixed together through the gas divider, and then constantly injected via the flow meter at 3LPM into the line source. The detailed line source design is provided in the next section.

3.5.3.1 Line Source Design and Locations

Line sources are usually designed for presenting the vehicle exhausts along a street (Meroney 1996). Since most vehicle exhausts are directed horizontally, vehicle exhaust is considered neutrally buoyant gas even for hot exhaust. The principles of the line source design are to reduce the vertical momentum and the deviation of concentration along the line source. Meanwhile, tracer gas emission from the line source should not be effected by the wind environment either, for instance, the wind direction and the wind speed.

Two types of line source design are available in practice. One type is drilling regularly spaced holds in the pipes or tubes (Kitabayashi et al. 1977; Builtjes, 1984). Kitabayashi et al. (1977) drilled 2mm holes spaced at an interval of 1cm on a 1m long and 1cm thick tube which is placed above the street. To eliminate vertical lofting momentum, the holes are placed facing downwards. Builtjes (1984) changed the hole diameter and spacing to 1.5mm and 1.5cm respectively. However, Meroney et al. (1996) proposed the source was laterally inhomogenous in the near field due to the over-large spacing between holes. The other type of line source design is relatively more popular, which utilises plenum chambers for gas distribution beneath drilled plates or sintered porous metal plate (Murphy & Davies, 1988). Murphy & Davies (1988) investigated three prototype line source designs intensively. There are two chambers for the first source prototype. The tracer was injected into the primary chamber, then gas is delivered to the second chamber or many compartments through the holes drilled between the chambers. For the third prototype, the second chamber was also divided into four sections but with three holes in each section. Foams or other porous media were applied to fill the plenum chamber to prevent expanding pressure loss across the exit (Murphy & Davie, 1988). But this method is unable to create a laterally homogeneous flow.

The homogenous concentration and pressure drop across the street is enlarged by using porous materials (Meroney et al. 1996).

Meroney et al (1996) found the key characteristic influencing the gas flow from the source is the pressure drop through the exhaust holes. Therefore, the line source design of Meroney et al's (1996) was employed 25-mm long hypodermic needles 0.25mm in diameter to achieve high discharge pressure drop and a plenum-type linear source design by Kitabayashi et al. (1974). Smaller changes were also made individually to optimise the design. Klein et al. (1999) applied the same principle of Meroney et al's (1997) line source design to their design. But Klein et al. (1999) modified their design for the line source to length $L_s = 1.42\text{m}$, 25-mm long outlet pipes 0.5mm in diameter. The distance between the pipes along the source was 5mm and the distance between the each inlet port along the source was 10-cm. Both Meroney et al's (1997) and Klein et al's (1999) design were applied with a shelter of 10mm wide and 2mm thick metal strips on top of the source outlets to laterally deflect the vertical momentum of large discharges. Therefore, potential flow disturbances could be minimized. The overall discharge rate was generally regulated by the wind tunnel airflow rate Q_a as the tracer gas flow rate Q_t from the line source was much smaller than the airflow rate Q_a .

The line source design adopted in this experiment was based on Meroney et al's (1996) design. Line sources of the length $L_s=780\text{mm}$ was equipped with 25mm long pipes with internal diameter 0.5mm. The distance between the pipes along the sources was 3mm. The pipes were integrated in a chamber. A mixture of air and tracer gas (SF6) was injecting through 16 inlet ports placed along the line source at 50mm spacings from each other. In order to avoid potential flow disturbances by relatively high gas discharge velocities at the pipe outlets, the source outlets were sheltered by 10mm wide and 2mm thick plastic strips that laterally deflected the vertical momentum of discharge. The distance between the outlets

and the stripes was 1mm. In this investigation, the tracer gas was injected through a flow meter at 3LPM into the line source first. Then it was released at 2.5mm model height above the tunnel ground level. The reason of choosing 2.5mm is because vehicle exhausts, specifically double-decker buses are approximately 0.5m in full scale. The dimensions of the chamber, the dimensions and distribution of tubing inside the chamber and the inlet ports, dimensions of the capping brass bar over the line source top have been illustrated clearly in Figure 3-12-- Figure 3-14.

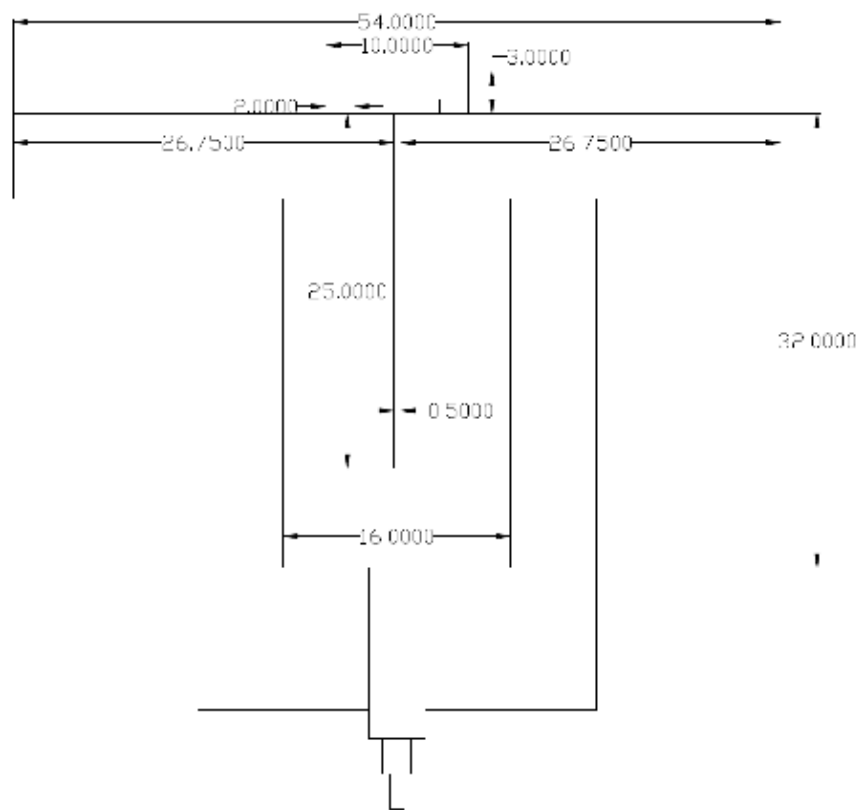


Figure 3-12. Cross section of individual trace gas injector

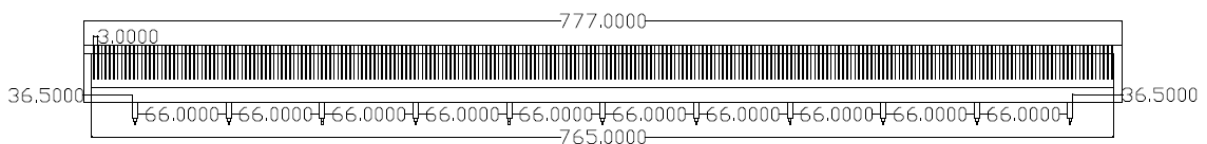


Figure 3-13. Cross section of 255 tubes along the line source

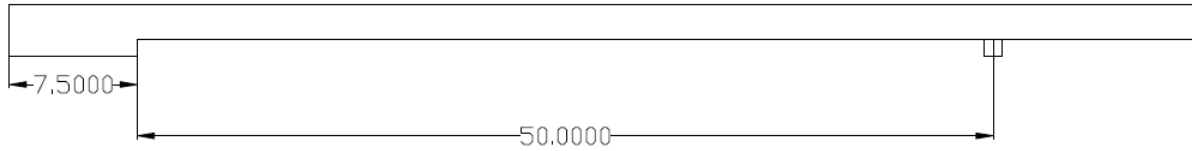


Figure 3-14. Capping brass bar design over the top of the line source

3.5.3.2 Measurement equipment

The INNOVA Air Tech Instrument 1312 Photoacoustic Multi-gas Monitors and the Multipoint Sampler and Doser Type 1303 were used for collecting and analysing the gas measurements. For mixing the SF₆ gas and compressed air, a gas divider was employed. The monitoring system relied on the photoacoustic infrared detection method and operated directly via a notebook where data were displayed and stored. An INNOVA Instruments Application Software Type 7620 was used to co-ordinate and to control all the sampling and monitoring function from a notebook PC. The air samples collected from the sampling points are delivered into the multipoint sampler 1303 via tubing. These air samples were delivered to the Multi-gas monitor 1312 for analysis. In total, there were 6 measurement points that can continuously collect the data in sequence, each point took approximately 60 seconds to collect and analyse the data. Therefore, the long sampling periods was one of main issues to be considered for pollutant dispersion measurement. The detailed measurement layout for pollutant measurement for each different building configuration is given in the next section.

3.5.3.3 Measurement layout

As described in the earlier section, due to the time constraints, the number of pollutant measurement for each case is limited. In total, there were 18 measurements for singular building with and without lift-up design, 21 measurements for a row of building with and without lift-up design and podium building with and without lift-up design. The line source was located upstream and downstream of the building respectively. Each measurement point

took approximately 60 seconds. In order to have a fully turbulent environment inside the wind tunnel, each measurement point was recorded at least 15 times. The reading from the analyser for each measurement point was compared. The difference between the 15 times reading and 20 times reading was within 5%. Consequently, 15 times reading was believed to be sufficient to show the concentration value for each measurement point is accurate. In order to illustrate how these measurement points are distributed, a plan view of pollutant measurement points for a singular building with and without the lift-up design when the line source was placed upstream and downstream of the building is given below. The remaining plan views for other cases are given in Appendix 1.

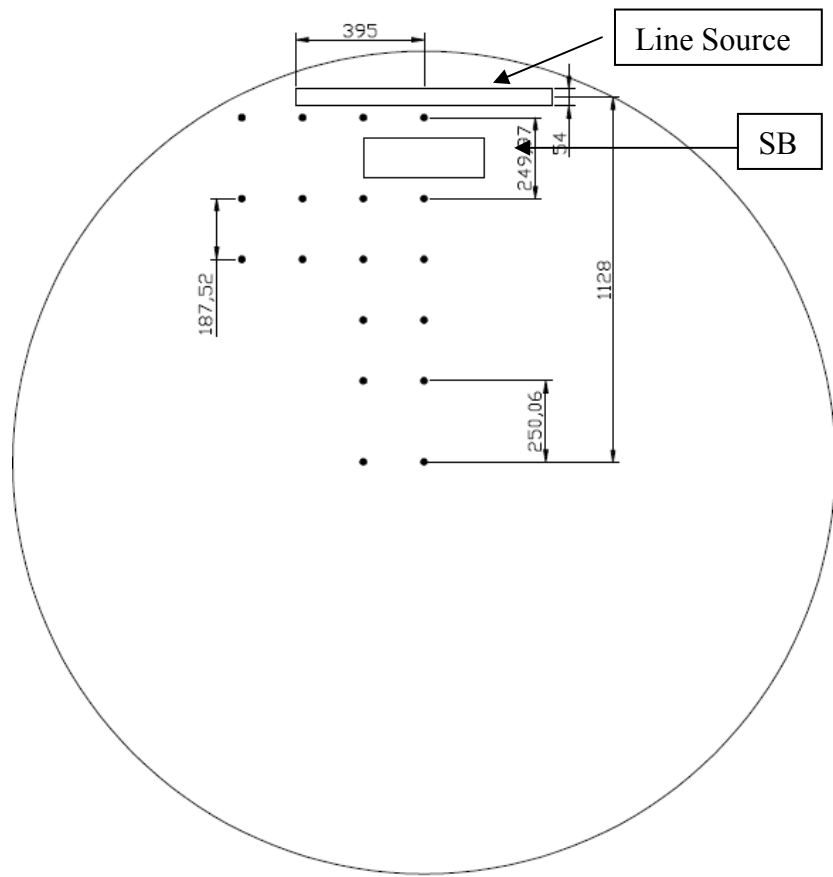


Figure 3-15. Pressure distribution for podium buildings with or without lift-up design when line source lined upstream

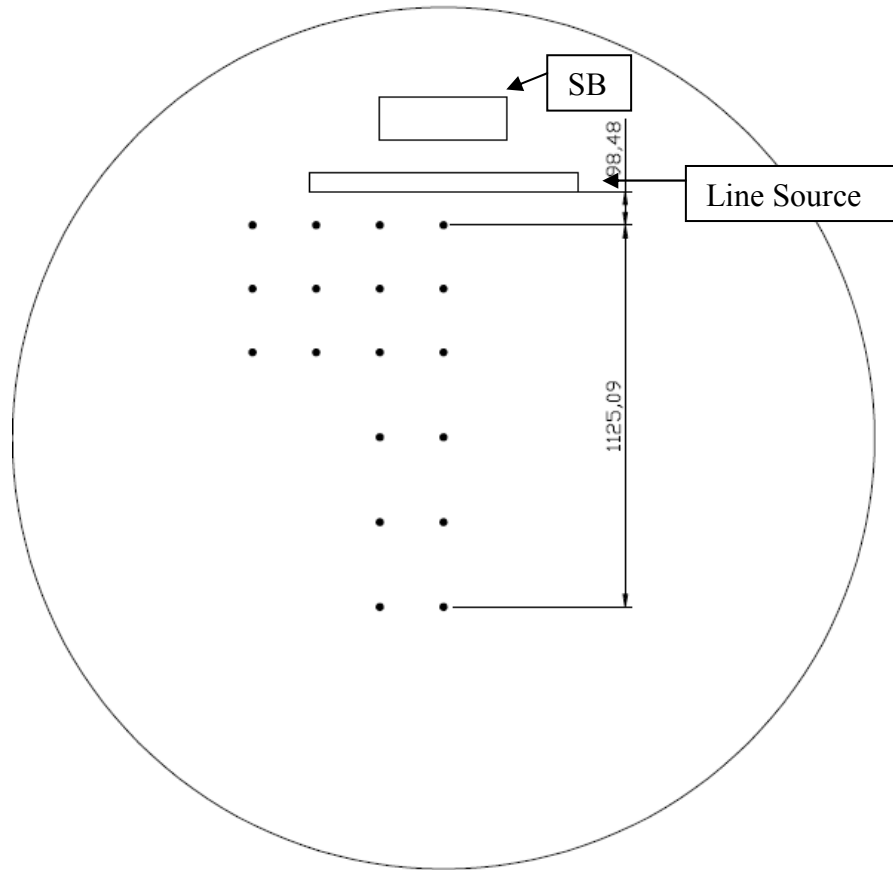


Figure 3-16. Pressure distribution for podium buildings with or without lift-up design when line source lined downstream

For these experiments, the concentration measurement for pollutant dispersion for singular building with and without the lift-up design took approximately 4.5 hours each excluding the time required for changing the measurement points. For the case with a row of building with and without the lift-up design, podium building with and without the lift-up design, the measurement periods required approximately 5.25 hours each.

The measured concentrations at different locations were scaled using the form of non-dimensional concentration K_c :

$$K_c = CU_H H^2 \quad (3.16)$$

, where C is the measured mean concentration (ppm), U_H is the mean wind speed (m/s) at building model height H (m) and Q is the volumetric flow rate of the tracer gas (ml/s). This scaling accounts fully for all aspects of plume dispersion at any scale, wind speed or source flow rate.

3.6 Summary

In this chapter, the methods that used to study pressure, flow and pollutant dispersion around singular building, a row of buildings and podium building (with and without lift-up design) have been presented. The fundamentals of these methods have been introduced. For this study, only the wind tunnel experiment method had been selected. The overall arrangement, measurement methods, measurement equipment and analysing methods are all described. The pressure, wind speed and pollutant concentration data will be discussed in detail in Chapters 4, 5 and 6 respectively.

Chapter Four: Effects of natural ventilation potential by using the lift-up design

4.1 Introduction

Building ventilation is used as a means for controlling indoor air quality by diluting internal air contaminants with cleaner outdoor air. Building ventilation is also used as a tool to provide the thermal comfort for the occupancies. This is typically achieved by either direct or indirect cooling systems. Direct cooling of building interiors and occupants functions by replacing or diluting warm indoor air with cool outdoor air to enhance the convective transport of heat and moisture. Indirect cooling involves pre-cooling the thermal mass of the building fabric or a thermal storage system with cool nighttime outdoor air. Natural ventilation is the most energy efficient solution for ventilating a building, with the potential to reduce the energy cost compared to air conditioning. Natural ventilation potential (NVP) is defined as the possibility of ensuring an acceptable indoor air quality through natural ventilation only. Passive cooling potential (PCP) can also be defined as the possibility of ensuring an acceptable indoor thermal comfort in summer solely by using natural ventilation. Indoor air quality, thermal comfort and energy savings are three key objectives of natural ventilation in buildings. A number of factors should be carefully considered to ascertain whether natural ventilation can be implemented to achieve the 'comfort' requirements. For instance, outdoor air quality, outdoor air temperature and moisture, outdoor noise, local noise, local winds or global winds, urban structure, indoor pollutant sources, indoor heat sources and stored heat, indoor air quality requirements, position and size of ventilation openings, indoor temperature, orientation of building, internal air-path distribution etc.

There are two main driving forces of natural ventilation; one is wind driven natural ventilation, the other is buoyancy driven natural ventilation. Wind driven natural ventilation is governed by exposure to wind and can be calculated as a function of wind pressure. Pressure coefficients of wind driven natural ventilation are determined either experimentally, in the wind tunnels, or numerically, using computational fluid dynamics software. The driving wind pressure can be determined by the difference between inlet and exhaust wind pressure coefficients and the kinetic energy content of the approach wind velocity. The driving force of buoyancy natural ventilation is stack pressure, or pressure due to buoyancy. It is induced by density differences between the indoor and outdoor air and the height difference from the stack exhaust and the floor-level inlet location. If the internal air temperature is higher than the external air temperature, the air enters through the lower openings and goes out through the upper ones. Therefore, an upward flow is generated in the absence of wind. On the contrary, a downward flow is produced when the internal air temperature is lower than the external air temperature. The airflow can also be predicted if both openings are of the same area and same discharge coefficient. In this study, wind pressure coefficients for the building surfaces have been measured in the wind tunnel experiments (Germano and Roulet, 2006). Consequently, the emphasis on this study is wind driven natural ventilation. In the past, numerous researchers have studied the natural ventilation on different types of buildings (Germano and Roulet, 2006; Orme, 1999; Yang et al., 2013; Faure and Demouge, 2013; Stavrakakis et al. 2008; Moonen et al., 2011; Yao et al., 2009). A large majority of the publications on natural ventilation deal with its behaviour within a singular building, like single and multi-zone models, possibly coupled with thermal models (Orme, 1999). Yang et al. (2013) examined the micro-scale effect of urban form and density (of buildings and/or greenery) on outdoor ventilation potential, using empirical data from an extensive field measurement for a selected ten high-rise residential sites in inner-city

Shanghai. Wind velocity rate could increase 7 to 8% with 10% sky view factor arising. A more strictly controlled experiment environment, ideally using a physical boundary wind tunnel is suggested for examining the effects of varying building densities. Faure and Demouge (2013) used a combined approach of OpenTurns software and a genetic algorithm to do sensitivity analyses between discharge coefficient and areas of internal door areas. A one-storey building has been used for this investigation. Stavrakakis et al. (2008) studied natural cross-ventilation experimentally and numerically for a test chamber with openings at non-symmetrical locations. It concludes natural cross-ventilation can provide well-mixed condition, leading to low temperature differences in the occupied zone and minimize local air draughts. However, no one has ever done any research on the influence of natural ventilation by utilizing lift-up design yet.

As discussed in previous chapters, there are three building configurations, each with and without the lift-up design have been investigated (Singular building, a row of buildings and podium building). The aims examined in this chapter are:

- 6) To study the ventilation potential of singular building, a row of buildings and podium building.
- 7) To investigate the ventilation potential of singular building, a row of buildings and podium building with lift-up design.
- 8) To determine whether lift-up design can improve cross ventilation or not.

4.2 Methodology

Surface pressures were measured simultaneously by pressure taps (0.5mm diameter), which were mounted on the model and connected to 16-channel electronic pressure scanners manufactured by Pressure System Inc. The main control unit can manipulate and record the data sent from 32 Easterline miniature ESP-16HD electronic differential pressure transducers.

Each transducer has 16 measurement channels that are connected to a common reference which is atmospheric pressure. Fluctuating pressure signals for each channel can be recorded at sampling frequencies up to 1200Hz. Both the tubes and the pressure scanners were concealed within the building model and connected to the data acquisition system under the wind tunnel floor. This arrangement ensures that the tubes and scanners do not interfere with the airflow in the wind tunnel. Equipment details and layouts for the pressure measurement points for different building configurations are given in Chapter 3.

4.3 Results and Discussions

4.3.1 Singular building with and without lift-up design

When planning the pressure measurement points, only half of the building was installed with pressure taps. Since the flow should be symmetric about the vertical centreline of the building. In order to facilitate the discussion later, each façade has been illustrated in **Figure 4-1**. The layout of the pressure measurement points have only been distributed at the lower floors of the building. The purpose of this is to investigate the variation of the pressure distribution of the lower floor levels and the improvement of the ventilation potential by implementing the lift-up design. For singular building with and without lift-up design, only 7 floors of the lower part have been investigated in this study.



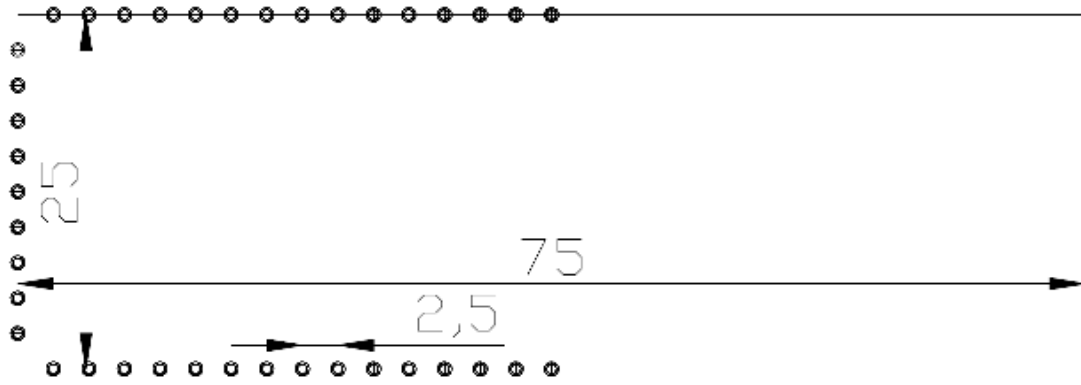
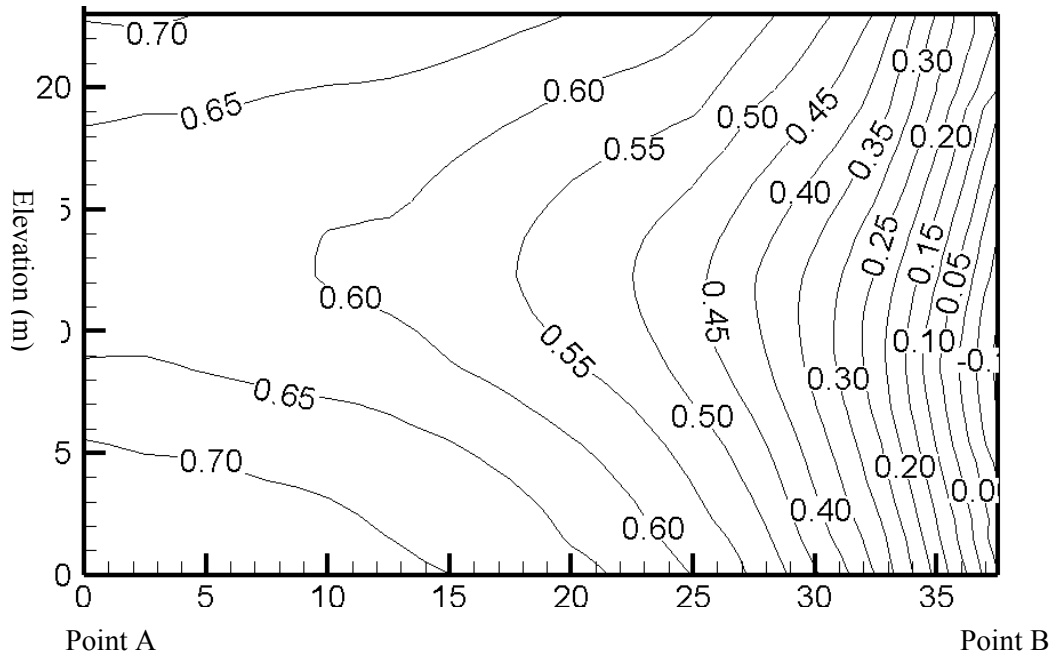
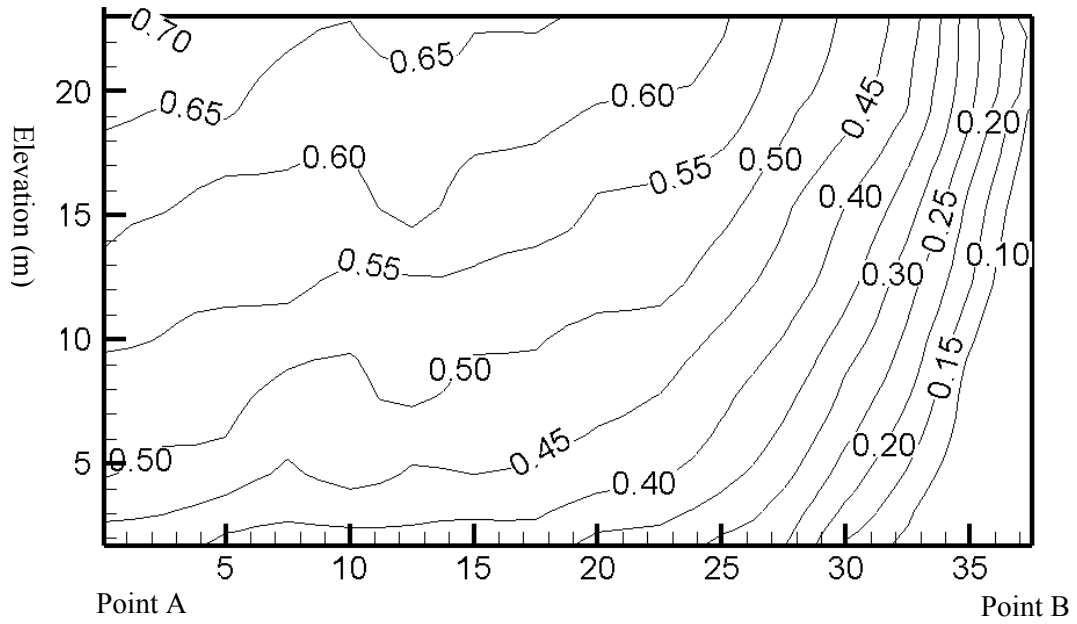


Figure 4-1. Plan of pressure measurement locations for singular building with and without lift-up design

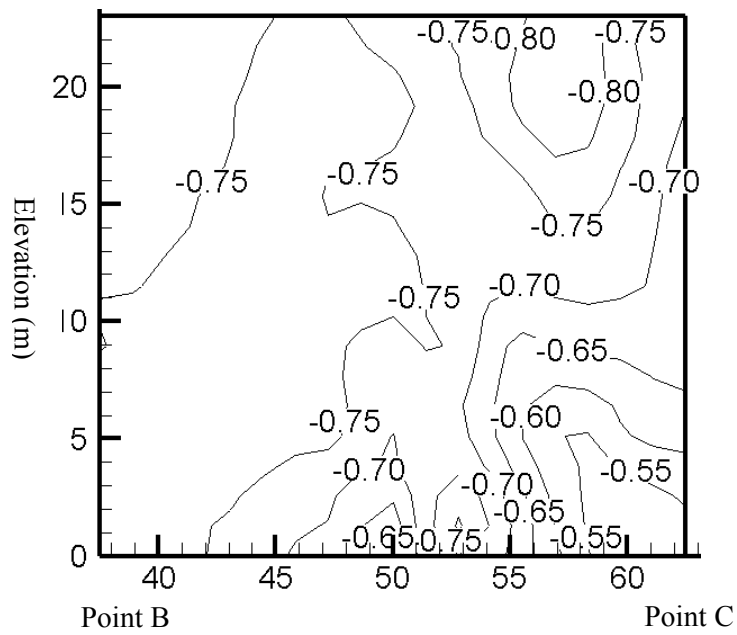


a) Façade A-B for singular building

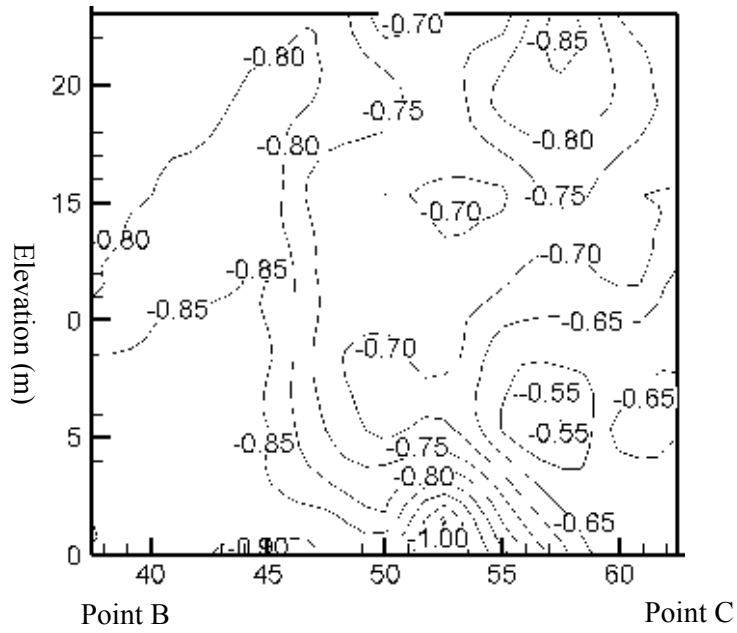


b) Façade A-B for singular building with lift-up design

Figure 4-2. Pressure contours diagram for facade A-B for singular building with and without lift-up design

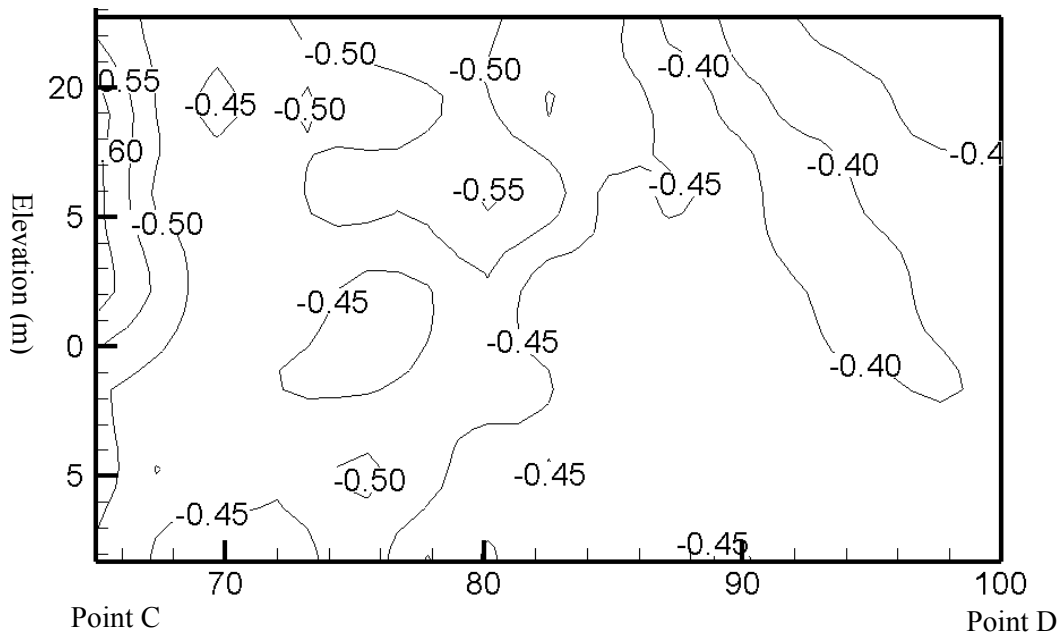


a) Façade B-C for singular building

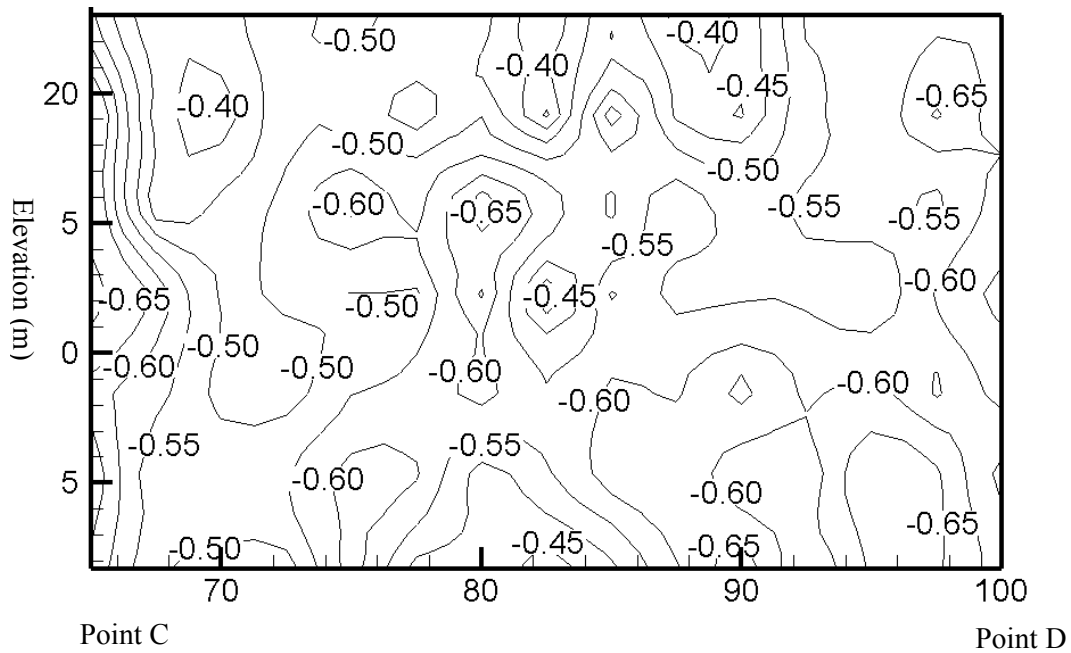


b) Façade B-C for singular building with lift-up design

Figure 4-3. Pressure contours diagram for facade B-C for singular building with and without lift-up design



a) Façade C-D for singular building



b) Façade C-D for singular building with lift-up design

Figure 4-4. Pressure contours diagram for facade C-D for singular building with and without lift-up design

When the approaching wind was normal to the façade A-B, only positive pressures were recorded for this façade. Conversely, only negative pressures occurred for façades B-C and C-D for singular building and singular building with lift-up design. This was due to the suction effect of the wind flow. Interestingly, with the lift-up design, the pressure distribution generally was much more varied for the façade B-C and façade C-D compared to the singular building without lift-up.

For façade A-B, pressure coefficients appeared to be positive for most of the areas of singular building and singular building lift-up design. The highest pressure coefficient for singular building and singular building lift-up design was 0.70, which occurred at the highest measured floor for both singular building and singular building lift-up design and also occurred at the lowest floor near point A for singular building. This implied the highest pressure coefficient was recorded at the centre of the windward façade of the singular building with and without

the lift-up design. In general, with the lift-up design for the singular building, the pressure coefficients were highest at the area near point A and progressively decreased towards point A, the corner of the building.

For façade B-C, the pressure coefficients variations have increased from -0.55 to -0.80 for the singular building, to a range of -0.55 to -1.00 when the lift-up design was applied. The negative pressures for façade B-C increased slightly for the lift-up design, particularly at the lower floors of the building. This indicates that the lift-up design has some influence on the pressure distribution for the side facades of singular building or a slab of building, which are more prominent on the lower floors for the side facades.

For façade C-D, the façade on the leeward side of the building, the negative pressures at corner point c remained relatively unchanged when compared to the lift-up design. When progressing along the façade towards point D – the centre of the leeward face, there is a general increase of negative pressures compared to the lift-up design. This is likely due to the stronger vortices and recirculation flow generated.

Natural Ventilation Potential

The natural ventilation potential is the possibility to ensure an acceptable indoor air quality by natural ventilation only. It hang on many conditions depending on the site (outdoor air quality, outdoor air temperature and moisture, outdoor noise, local winds or global wind and urban structure, etc.) or on the building (indoor pollutant sources, indoor heat sources and stored heat, indoor air quality requirements, position and size of ventilation openings, indoor temperature, orientation of building, internal air path distribution, etc). In the current study, the natural ventilation potential has been estimated by calculating the difference between the measurement point on the windward face and the corresponding point on the leeward face that is directly in line with the theoretical wind tunnel flow direction. For example, the

measurement point at A on third floor would correspond with point D also on third floor. The natural ventilation potential is interpreted from the pressure difference between the two. The greater the pressure difference, the greater the potential for natural ventilation.

The following discussion presents the findings of the results for each pair of pressure measurement points and at every measured floor. Point A and D at the centre of the building are represented by point 1 and point 15 is at the left hand end of the building, corresponding with points B and C.

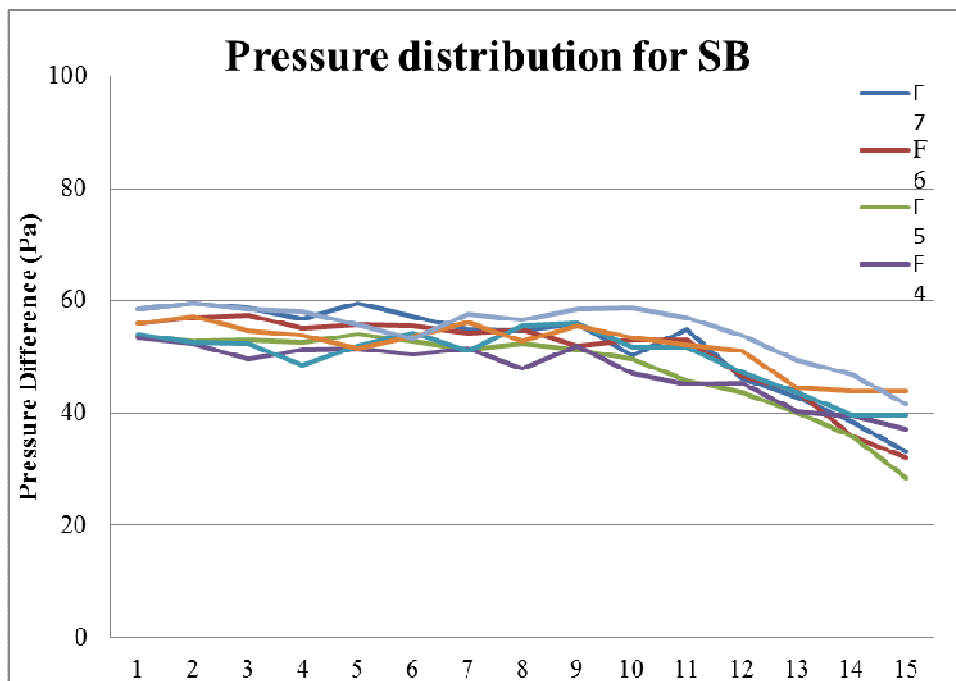


Figure 4-5. Pressure difference distribution for singular building for different floors

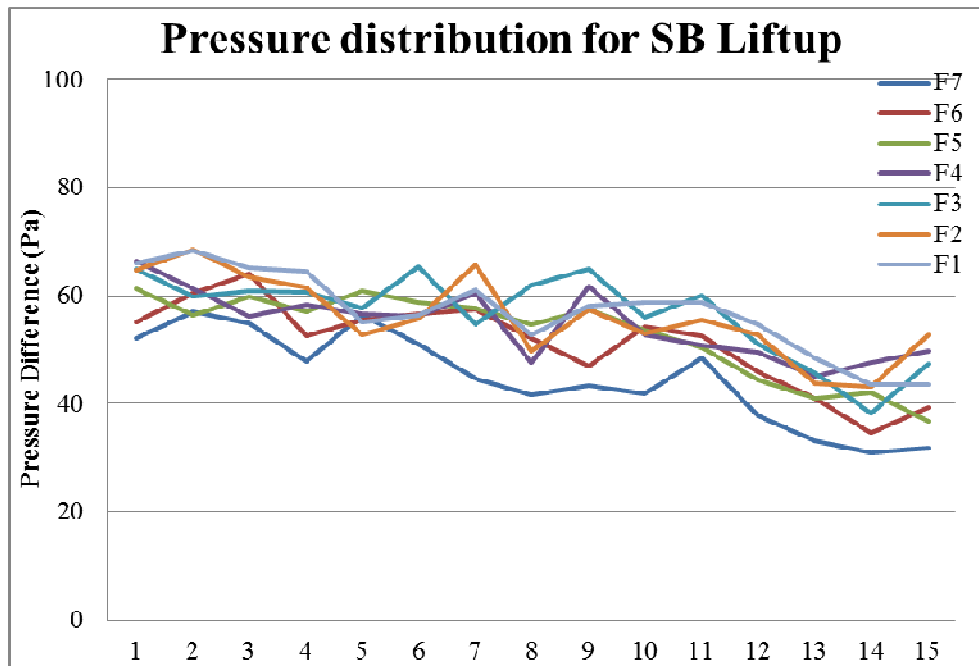
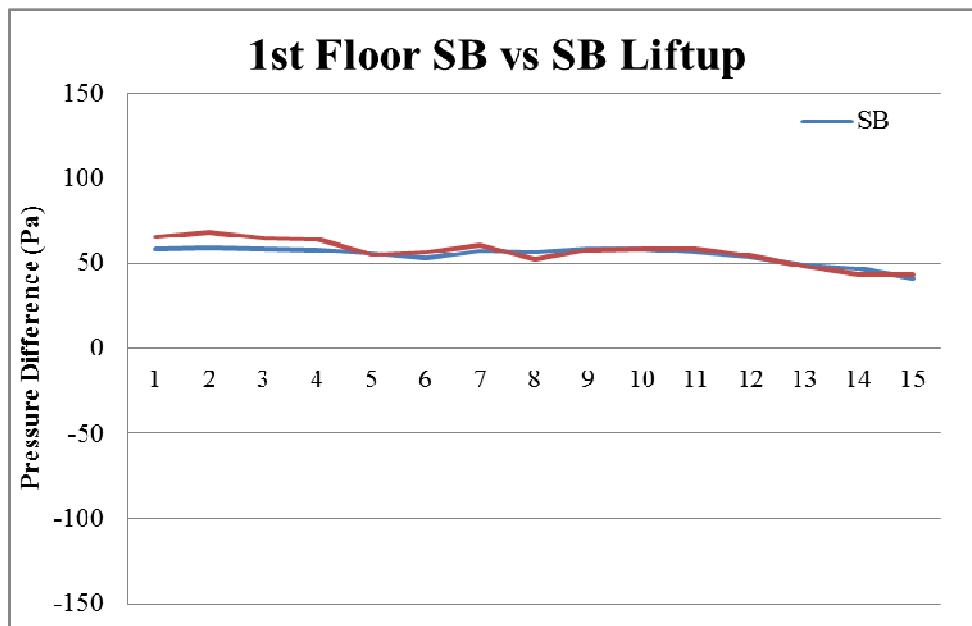


Figure 4-6. Pressure difference distribution for singular building with Lift-up Design for different floors

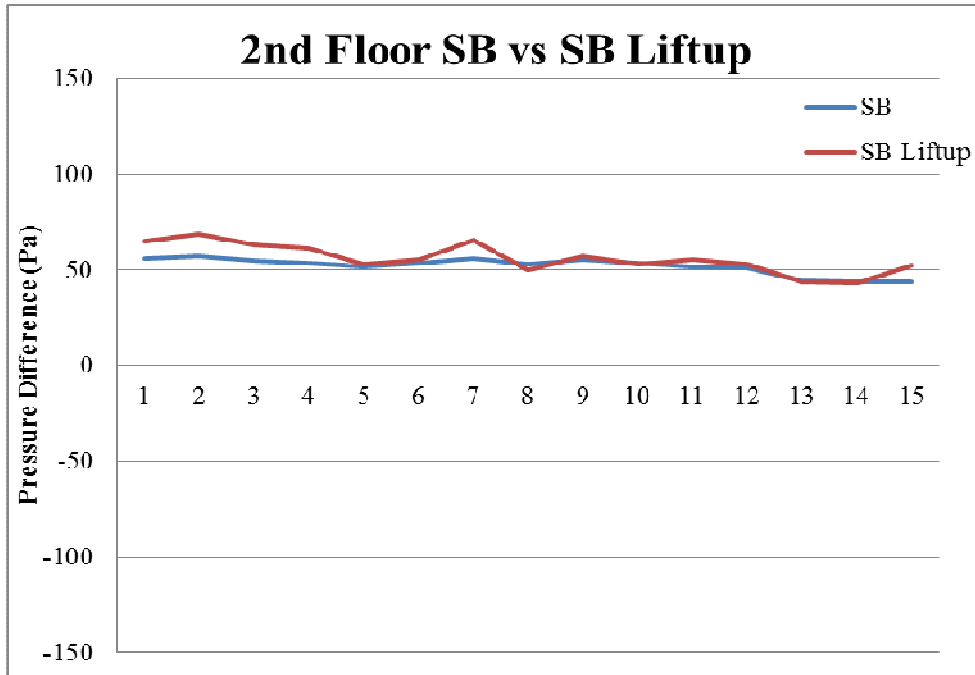
The pressure difference distributions for the SB are given in Figure 4-5 and pressure difference distribution for the SB with lift-up design was shown in Figure 4-6. In both cases, the largest pressure difference point occurs at the centre of the building which is at point 1; the lowest pressure difference point occurs at the corner of the building, point 15. Simply put, the greatest and least ventilation potential occurred at the centre and corner of the building respectively. On the lift-up design, the highest pressure difference point was found on the second floor, while the lowest pressure difference point was recorded on the fifth floor. Without the lift-up design, the highest pressure difference point was on the second floor, while the lowest pressure difference point was on the seventh floor.

In terms of the general trend for all the measurement points, the highest pressure differences for singular building were on the first floor. The second highest pressure differences were on the second floor. But interestingly, the smallest pressure differences occurred at floor four for singular building. With the lift-up design, seventh floor had the lowest pressure differences,

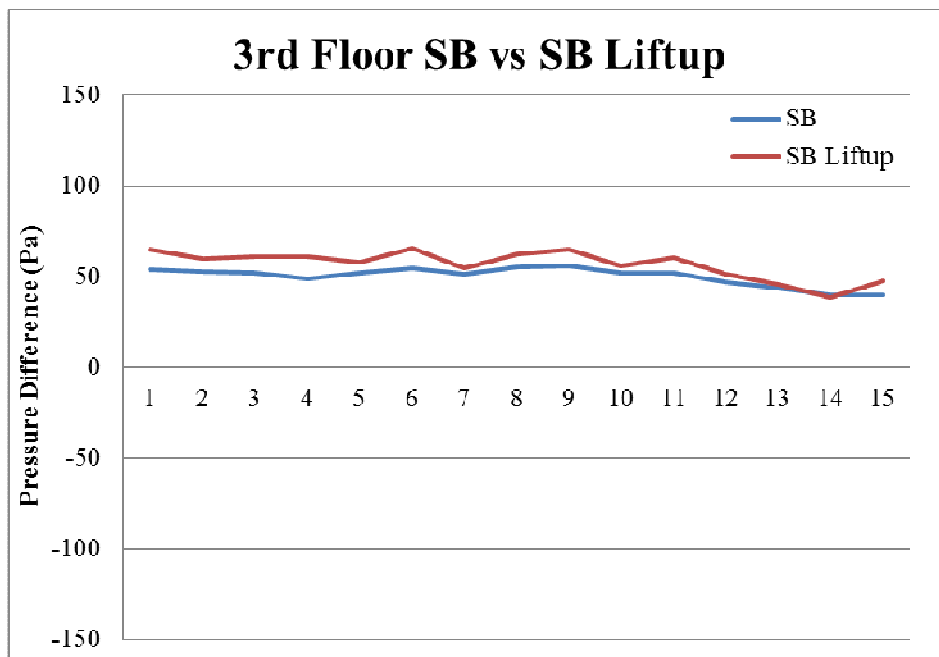
while third floor had the highest pressure differences. In the lift-up design, the air can flow through the lift-up zone, the positive pressures for the lower two floors reduce. Consequently, the highest pressure differences for all the measurement points switch from the first floor to the third floor when the lift-up design is implemented. In order to have a better understanding of how the lift-up design affects ventilation potential on the singular building, a direct comparison for different floors was conducted and presented below.



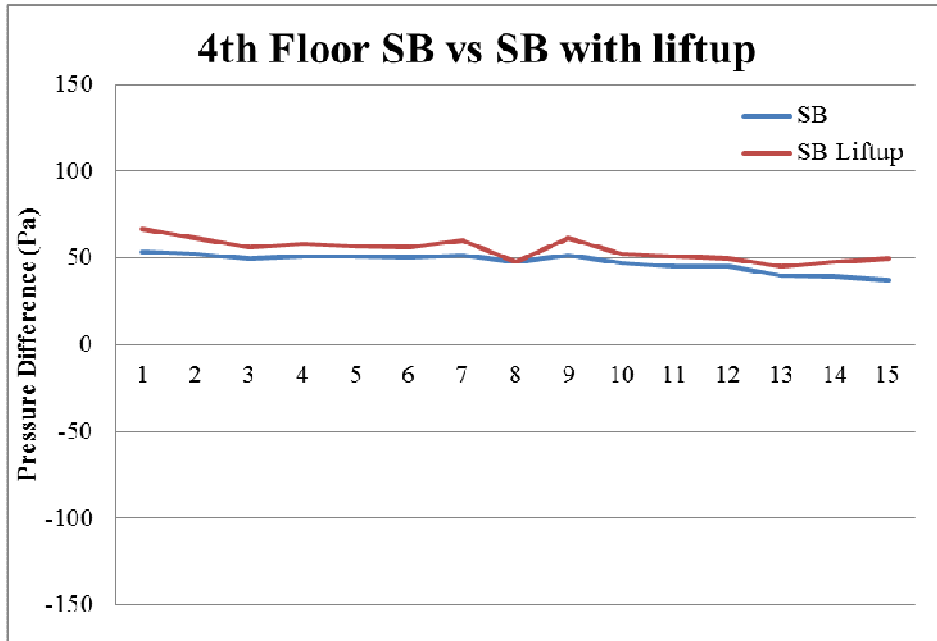
a) 1st Floor SB vs SB Lift-up Design



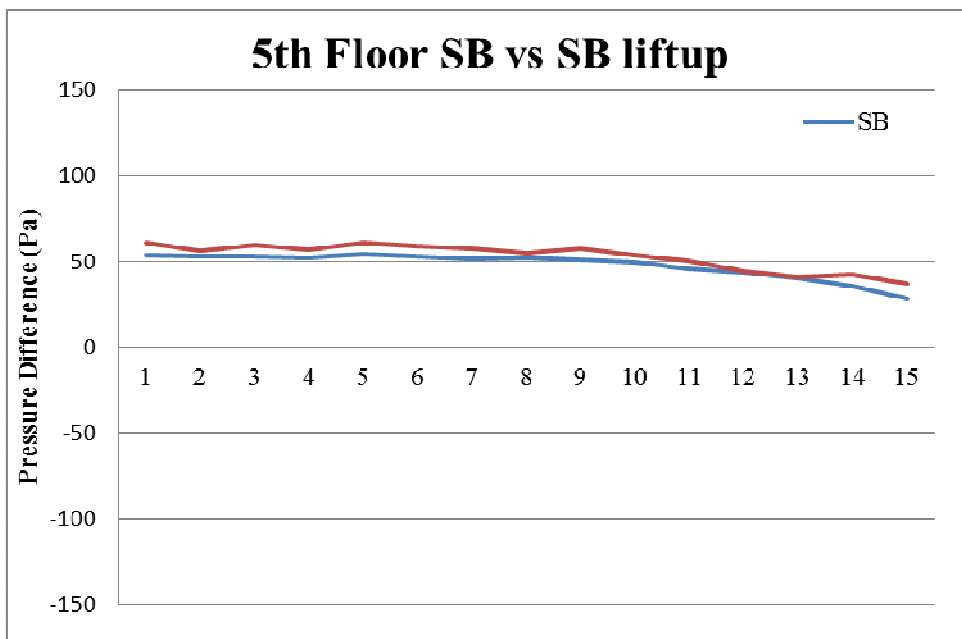
b) 2nd Floor SB vs SB Lift-up design



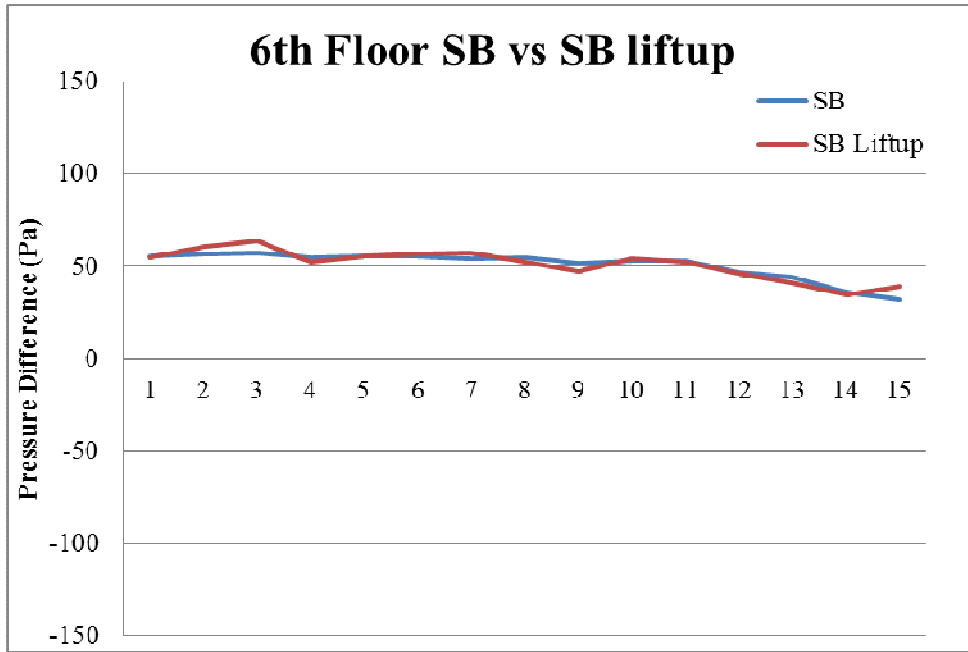
c) 3rd Floor SB vs SB Lift-up Design



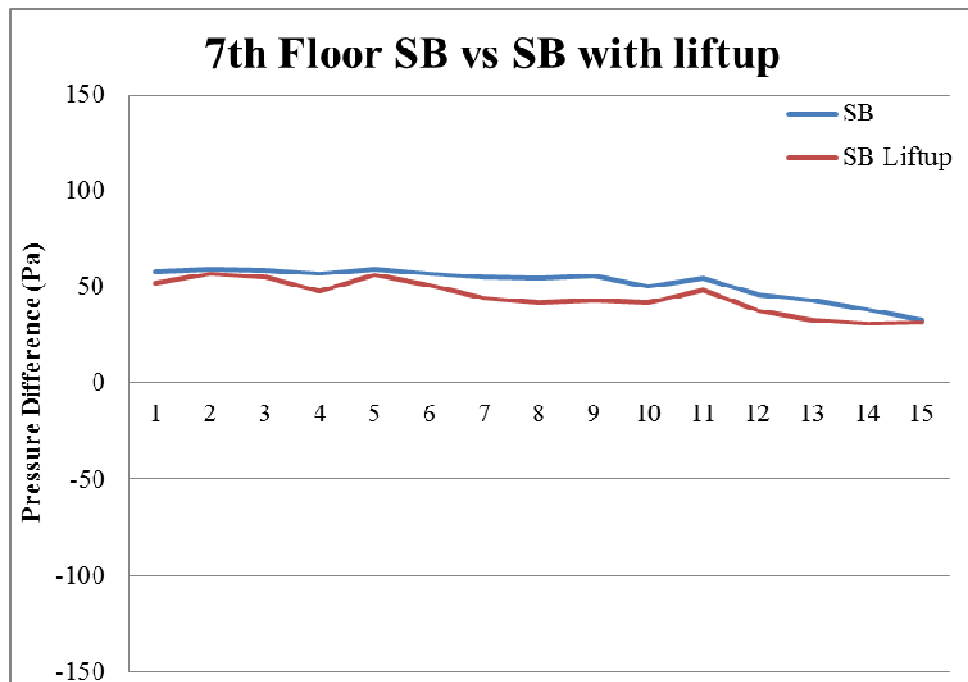
d) 4th Floor SB vs SB Lift-up Design



e) 5th Floor SB vs SB Lift-up Design



f) 6th Floor SB vs SB Lift-up Design



g) 7th Floor SB vs SB Lift-up Design

Figure 4-7 Pressure differences for different floors of singular building with and without lift-up design

Ventilation potential for different floors of the singular buildings with and without lift-up design are illustrated in Figure 4-7. It suggests that ventilation potential had been enhanced from 2nd to 5th floor with the lift-up design for singular building. This could be due to the greater negative pressure that was generated by the lift-up design for the leeward façade. When the air is able to flow through the lift-up area, some air also flows downwards on the leeward face and results in forming recirculation vortices. As the wind approaches normal to the building, some of the wind flows around the building, which also generates recirculation vortices as well. When two vortices meet each other, even lower negative pressures are resulted.

Ventilation potential change was less noticeable for 1st and 6th floor for the singular building with lift-up design. Interestingly, the singular building with lift-up design definitely was not helpful for 7th floor ventilation potential, which had actually decreased. The reason that ventilation potential decreases along the height of a building is because the approaching wind is split into two flows when the lift-up design is used. One is flowing across the lift-up area and the other flow is across the building height. As the measurement points are only located at the lower part of the building the 7th floor is about half of the singular building height. Consequently, the positive pressure at the windward façade decreases at the 6th or 7th floor. So the pressure difference is less and the ventilation potential is reduced on the higher floors. It is concluded that the lift-up design is helpful for improving the ventilation potential for the occupancies in the lower floors of a cluster of building or a slab of building. But its effectiveness is less noticeable for the 1st floor or floors above 6th in this case. For higher floors, it may reduce ventilation potential.

4.3.2 A row of buildings with and without lift-up design

4.3.2.1 Surface pressure distribution

As in section 4.3.1, only half of the building structure had been considered by assuming the flow is symmetric for both sides. There are four building blocks for the case of a row of buildings. Consequently, the pressure measurements were conducted on two adjacent building blocks. In order to facilitate the discussion, each façade for these two buildings has been illustrated in Figure 4-8. The building on the left hand side is labelled RB1 and the right one labelled RB2.

The layout of the pressure measurement points have only been distributed at the lower floors of the building. The purpose of doing this was to investigate the variation of the pressure distribution of the lower floor levels and the improvement of the ventilation potential by implementing the lift-up design. Only the bottom six floors of both building had been measured in this study.

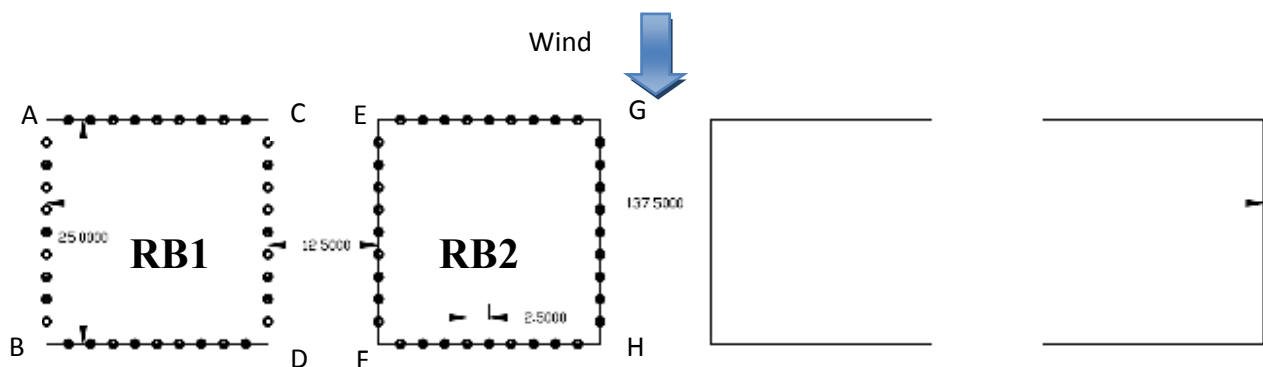
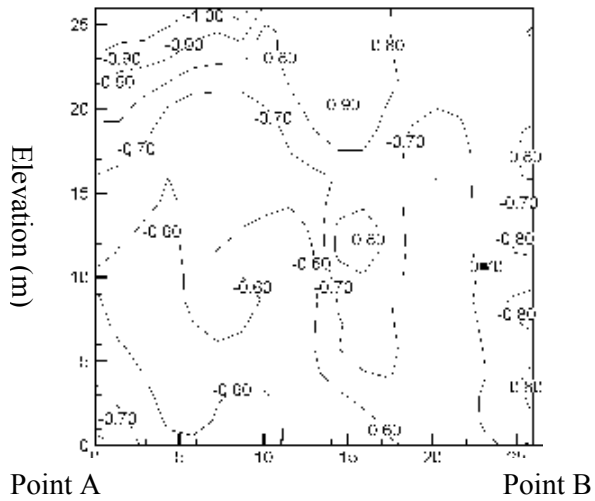
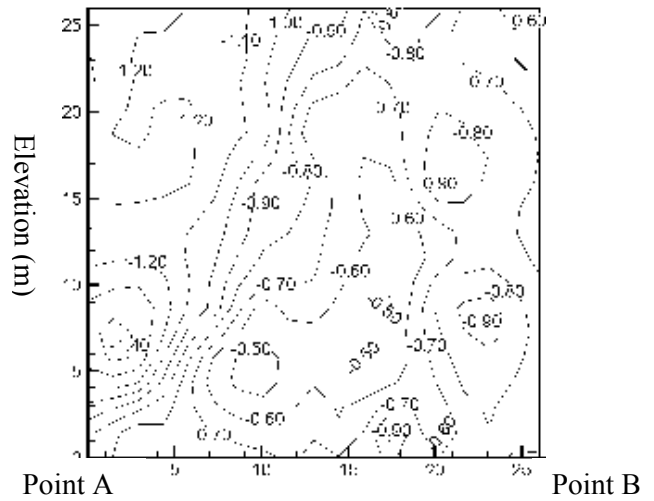


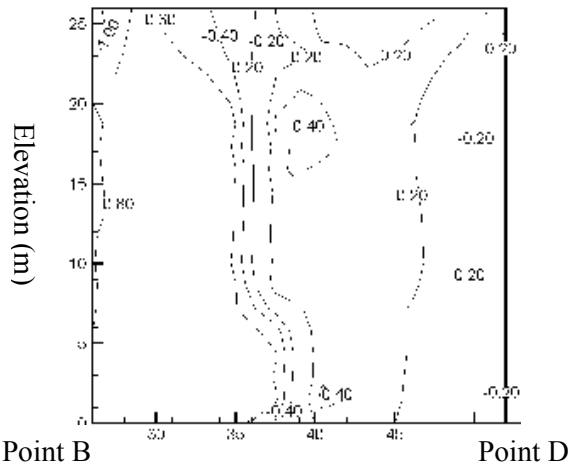
Figure 4-8. Plan of pressure measurement for a row of buildings with and without lift-up design



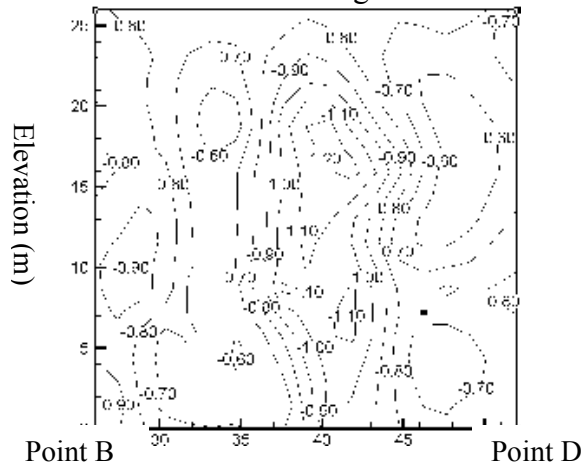
a) Façade A-B for RB 1



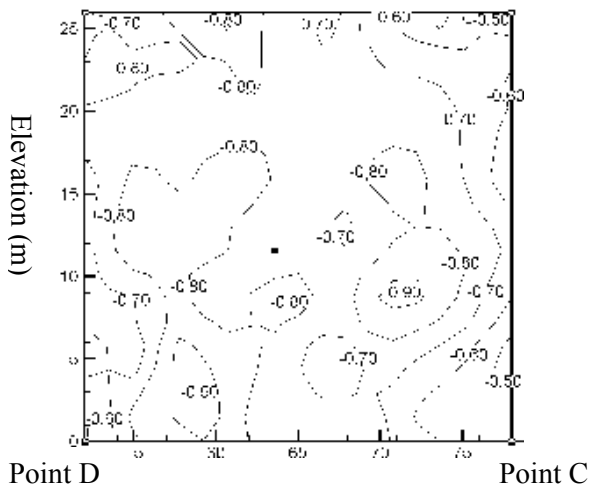
b) Façade A-B for RB 1 with lift-up design



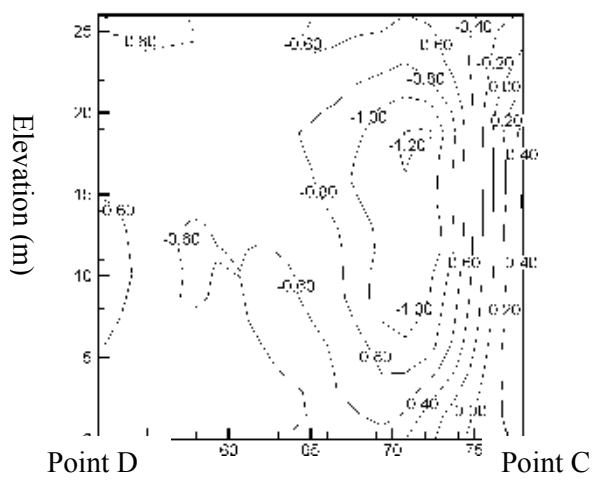
c) Façade B-D for RB 1



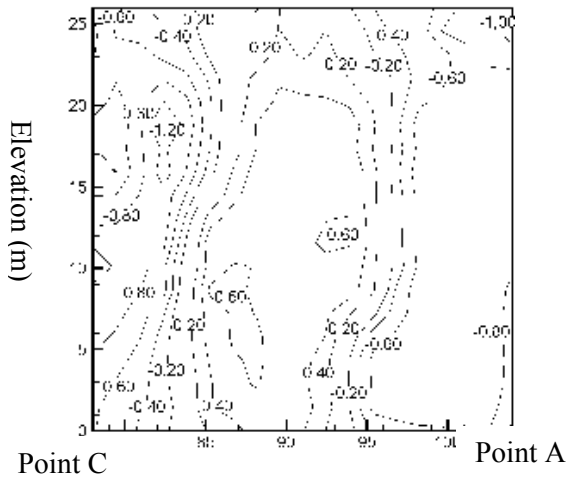
d) Façade B-D for RB 1 with lift-up design



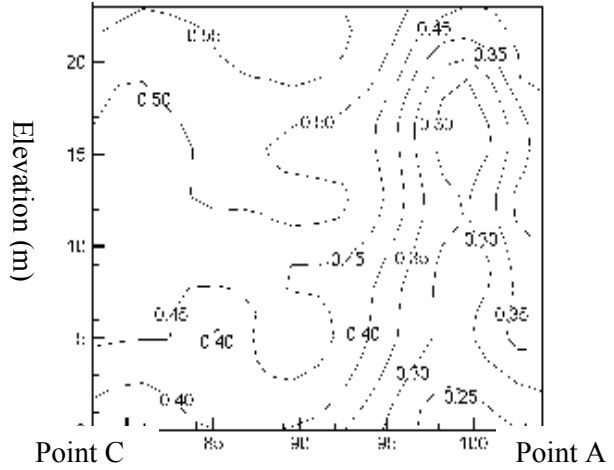
e) Façade D-C for RB 1



f) Façade D-C for RB 1 with lift-up design

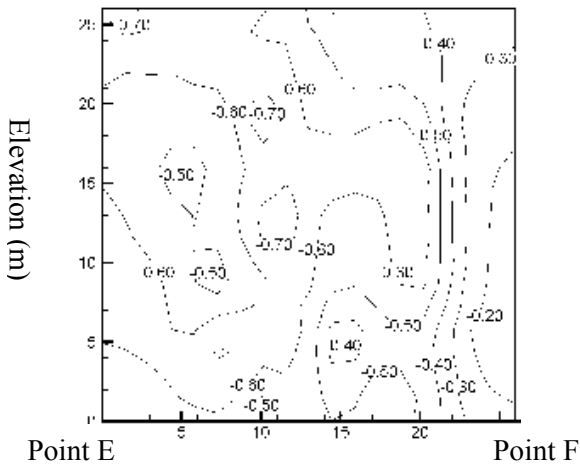


g) Façade C-A for RB1

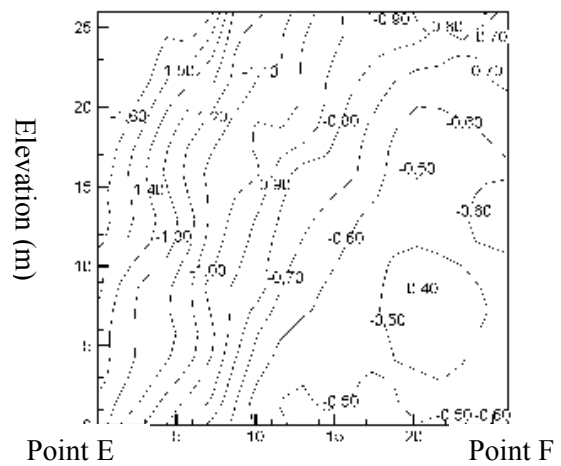


h) Façade C-A for RB1 with lift-up design

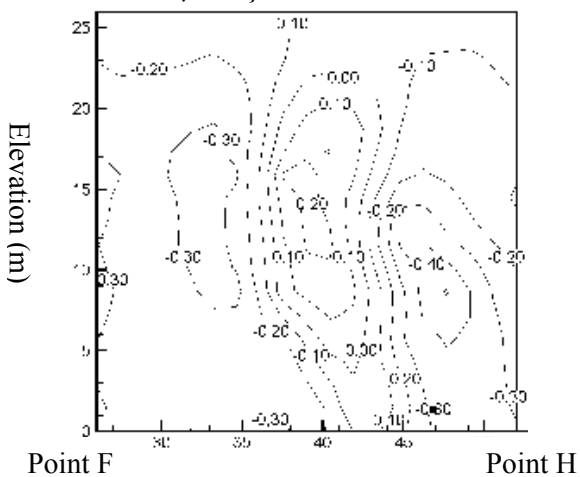
Figure 4-9. Pressure contour diagram for RB1 for a row of buildings with and without lift-up design



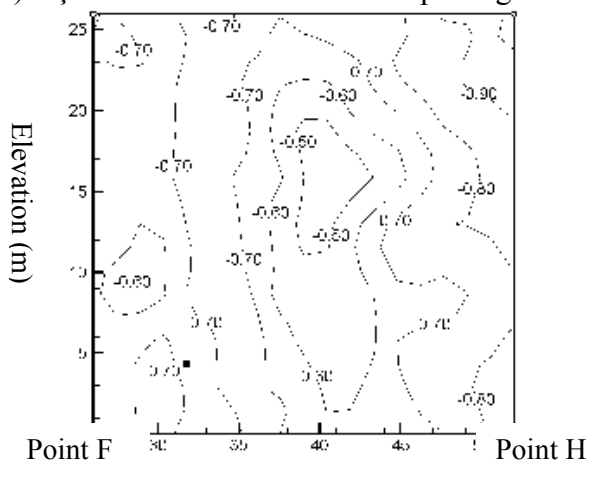
a) Façade E-F for RB 2



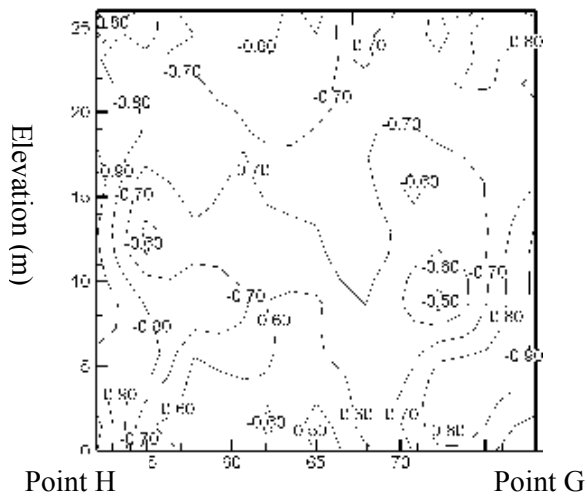
b) Façade E-F for RB2 with lift-up design



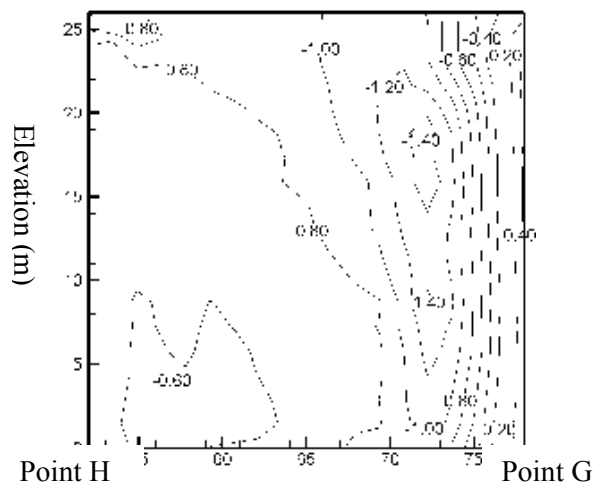
c) Façade F-H for RB 2



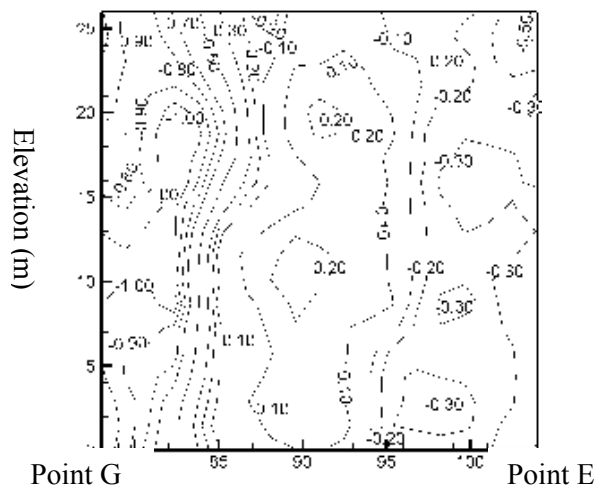
d) Façade F-H for RB2 with lift-up design



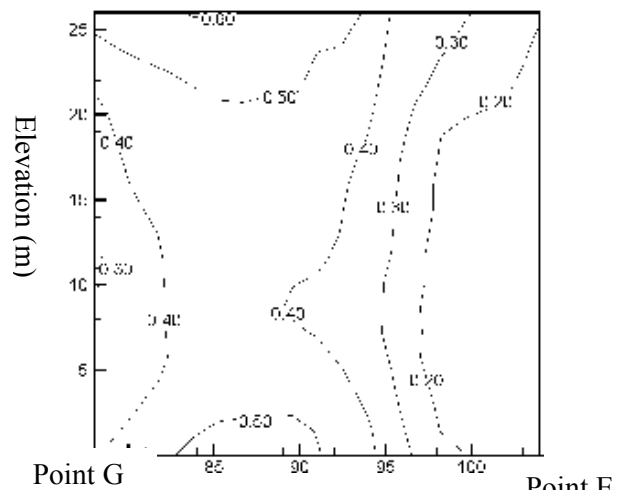
e) Façade H-G for RB 2



f) Façade H-G for RB 2 with lift-up design



g) Façade G-E for RB 2



h) Façade G-E for RB 2 with lift-up design

Figure 4-10. Pressure contours diagrams for RB2 for a row of buildings with and without lift-up design

The approaching wind was perpendicular to façade C-A and G-E for RB1 and RB2. According to Figure 4-8 , these two façades were the windward façades. High positive pressures occurred at the centre part and negative pressure happened at both side of the façade C-A for RB1. Positive pressures ranged from 0.20 to 0.60; negative pressures were from -0.20 to -1.20. However, for RB1 with the lift-up design, all the pressure coefficients had become positive varying from 0.25 to 0.55. Similar phenomena could also be noticed for façade G-E for RB2 with or without lift-up design. With the non-lift-up design, positive

pressures dropped from 0.10 to 0.20 and negative pressures were from -0.10 to -1.00. With the lift-up design, positive pressure varied from 0.20 to 0.60. Therefore, RB2 had both lower positive pressure and negative pressure compared to RB1. RB1 with lift-up design achieved slightly higher positive pressure than RB2 with lift-up design.

Façade A-B and D-C were the side façades for RB1; façade E-F and H-G were the side façades for RB2. As before, with the lift-up design, pressure contours were much more complicated compared to the one without the lift-up design. For façade A-B for RB1, the pressure varied from -0.60 to -1.00 and increased to the range of -0.60 to -1.40 with lift-up design. The highest negative pressure was generated near to point A. Without the lift-up design, the highest negative pressure occurred at the highest floor of point A, but it changed to the lower floor of point A with the lift-up design. Pressure coefficients varied from -0.20 to -0.70 for façade E-F for RB2 and to the range of -0.40 to -1.60 for the same façade but with the lift-up design. For façade D-C for RB1, the pressure varied from -0.50 to -0.90, but changed to the range of -0.20 to -1.20 with the lift-up design. For façade H-G for RB2, the pressure varied from -0.50 to -0.90. It changed to a greater negative pressure range of -0.40 to -1.40 when lift-up design was utilized for RB2. But interestingly, some positive pressure was generated near to point C for façade D-C with the lift-up design for RB1 and near to point G for façade H-G with the lift-up design for RB2.

Façade B-D and F-H are the leeward façade for RB1 and RB2 with and without lift-up design. Without the lift-up design, only part of the negative pressure occurred at both sides of façade B-D for RB1, which varied from -0.20 to -1.00. But the central part of façade B-D recorded positive pressures up to 0.40. Similar pressure patterns could also be observed for the façade F-H on RB2. But the negative and positive pressures were much lower compared to RB1, which are in the range of -0.10 to -0.40 and 0.10 to 0.20 respectively. With the lift-up design,

only negative pressure were generated at the leeward façade of RB1 with the lift-up design, which was in the range of -0.60 to -1.20. The highest negative pressure occurred at the centre of the façade B-D. The leeward façade F-H also had a much lower negative pressure range, which was from -0.50 to -0.80.

In conclusion, the pressure pattern for the lower part of the building for RB1 and RB2 were similar, but the values were slightly different. For the windward side for RB1 and RB2 alone, only some positive pressure was generated at the centre for the façade, but the remaining areas were negative. With the lift-up design, positive pressure was recorded for the entire façade. For the leeward façade for RB1 and RB2 with or without the lift-up design, only negative pressures were generated. But with the lift-up design, it could help to reduce the negative pressure to a lower level and some positive pressure could be produced at the centre of the façade. For the side facades, lift-up design could help to moderate the negative pressure to a much lower level.

4.3.2.2 Natural Ventilation Potential

The following discussion presents the findings of the results for each pair of pressure measurement points and at every measured floor. Point A and B at the left side of the building RB1 are represented by point 1 and point 9 is at the right hand end of the building, corresponding with points C and D. Point E and F at the left side of the building RB2 are represented by point 1 and point 9 is at the right hand end of the building, corresponding with points G and H.

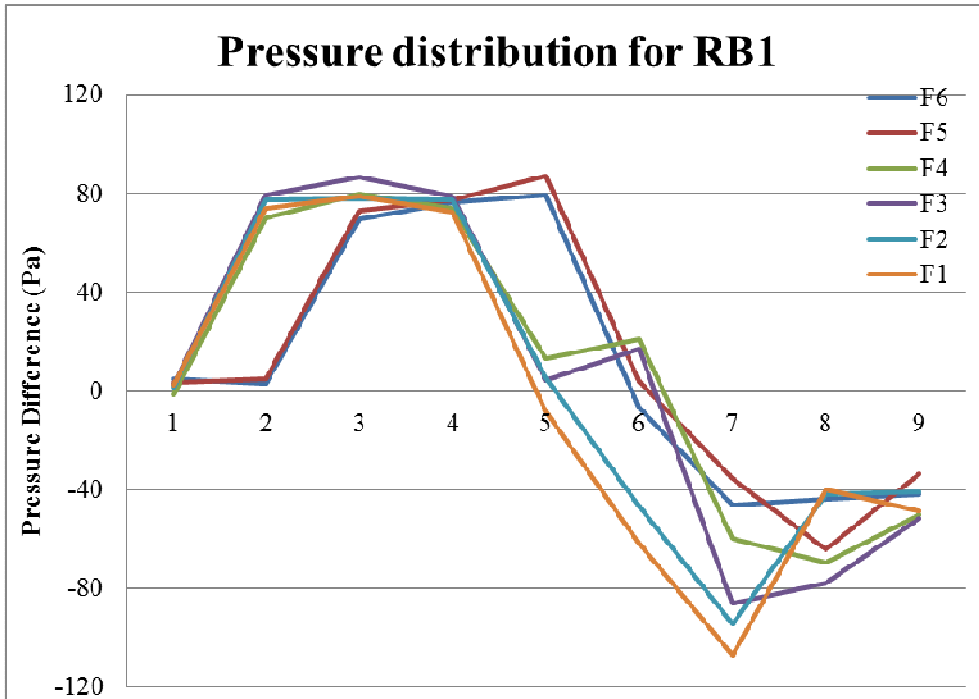


Figure 4-11. Pressure difference distribution for RB1 for different floors

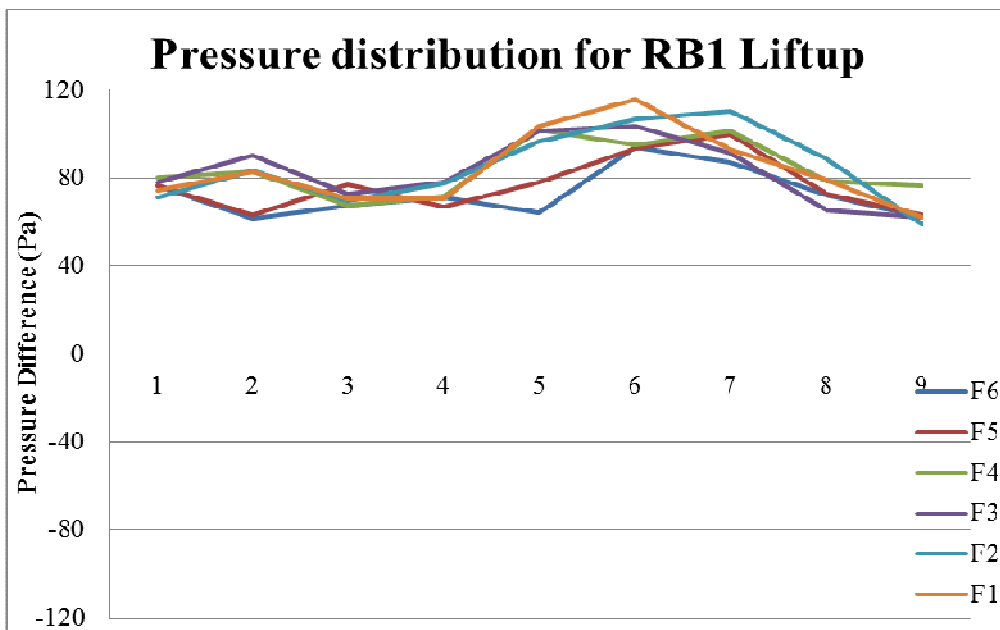


Figure 4-12. Pressure difference distribution for RB1 with lift-up design for different floors

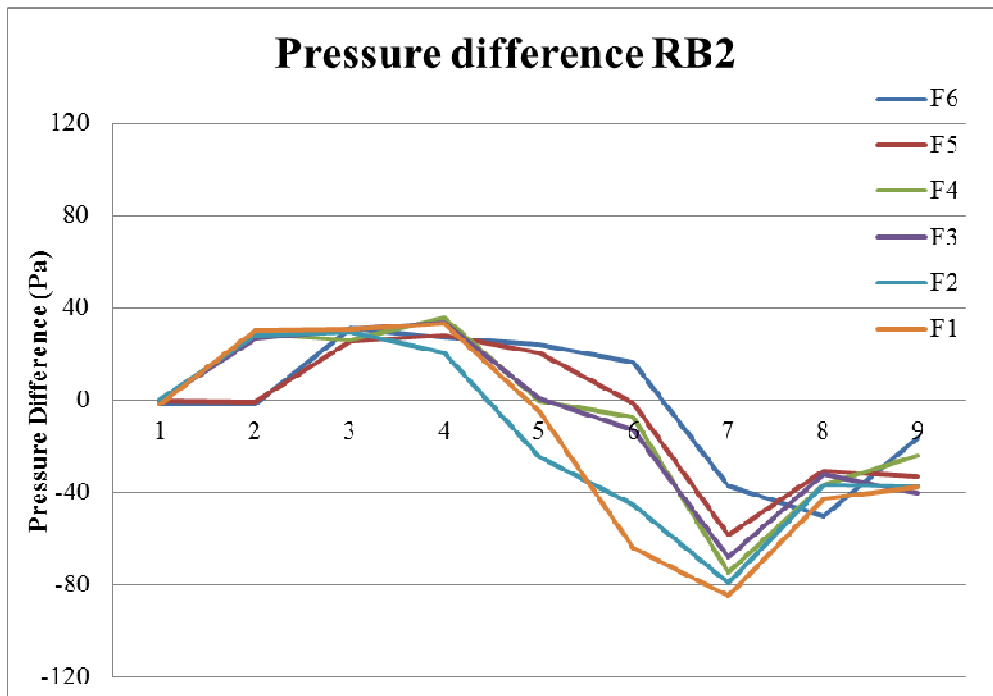


Figure 4-13. Pressure difference distribution for RB2 for different floors

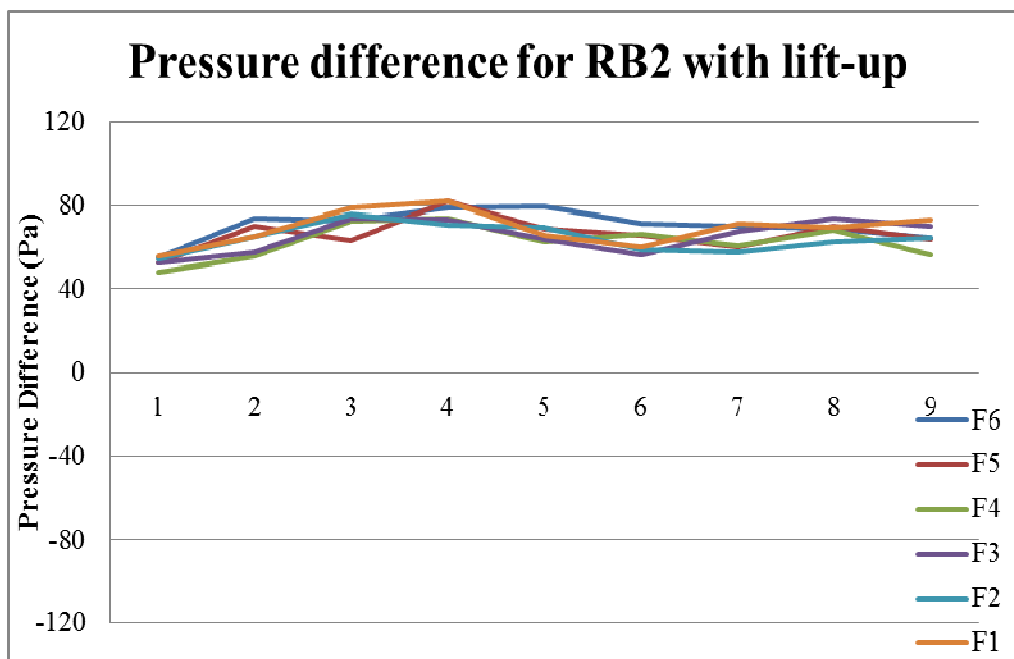
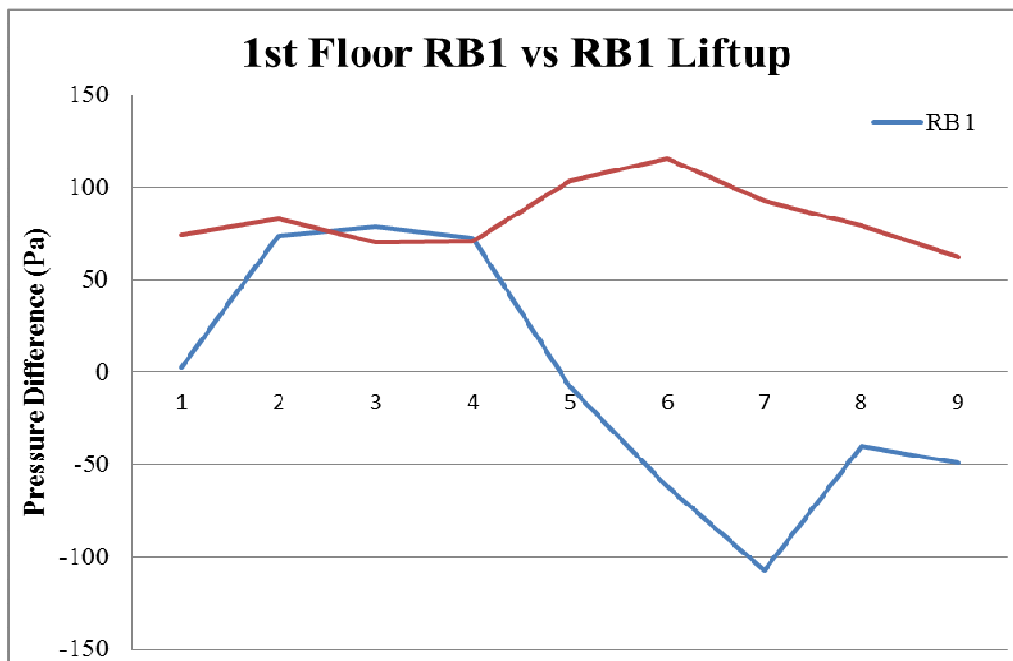


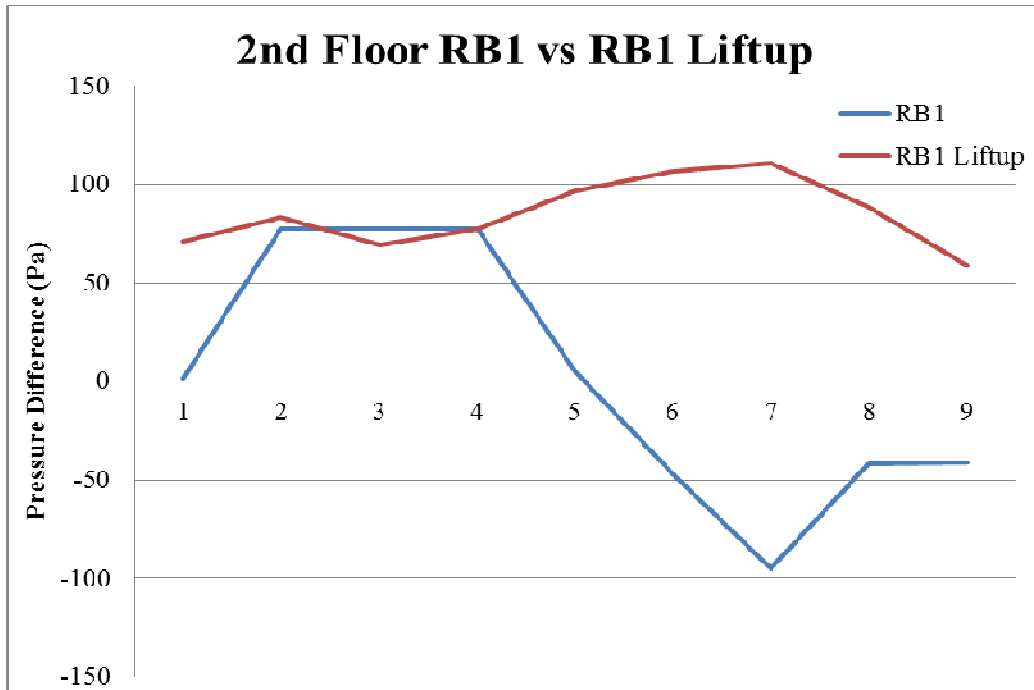
Figure 4-14. Pressure difference distribution for RB2 with lift-up design for different floors

Pressure difference distribution for RB1 and RB2 are given in Figure 4-11 and Figure 4-12 and pressure difference distribution for RB1 and RB2 with lift-up design are shown in Figure

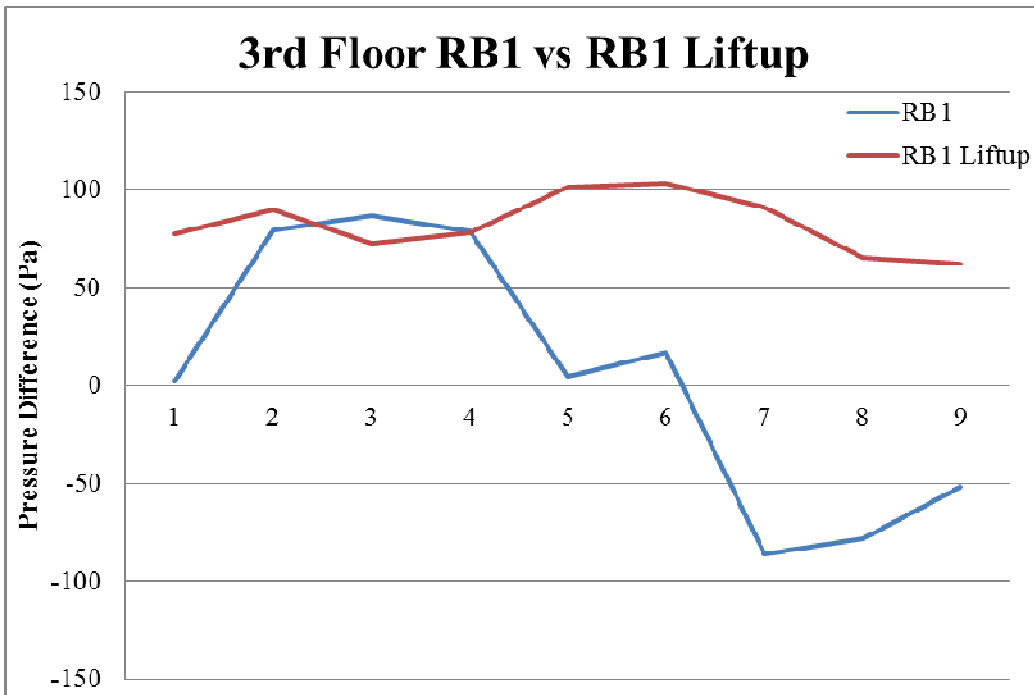
4-13 and Figure 4-14. With the lift-up design, the highest pressure difference point for RB1 was found on the first floor, while the lowest pressure difference point for RB1 was on the second floor. Without the lift-up design, the highest pressure difference point for RB1 was on the fifth floor, while the lowest pressure difference point for RB1 was on the first floor. But with the lift-up design, the highest pressure difference point for RB2 was on the first floor, while the lowest pressure difference point for RB2 was on the fourth floor. Without the lift-up design, the highest pressure difference point for RB2 was on the fourth floor, while the lowest pressure difference point for RB2 was on the third floor.



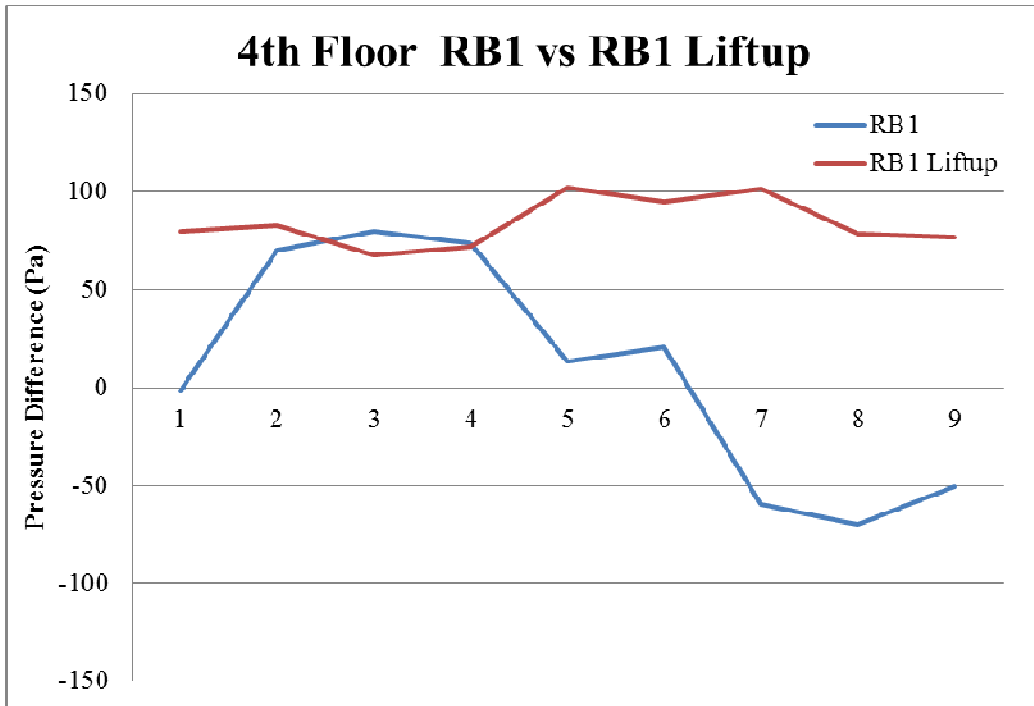
a) 1st Floor RB1 vs RB1 Lift-up Design



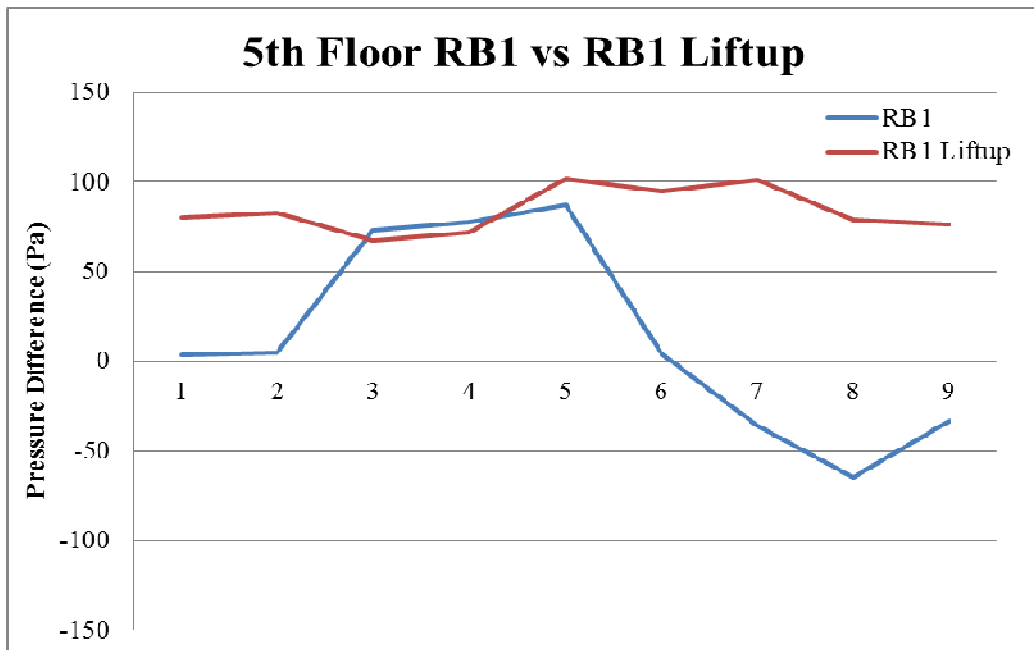
b) 2nd Floor RB1 vs RB1 Lift-up Design



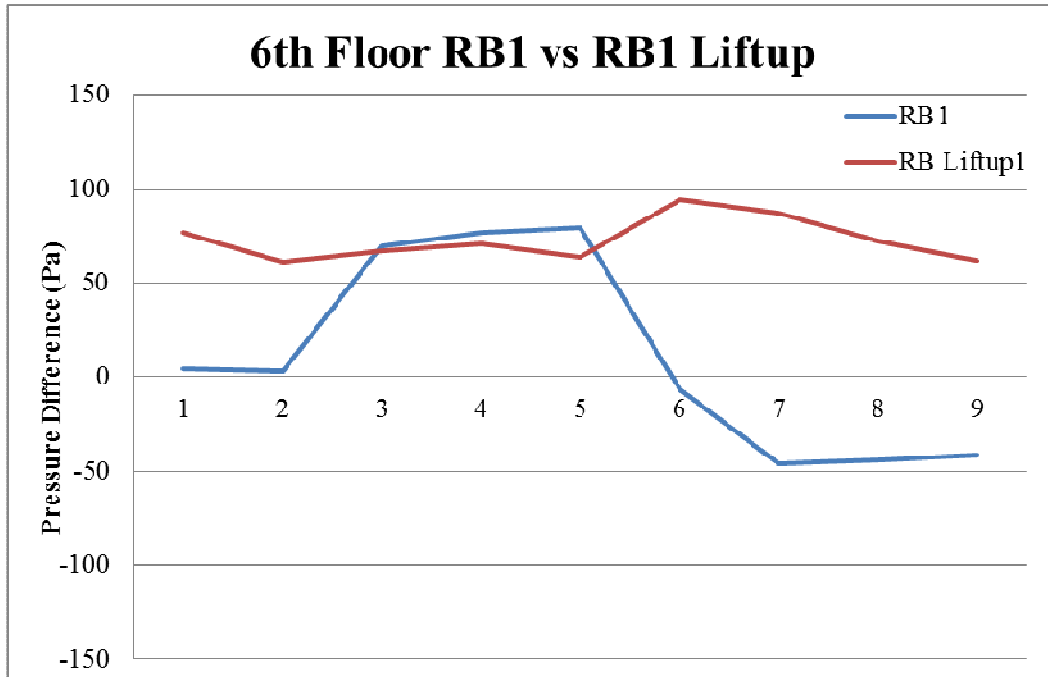
c) 3rd Floor RB1 vs RB Lift-up Design



d) 4th Floor RB1 vs RB1 Lift-up Design

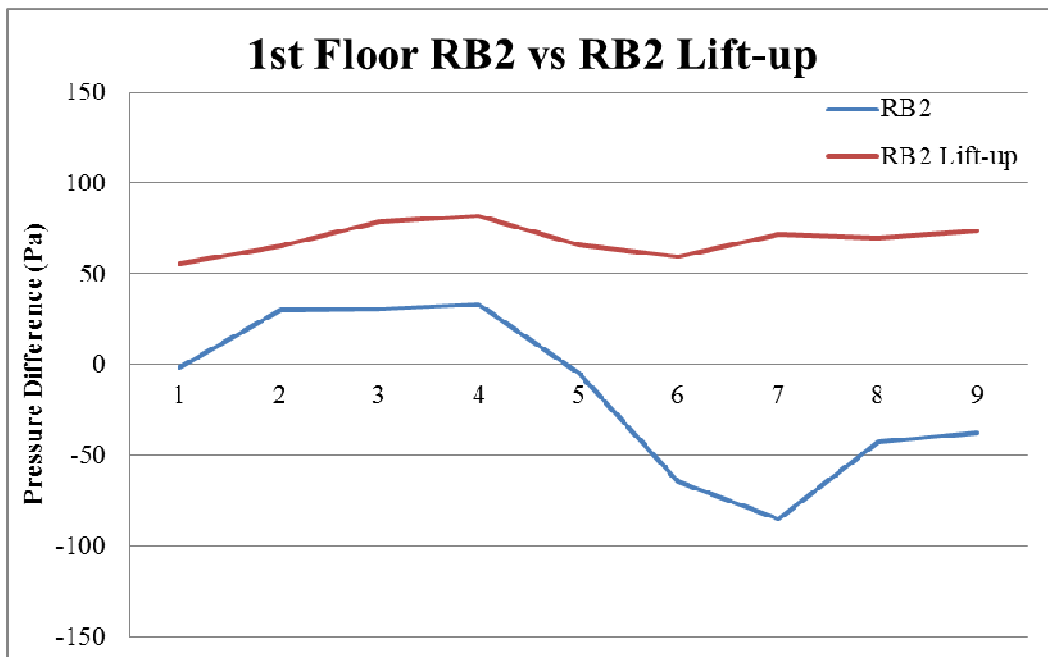


e) 5th Floor RB1 vs RB1 Lift-up Design

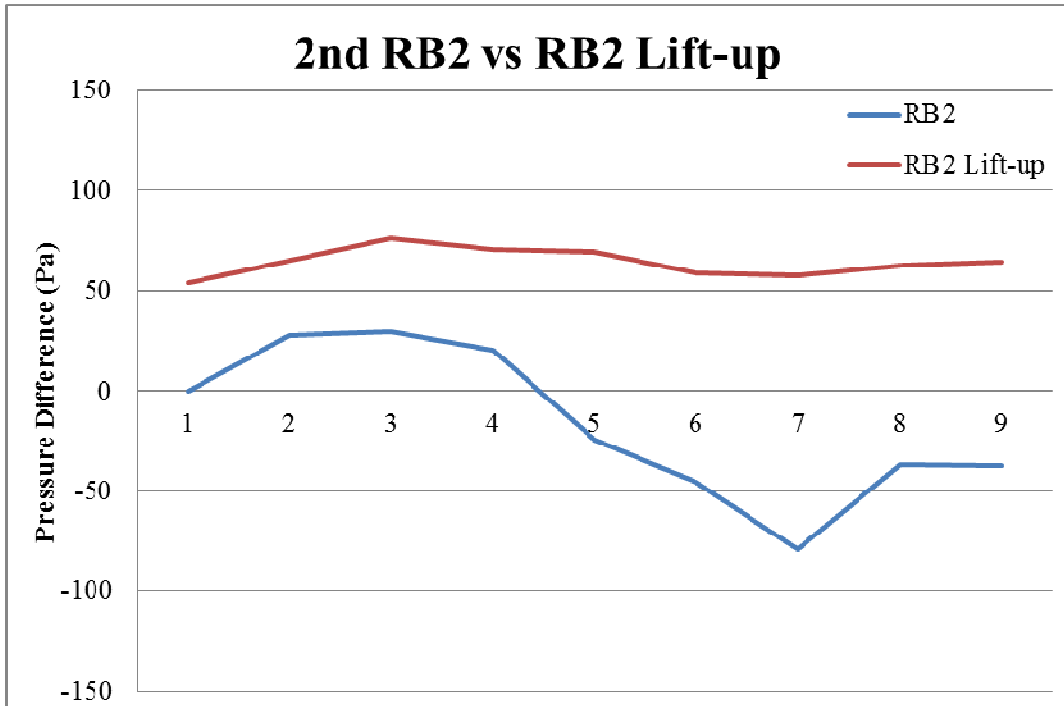


f) 6th Floor RB1 vs RB1 Lift-up Design

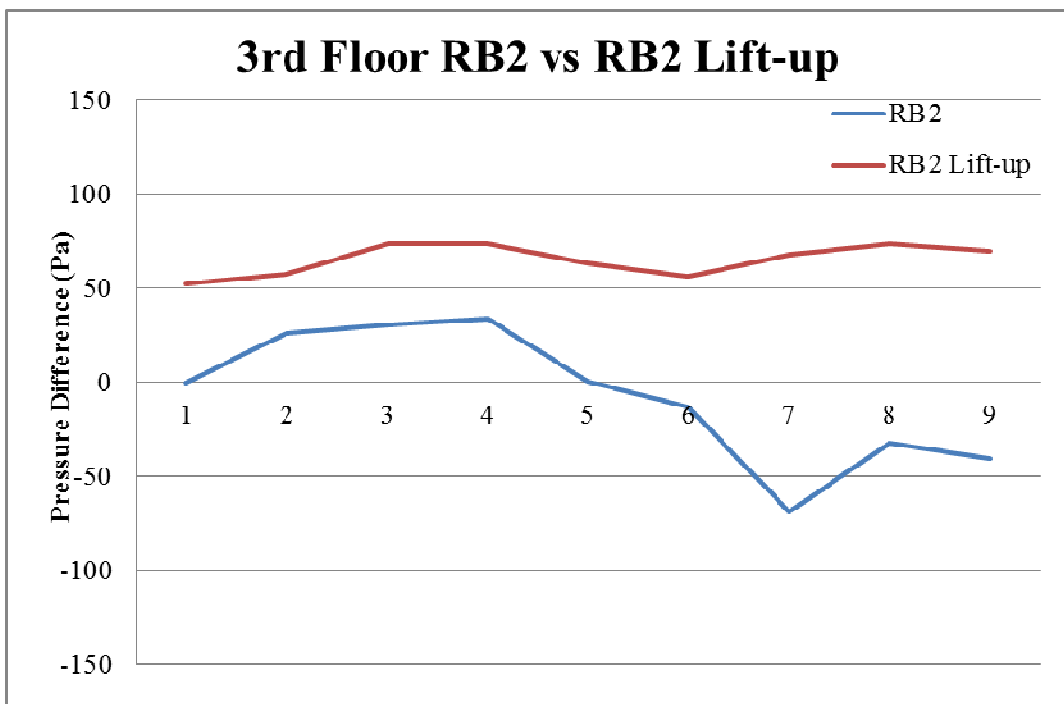
Figure 4-15. Pressure differences for different floors of RB1 with and without lift-up design



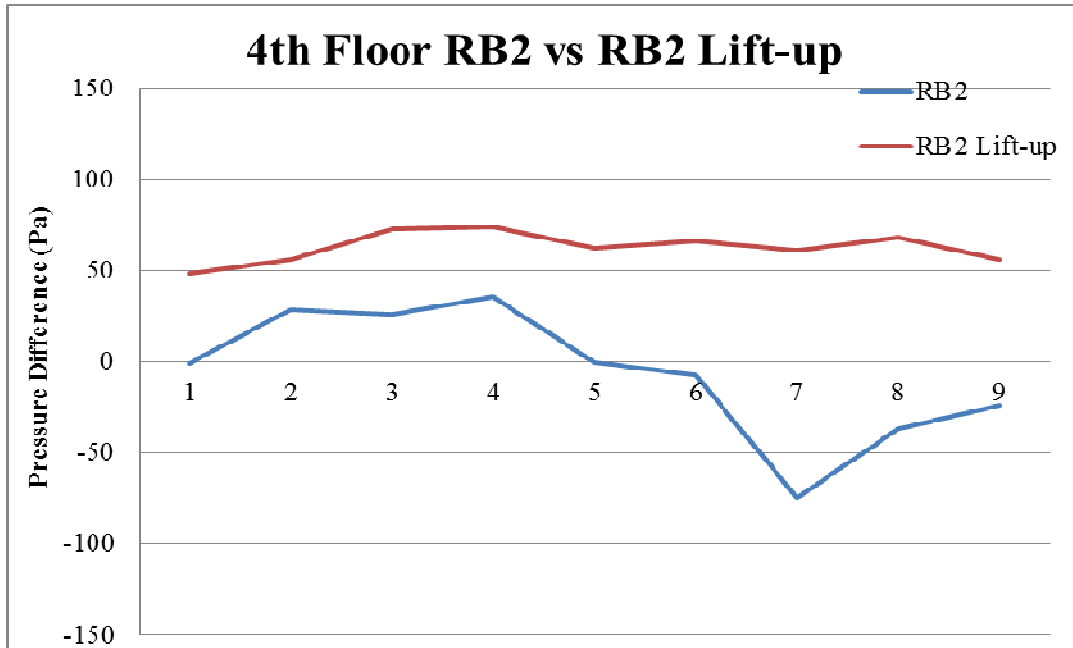
a) 1st Floor RB2 vs RB2 Lift-up Design



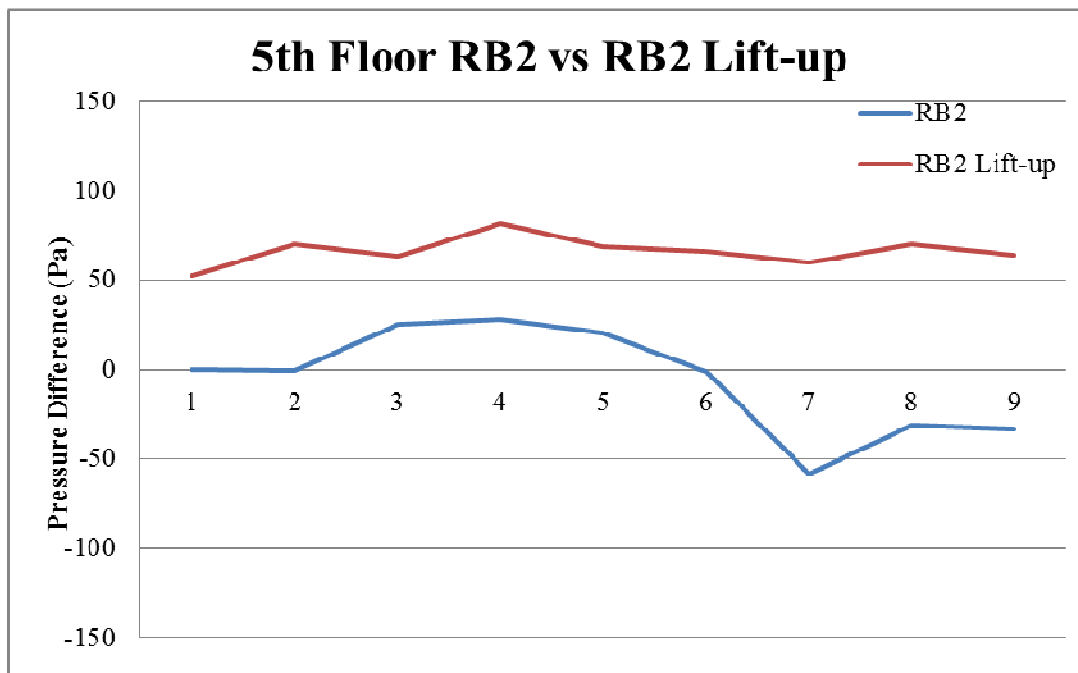
b) 2nd RB2 vs RB2 Lift-up Design



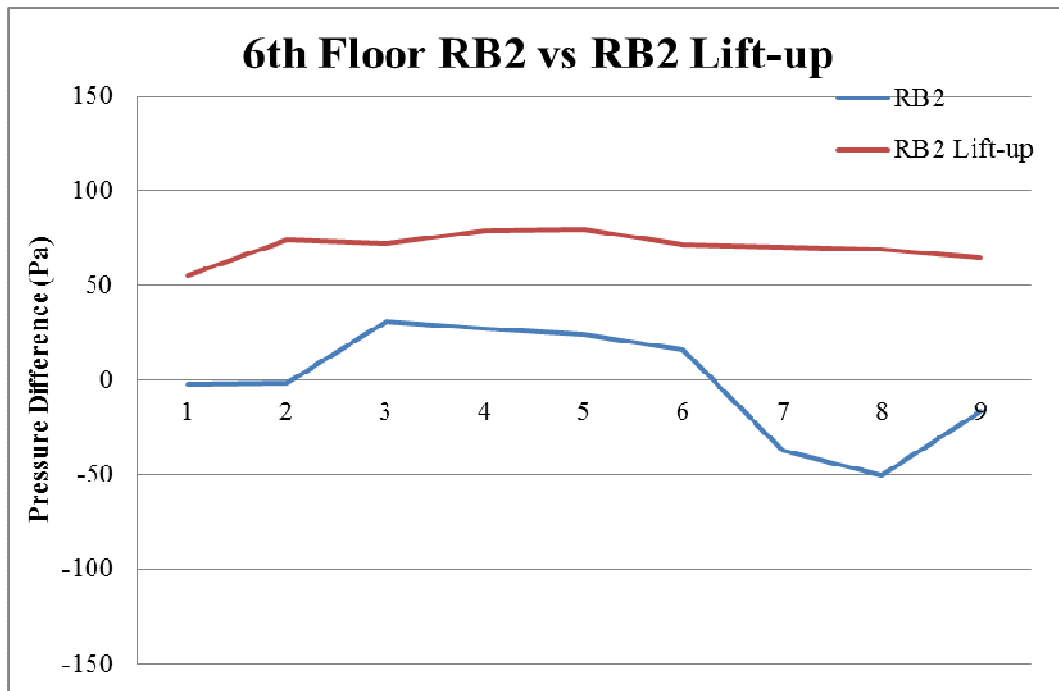
c) 3rd Floor RB2 vs RB2 Lift-up Design



d) 4th Floor RB2 vs RB2 Lift-up Design



e) 5th Floor RB2 vs RB2 Lift-up



f) 6th Floor RB2 vs RB2 Lift-up Design

Figure 4-16. Pressure differences for different floors of RB2 with and without lift-up design

Pressure differences for different floors of RB1 with and without the lift-up design is given in Figure 4-15. Pressure differences for different floors of RB2 with and without the lift-up design is shown in Figure 4-16. It was found that utilizing the lift-up design could increase the pressure differences between the windward and leeward façade, which means that the ventilation potential for all the floors for RB1 and RB2 could be raised by utilizing lift-up design. But the ventilation potential of the central part of RB1 slightly decreased with the lift-up design. RB2 with lift-up could increase more pressure differences than RB1 with lift-up. Consequently, cross ventilation for different floors of RB2 could rise more than RB1 when the lift-up design was applied. Comparing the increase of cross ventilation of different floors between RB1 with and without the lift-up design, ventilation potential appears similar, but the lower floors generally had higher ventilation potential than the higher floors. Similar characteristics could also be observed for RB2 with or without lift-up. It can be concluded

that the lift-up design can increase the cross ventilation for occupants inside a row of buildings, more enhanced effects were observed for lower floors and the central two buildings in a row of building.

4.3.3 Podium building with and without lift-up design

As in sections 4.3.1 and 4.3.2, only half of the building structure had been considered by assuming the flow was symmetric for both sides. In order to facilitate the discussion later, each façade for this building has also been illustrated in Figure 4-17. The pressure measurements were only carried out on the lower part of the podium level rather than on the four buildings erected on top of the podium. The purpose for doing this was to investigate the variation of the pressure distributions of the lower floor levels and the possible improvement of the ventilation potential by implementing the lift-up design. Only the bottom seven floors of both buildings have been investigated for this section of study.

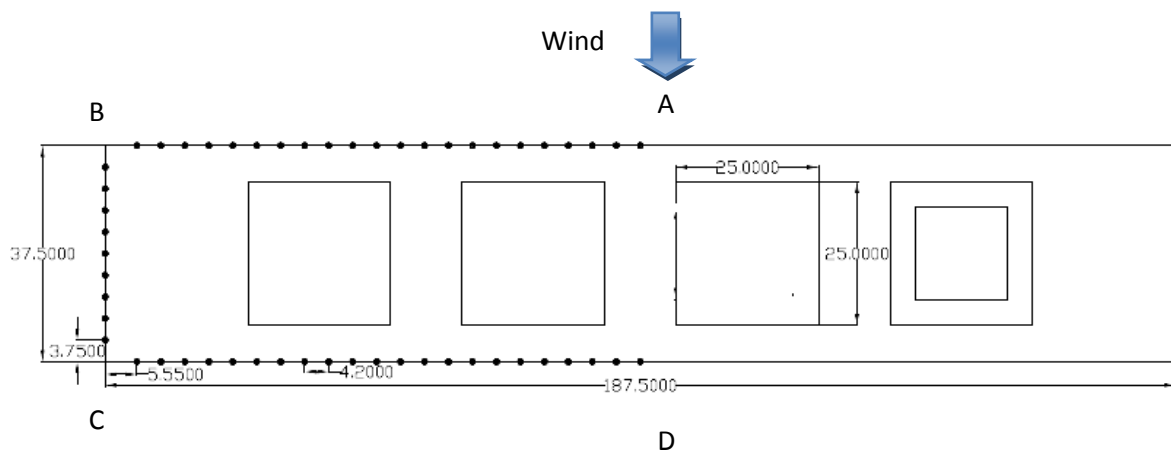
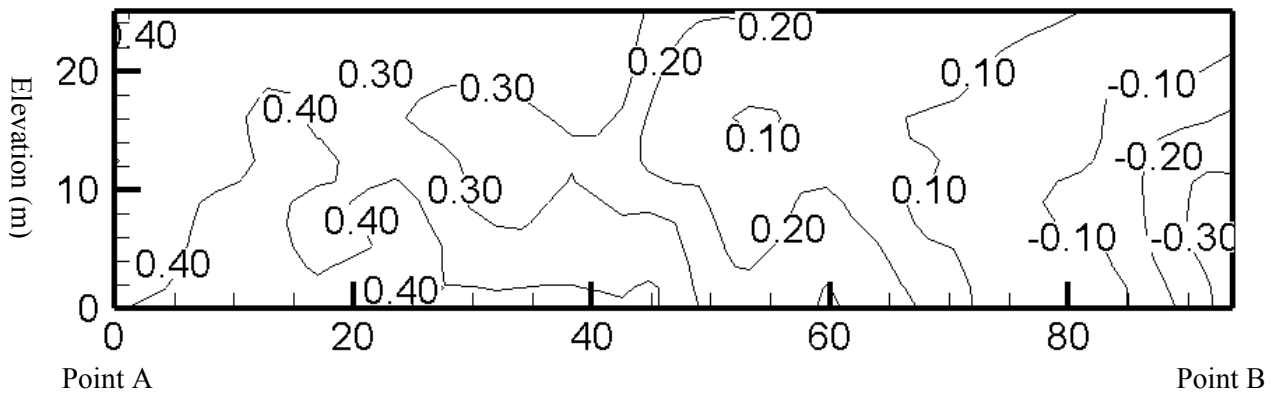
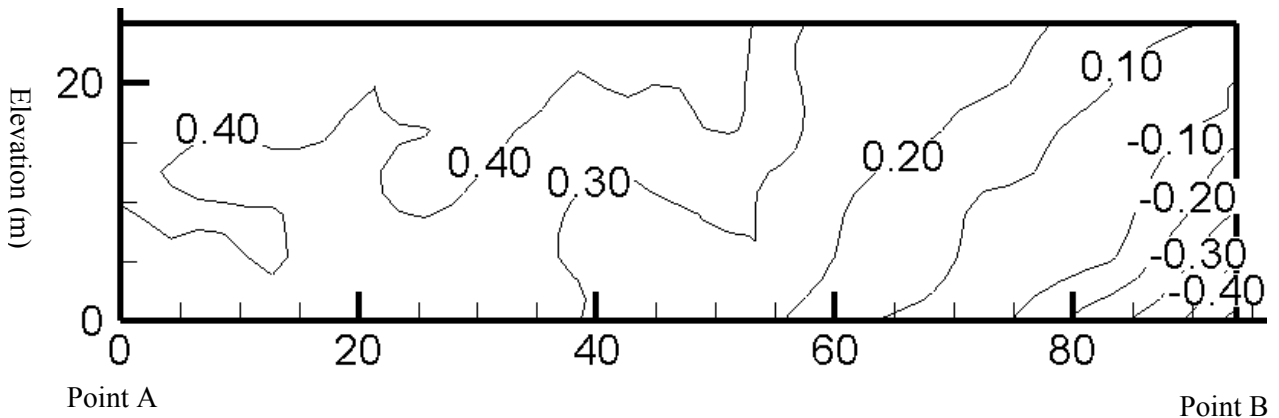


Figure 4-17. Plan view of pressure coefficient distribution for PB



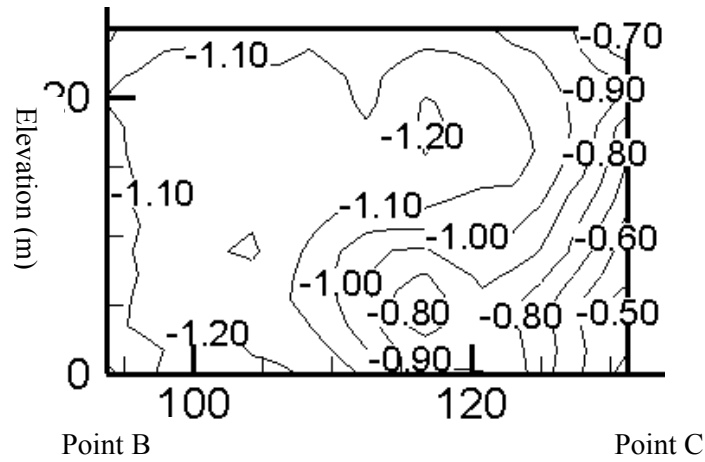
a) Façade A-B for Podium Building only



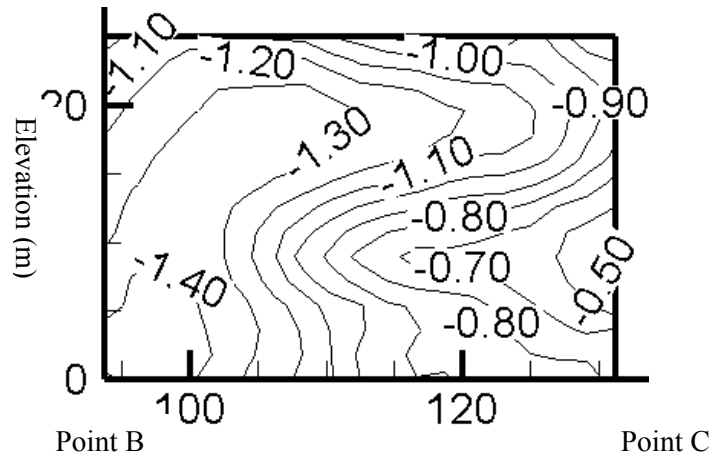
b) Façade A-B for Podium Building with lift-up design

Figure 4-18. Pressure contour diagram for facade A-B for podium building with and without lift-up design

On façade A-B, the measured pressure coefficients were generally positive for most of the areas of the PB and PB with lift-up design. The highest pressure coefficient for the PB and PB with lift-up design was 0.40. Yet the area for positive pressure coefficient was larger for PB with lift-up design compared to the PB only. The lowest pressure coefficient for PB was -0.30, but the lowest pressure coefficient for PB lift-up was decreased to -0.40. Negative pressures normally occurred at the corner near to the façade B-C. And the area of the negative pressure coefficient for façade A-B reduced for PB with lift-up design compared to PB.



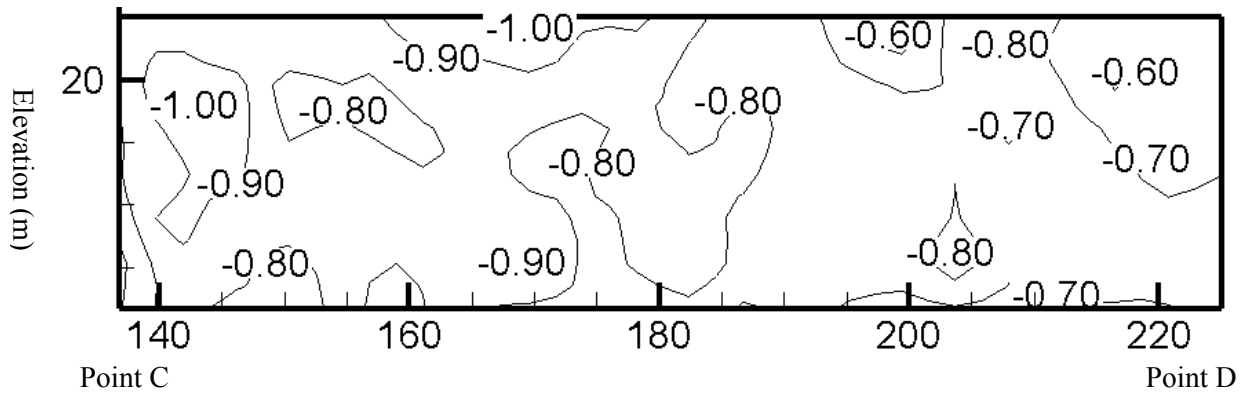
c) Façade B-C for Podium Building only



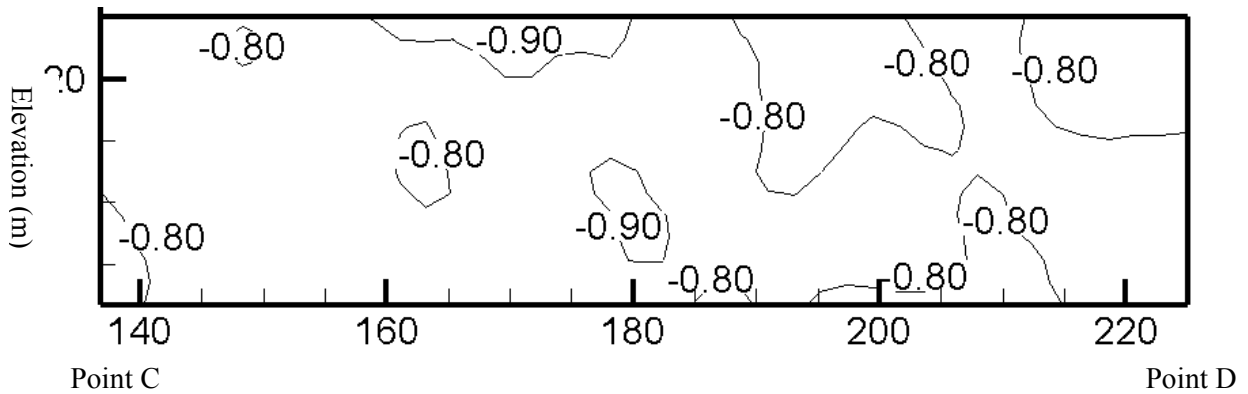
d) Façade B-C for Podium Building with lift-up design

Figure 4-19. Pressure contour diagram for facade B-C for singular building with and without lift-up design

On façade B-C, the PB pressure coefficients varied from -0.50 to -1.20. However, these deviated from -0.50 to -1.40 with the lift-up design. Therefore, with the lift-up design, the negative pressure coefficients on the side façade increased, particularly at the lower floors near to point B.



e) Façade C-D for Podium Building only



f) Façade C-D for Podium Building with lift-up design

Figure 4-20. Pressure contour diagram for facade C-D for singular building with and without lift-up design

Generally speaking, the pressure coefficients were all negative for façade C-D. Without the lift-up design, negative pressures ranged from -0.60 to -1.00 and varied from -0.80 to -0.90 with the lift-up design. The lift-up design increased the negative pressures at the upper and lower floors near to point D, whereas the negative pressures decreased at the upper and lower floors near to point C. The negative pressures were also remarkably consistent across the entire façade C-D with the lift-up design.

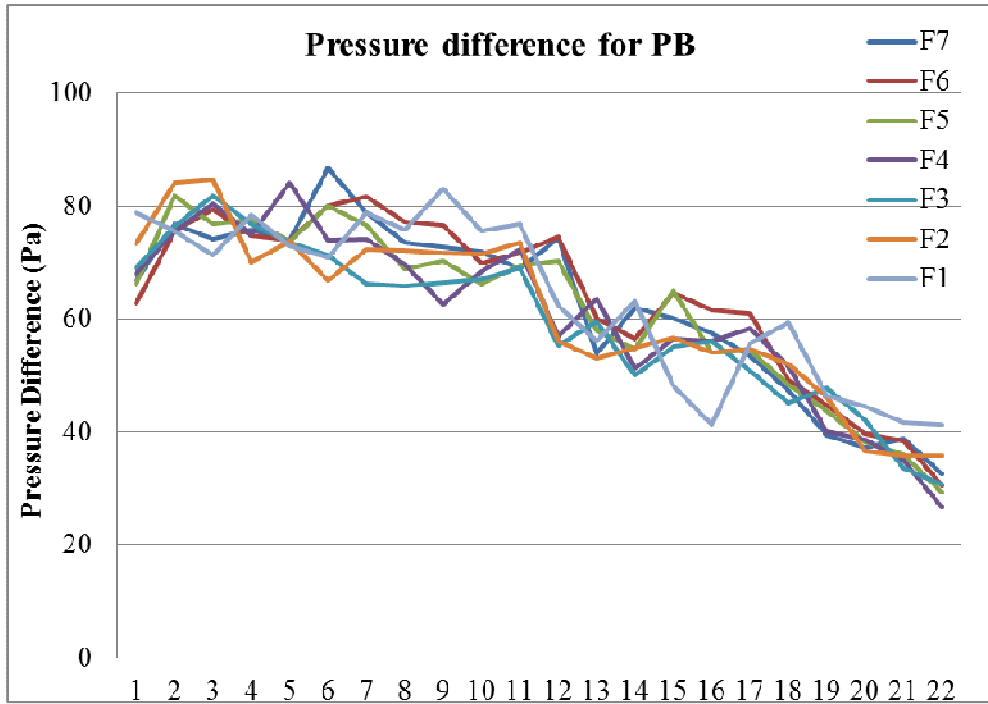


Figure 4-21. Pressure difference distribution for podium building for different floors

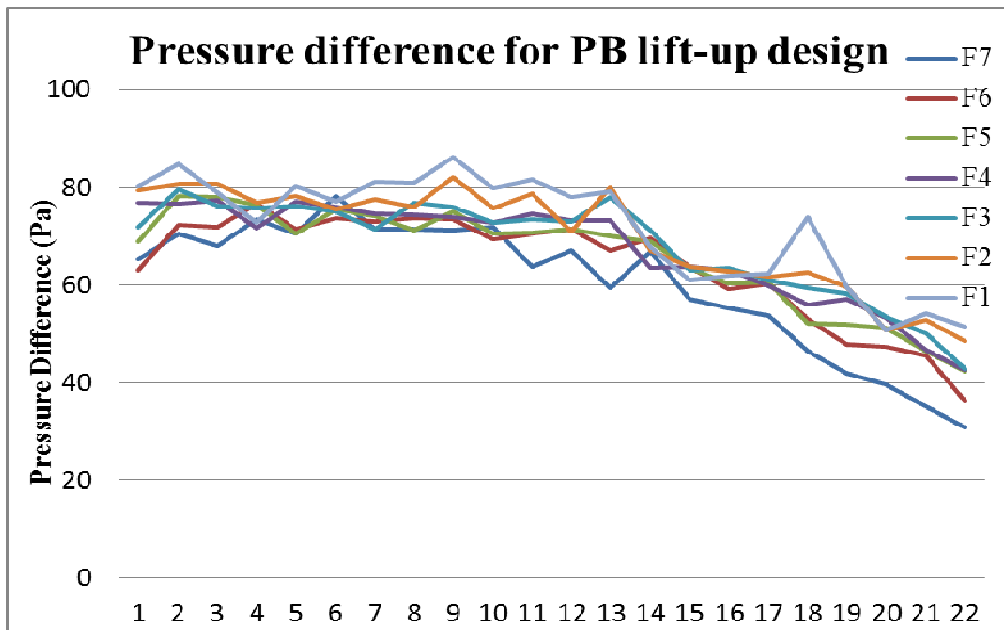
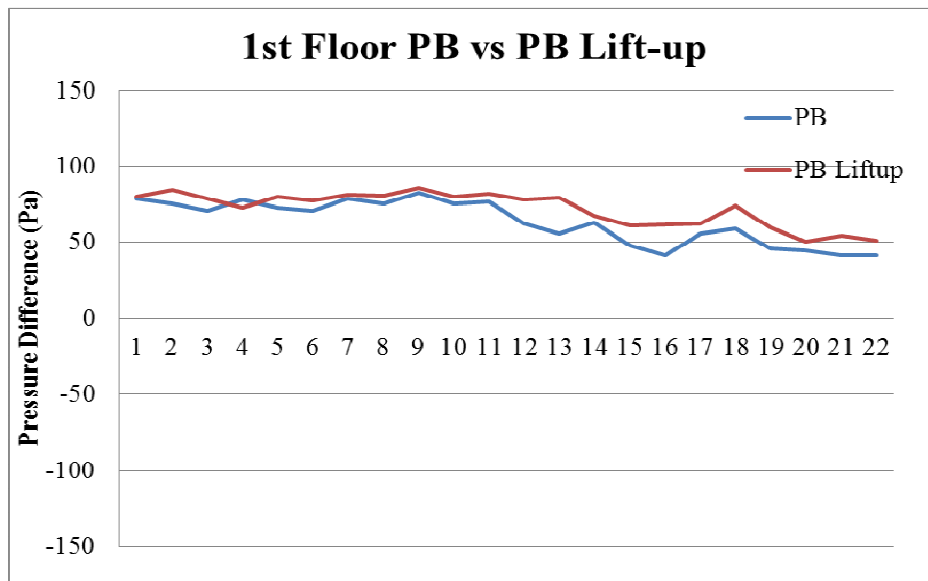


Figure 4-22. Pressure difference distribution for podium building with lift-up design for different floors

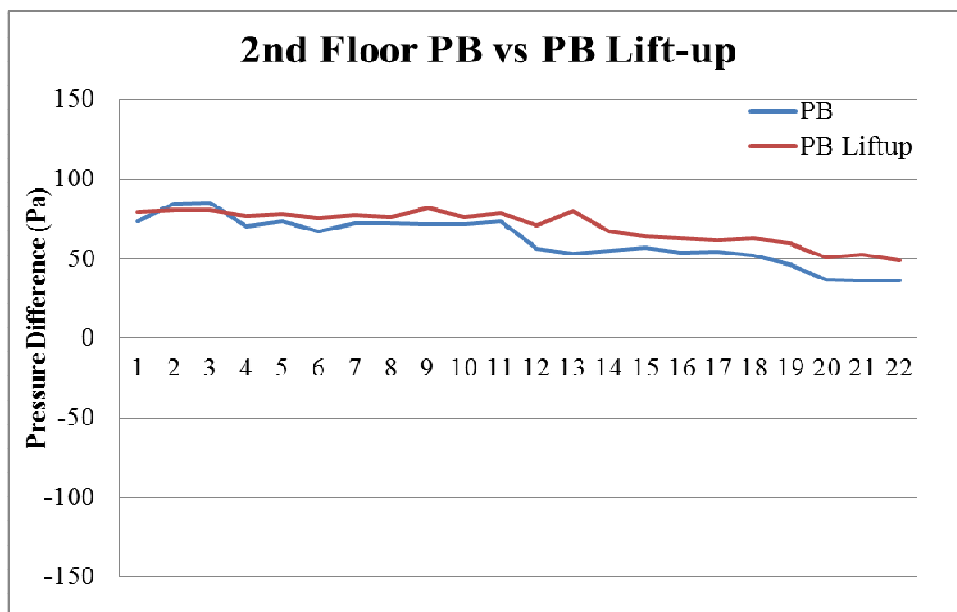
The pressure difference distribution for the PB are given in Figure 4-21 and pressure difference distribution for the PB with lift-up design was shown in Figure 4-22. Generally speaking, the largest pressure difference point occurred near to the centre of the building where was near to point 1. The lowest pressure difference point was recorded at the corner of the building, which was at point 93.75. Simply put, the largest and lowest ventilation potential occurred near to the centre and at the corner of the building respectively. With the lift-up design, the highest pressure difference point was found on the first floor, while the lowest pressure difference point was found on the seventh floor. Without the lift-up design, the highest pressure difference point was on the seventh floor, while the lowest pressure difference point was on the fourth floor.

In terms of the general trend for all the measurement points, the highest pressure differences for the podium building were on the sixth floor. The second highest pressure differences were on the seventh floor. But interestingly, the pressure differences for first and second floor fluctuated dramatically along the measurement points. The smallest pressure differences occurred at floor third for podium building. With the lift-up design, the seventh floor showed the lowest pressure differences, while first floor displayed the highest pressure differences. Without the lift-up design, some blocking effects were found in front of the podium. The higher the floors were, the higher the cross ventilation potential of those floors. With the lift-up design, air can flow through the lift-up area. The vortices at the leeward face of the building could be reduced. So the negative pressures at the back the podium building decreased. In order to have a better understanding of how the lift-up design affects façade pressures on the podium building, a direct comparison for different floors are presented below. Pressure differences of podium building with and without the lift-up design for

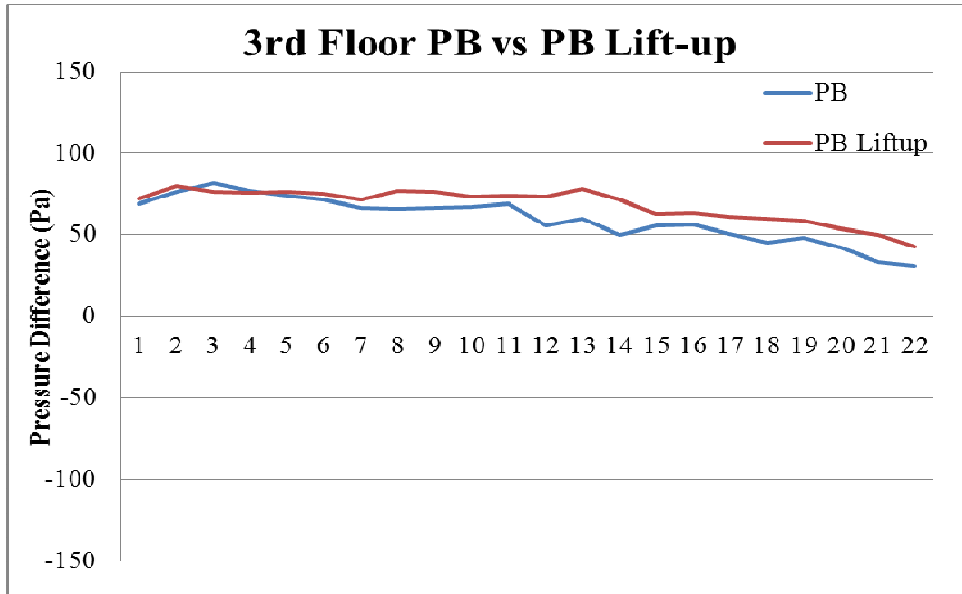
different floors have been compared to determine whether the lift-up design can induce better cross ventilation for the lower levels of the podium building.



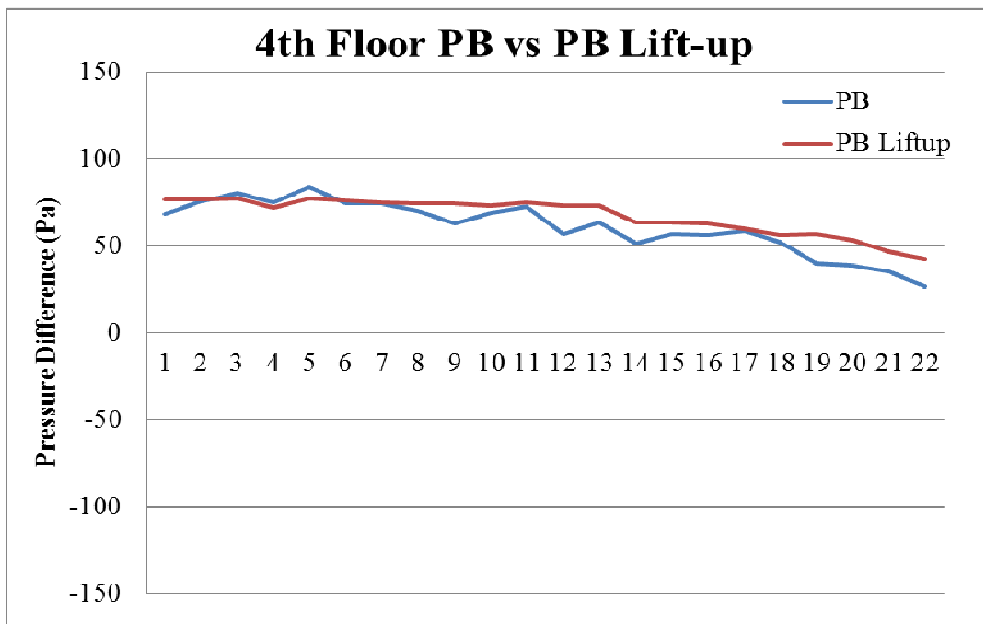
a) 1st Floor PB vs PB Lift-up Design



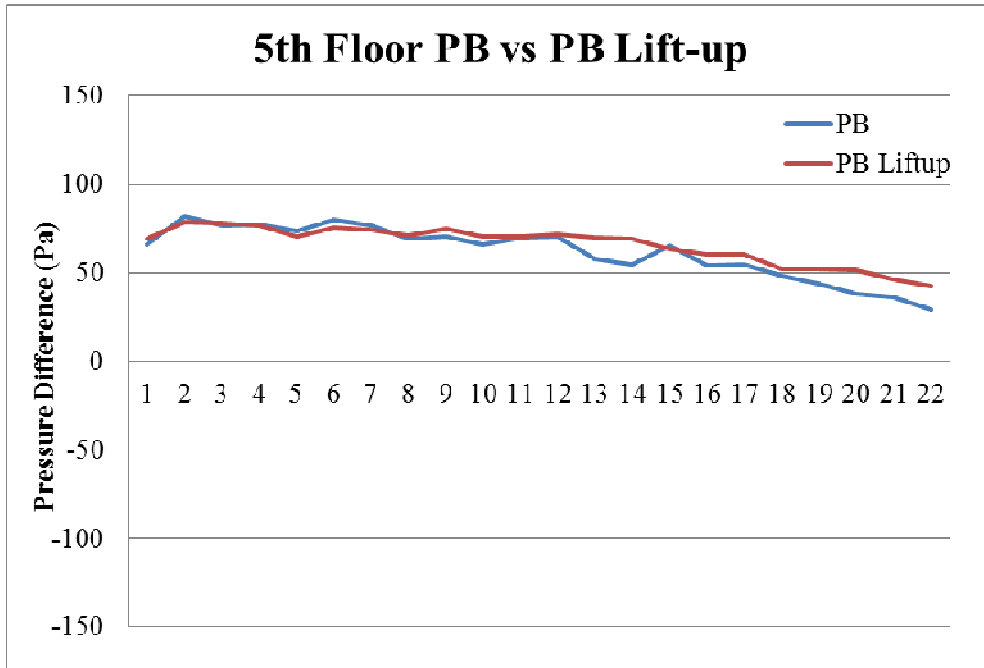
b) 2nd Floor PB vs PB Lift-up Design



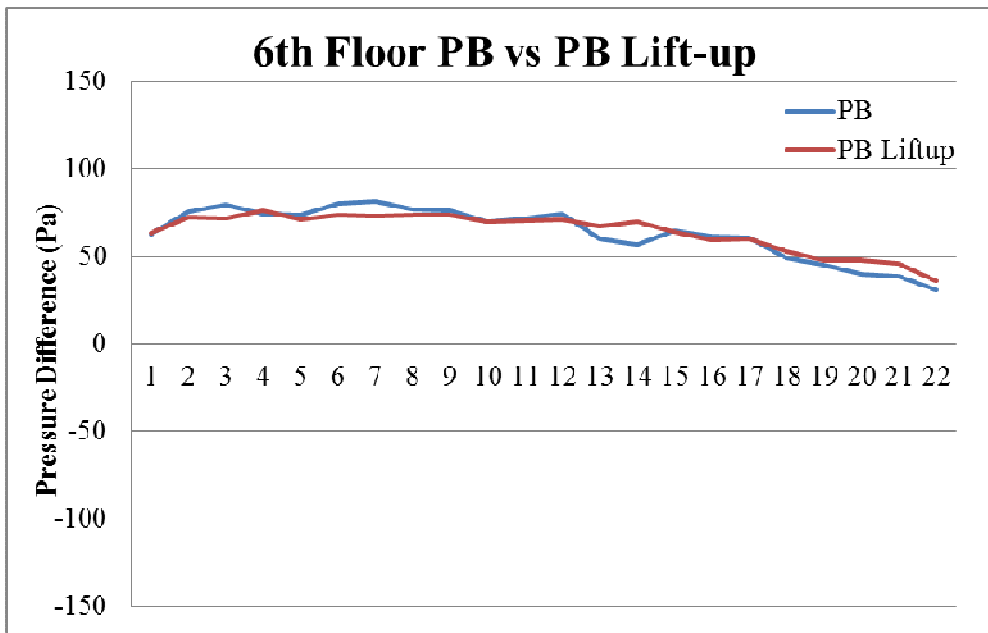
c) 3rd Floor PB vs PB Lift-up Design



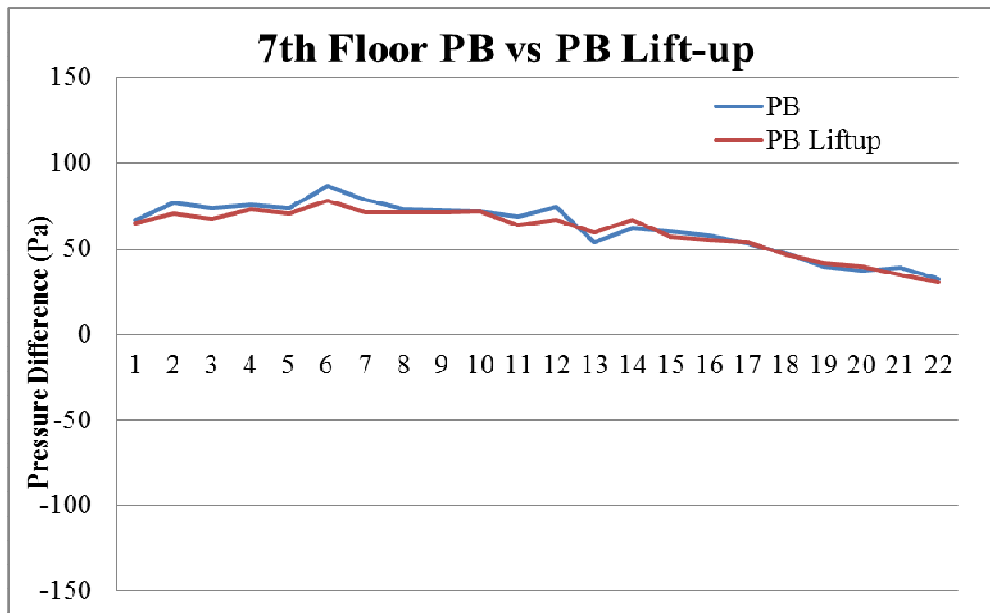
d) 4th Floor PB vs PB Lift-up Design



e) 5th Floor PB vs PB Lift-up Design



f) 6th Floor PB vs PB Lift-up Design



g) 7th Floor PB vs PB Lift-up Design

Figure 4-23. Pressure differences for different floors of podium building with and without lift-up design

Ventilation potential for different floors of podium building are shown in Figure 4-23. The increase is more obvious for 1st to 4th floors when lift-up design was employed for the podium building. But ventilation potential was not improved for 5th to 7th floor when lift-up design was implemented.

4.4 Summary

In summary, the ventilation potential of the lower floors of the singular building, a row of buildings and the podium building with or without lift-up design has been evaluated. For the natural ventilation potential section, the current results are only for a single building block, if this building block is located in a dense city, the natural ventilation potential will be affected as the approaching wind is much smaller. But it can provide more natural ventilation potential when lift-up design is used.

With the lift-up design for the singular building, the pressure coefficients reduced at the area near to point A and increased at the area near to point B. The lift-up design has some influences on the pressure distribution for the side facades of the singular building or a slab of building, particularly the lower floors. The nearer to the building centre for the leeward façade, the more dramatic the increase of the negative pressures were found when lift-up design was implemented. The highest cross ventilation potential for the singular building was found on the first floor, while the smallest cross ventilation occurred at floor four for singular building. With the lift-up design, seventh floor had the lowest cross ventilation, while third floor had the highest cross ventilation. The lift-up design was helpful for the ventilation potential of the lower floors of a cluster of buildings or a slab of building. But its effectiveness is less noticeable for the 1st floor or slightly higher floor. For higher floors, ventilation potential was adversely affected.

The pressure patterns for the lower part of the building for RB1 and RB2 were similar. On the windward side for RB1 and RB2 alone, there were some positive pressures generated at the centre of the facades, but the remaining facades were negative. With the lift-up design, positive pressures were recorded on the entire façade. RB2 had both lower positive pressures and negative pressures compared to RB1. RB1 with the lift-up design achieved slightly higher positive pressure than RB2 with the lift-up design. For the side faces, some positive pressures were recorded near to point C for façade D-C with the lift-up design for RB1 and near to point G for façade H-G with the lift-up design for RB2. With the lift-up design, it helped to reduce the negative pressures to a lower level and some positive pressures were generated at the centre of the leeward façade. The ventilation potential for all the measured floors for RB1 and RB2 could be raised by utilizing the lift-up design. But the ventilation

potential of the central part of RB1 slightly decreased with the lift-up design than RB1 alone. RB2 with lift-up increased more pressure differences of different floors than RB1 with lift-up. According to this study, it has observed that the RB with the lift-up design is the building configuration that produces the greatest cross ventilation potential of all three building configurations.

The area of positive pressure coefficient was larger for the PB with lift-up design compared to the PB only. The negative pressure values were higher for the PB with the lift-up design, but the area of negative pressures was smaller when the lift-up design is applied. With the lift-up design, the negative pressure coefficients for the side façade increased more at the lower floors near to point B. The lift-up design decreased the negative pressure at the upper and lower floors near to centre of the building of the leeward façade. But it increased the negative pressures at the upper and lower floors near to point C of the leeward façade. The highest pressure differences for the podium building were found on the sixth floor. The smallest pressure differences occurred at third floor for the podium building. With the lift-up design, seventh floor had the lowest pressure differences, while first floor had the highest pressure differences. Ventilation potential increases were more obvious for 1st to 4th floors when lift-up design was employed for podium building. But ventilation potential did not improve for 5th to 7th floor with the lift-up design.

Chapter Five: Effects of building lift-up design on pedestrian wind environment

5.1 Introduction

Urban renewal is significant for many metropolises around the world. It is also a sustainable way of developing the community in terms of using land and infrastructure effectively. But constructing a new building will always affect the microclimate within its surrounding area, especially building some high-rise buildings inside the closely packed old areas. This can lead to low airflow or poor outdoor ventilation around the building blocks, which can negatively influence pollutant dispersion in the surroundings, indoor air quality and even increase risks of airborne transmission of infectious diseases. In recent years, emissions from vehicle exhaust have become one of the major urban air pollutions due to the dramatic growth of vehicle population despite significant improvements in fuel and engine technology (Vardoulakis et al, 2003). There are more than 100 types of harmful substances emitted from vehicular exhausts, such as tiny suspended particles (particulate matter), carbon monoxide (CO), nitrogen oxides (NO_x), sulphur dioxide (SO_x), hydrocarbons (HC), formaldehyde, benzene, lead etc. High concentrations of these pollutants due to ventilation stagnant or slow air movement area can exacerbate the harmful effects on the health of urban inhabitants. Conversely, high winds speeds can also be encountered in densely built up areas that can introduce discomfort or danger, such as flying debris or knocking over pedestrians. After the severe acute respiratory syndrome (SARS) epidemic hit Hong Kong in 2003 and the recent bouts of swine flu, awareness of wind environment and pollutant dispersion has been raised, especially in those environments with significant alterations by new constructions where either poor ventilation or strong wind concerns have been reported from the communities

(HKSAR Building Department, 2004). But maintaining the optimum air flow rate within a complex urban environment is always a challenge to achieve and quantify. Different buildings and urban designs can dramatically influence the wind environment but a balanced and satisfactory urban wind environment should be achievable through the effective planning and analysis of the designs.

The air flow patterns at pedestrian level around buildings and in particular, high-rise buildings, are generally complex. Although the wind environment has been investigated from the 1960s, Blocken and Carmeliet (2004) found that most of the studies conducted in the Wind Engineering community were mostly for investigating the numerous wind comfort criteria (Davenport, 1972, Hunt et al., 1976, Isyumov and Davenport, 1975, Lawson, 1973, Lawson, 1975, Lawson and Penwarden, 1975, Lawson, 1990, Melbourne, 1978, Penwarden, 1973, Penwarden and Wise, 1975, Tsang et al., 2012). With only a few studies focusing on the pedestrian level low wind speed and discomfort wind environment (Tsang et al., 2012) for different building designs. Buildings with the lift-up design have been particularly overlooked. But this kind of design is very common in dense metropolises such as Hong Kong. The majority of the city's large residential and retail developments have bus stops located underneath of the high-rise buildings. Pedestrian routes in and around these developments are inevitable which make these lift-up building designs an important and necessary area of investigation for future planning.

This research work studies three tall building configurations; singular building (SB), a row of buildings (RB) and a row of building with podium (PB). These were selected from a number of building designs that resulted in the lowest wind speed zones, identified in a previous study by Tsang et al. (2012). A 3.5m lift-up in prototype scale was added to each of the three

configurations producing three lift-up designs for comparison with the original designs. The purposes of this research are:

- To study the pedestrian level wind environment around three kinds of building configurations with and without lift-up designs.
- To assess the potential improvement of low wind speed zone at the pedestrian level by lift-up design.
- To discover the discomfort zone at the pedestrian level of these different building types and to research whether the lift-up design can exacerbate the discomfort area.

5.2 Research Methodologies

More than 200 Irwin probes have been used to measure the mean and simultaneous wind speed at the pedestrian level at the same time which is 2m in prototype size. The detailed measurement equipment and procedures, please refer back to Chapter two.

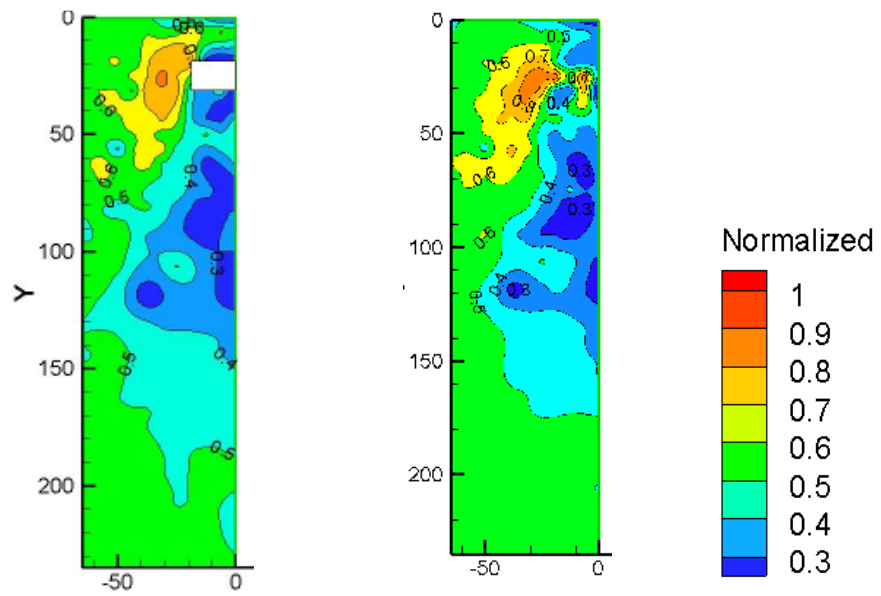
5.3 Results and Discussion

Tsang et al's (2012) work investigated pedestrian level winds with emphases on the features and impacts of low speed winds over a large extent of areas downstream of the modern building configurations (i.e. singular building, a row of buildings, podium building). Effects on pedestrian comfort under strong wind conditions were also examined. In the current study, all these investigations have been reproduced. Meanwhile, low wind speed and gust wind speed for the selected modern configurations from Tsang et al's (2012) with the lift-up design had also been provided in this study. The results between the lift-up design and non-lift-up design had been compared.

5.3.1 Pedestrian mean wind conditions

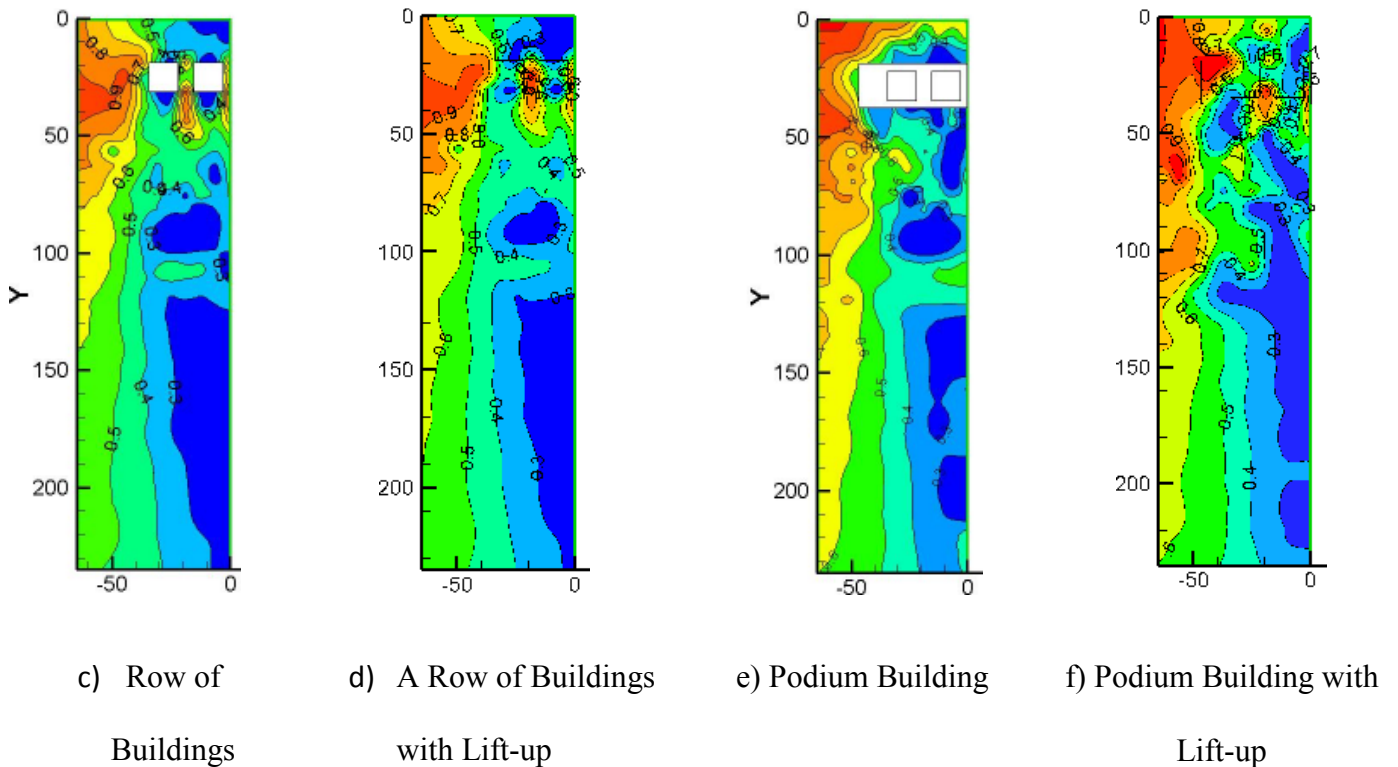
An average wind flow can be represented by an average or mean wind speed with an averaging time, such as 10 min or an hour. However, the gust wind typically measures with an averaging period of 2 to 3 seconds. For maintaining a good naturally ventilated environment, an average wind flow is a more appropriate measure. Consequently, in this study, mean wind speeds were used to characterize the low wind speed zones where inadequate or poor air ventilation may occur due to insufficient available winds or the wind blocking effects by obstacles. Mean wind speed at pedestrian level at any interested point was normalized by the reference mean wind speed of the approach flow at 150m in prototype scale. The normalized mean wind speed (U/U_r) was applied due to its ability to readily incorporate a particular wind climate to determine the statistics of wind speeds, in terms of magnitude and probability of occurrence. For instance, in Hong Kong, the mean wind speed at 150m is around 5m/s to 6m/s for 50% probability of exceedance (Irwin et al. 1969). The minimum wind speed for human at the pedestrian level is around 1.5m/s in order to achieve thermal comfort or pollutant dispersion (Lawson & Penwarden, 1975). This means a normalized mean wind speed (U/U_r) around 0.3, and areas with U/U_r lower than 0.3 can be designated as low wind speed zones (LWS), which is unfavourable for maintaining a good natural ventilation environment. On the other hand, the gust wind is a more representative measure for the pedestrian discomfort caused by overspeed wind. High speed steady winds and instantaneous strong winds are both important elements for pedestrian comfort under strong wind conditions.

5.3.1.1 Mean wind speed pattern of SB, RB and PB with and without lift-up design



a) Singular Building

b) Singular Building
with Lift-up



c) Row of
Buildings

d) A Row of Buildings
with Lift-up

e) Podium Building

f) Podium Building with
Lift-up

Figure. 5-1. Distribution of the normalized mean wind speed with and without lift-up design for different building configurations

The general features of the normalized mean wind speed distribution of singular building, a row of buildings and podium building without 3.5m height lift-up design are shown in Figure. 5-1a), Figure. 5-1c) and Figure. 5-1e) respectively. On aggregate, there are four low wind speed zones for these three building configurations with or without the lift-up design: an upstream far-field low wind speed (UFLWS) zones; an upstream near-field low wind speed (UNLWS) zones; a downstream near-field low wind speed (DNLWS) zone and a downstream far-field low wind speed (DFLWS) zone (Tsang et al, 2012). In all these figures, the normalized pedestrian-level mean wind speed distribution (U/U_r) ranges from 0.0 to 1.0. The normalized mean wind speeds is approximately 0.5 when no building is installed. Reasonable threshold values for outdoor wind comfort and air ventilation purpose are from 0.3 to 0.8. Areas with the normalized mean wind speed lower than 0.3, illustrated in dark-blue in the Figures are designated as low wind speed zones, which is equivalent to mean wind speeds roughly 1 to 2m/s for an annual probability of exceedance of 50% in an environment like Hong Kong.

For the building configurations without the lift-up design, the wind hits the windward façade of the building and a downwash flow is generated. This downwash effects on the windward face of the building can form the UFLWS zone. It also results in a revised flow in front of the building at pedestrian level, approximately along the centreline upstream of the building. When the two opposing windward and backflows encounter each other, a low wind speed zone is created at the upstream of buildings. The UNLWS zone is located at the stagnant area bounded by the ground and the windward face of the building. In terms of wake flow for non-lift-up design, recirculation due to building blockage is occurring in the downwind near-field which generates the rotational flow that induces the formation of vortices. This is indicated by the low pressure zone on the leeward side of the building, caused by both the horizontal

and the vertical recirculation. This poor ventilation zone is called the DNLWS zone. As for the downwind far-field area, the observed low wind speed zone is due to the reattachment of vertical recirculation behind the building and strength of the horizontal recirculation. This low wind speed zone is addressed as the DFLWS zone. All these types of flow features had already been identified in Tsang et al's study (2012). In the current study, these results can be well reproduced.

The general patterns of the normalized mean wind speed distribution of a singular building, a row of buildings and podium building with 3.5m height lift-up design are provided in Figure. 5-1b), Figure. 5-1d) and Figure. 5-1f) respectively. On the whole, the low or poor ventilation situation of the upstream near-field has been improved due to 3.5m lift-up areas underneath. This is because part of the downwash and the approaching wind can flow through the lift-up area of the buildings that can reduce blocking of the flow. Consequently less backflow wind and approaching wind meets in front of the building at the pedestrian level. But the natural ventilation for the UNLWS zone is getting larger for a row of buildings with the lift-up design. A reduction of wind speeds at the far-field upstream is observed for all the lift-up buildings. This is likely due to the increased downwash effects because the lift-up design increased the building height by 3.5m. From Figure. 5-1, it can be noted that the largest UNLWS and UFLWS zones are RB with lift-up, and take up 2/3 of the upstream area right in front of the buildings. By contrast, singular building with lift-up design for has the minimum low wind speed area among the three.

In the downstream area, it is found that the singular building with lift-up can not only improve air flow for the surrounding area of the building, but also significantly shorten the length of the wake flow. A row of buildings with the lift-up design also remarkably reduces the size of the DNLWS zone. But only slightly diminishes the DFLWS area. Contrarily,

although these effects can still be identified for the DNLWS zone for podium building with lift-up design, area for the DFLWS zone is getting even larger. This can be attributed to stronger horseshoe vortices, created by the stronger downwash which covered around the building and strengthened right behind the building. Therefore, the DFLWS zone for all these three building configurations with the lift-up is smaller. Despite there being three to four central cores for these three building configurations, mean wind speeds at the pedestrian level of the underneath part of the building with the lift-up design are all higher than 0.3.

5.3.1.2 Improvement of mean wind speed distribution with lift-up design

In order to better illustrate the improvement of wind distribution at the pedestrian level with lift-up design, the ground area is separated into eight different zones. This enables simpler and more direct comparisons between the non-lift-up design and lift-up design. One of the key criteria of splitting these zones is based on the building width (b). But splitting the podium building, it depends on the podium width (b) for podium building. The detailed separation is illustrated below in Figure. 5-2.

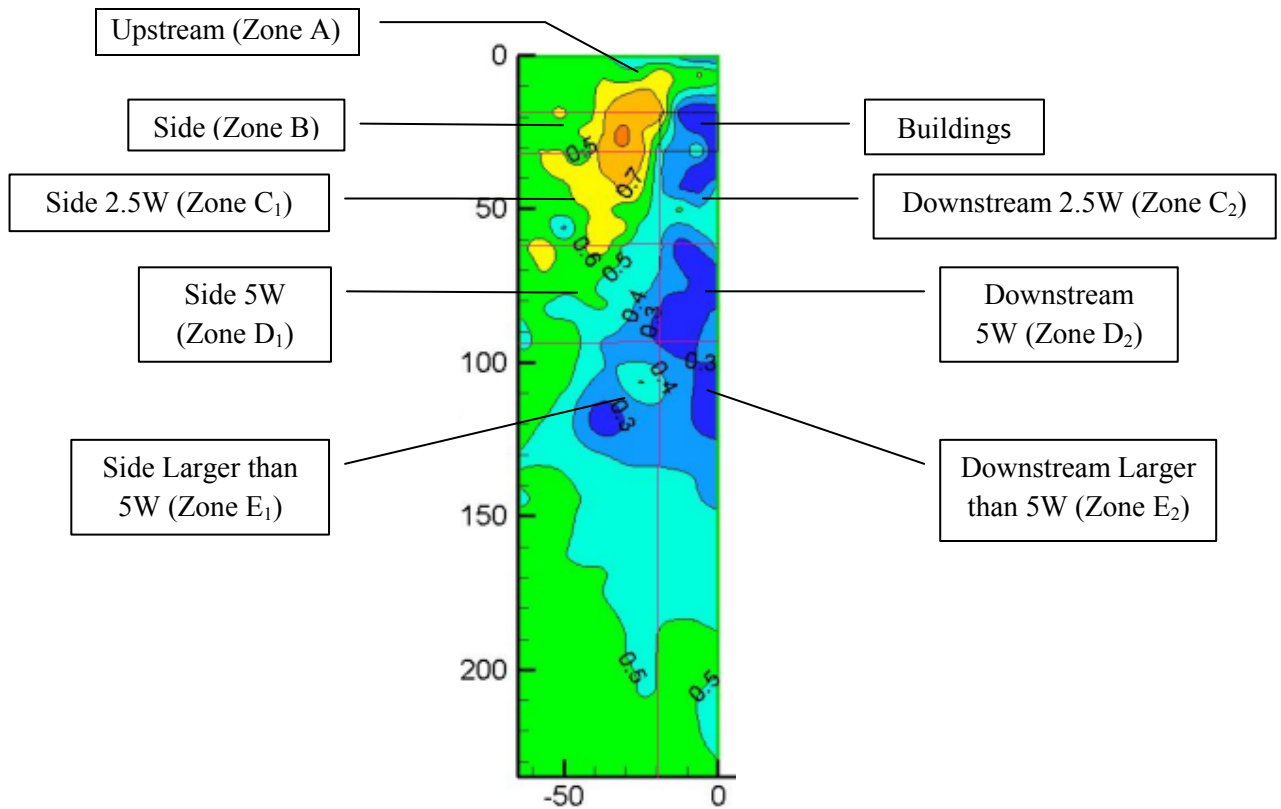
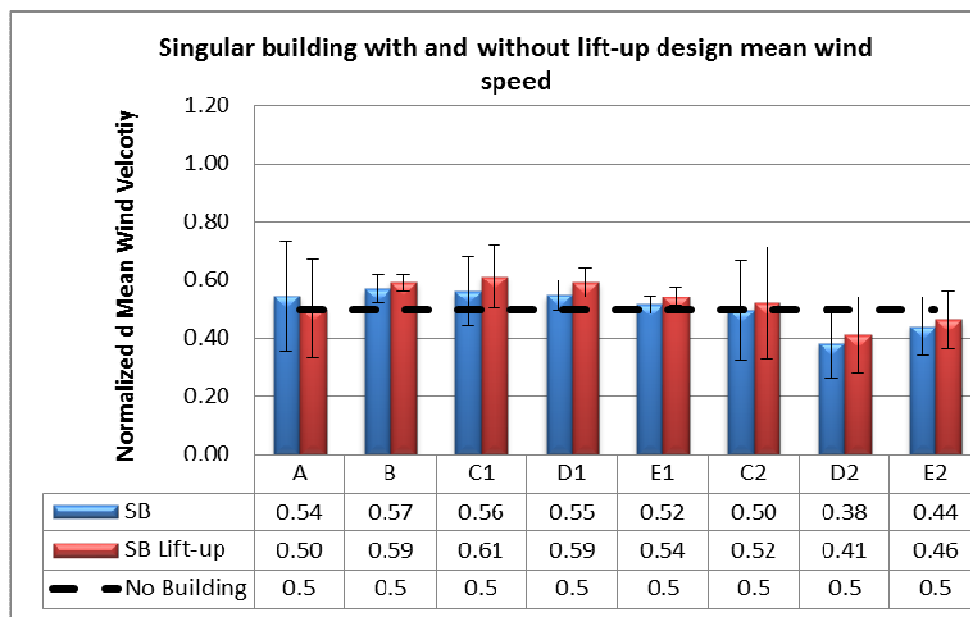


Figure. 5-2. Eight different zones for pedestrian wind speed measurement

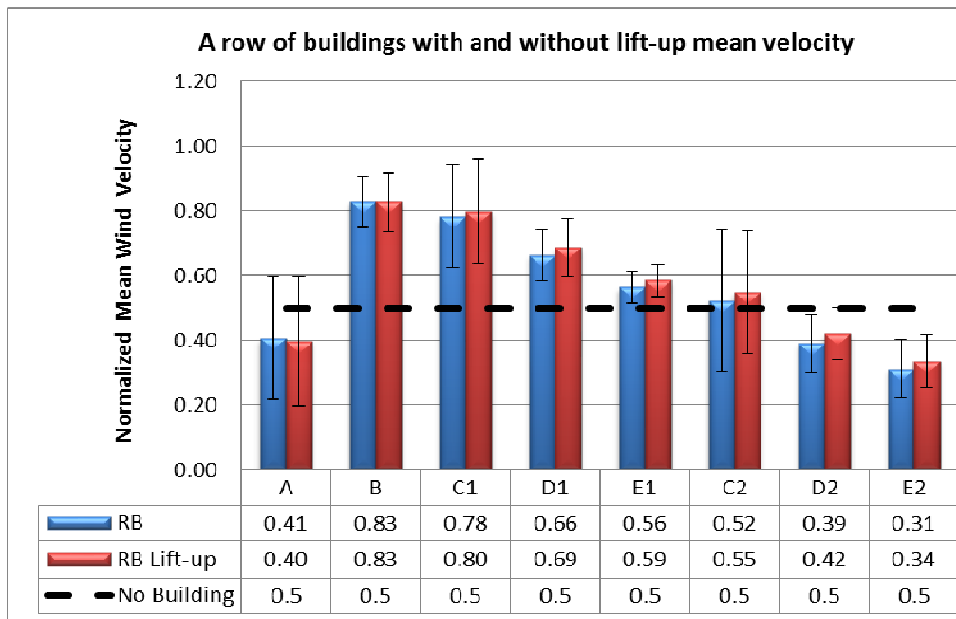
Mean wind speed for these eight different zones for singular building, a row of buildings and podium building with and without lift-up design are presented in Figure. 5-3a) to Figure. 5-3c). They all show lower mean wind speeds for the upstream areas in all buildings configurations with the lift-up. Whereas mean wind speeds are consistently higher in the remaining seven areas of singular building with the lift-up design. The rising percentages of the mean wind speed are from 4% to 10%. This suggests that urban planners and/or buildings architects can improve ventilation in ground level public areas by introducing the lift-up design for singular buildings. This can benefit public and communal facilities such as playgrounds, parks, car parks, swimming pool, etc. Those facilities would see improved ventilation if placed in any of the areas except for zone A or at least a building width away from the building to account for changing wind directions.

For the row of buildings, Zone A results show a very marginal increase in wind speed of 1% whereas zone B shows no change, and all the remaining zones show increased mean wind speeds with the lift-up. The percentage increase of the mean wind speed range from 3% to 11%. Consequently, similar to the singular lift-up building, public facilities located in areas other than zone A or B would see improved natural ventilation.

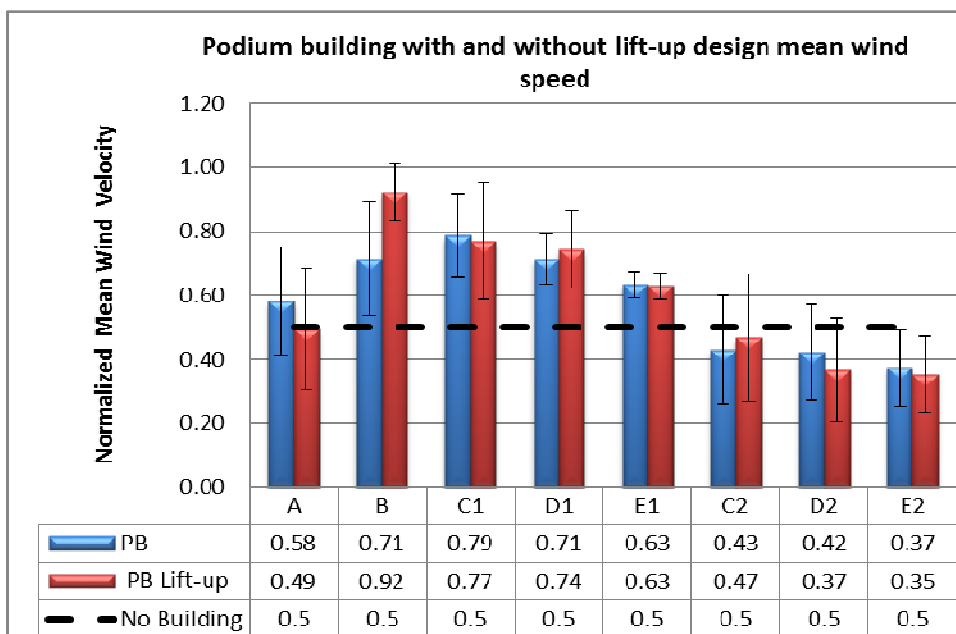
The mean wind speed results for the podium buildings are much more variable with a similar number of zones showing increases as decreases. For the downstream areas, normalized mean wind speed has been improved 4% for the lift-up design at zone F, whereas airflow is reduced at zones D₂ and E₂. This is contrasted by improved air flow down the side parts of the building, particular at zone B which has the best improvement a. Zone C shows a significant reduction in wind speed with the lift-up design. Therefore, areas of public congregation located in zones B, D, E₁ and C₂ will see improved ventilation if a lift-up design is introduced. Zone B exhibits the most enhanced wind as it improves approximately 30% with the lift-up design.



a). Singular building with and without lift-up design



b). A row of buildings with and without lift-up design



c). Podium building with and without lift-up design

Figure. 5-3. Normalized wind speed distribution for different zones for different building configurations

5.3.1.3 Measurements underneath the buildings with lift-up design

A limited number of measurement probes have been employed for the singular building and podium building with lift-up designs, while no wind speeds were measured underneath of a row of buildings with lift-up design, which are occupied by the large central cores (Table 1).

The two wind speed measurement points are located right beneath singular building. Probe 031 is between two central cores and the other probe 071 is on the other side of one of the central cores. Plan of measurement points underneath singular building is giving in Figure 5-4a). The normalized wind speeds in these two points are about 0.9, indicating relatively high speed.

The normalized mean wind speeds underneath the podium building with lift-up design are shown in Figure. 5-b). 20 measurement points under the podium building are provided in Figure. 5-a). Most of the normalized mean wind velocity beneath the building is from 0.4 to 1.2. Only four measuring points show the normalized a mean wind velocity of under 0.4. Therefore, most of these areas exceed the low wind speed zone classification. These results all confirm that the open ground floor has a good wind velocity.

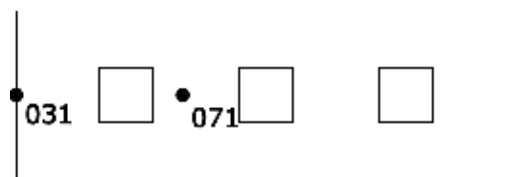


Figure 5-4a). The two measurement points underneath the singular building

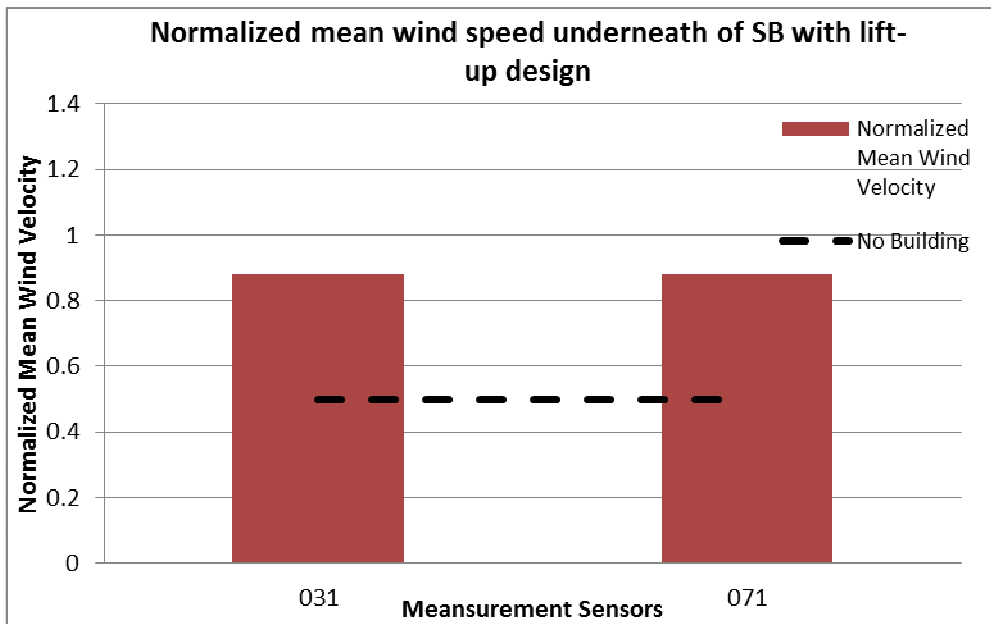


Figure. 5-5b). Normalized mean wind speeds at the two points beneath the singular building with lift-up design

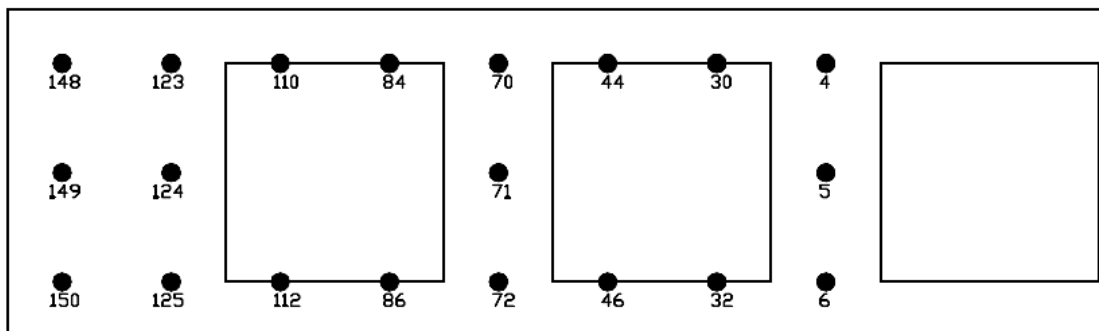


Figure. 5-6a). Measurement points underneath podium building

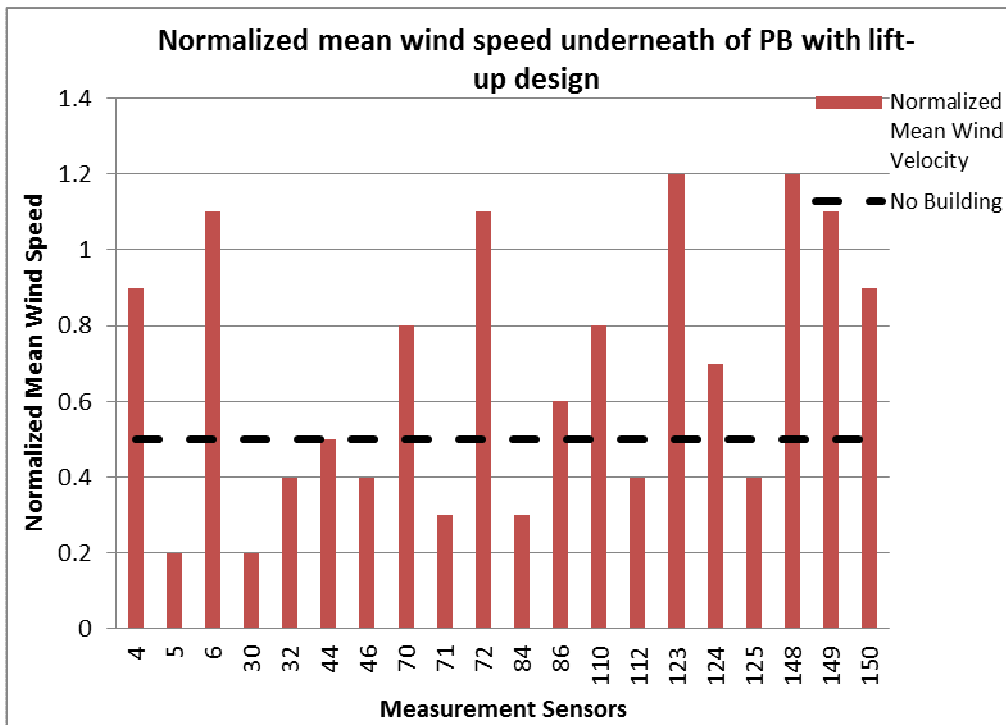


Figure. 5-7b). Normalized mean wind speed beneath podium building with lift-up design

5.3.2 Pedestrian comfort under strong wind conditions

5.3.2.1 Gust Equivalent Method (GEM) wind speed analysis

The method utilised for analysing gust wind is called the ‘multiple extremes method’. This method determines the 3 second gust wind speed by averaging the maximum wind speed in each of the five independent samples. The duration of each independent sample is exactly 1 hour at prototype scale. In this analysis, the GEM wind speed (U_{GEM}) was normalized by the reference mean wind speed U_r of the approaching flow at 150m above ground level at full scale.

According to Lawson’s comfort criteria, the threshold for the maximum allowable GEM wind speed for comfortable business walking at pedestrian level is 10m/s with a 5% probability of exceedance (Lawson, 1990). However, in Hong Kong, the equivalent wind speed at 150m is around 12m/s to 13m/s for a probability of exceedance of 5%. Thus, the

corresponding U_{GEM}/U_r for Hong Kong is approximately 0.8 and areas with a U_{GEM}/U_r value higher than 0.8 were designated as high wind speed zones. This level is considered to cause potential discomfort from the strong winds at pedestrian level.

5.3.2.2 GEM wind distribution around singular building, a row of buildings and podium building with and without lift-up design

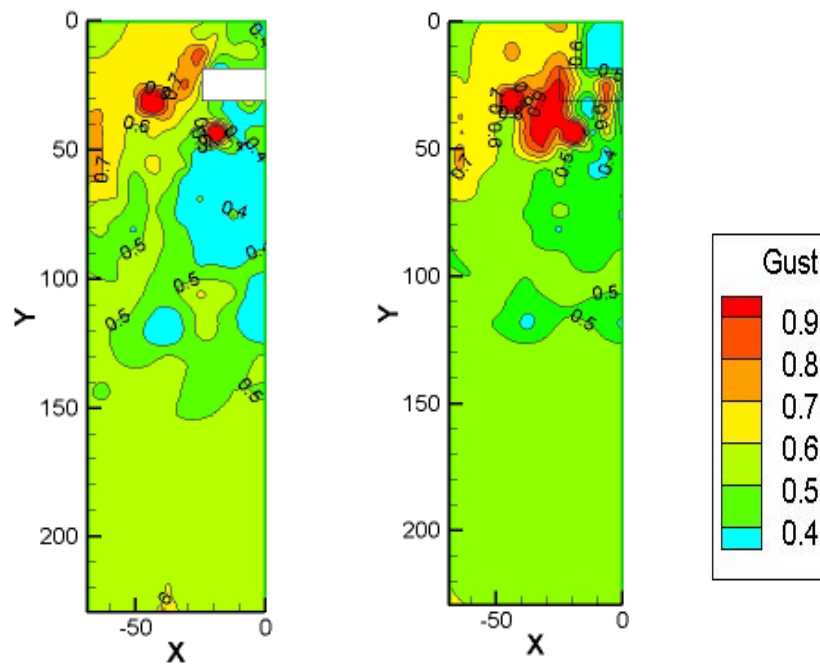
The normalized GEM wind speed distributions (U_{GEM}/U_r) are given in Figure 5-8, or singular building, a row of buildings and podium building with and without the lift-up design.

Generally, for every building configuration, the maximum GEM wind speed occurred at the upstream or side corner of the building, which can be divided into Lateral High Wind Speed (LHWS) zone; the other high speed zone occurs between two adjacent buildings while can be called Middle High Wind Speed (MHWS) zone, indicated in Figure 5-8c) respectively. The downwash from the windward façades of the building generates the high wind speed horseshoe vortices. It accelerates around the building group. Therefore, LHWS zone is created. On the other hand, MHWS zone has only been observed for a row of buildings and singular building with lift-up and podium building with lift-up.

The side corner LHWS zone for the singular building with lift-up is much larger than that without lift-up. In Figure 5-8a) and Figure 5-8b) it is apparent that the wake flow has increased dramatically with the 3.5m lift-up design for the singular building, whereas the upstream area is reduced. A new high wind speed area is introduced between the two central cores which lift-up the building.

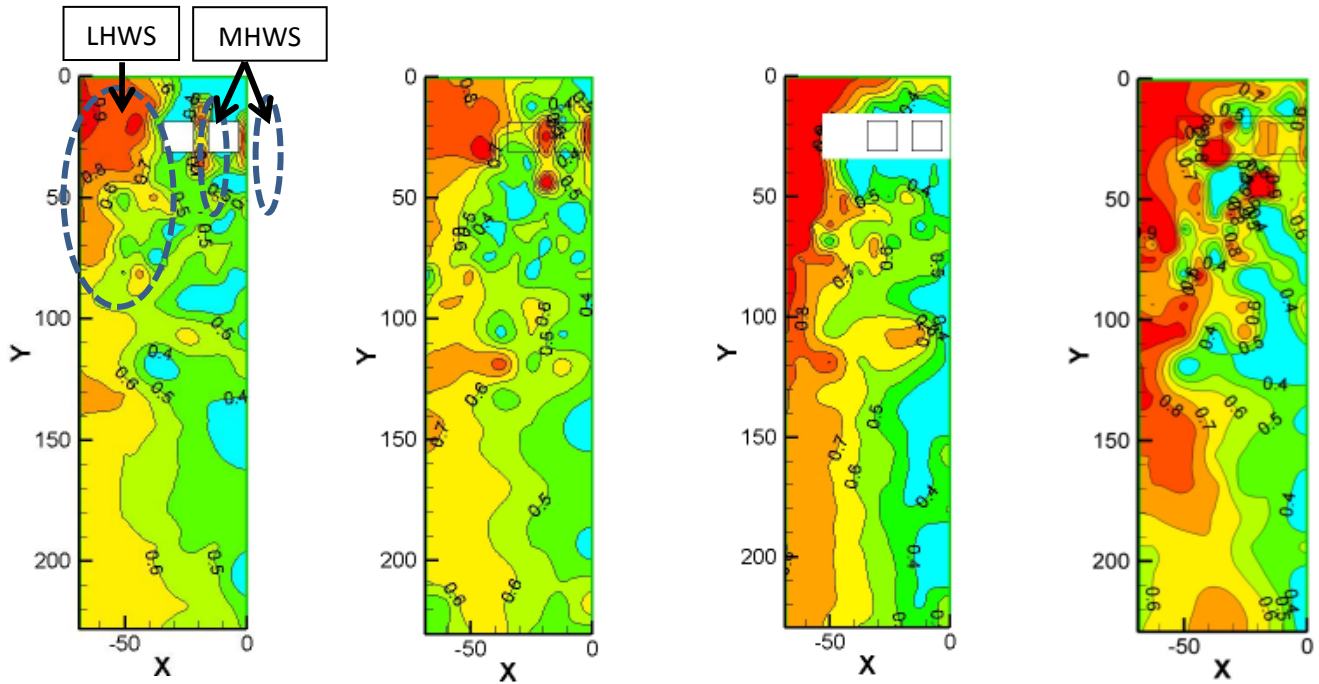
For a row of buildings, the air flow upstream of the building elevates notably by the lift-up design. The size of LHWS zone is slightly smaller for the lift-up design. In contrast, the MHWS zone becomes greater (Figure 5-8c) and Figure 5-8d)).

For the podium buildings, the LHWS zone can reach $5W$ ($W = \text{Podium Width}$) downstream from the building. But the LHWS zone covers approximately half of the upstream area of podium building (Figure 5-8e)). With the lift-up design, the flow pattern changes slightly though the LHWS zone still occupies nearly half of the upstream. In the wake area, the LHWS zone extends $3W$ along the size of the building, and a second LHWS zone stretches from $5W$ to $6W$ in the leeward direction. Interestingly, there is no MHWS zone between the 3.5m high centre cores, but another high wind speed zone appears right after the building.



a) Singular Building

b) Singular Building
with Lift-up



c) A Row of Buildings d) A Row of Buildings with lift-up e) Podium Building f) Podium Building with lift-up

Figure 5-8. Distribution of the normalized GEM wind speed with and without lift-up design for different building configurations

5.3.2.3 Gust wind speed distribution with lift-up design

In this section, a clear discussion regarding to gust wind speed distribution for different building types has been carried out below. It is complicated to conclude whether the lift-up design can induce more discomfort zones than the one without. In order to have better illustrations of the gust wind distribution at the pedestrian level with lift-up design, the Irwin probe measurement layout has been split into the same eight different zones as used in Section 3.1.2. After calculating the gust wind speed for each point, the gust wind speed for each zone is estimated by averaging number of probes inside that zone.

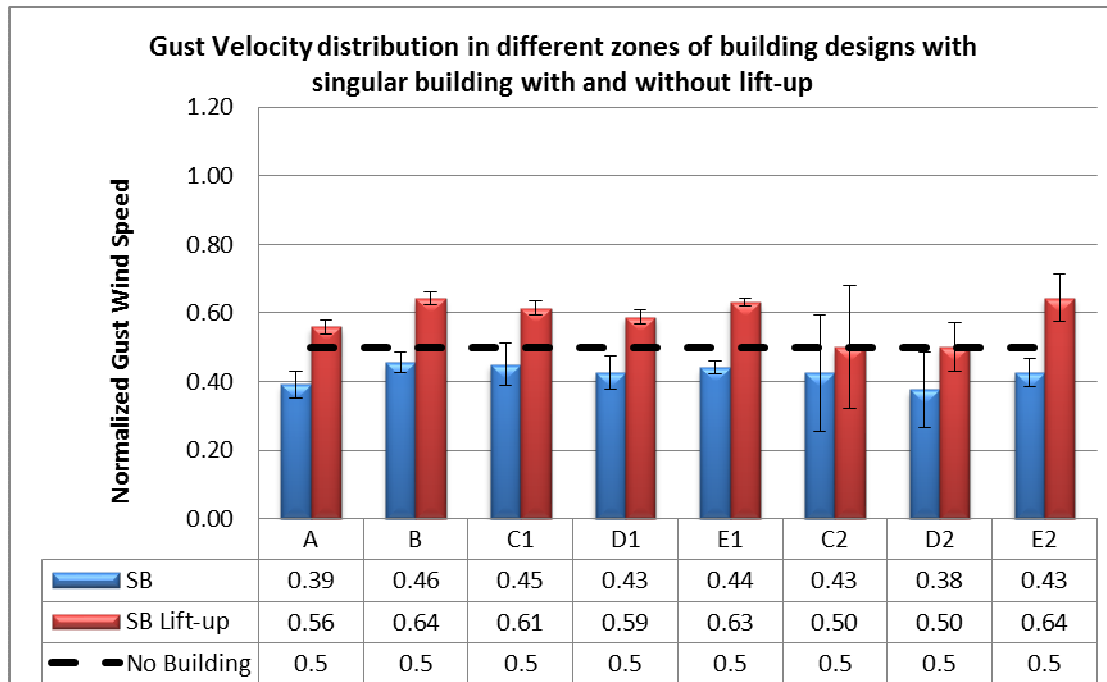
Generally speaking, the lift-up design increases the gust velocity magnitudes for the majority of the zones, particularly for the singular building. This sees significant increases in gust wind speeds for all zones of up to 16% as shown in Figure. 5-7a). However, gust velocity

speeds for zone D_1 and C_2 are slightly less due to the blockage effect of the singular building. The technique of averaging the wind speeds within each zone has masked the localised discomfort zones that were evident in Figure 5-9a) and Figure 5-9b) and discussed previously in Section 5.3.2.2.

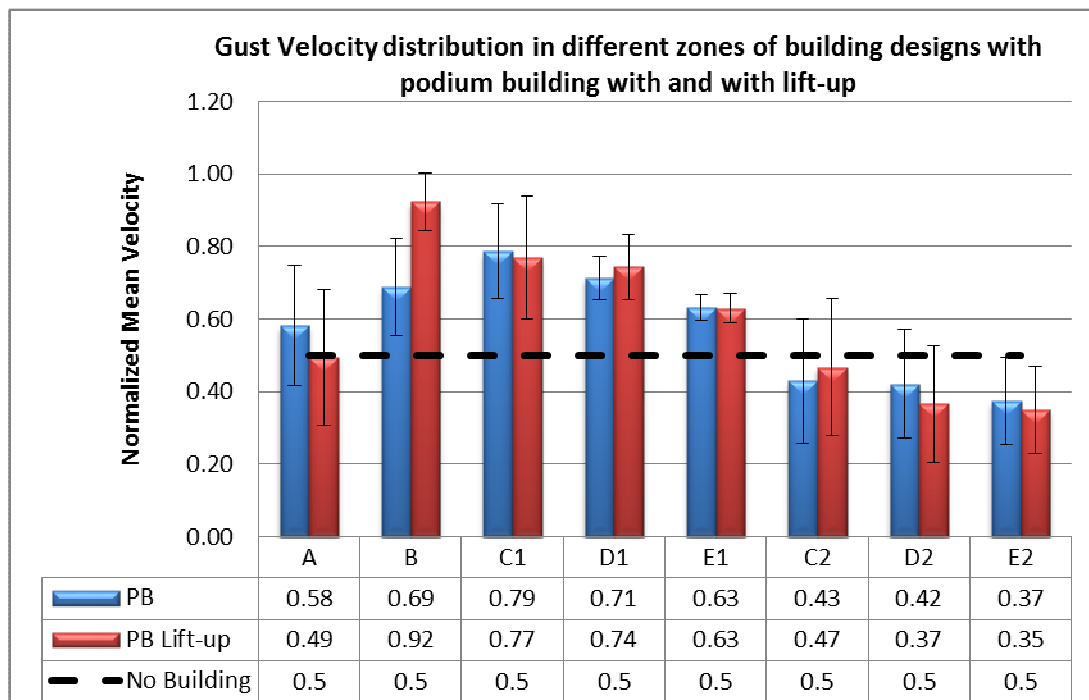
For a row of buildings, the lift-up design shows the greatest increase in gust wind speed at the upstream and adjacent to the buildings zones. Though moderate increases are also seen in zones A, B, C_1 and D_1 . But for the downstream areas zones D_2 and E_2 show lower gust wind speeds. In general, the variation for the gust wind speed among these eight zones with the lift-up design for a row of buildings is small, which means the lift-up design has limited affects in reducing discomfort for pedestrians under a strong wind environment. Figure 5-7b) also shows that a high wind speed zone appears at zone B where normalized gust wind speed exceeds 0.8. When the standard deviation is included into the results, zone C_1 also exceeds 0.8. Therefore, zones of pedestrian discomfort will appear at zones B and C_1 for a row of buildings with and without lift-up design.

A similar result is observed for the podium building as shown in Figure 5-7c). But a dramatic rise in gust wind speed for podium building with lift-up design is seen of up to 30% in zone B. The results show potential high wind speed zones for podium building with lift-up design occurring at zones B, C_1 and D_1 as their standard deviation 0.8. But the potential high wind speed zones for the podium building alone occurred only at zones B and C_1 . This suggests that the areas of the high wind speed zones have been enlarged by the lift-up design. With the lift-up design, it is only the podium building that has seen a reduction in upstream gust wind. The reduction is also seen in zones D_2 and E_2 which are further away from the building. But higher magnitude of gust wind speed is recorded in zone C_1 with the lift-up design.

Nonetheless, downstream gust wind speed distribution is under a comfortable gust speed range with and without the lift-up design.



a). A row of buildings with and without lift-up design



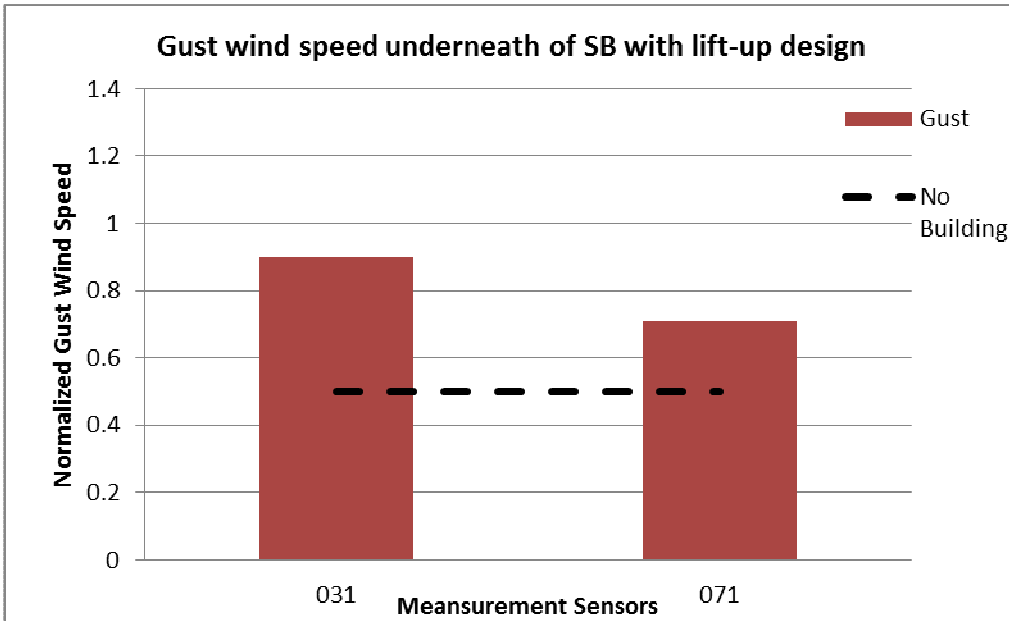
b). Podium building with and without lift-up design

Figure 5-9. Gust velocity distribution in different zones for different building configurations

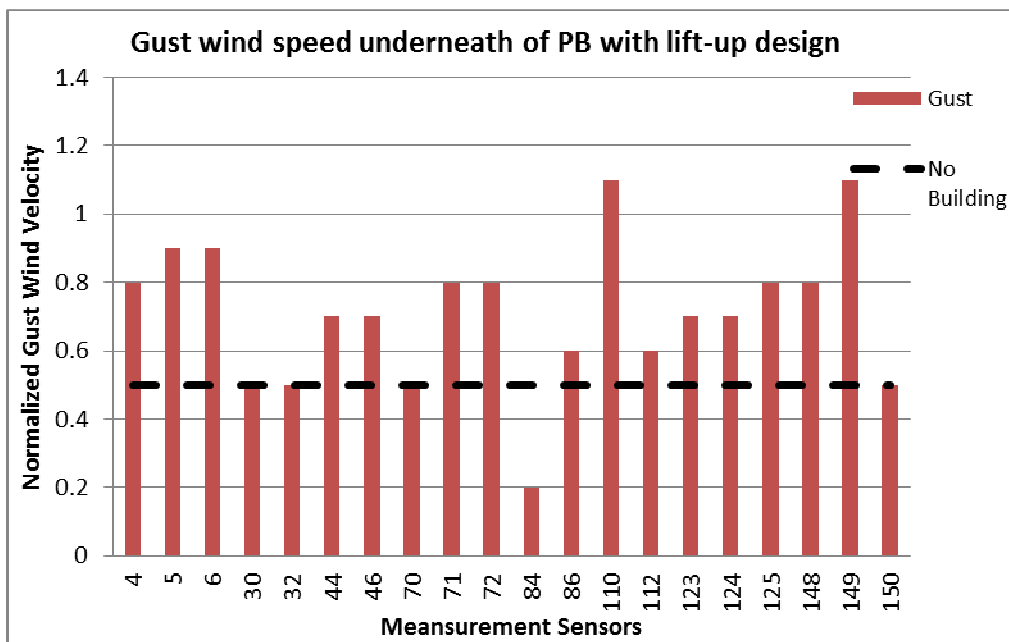
5.3.2.4 Measurements underneath of the buildings with lift-up design

In this section, normalized gust wind speeds underneath of singular building and podium building with the lift-up design have been plotted in Figure 5-10a) and Figure 5-10b) to illustrate the discomfort areas of the lift-up area caused by the gust wind speed. The measurement probes beneath the singular building and podium building with lift-up designs are exactly the same as in Section 5.3.1.3. For the singular building with lift-up design, probe 031 records a high normalized gust wind speed of around 0.9. The probe is located in a particularly sensitive position between two central cores, where funnelling of the wind flow is occurring as it flows between the constricting building cores which results in a discomfort zone. Probe 071 is on the other side of one of the central cores, the normalized gust wind velocity is only at 0.7 which is within the comfortable range.

Underneath the podium building, normalised gust values from the majority of the probes lay within the range from 0.5 to 0.9 and at reach 1.12 probes. Almost half of the probes below the podium show a normalized gust wind speed over 0.8, which shows the lift-up design for the podium building does introduce quite significant areas and magnitudes of wind discomfort for pedestrians beneath the podium.



a). Singular building with lift-up design



b). Podium building with lift-up design

Figure 5-10. Normalized gust wind speed distribution underneath different building configurations

5.4 Summary

The general features of the low and gust wind speed areas around singular building, a row of buildings and podium building with and without lift-up designs were identified experimentally. It was found that there is an improvement for the low speed areas at the pedestrian level with lift-up design for singular building and a row of buildings. But for the podium building where wind speeds are generally greater, the lift-up design does not necessarily improve the pedestrian level wind environment. In terms of discomfort caused by a strong wind environment, the lift-up design brings a significant increase of the normalized gust wind speed, particularly for the singular building. There are more areas of wind discomfort created by the lift-up design compared to the one without. But the downstream low wind environment is substantially improved with better natural ventilation.

The variations of the normalized gust wind speed between a row of buildings with and without the lift-up design is very minor. With the introduction of the lift-up design in the podium building, there is a significant change in the gust wind speeds adjacent and upstream of the building but downstream is largely very similar. Beneath the singular building and podium building with lift-up, there is significant likelihood of discomfort caused by strong winds.

For a tropical and sub-tropical climate, a lift-up design for a slab building or a cluster of buildings may be considered by architects or urban planners as an effective means to improve the air movement for pedestrians. But conversely, excessive air movement due to strong winds would also need to be considered. Central cores of the buildings should not be placed too close to each other to avoid generating discomfort zones due to the channel effect. In a temperate or cold climate, the lift-up design may not be desirable when increased wind speeds coupled with low temperature may cause additional discomfort to pedestrians. A lift-

up design for a row of buildings for enhancing pedestrian level wind is not as noticeable as for a singular building; the arising normalized gust wind speed with lift-up design is minor as well. Basically, the wind environment is fairly unchanged if a 3.5m lift-up design is implemented. The podium building with lift-up design improves air flow in selective areas without causing additional wind discomfort zones to pedestrians. Additional studies are recommended to determine the effectiveness of lift-up design by considering the influence of lift-up height, spacing between cores, interference/shielding by upstream and/or downstream buildings, and angle of wind incidence.

To satisfy both thermal comfort and maximum mean wind speed is always difficult. For this stage of the research, it is only goes so far as investigating how effective the lift-up design is in changing the natural ventilation potential, wind environment and thermal comfort and finding out which building configuration is the most effective design on all these aspects while lift-up design is implemented. From a building-services-engineering perspective, deciding whether mean wind speed or gust wind speed is the most important wind speed depends on the location being investigated. For instance, in Hong Kong, stagnant flow is much more common compared to the gust wind speed. In this case, mean wind speed will be looked into more than the gust wind speed. After that, during typhoon season, strong wind might also cause potential problems for pedestrians as well if the lift-up design is implemented. In this case, wind breaks could be used for the safety of the pedestrians.

Chapter Six: Thermal Sensation of different building configurations with and without lift-up design under different weather conditions

6.1 Introduction:

After the outbreak of the severe acute respiratory syndrome (SARS) in 2003, creating an acceptable macro wind environment in the city for people's health and comfort has become a major issue of the Planning Department of the Hong Kong Government. Thermal sensation is one aspect of urban environment quality. Therefore, it is necessary and interesting to analyse the thermal comfort environment of buildings with and without the lift-up design under different seasonal data.

Many different models and indices were developed during the second half of the 20th century for estimating the complex influence of atmospheric thermal environment on human being. Thermal bioclimatic assessment has been done, and many different indices, such as heat stress index, discomfort index (Thom, 1959), wind-chill index (Steadman, 1971) or similar ones, have been developed that are based on atmospheric parameters such as air temperature, humidity, wind speed etc, but do not include the effect of radiation fluxes. Therefore, thermo-physiological regulatory processes were not taken account into and there were various limitations (Mayer and Hoppe, 1987; Hoppe, 1999). In order to estimate the relationship between atmospheric environment and human health in a more relevant way the methods of heat balance of humans are used (Burton and Edholm 1955; Fanger, 1972; Hoppe, 1999). Two different main thermal indices had been introduced. One is called predicted mean vote (PMV) combined with predicted percentage discomfort (PPD). The other is called physiological equivalent temperature (PET). But they are applied under very different conditions. PMV is a thermal index developed by Fanger (1972). It has been used for

predicting the mean value of the thermal sensation votes of a large group of people based on six variables: metabolic rate, clothing insulation, air temperature, radiant temperature, air speed, and humidity. It is rated on a 7-point scale ranging from -3 (cold) to +3 (hot) (ASHRAE 2004). PMV has been widely used for estimating the subjective thermal comfort of an indoor environment at steady state. But Hoppe (2002) and Nikolopoulou et al. (2001) reported that PMV could inaccurately predict the thermal comfort level for outdoor environment. Often, thermal sensation in hot climates has been overestimated towards the warmer end of the scale by PMV. It has been underestimated by PMV towards the colder end of the scale in cold climates. PET is a thermal index from the Munich Energy Balance Model for Individual (MEMI) which is a heat balance model of the human body. It is equivalent to the air temperature in a typical indoor sitting at which the heat balance of the human body is maintained, with core and skin temperature equal to those under the conditions being assessed (Hoppe 1999; Matzarakis et al. 1999). PET is normally used under steady state outdoor environment, but it does not require pre-calibration of the range of PET for different grades of thermal stress. Comparing two methods, PET has been chosen for this research the outdoor environment is going to be analysed.

In the current study, the primary aims are:

- To study the pedestrian-level thermal comfort environment around SB, RB and PB configurations with and without lift-up design under summer and winter climatic conditions.
- To assess the potential improvement of thermally discomfort area at the pedestrian level by lift-up design during summer and winter season.

- To conclude the benefits and drawbacks of utilising the lift-up design on the thermal sensation at different seasons and how to make the building designs to be more efficient for providing a neutrally thermal conditions for the pedestrians.

6.2 Research Methodology

According to Cheng et al's (2010) study, two predictive formulas have been adopted for analysing the thermal sensation and overall comfort, which is based on PET. Formulas for predicting thermal sensation were developed using linear regression analysis with four independent variables: air temperature, wind speed, solar radiation intensity and absolute humidity. Absolute humidity truly represents the moisture content of air.

The following two equations are representing summer and winter respectively.

Summer data:

$$TS = 0.1895TA - 0.7754WS + 0.0028SR + 0.1953HR - 8.23 \text{ (correlation coefficient } R = 0.87) \quad (7.1)$$

Summer + winter data, without humidity:

$$TS = 0.1185TA - 0.6019WS + 0.0025SR - 2.47 \text{ (correlation coefficient } R = 0.90) \quad (7.2)$$

Where,

TA = dry bulb air temperature (°C)

WS = wind speed (m/s)

SR = solar radiation intensity (W/m²)

HR = absolute humidity (g/kg air)

Absolute humidity is used here because it is a truer representation of the moisture content in the air sample, whereas relative humidity represents moisture content relative to saturation at a given temperature. Therefore the temperature variable adds an additional parameter that unnecessarily complicates the formula adopted by Cheng et al. (2010). By using the above two equations, thermal sensation can be calculated and be rated on a 7-point scale from -3 (cold) to +3 (hot). Normally, neutral thermal sensation (TS=0) is corresponding to a state of thermal comfort. Different levels of thermal sensation (TS) is given in the below table.

Table 6-1: Different levels of thermal sensation

Thermal Sensation	
-3	Cold
-2	Cool
-1	Slightly Cool
0	Neutral
1	Slightly Warm
2	Warm
3	Hot

In the current project, only summer and winter have been considered for calculating the thermal sensation at the pedestrian level. The climatic data showing below has been selected from the Hong Kong Observatory website. Only the weather data from 2013 has been used here. Mean wind speed is measured at the height of 83m above the sea level by an

anemometer in Waglan Island in Hong Kong. Two extreme weather conditions have been selected for this study: one is the hottest month; the other is the coldest month. From the below table, it can be noticed that the hottest month is August which provides 28.6°C dry bulb temperature; and the coldest month is December which has 16.1 °C dry bulb temperature.

Table 6-2: 2013 weather data from Hong Kong Observatory

Month	Dry Bulb Temp (deg.C)	Mean Dew Point (deg.C)	Mean Relative Humidity (%)	Total Bright Sunshine (hours)	Mean Daily Global Solar Radiation (MJ/m ²)	Mean Wind Speed (km/h)
January	16.7	11.3	71	184.0	12.62	21.2
February	19.1	15.4	80	98.7	11.51	22.6
March	20.5	16.5	79	12.4	11.78	19.5
April	21.5	19.0	86	53.6	8.98	22.9
May	25.7	23.2	86	90.7	12.29	19.7
June	28.2	25.1	84	146.1	15.83	23.4
July	28	25.1	85	156.9	16.18	20.3
August	28.6	25.3	83	148.1	14.50	22.7
September	27.5	23.9	82	186.0	15.98	27.4

October	25.7	18.6	66	247.3	17.11	23.6
November	21.7	16.2	72	133.4	11.14	30.5
December	16.1	8.6	63	197.4	12.20	24.9

It is known that the normalized mean wind speed at the pedestrian level is calculated by measured mean wind speed over the reference wind speed at 150m prototype height. Based on the mean wind speed from the above table, the reference equivalent mean wind speed at prototype 150m height in the wind tunnel experiment can be calculated, using the power law formula. Additionally, the measured mean wind speed data at the pedestrian level for singular building, a row of buildings and podium building with and without the lift-up design can be utilized for thermal sensation analysis. Assuming the same normalized mean wind speed for different measured points at the pedestrian level for August and December, all the measured mean wind speed at the pedestrian level in August and December can be estimated accordingly.

With regards to solar radiation intensity, the above table only provides the total bright sunshine hours and mean daily global solar radiation. The sunshine hours per day can be assessed by the total bright sunshine hours over number of days in the relevant month. Mean daily global solar radiation over the total sunshine seconds per day can give the solar radiation intensity.

6.3 Results and Discussion

6.3.1 Thermal sensation under summer conditions

In summer, overall speaking, the thermal sensation values are positive in most of the area due to the high temperature, solar radiation and moisture content.

In the below figure, contour diagrams of singular building, a row of buildings and podium building with and without lift-up design under summer conditions has been given. During summer season, most of area is in the range of thermal sensation value from 0 to 2.5 for singular building. Some area next to the building side is in the range of -1 to -1.5. at downstream area drops from a higher value to neutral thermal sensation level which is 0. This implies that more area at the pedestrian level can achieve better thermal comfort when lift-up design is used for singular building, particularly in the downstream area. But, the thermal sensation value right in front of the singular building is slightly higher when lift-up design is implemented. Comfort area is created underneath and adjacent part of the singular building when lift-up is utilized.

For a row of buildings with and without lift-up design, the contour diagram does not vary too much for thermal sensation distribution. This suggests that the effect of lift-up design is not obvious at the pedestrian level for a row of buildings. Therefore, lift-up design does not bring a better thermal environment for people at the pedestrian level, particularly at some upstream are , slightly higher thermal sensation value can be achieved.

Interestingly, when lift-up design is implemented, the overall thermal pattern at the pedestrian level has changed much the most obviously for podium building compared to singular building and a row of buildings. For podium building alone, majority of the area is in the range of 0 to 2.5 for thermal sensation value. Some area at the side of the building is within

the range of 0 to -2. But on the far left hand corner side, thermal sensation with the range of -0 to 3.5 appeared, which means this area is cold even for the hottest month of the year. When lift-up design is used thermal sensation value at the left-hand corner became very hot. Its value can reach as high as 3.5. Most of the remaining upstream area keeps its thermal sensation value at the neutral level when lift-up design is used. Right behind the building, thermal sensation value is also lower when lift-up design is utilized.

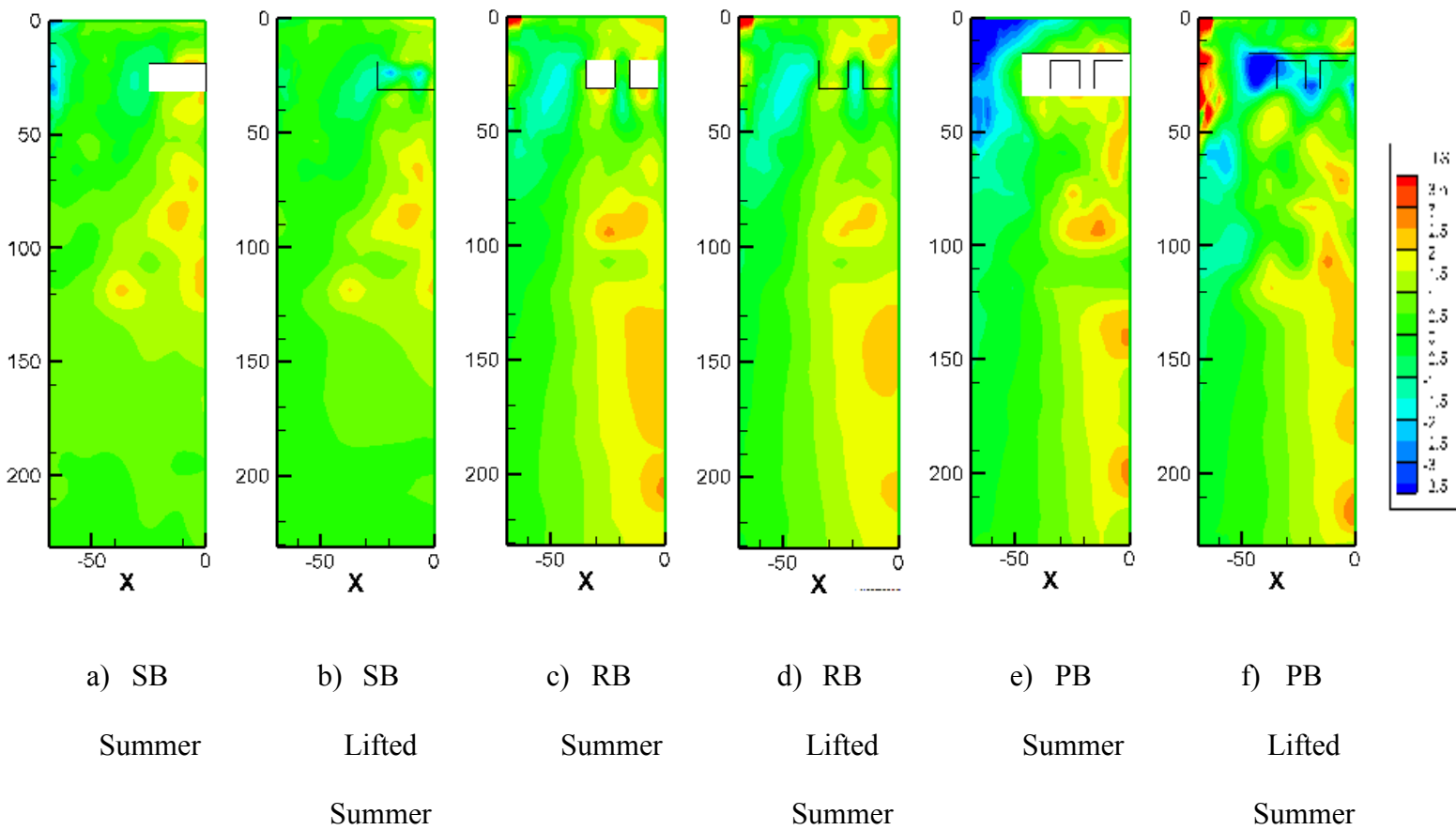


Figure 6-1: Contour diagram of SB, RB and PB with and without lift-up design under summer climatic conditions

In order to have a better illustration of comparing how effective lift-up design is for thermal sensation at the pedestrian level for different building configurations. An exact the same method of separating measuring area into different zones in Chapter five has been adopted in this chapter. One of the key criteria of splitting these zones is based on the building width (b).

But splitting the podium building, it depends on the podium width (b) for podium building. The detailed separation is illustrated below in Figure. 6-2.

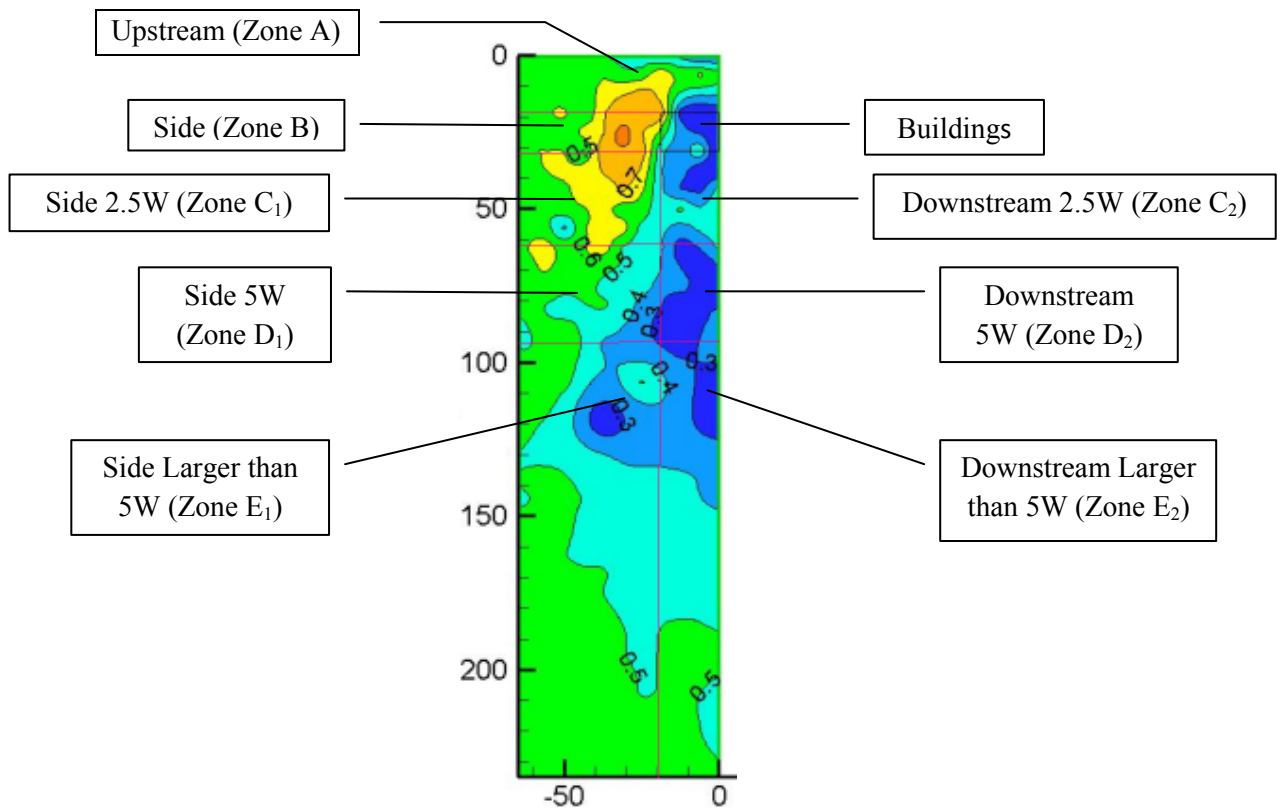


Figure. 6-2. Eight different zones for pedestrian wind speed measurement

7.3.2.1 Summer Conditions

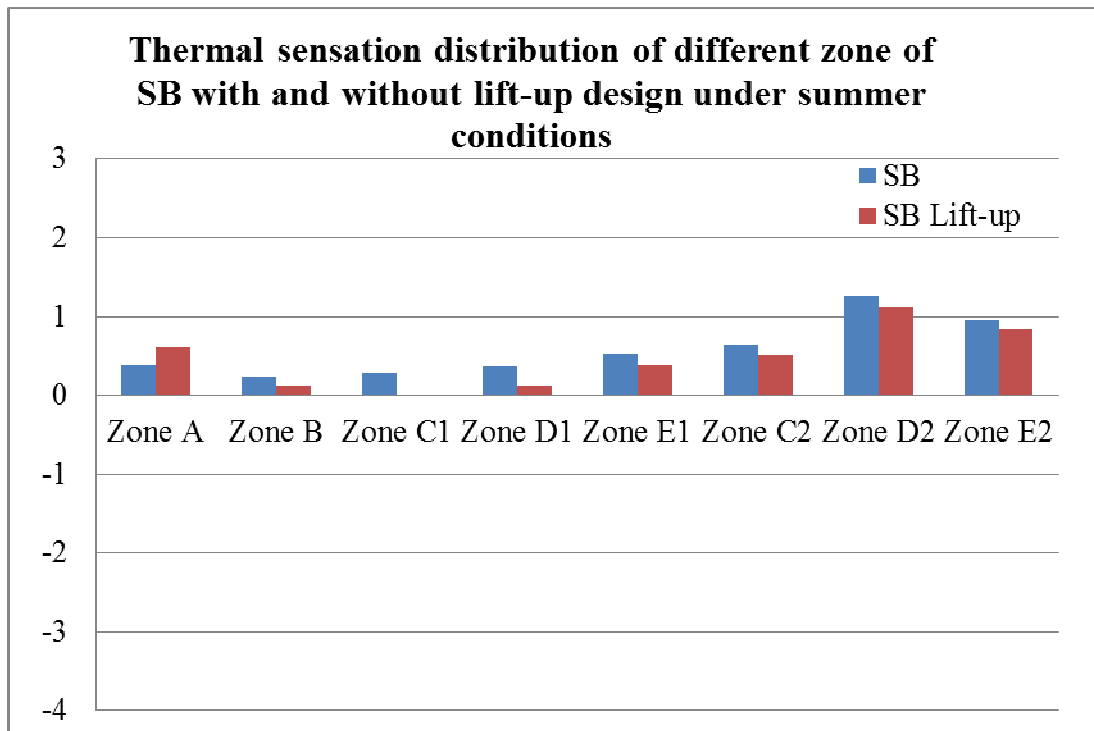
Thermal sensation distribution for these eight different zones for singular building, a row of buildings and podium building with and without lift-up design under summer climatic conditions are presented in Figure 6-3a) to Figure 6-3c). Generally speaking, all of the zones for singular building with and without lift-up design have positive values for thermal sensation at the pedestrian level and the thermal sensation level for most of the zones are under 1 apart from Zone D₂. This implies that people at the pedestrian level feels quite comfortable for singular building with and without the lift-up. In terms of the necessity of

lift-up design for singular building is concerned, interestingly, all the zones apart from zone A for singular building, thermal sensation value is getting lower when the lift-up design is used. The thermal sensation distribution has been dropped at least 14%, the most significant reduction zone is zone C_1 which can reach more than 52 times dropping. The second significant reduction zone is zone D_1 that can achieve more than 1.9 times dropping. It indicates that singular building configuration is the most efficient building configuration among the three to apply lift-up to improve thermal sensation at the pedestrian level. This also suggests that the lift-up is really useful for singular building, a slab of building to improve the thermal environment for people at the pedestrian level. This suggests that urban planners and/or buildings architects can improve thermal comfort in ground level public areas by introducing the lift-up design for singular buildings in summer. This can benefit public and communal facilities such as playgrounds, parks, car parks, swimming pool, etc, particularly in summer season. Those facilities would see improved thermal comfort if placed in any of the areas except for zone A.

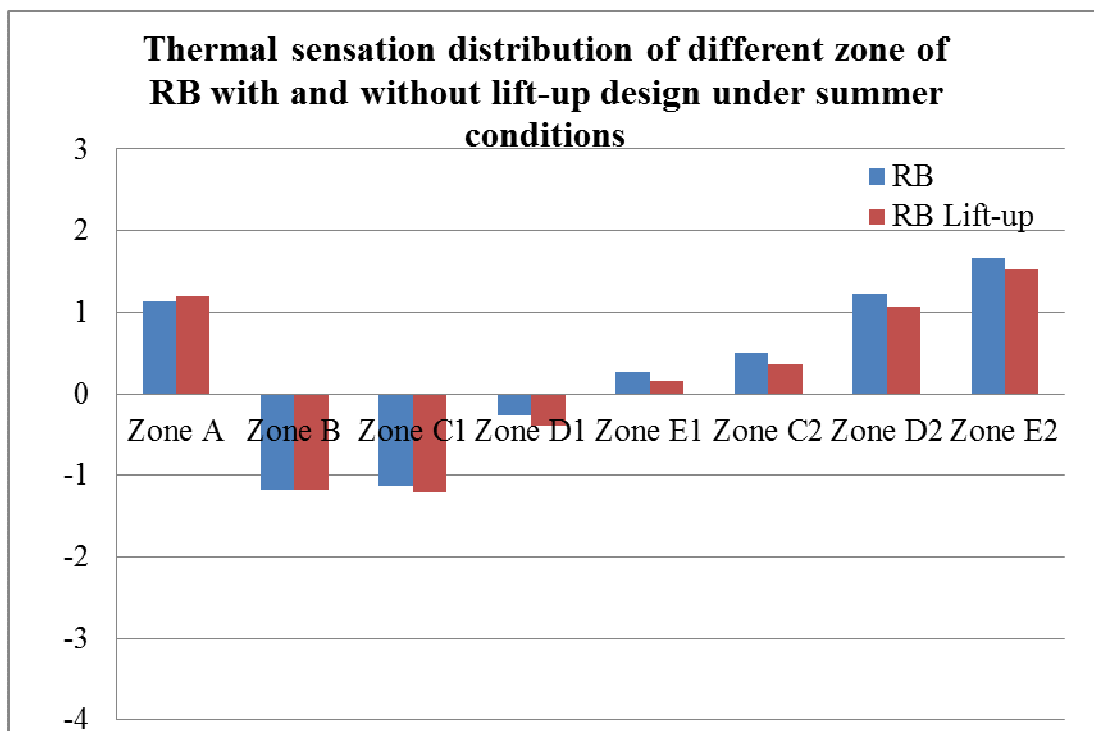
For a row of buildings, zone B and C_1 are having the negative thermal sensation level, the remaining zones are all having the positive thermal sensation level. Thermal sensation level in zone D_1 , E_1 and C_2 is under 1 or -1, which illustrates that the thermal sensation level is neutral and people feels comfortable at these zones. On the other hand, people at zone A, D_2 and E_2 feel slightly warm or near to warm while the thermal sensation level is over 1. Adversely, pedestrians feel slightly cool for zone B and C_1 . For all the downstream zones, thermal sensation levels are decreasing varied from 8% to 41% while lift-up design is utilized. But the largest decreasing zone for thermal sensation level is not locating at downstream of a row of buildings when lift-up design is applied. It is placed at the side of the building zone E_1 . The reduction of thermal sensation level while lift-up design is implemented can reach to

77%. Additionally, marginal decrease in thermal sensation could be found for zone B when lift-up design is used, and the remaining zones show increase of thermal sensation while lift-up design is adopted. Consequently, public facilities located in areas other than zone A or C₁. Although people feel slightly warmer while lift-up design is used for zone D₁, the average zonal thermal sensation level is still pretty low, which is lower than -1. Therefore, people at the pedestrian level should still feel quite comfortable here. This implies that lift-up design is only useful to improve the thermal environment for certain zones at the pedestrian level, particularly for the downstream level.

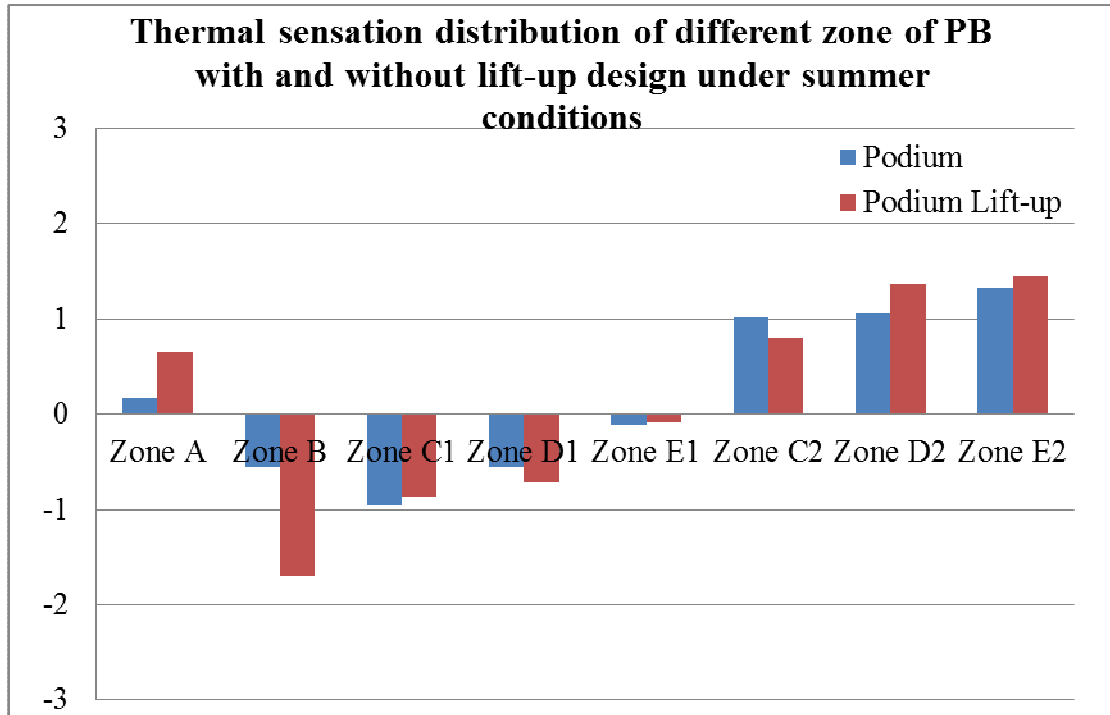
The thermal sensation results for the podium buildings are much more variable with a similar number of zones showing increases as decreases. For the downstream areas, thermal sensation has been decreased 3% for the lift-up design at zone C₂, whereas it is increased at zones D₂ and E₂. While for the side areas, thermal sensation has been decreased 1% at zone D₁ and 2% at zone E₁, whereas it is increased at the rest of zones. Additionally, people should feel comfortable for zone A, B, C₁, D₁, E₁ and C₂ for podium building at the pedestrian level, but slightly warm at the remaining zones. When lift-up design is used, people will feel slightly warm at zone, D₂ and E₂ and cool at zone B. These data for podium building with and without the lift-up design indicates that lift-up design does not improve the thermal environment for the pedestrians much.



a) Singular Building



b) A row of buildings



c) Podium building

Figure 6-3. Thermal sensation distribution of different zone of different building configurations with and without lift-up design under summer conditions

6.3.2 Thermal sensation under winter conditions

In winter, generally speaking, majority of the measured area provides negative thermal sensation value when lift-up design is implementing or not. This means lower mean wind speed, lower temperature, lower solar radiation and no humidity can bring much lower thermal sensation for pedestrians in winter compared to summer.

In the below figure, contour diagrams of singular building, a row of buildings and podium building with and without lift-up design under winter conditions has been given. During winter season, most of area is in the range of thermal sensation -1 to -2 for singular building. Some area next to the building side is in the range of -2 to -3.5. When lift-up design is utilized, thermal sensation value at the side of the building increases till -1.5 or -2. This indicates that lift-up design can eliminate the cold environment to cool environment at the

side of the building. Although it might still causes discomfort for the pedestrians, the uncomfortable thermal sensation level is much lower. In terms of neutral thermal sensation level is concerned, singular building with or without the lift-up design brings similar area, but some area underneath of the singular building with the lift-up design has neutral thermal sensation level at the pedestrian level.

For a row of buildings with and without lift-up design, the contour diagram does not vary too much not only in the thermal sensation value but also in the thermal pattern. This suggests that the lift-up design does not bring a better thermal environment for people at the pedestrian level for RB. Adversely, when lift-up design is used, slightly lower thermal sensation value can be achieved at some side area of a row of buildings. In terms of neutral thermal sensation is concerned, its coverage area is even less when lift-up design is implemented. But thermal sensation values underneath of the a row of buildings with the lift-up design are all neutral, which implies people should have a comfortable thermal environment at those area in winter.

Interestingly, when lift-up design is implementing, the overall thermal pattern at the pedestrian level has changed much more dynamically for podium building compared to singular building and a row of buildings. For podium building alone, there is a large area at the side the podium building covers thermal sensation value from -2.5 to -3.5. The neutral thermal sensation area mainly appears downstream of podium building. When the lift-up design is utilized, the coverage of thermal sensation value from the range of -2.5 to -3.5 is reduced significantly at the side of the building. Even some area becomes neutrally thermal comfort. On the other hand, the thermal environment underneath of podium building with lift-up is generally quite cold at the pedestrian level.

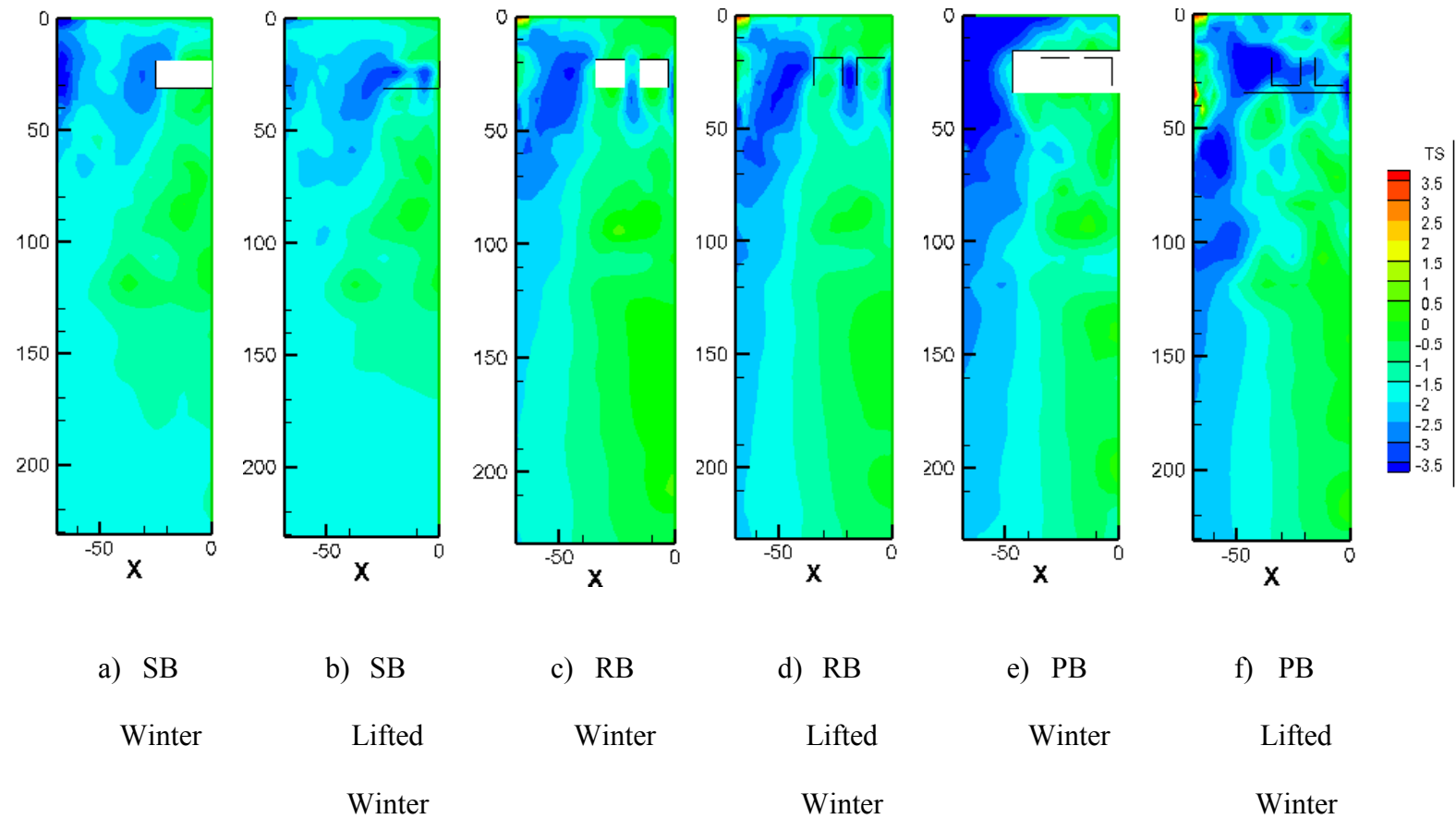


Figure 6-4: Contour diagram of SB, RB and PB with and without lift-up design under winter climatic conditions

6.3.2.2 Winter Conditions

Thermal sensation distribution for these eight different zones for singular building, a row of buildings and podium building with and without lift-up design under summer climatic conditions are presented in Figure 6-5a) to Figure 6-5c).

Generally speaking, all of the zones for singular building with and without lift-up design have negative values for thermal sensation at the pedestrian level and the thermal sensation level for all the zones are under -1. This implies that people at the pedestrian level for all the zones feels slightly cold for singular building with and without the lift-up. In terms of the necessity of lift-up design for singular building is concerned, interestingly, all the zones apart from zone A for singular building, thermal sensation value is getting higher negative when the lift-

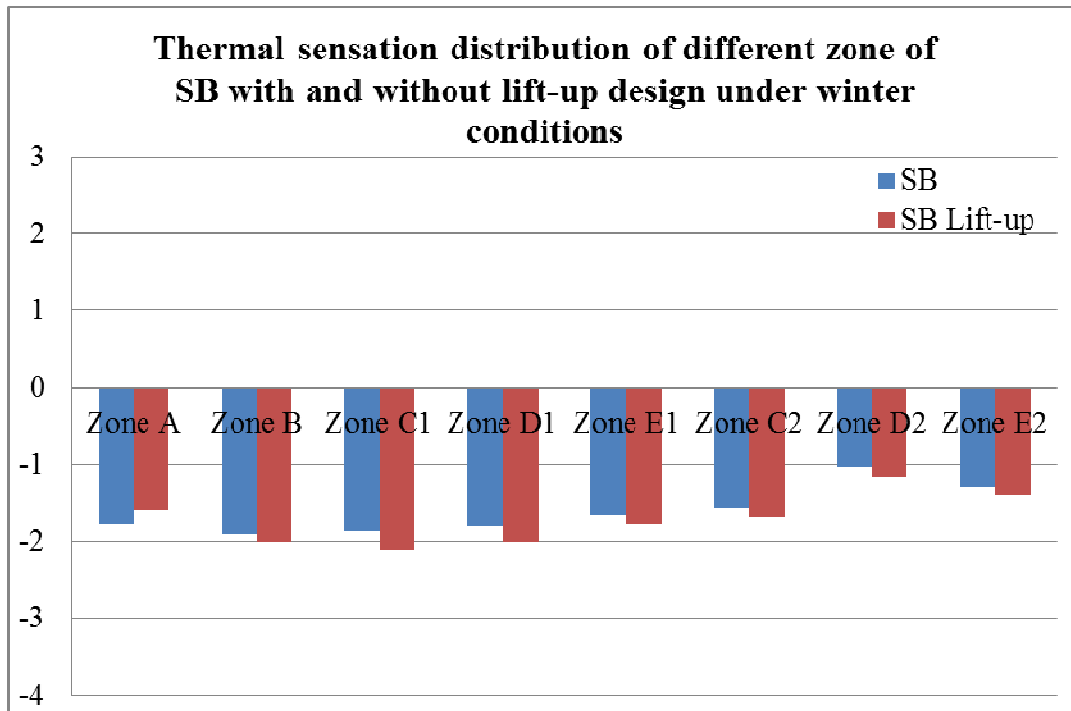
up design is used. The increase in thermal sensation discomfort varies from 5% to 11%, the most significant increasing zone is zone C₁. The second significant increasing zone is zone D₁. On the contrary, zone C₁ and D₁ are the two most significant decreasing zones in thermal discomfort during summer period for singular building when lift-up is used. This is probably because of the much colder air temperature in winter. Consequently, pedestrians do not require a much cooler environment in winter to bring down the equivalent temperature like in summer. Adversely, people probably need to have a warmer environment. But with higher wind speed due to lift-up design, less solar intensity and colder air temperature in winter, lift-up design might bring even more discomfort.

For a row of buildings, thermal sensation values are all negative values in winter. Generally speaking, people at the side of a row of buildings with and without lift-up design are generally feeling cold. People located at the downstream or upstream of a row of buildings with and without lift-up are feeling cool or slightly cold. Apart from zone A and zone B are providing marginally lower thermal sensation values, the remaining zones are all giving higher thermal sensation levels which varies from 2% to 13%. Zone E₂ increased the highest discomfort while lift-up design is used; zone D₂ has the second highest discomfort while lift-up is used. Therefore, the increase of discomfort level is much more obvious in the downstream area of a row of buildings while lift-up design is implemented. But it is slightly less at the side and in the upstream of a row of buildings while lift-up is used. People can feel most uncomfortable in zone B, C₁ and D₁ no matter the lift-up is implemented or not. Pedestrians can feel slightly cold in zone A, E₁, C₂ and D₂ no matter the lift-up is used or not. On the other hand, people in zone E₂ have the least discomfort whether the lift-up is utilized or not.

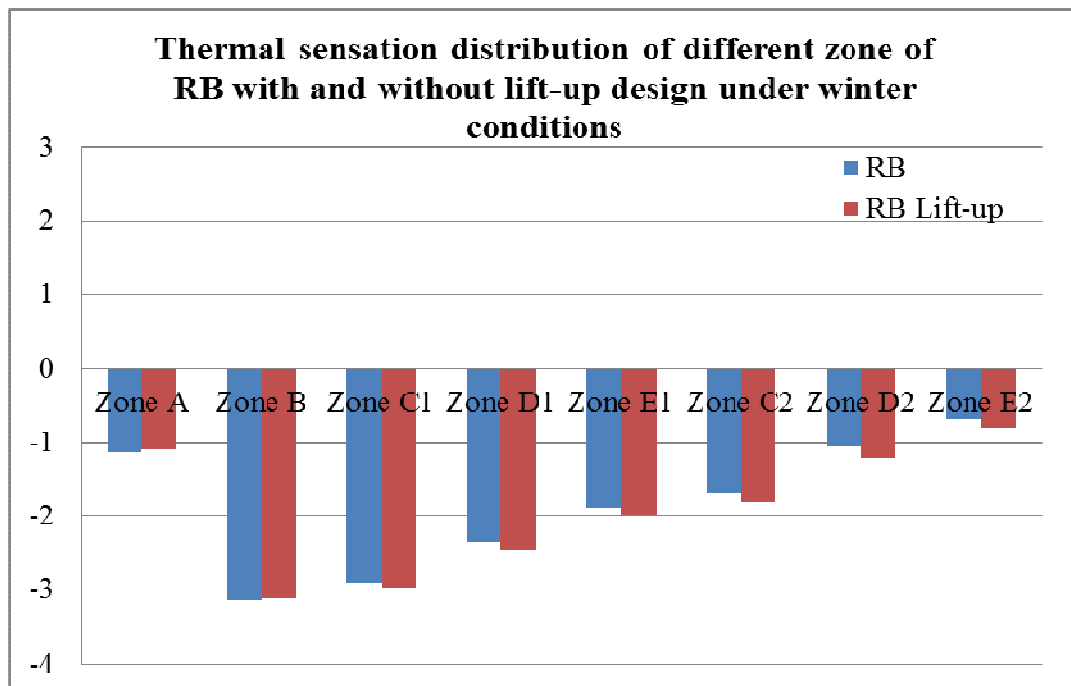
The thermal sensation results for the podium buildings are much more variable with a similar number of zones showing increases as decreases. All the zones are showing negative thermal sensation levels. People at the side of the podium building with and without lift-up design are generally feeling cold. People located at the downstream or upstream of the podium building with and without lift-up are feeling cool or slightly cold. Zone D₂ and E₂ at the downstream area reduced thermal sensation level most dynamically while lift-up is used, which was from 11% to 27%. People could feel different thermal comfort environment while lift-up is implemented at these two zones, while is from slightly cold to cool. The increase of thermal sensation level for zone A while lift-up design is used is 26%. But zone C₁ and E₁ at the side of the podium building only provide marginally increase of thermal sensation level while lift-up design is used. These suggest that the lift-up design is quite useful for decrease thermal sensation level for most of the zones for podium building under winter conditions, the most significant decreasing area is downstream area. Interestingly, zone B is the area has the highest increasing thermal discomfort for podium building no matter in winter or summer climatic conditions while lift-up design is implemented.

Among the thermal sensation distribution of different zones of these three different building configurations with or without the lift-up design under winter conditions, it can conclude that in winter, all the zones only provide negative thermal sensation values for these three building configurations with and without the lift-up design. Comparatively, singular building with or without the lift-up design can provide the most comfort thermal environment among the three building configurations in winter, particularly at the side area of the building. Lift-up design does not benefit so much significantly for singular building or a row of building at the pedestrian level under the winter climatic conditions, but it does benefit for quite

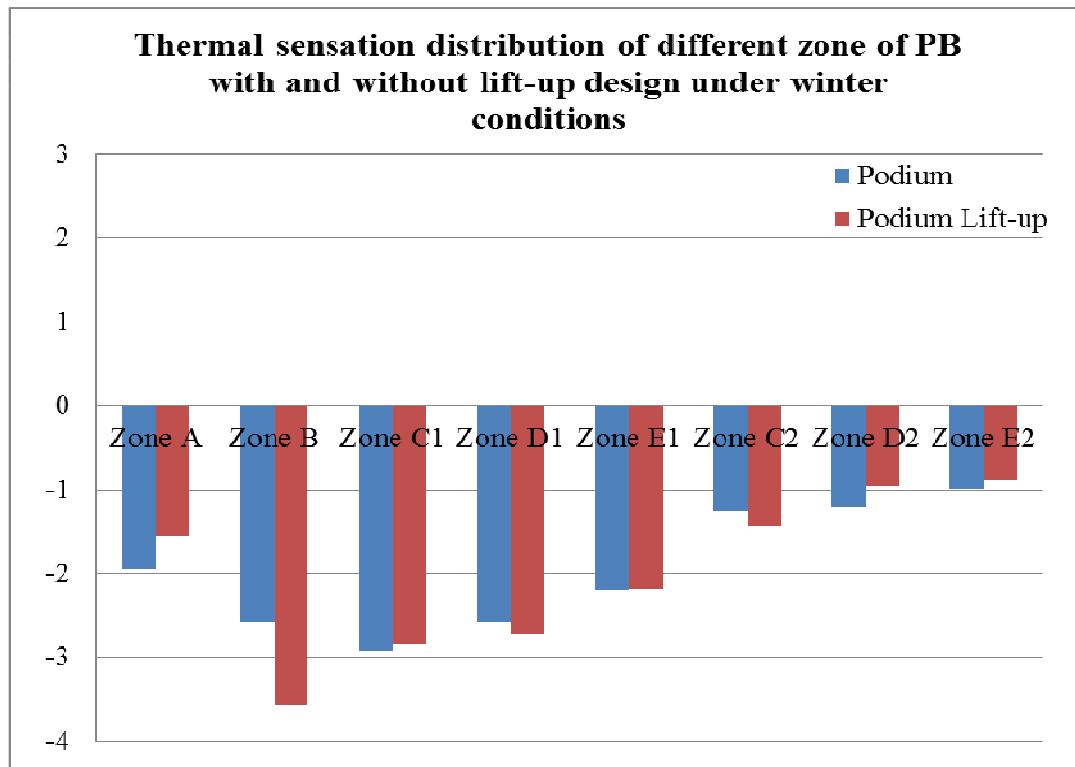
reasonable amount of zones at the pedestrian level for podium building under the winter climatic conditions.



a) Singular building



b) A row of buildings



c) Podium building

Figure 6-5. Thermal sensation distribution of different zone of singular building with and without lift-up design under winter conditions

6.4 Conclusion

In conclusion, based on Cheng et al's (2010) investigation, two predictive formulas have been utilized for analysing the thermal comfort distributions at the pedestrian level for singular building, a row of buildings and podium building with and without the lift-up design by using the weather data from two extreme months (August and December which were the hottest and coldest month of 2013) in Hong Kong. Thermal contour diagrams for different building configurations with and without lift-up design under summer and winter climatic conditions have been described separately. In order to have a better illustration, thermal sensation distribution at eight different zones of different building types under different climatic conditions has been discussed as well.

In summer, only positive thermal sensation for all the zones at the pedestrian level for singular building with lift-up or not is discovered. The thermal sensation level apart from zone D₂ is under 1. Even without the lift-up, people at the pedestrian level feel quite comfortable for singular building. But with the lift-up design, it reduces the thermal sensation level dramatically apart from zone A. Zone C₁ is the most significant reducing zone which can reach 52 times. Additionally, singular building configuration is the most efficient building configuration among the three to apply lift-up to improve thermal sensation at the pedestrian level. This design is really useful for singular building, a slab of building to improve the thermal environment for people at the pedestrian level. This suggests that urban planners and/or buildings architects can improve thermal comfort in ground level public areas by introducing the lift-up design for singular buildings in summer. This can benefit public and communal facilities such as playgrounds, parks, car parks, swimming pool, etc, particularly in summer season. Those facilities would see improved thermal comfort if placed in any of the areas except for zone A. For a row of buildings, all the zones are having positive thermal sensation level apart from zone B, C₁ and D₁ in summer. These phenomena can also be found for podium building with and without the lift-up design in summer. For all the downstream zones, thermal sensation levels are decreasing while lift-up design is utilized. But it is not reducing for all the side zones while lift-up design is used. Therefore, lift-up design is only useful to improve the thermal environment for certain zones at the pedestrian level, particularly for the downstream level. For podium building, lift-up design does not improve the thermal environment for the pedestrians much in summer.

In winter, generally speaking, all of the zones for singular building with and without lift-up design have negative values for thermal sensation at the pedestrian level. All the zones apart from zone A for singular building, thermal sensation value is getting higher negative when

the lift-up design is used. Due to the colder air temperature in winter, pedestrians do not require a much cooler environment in winter to bring down the equivalent temperature like in summer. Adversely, people probably need to have a warmer environment. But with higher wind speed due to lift-up design, less solar intensity and colder air temperature in winter, lift-up design might bring even more discomfort. People at the side of a row of buildings or podium building with and without lift-up design are generally feeling cold. People located at the downstream and upstream are feeling cool or slightly cold for a row of buildings or podium building with and without lift-up. Comparatively, singular building with or without the lift-up design can provide the most comfort thermal environment among the three building configurations in winter, particularly at the side area of the building. Lift-up design does not benefit so much significantly for singular building or a row of building at the pedestrian level under the winter climatic conditions, but it does benefit for quite reasonable amount of zones at the pedestrian level for podium building under the winter climatic conditions.

Furthermore, in terms of thermal comfort evaluation is concerned in this project is concerned, two predictive formulas were based on the experimental data direct under the sun. Cheng et al. (2010) has not carried out any research for the experiments in shade. It is necessary to conduct some survey and experiments with shading devices to derive some other formulas which should be more precisely represent the real outdoor situations. Therefore, the outdoor thermal environment can be analysed by those equations.

In the real urban environment, wind speed and solar radiation is much smaller than those in Waglan Island. The reason this date is used is because there are 13 weather data for 13 different districts in Hong Kong on the Planning Department website. But for our studies, the buildings were not located at any location first of all. Secondly, we are only concerned with

how affective these building configurations are to thermal sensation when lift-up design is used. Therefore, we chose a relatively higher weather date to find out which design is the most effective design for thermal sensation. In the real urban areas, the conclusions of effectiveness of different building configurations are still applicable, but for the more precise results and how effective they are, the exact weather data has to be used and recalculated by the equations provided by Cheng et al. (2012). But a specific district has to be selected first. Additionally, the variations of the humidity and solar radiation have not been considered, in further studies, these should be carefully considered to provide a more complete results.

Chapter Seven: Wind tunnel study of the pedestrian wind environment and pollutant dispersion in building lift-up design

7.1 Introduction

Air pollution is the introduction into the atmosphere of chemicals, particulates, or biological materials that cause discomfort, disease, or death to humans, damage other living organisms such as food crops, or damage the natural environment or built environment. According to Blacksmith Institute's World's Worst Polluted Places Report, 2008, indoor air pollution and urban air quality has been listed as two of the World's Worst Toxic Pollution Problems (Blacksmith Institute's World's Worst Polluted Places Report, 2008). So far as urban air pollution is concerned, emissions from vehicle exhaust have become one of the major pollutants due to the dramatic growth of vehicle population, even though there have been significant improvements in fuel and engine technology (Vardoulakis et al. 2003). Human exposure to hazardous substances is expected to be higher especially in areas with highly dense populations and traffic density. Concentration of these pollutants due to ventilation stagnant or slow air movement area can exacerbate the harmful effects on the health of urban inhabitants, which can cause numerous health issues including respiratory infections, cardiovascular diseases, and lung cancer, according to the WHO (Air quality guidelines for Europe, 2000). These effects can result in increases of medication use, doctor or emergency room visit, hospital admissions and premature death. Therefore, understanding flow and dispersion in urban area is extremely important for air quality management and urban planning. Additionally, concerns and awareness regarding the discharge of toxic material in populated area has been raised by the current international political situation.

The atmospheric pollutant dispersion depends on meteorological and topographical parameters, like wind speed and atmospheric stability which are decided by adiabatic and

environmental lapse rate in the lower atmosphere above the ground, terrain roughness and topography, releasing height of the source, temperature and velocity of effluent gaseous source. The urban-canopy pollutant dispersion normally takes place in the close vicinity of pollutant source and impact targets. The main urban pollutant sources are emissions from smoke and ventilation stacks (they may be represented as point sources), and car exhausts (they may be regarded as line sources stretched along street). Typical impact targets are pedestrian zones and living zones. Although extensive physical experiments or computational fluid dynamics studies are available in the literature to investigate the issues of air flow or pollutant dispersion, only few studies were related to pedestrian zones. Especially one particular architectural feature, the lift-up design, by which the high-ceiling ground floor is void and almost fully opened to the street, may have drastic effects on the pedestrian level pollutant dispersions. This feature has been adopted in some landmark buildings although the original intention might have been to serve other purposes.

With non-lift-up design, the pollutant normally is ascending within the recirculation area if the source is located downstream of the building as there is relatively lower wind there; but it could be separated to both side of the building due to the flow separation when the source is placed upstream side. When the lift-up design is implemented, the air flow is much more complicated compared to the non-lift-up design, as there is an opening space underneath of building, therefore, some of the pollutant is still ascending to the higher level when the source is located downstream. But air flow can penetrate through the opening space underneath the building, plus the revised flow generates from the ascending pollutant, these two flow streams can encounter to produce a much complicated flow situation. Therefore, understanding and using the reattachment length is extraordinarily important in this case. In the past, different researchers have used different research methodologies (Rodi, 1997;

Tominaga et al. 2008; Murakami 1998; Meng and Hibi, 1998; Yoshie et al. 2007; Lu et al. 2001) to study the impacts on these zones when flows past bluff bodies, particularly to study the complex phenomena like reattachment where the air flow and pollutant dispersion could be extremely complicated. Reattachment length is one of the most significant parameters to research the length of the primary recirculation zone. It strongly depends on the initial boundary layer, the specific geometry of the tunnel and the fluid Reynolds number (Tihon et al. 2001). The reattachment length has been defined as the length of the time-mean separation region behind an obstacle. Generally, reattachment point produces the zero velocity point on the downstream ground surface (Lu et al. 2001).

But they all reported different reattachment lengths. Rodi et al. (1997) did a systematic study on reattachment length when flow pasts a square cylinder by using different LES and RANS model. The reattachment length varies from 0.94 to 1.68 and 0.98 to 2.8 when different LES and RANS model applied respectively. Murakami (1998) also used LES to predict and to cross compare the reattachment length of a square shape building of 1:1:1 (height:width:depth) with experimental and RSM result. The LES model produced 1.4 for reattachment length, which is the closest to the experimental result which is 1.2. But RSM model calculated it between 2 to 2.3. Tominaga et al. (2008) did the cross comparison of the reattachment lengths generated by different revised κ - ε and LES models with experimental data (Meng and Hibi, 1998) for a single square prism of 2:1:1 (height:width:depth). In Meng and Hibi's test (1998), the reattachment length is 1.42. The reattachment length generated by the revised κ - ε models are from 2.7 to 4.22. The closest agreement with the experiment among all revised κ - ε models is Durbin's revised κ - ε model. But in general, revised κ - ε models overestimated the reattachment length behind the building. Although the overestimation of reattachment length behind the building in Durbin's revised κ - ε model was

improved in the LES computations to 1.02 and 2.1 due to the well reproduction of the periodic velocity fluctuation due to the vortex shedding behind the building, the inflow turbulence should be produced with the LES computation to avoid too much vortex shedding behind the building. Yoshie et al. (2007) used the standard κ - ϵ model to study the pedestrian wind environment for the same building in Meng and Hibi's experiment (1998). Yoshie et al. (2007) found the reattachment length is 2. Lu et al. (2001) discovered the reattachment length for a refuge floor is 2.5. Although the reattachment length has been reported in different values for different obstacles, it can be found that reattachment length for these different obstacles are lined within 1 to 3. And the experiment and LES can predict a relatively more accurate reattachment length.

In this chapter, As a proof of concept study, a 3.5m fully open ground floor in prototype scale was added to each of the three configurations (singular building, a row of buildings and podium building), producing three lift-up designs for comparison with the original configurations. Scale models of the designs were studied in the wind tunnel for the following reasons:

1. To ascertain the lift-up design influence on airflow and ventilation around the buildings.
2. To learn the significance of the lift-up design on pollutant dispersion around these three tall building configurations with upstream and downstream pollutant emission sources.
3. To explore the improvement or deterioration of airflow or pollutant dispersion by deploying lift-up design among different building cases.

Some recommendations are given which are prudent to urban designers, architects, engineers and even urban policy makers.

7.2 Experimental setup

7.2.1 The atmospheric boundary layer wind tunnel

The experiments were conducted in the CLP Power Wind/Wave Tunnel Facility (WWTF) at The Hong Kong University of Science and Technology.

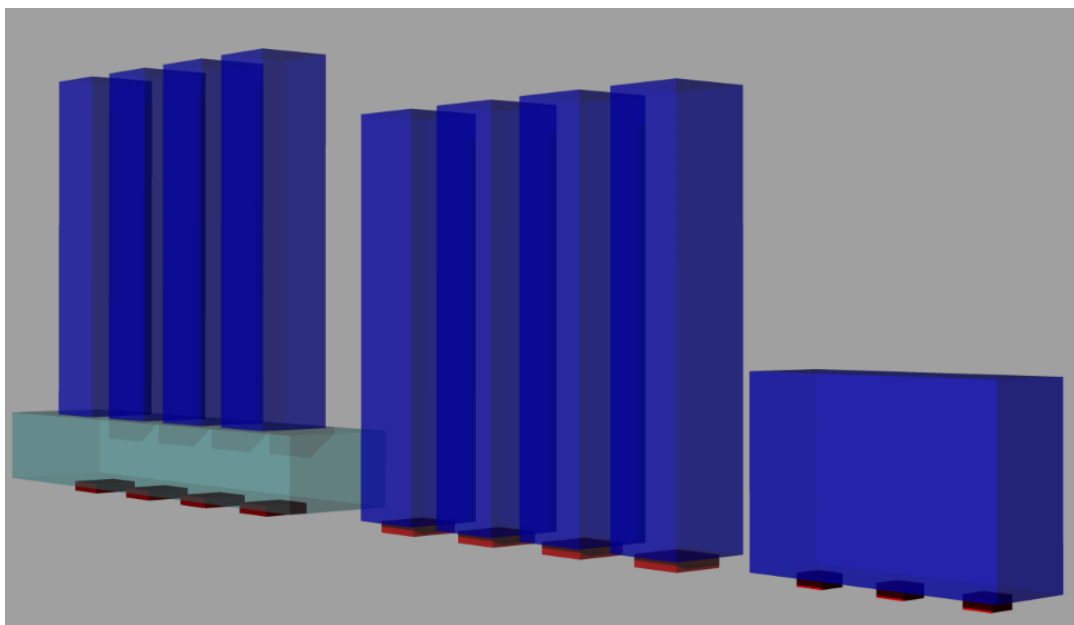


Figure 7-1. Isometric of Singular Building, A Row of Buildings, Podium Building with Lift-up Design

7.2.2 Measurement techniques

7.2.2.1 Velocity

Irwin Probes (1981) have been used for measuring pedestrian wind speed in this experiment. Only 18 to 21 Irwin Probes (1981) have been used for measuring pedestrian wind speed in this experiment. The implementation of number of Irwin Probes for measurements depends on different building configurations. The purpose of doing so is to keep the constancy

between the wind speed measurement and the pollutant measurement. Baseline studies without a building installed were studied as a reference at the beginning and at the end of tests.

7.2.2.2 Concentration

The constant injection method, in which the tracer gas is released at a constant rate, was applied in the current experiment. The tracer gas was injected through a flow meter at 3LPM into the line source first. Then it was released at 2.5mm model height above the tunnel ground level. The purposes of these concentration experiments are to simulate the pollutant dispersion of a line of stationary buses with their engines operating at either upstream or downstream of the building, and also to find out the impacts of the different building configurations on the pollutant dispersions due to these sorts of vehicular emissions. Therefore, a line source is implementing in these experiments, whose detailed design has been described in Chapter 3.

7.3 Results and discussions

An average wind flow can be represented by an average or mean wind speed with an averaging time, such as 10 min or an hour. For maintaining a good naturally ventilated environment, an average wind flow is a more appropriate measure. Consequently, in this study, mean wind speeds were used to characterize the low wind speed zones where inadequate or poor air ventilation may occur due to insufficient available winds or the wind blocking effects by obstacles. Mean wind speed at pedestrian level at any interested point was normalized by the reference mean wind speed of the approach flow at 150m in prototype scale. The normalized mean wind speed (U/U_r) was applied due to its ability to readily incorporate a particular wind climate to determine the statistics of wind speeds, in terms of magnitude and probability of occurrence. For instance, in Hong Kong, the mean wind speed

at 150m is around 5m/s to 6m/s for 50% probability of exceedance (Hitchcock et al. 2003). The minimum wind speed for human at the pedestrian level is around 1.5m/s in order to achieve thermal comfort or pollutant dispersion (Lawson and Penwarden. 1975). This means a normalized mean wind speed (U/U_r) around 0.3, and areas with U/U_r lower than 0.3 can be designated as low wind speed zones (LWS), which is unfavourable for maintaining a good natural ventilation environment. Meanwhile, the pollutant dispersion has also been researched for both the emitting source lined upstream and downstream of the buildings. The measurements of pollutant concentration and mean wind speed of the same zone have been compared to conclude the necessity of deploying lift-up design to improve the wind environment around the buildings or in an urban environment.

7.3.1 Distribution of mean wind speed

In order to better illustrate the improvement of wind distribution and pollutant dispersion at the pedestrian level with lift-up design, the ground measured area is separated into different zones. This enables simpler and more direct comparisons between the non-lift-up design and lift-up design. One of the key criteria of splitting these zones is based on the building width (b). But for the podium building, the building width is based on the podium width instead. The detailed separations for wind speed and pollutant measurements with upstream line sources are given below in Figure 7-2. In order to direct to see how far are the zones actually being away from the buildings, a dimensionless distance away from the building has been introduced here. This dimensionless distance is defined as the distance away from the building over the building width.

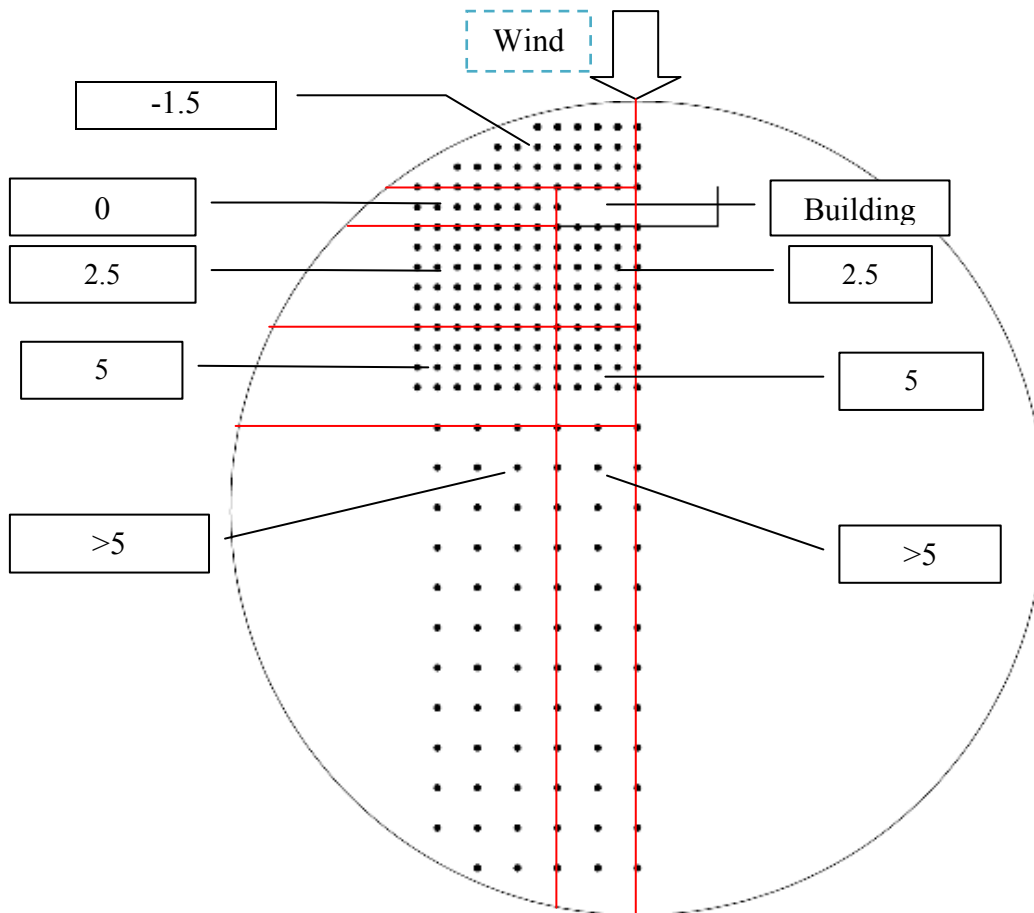


Figure 7-2. Eight different zones for pedestrian wind speed with upstream or downstream line source

Mean wind speed for these five different zones for singular building and seven different zones for a row of buildings and podium building with and without lift-up design are presented in Figure 7-3a) to Figure 7-3c). They all show lower mean wind speeds for the upstream areas in all buildings configurations with the lift-up. This could be caused by the revised flow in front of the buildings, which is generated by the downwash effects. When the two opposing windward and backflows encounter each other, a low wind speed zone is created at the upstream of buildings. Whereas mean wind speeds are consistently higher in majority of the areas of singular building with the lift-up design. The rising percentages of the mean wind speed are from 10% to 50%. The wind speed for all these zones are all higher than 0.3. Consequently, there is no LWS for this case no matter with or without the lift-up

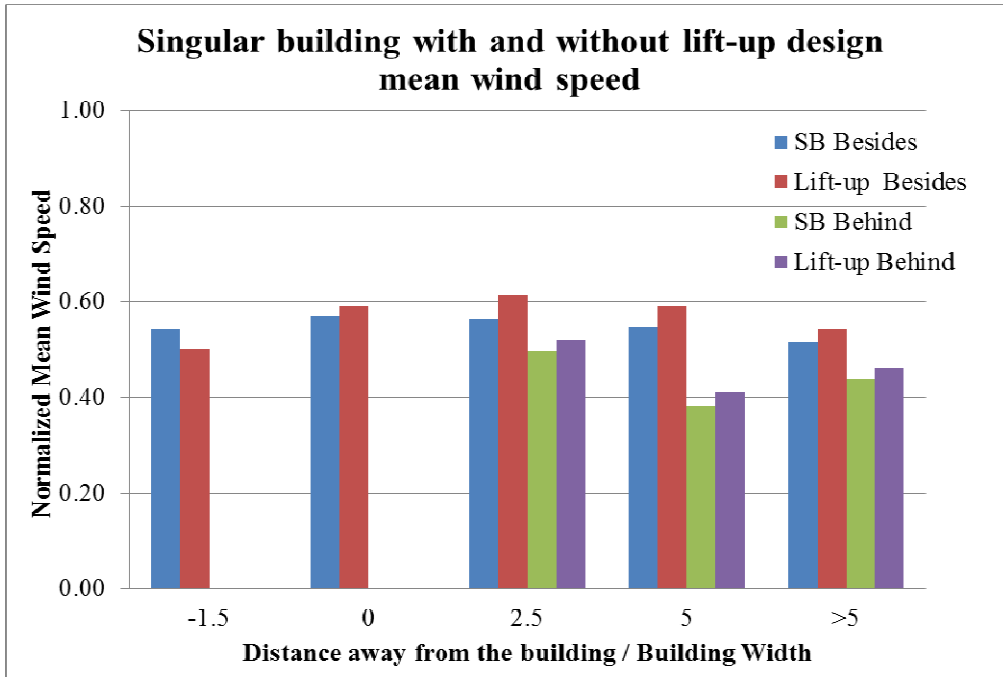
design. Therefore, a good natural ventilated environment can be maintained for all the zones. Using the lift-up design improves the majority of the downstream zones for a singular building. This suggests that urban planners and/or buildings architects can improve ventilation in ground level public areas by introducing the lift-up design for singular buildings. This can benefit public and communal facilities such as playgrounds, parks, car parks, swimming pool, etc. Those facilities would see improved ventilation if placed in any of the areas except for zone A or at least a building width away from the building to account for changing wind directions. But this needs to be confirmed by the normalized concentration level in the later section as well.

For a row of buildings, only the zone with -1.5 dimensional length results show a very marginal decrease in wind speed and the zone with 0 dimensional length (zone just next to the building itself) does not increase or decrease the normalized mean wind speed at all with the lift-up design, whereas all the remaining zones show increased mean wind speeds with the lift-up. The percentage increase of the mean wind speed range from 3% to 11%. Consequently, similar to the singular lift-up building, public facilities located in areas other than zone with -1.5 dimensionless length would see improved natural ventilation. In terms of LWS area is concerned, there is no LWS zone for a row of buildings with or without lift-up design. The flow separation for a row of buildings with the lift-up design brings more air flow to the besides of the buildings which are zone with dimensionless length 2.5, 5 and larger than 5 compared to the non-lift-up cases. Due to the blocking effect of the building itself, the air flow at immediate behind or far-field behind is much less compared to the side area of the building, which are zone with dimensionless length 2.5, 5 and larger than 5. Also, the normalized mean wind speed is decreasing gradually with the longer distance away from

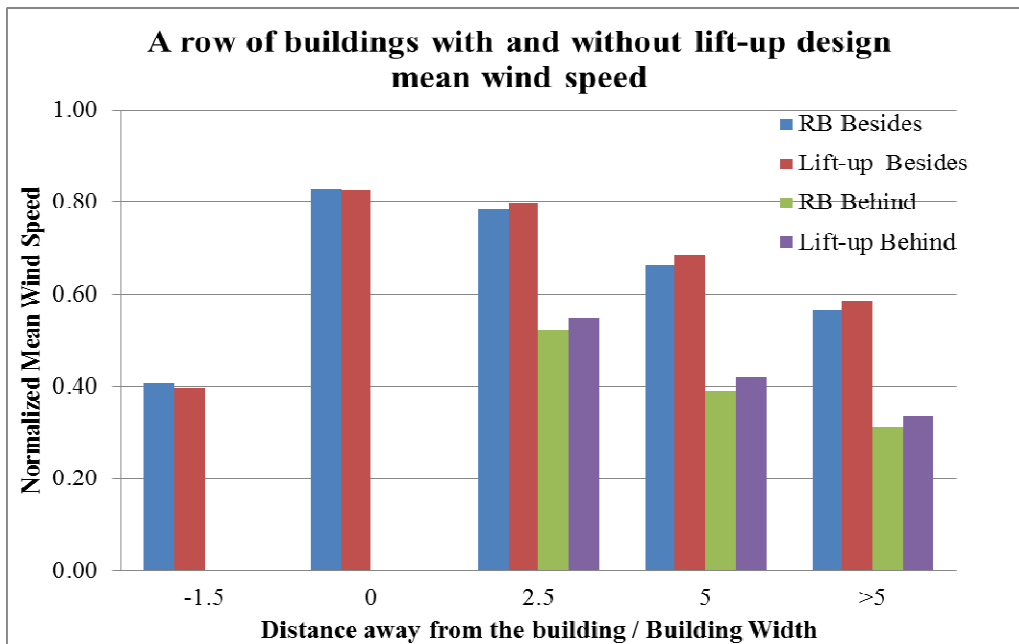
the building no matter in the besides zones or the behind zones. Interestingly, these sorts of flow characteristics can also be discovered for podium building with or without lift-up design.

The mean wind speed results for the podium buildings are much more variable with a similar number of zones showing increases as decreases.

For the behind areas, normalized mean wind speed has been improved 4% for the lift-up design at zone with 2.5 dimensionless length; whereas airflow is reduced at zones with 5 and larger than 5 dimensionless length. The reason that mean wind speed is reduced at zones with 5 and larger than 5 dimensionless length with the lift-up design for the behind of the building is because the reversed flow caused by the flow reattachment of vertical recirculation behind the building and strength of the horizontal recirculation. This is contrasted by improved air flow at the besides parts of the building, particular at zone with 0 dimensionless length which has the best improvement. Zone 2.5 shows a marginal reduction in wind speed with the lift-up design, whereas zone -1.5 shows a significant decrease in wind speed with the lift-up design. Therefore, areas of public congregation located in zones with dimensionless length 0 and 5 besides of the building and zone with dimensionless length 2.5 behind of the building will see improved ventilation if a lift-up design is introduced. But this needs to be confirmed by the normalized concentration in the later section. Zone 0 besides of the building exhibits the most enhanced wind as it improves approximately 30% with the lift-up design. Podium building with or without the lift-up design, there is no zone that can be classified as the LWS area.



a): SB V's SB with lift-up



b): RB V's RB with lift-up



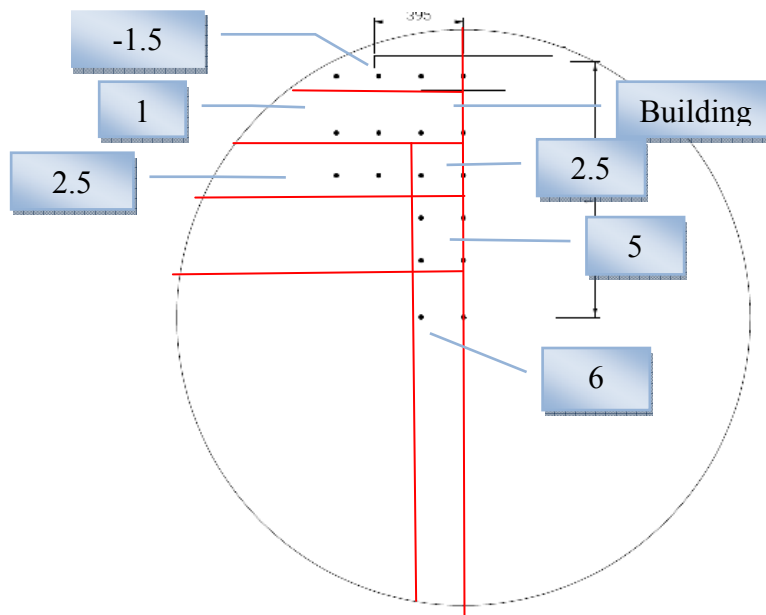
c): PB V's PB with lift-up

Figure 7-3. Normalized wind speed distribution for different building configurations with or without lift-up design

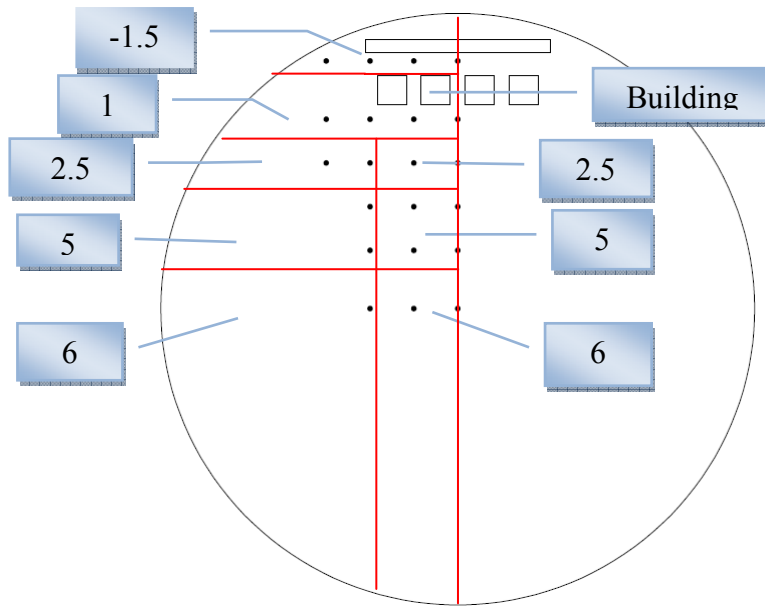
7.3.2 Distribution of pollutant distribution with lift-up design and line source upstream of building

For a row of buildings and podium building with and without lift-up design configurations, there are 21 measurement points in total. But for singular building with and without lift-up design, there are only 18 measurement points. This is due to the limited experimental time and simplicity of the building configuration itself. Therefore, when analysing mean wind speed distribution and pollutant dispersion for singular building with and without lift-up design, there are no zone with dimensionless length 5 and 6 besides of the building when the source line is upstream of the building. Consequently, there are only six zones for the singular building and eight for the other building configurations as indicated in Figure 7-4. For a more direct comparison between the pollutant dispersion with the upstream and

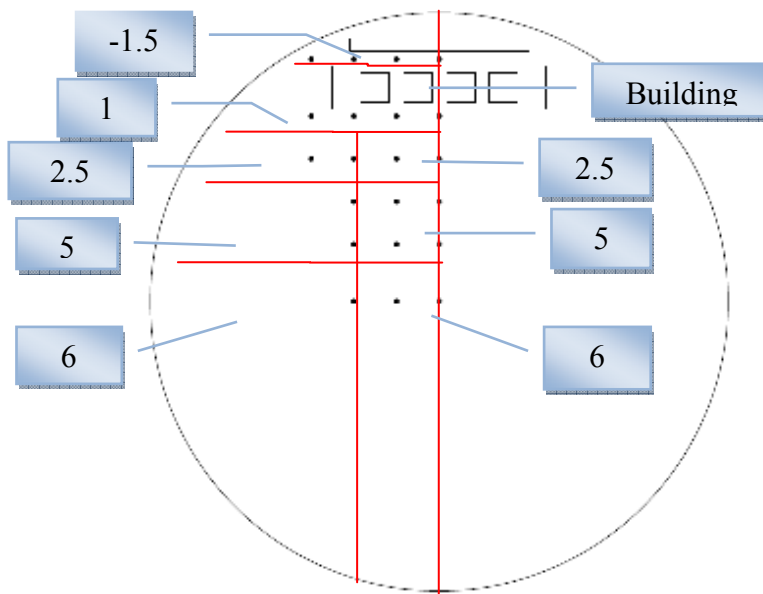
downstream line source, zone with dimensionless length 1 has been added up here for representing the downstream line source location.



a) Singular building



b) A row of buildings



c) Podium building

Figure 7-4. Different zonal distributions for pedestrian pollutant measurement with upstream line source for different building configurations

So far as pollutant dispersion with the upstream line source is concerned, the lift-up design can bring even higher pollutant concentrations, which is clearly indicated in Figure 7-5a) to

c). This is because the lift-up design helps to let more air flow through 3.5m lift-up gap, which can allow more pollution to get through the gap. The highest pollutant concentration always occurs at upstream of the building for all the cases when the source is emitting upstream. But from Figure 7-3a) to Figure 7-3c) above, air flow is always lower for the upstream zones when the lift-up design is applied. Therefore, pollutant can accumulate there. And the general feature of these three building configurations with the upstream line source is very similar. Apart from the highest normalized concentration happened at the upstream of the building, concentration level is generally higher at the side of any of the building configurations and it is relatively lower at the downstream of the buildings. This could be because of the flow generates by the building separation. Figure 7-5a) to c) also demonstrates that higher normalized concentration level happened at the zone with dimensionless length 2.5 behind the building for all the building configurations. Singular building and podium building with or without lift-up design also have higher normalized concentration at the zone with dimensionless length 2.5 besides the building compared to the zone with dimensionless length 1 besides the building. It is known that the velocity is equal to zero at the reattachment points on the downstream ground surface (Lu et al. 2001). Therefore, higher pollutant should be able to accumulate around this area. Consequently, although the normalized concentration differences between each zones behind the building is relatively small, this implies that the reattachment length for singular building, a row of buildings and podium building is approximately 2.5.

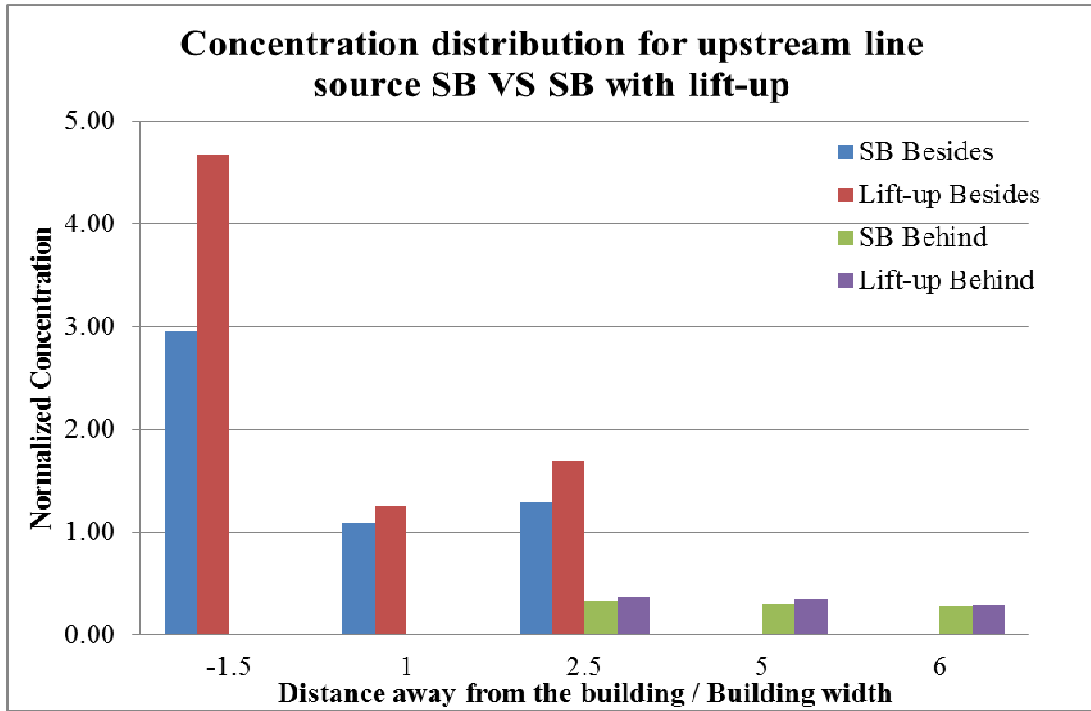
Normalized pollutant concentrations are rising for all zones when the line source is situated upstream of the singular building with lift-up design, whereas the mean wind speed is increasing for most of zones only in Figure 7-3a). For zone with dimensionless length 2.5 besides the building, lift-up design a 31% rise of pollutant flow through compared to the one

without the lift-up design, whereas lift-up design can increase 15% more pollution flowing through at the zone with dimensionless length 1 besides the building. For the downstream area behind the building block, the pollutant concentration is increasing marginally, which is from 3% to 13%. For zone with dimensionless length 2.5 and 5 behind the building, the percentage increase of pollutant concentration is just over 10%. Zone with dimensionless length 6 behind the building has the lowest percentage increase of pollutant concentration, which is lower than 3%. But still there is no zone decreasing the pollutant concentration level with the increasing air flow. In order to minimise the pollution concentration levels that would impair the wind environment, a mechanical ventilation system is recommended to be implemented for a singular building with lift-up design when line source is situated at the upstream side. The exhaust should be placed at or above the building height. But its flexibility and the environmental impacts of utilizing this sort system should be further investigated before it is fully implemented.

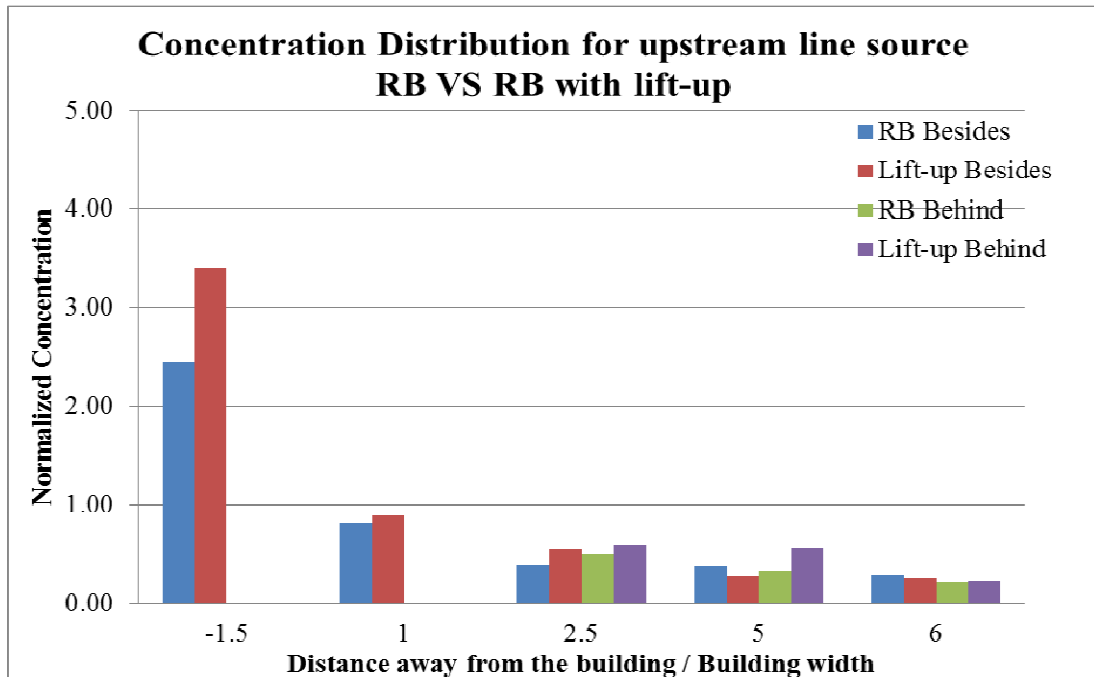
For a row of buildings with lift-up design, apart from zone with dimensionless length 5 and 6 besides of the buildings, normalized concentrations are all increasing for the remaining zones. The rising percentage varies from 10% to 72%. As shown in Figure 7-3b), the mean wind speed is rising for zone with dimensionless length 5 and 6 besides of the buildings, therefore, communal facilities with human activities that would benefit from better air quality, such as parks and leisure areas should be located in these zones for a row of building with lift-up design when the pollutant line source is upstream.

For the podium building with the lift-up design, normalized concentrations are rising for zone with dimensionless length -1.5, 1, 2.5 besides the building and 6 behind the building. Zone with dimensionless length 5 besides the building and 2.5 behind the building maintain the same concentration levels yet higher wind speeds when the lift-up designs are applied. While

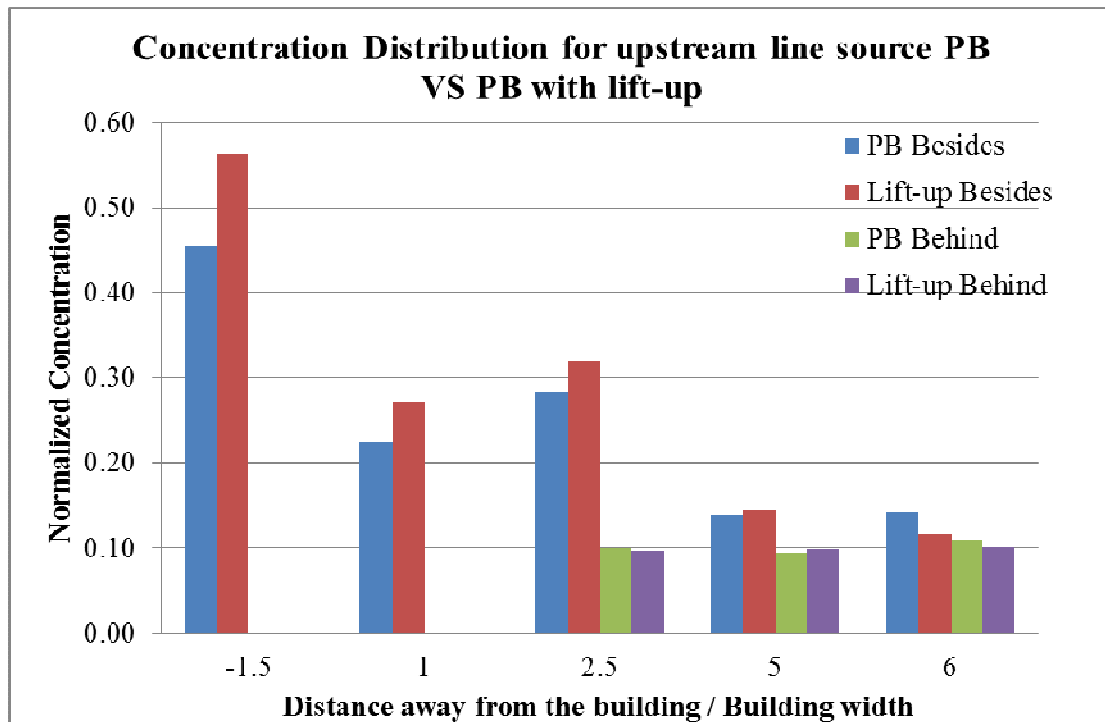
for zone with dimensionless length 5 besides and behind the building, although normalized concentration level is getting lower, but the mean wind speed either keeps the same for zone with dimensionless length besides the building or it is getting even lower. Therefore, there is no such a specific zone that can locate the communal facilities for podium building with the lift-up building when the pollutant line source is upstream. Ignoring the lift-up design, pollutant concentrations downstream are lower for podium building than a row of four building blocks. This is because podium building has larger geometric dimensions compared with a row of buildings, especially the podium underneath of a row of four building blocks. Similarly, singular building has the smallest dimensions among all these building configurations, so normalized pollutant concentration for singular building is the highest. This further demonstrates that the blockage of singular building is the smallest, consequently, the higher pollutant concentration can penetrate through. On the other hand, the concentration data shown in Figure 7-5a) to c) does not prove that reduced normalized concentration can be achieved with the higher air flow when applying lift-up design. In other words, although higher air flow can be obtained by employing lift-up design for some building configurations to avoid LWS area, it does not necessarily improve the air quality around it, particularly at the pedestrian levels, when the releasing source is located at the upstream of the building. Also, the higher the airflow is, the higher the concentrations recorded with the lift-up design. Therefore, the lift-up design does not benefit pedestrians through lowering pollutant concentration levels in the air quality.



a) SB V's SB with lift-up



b) RB V's RB with lift-up



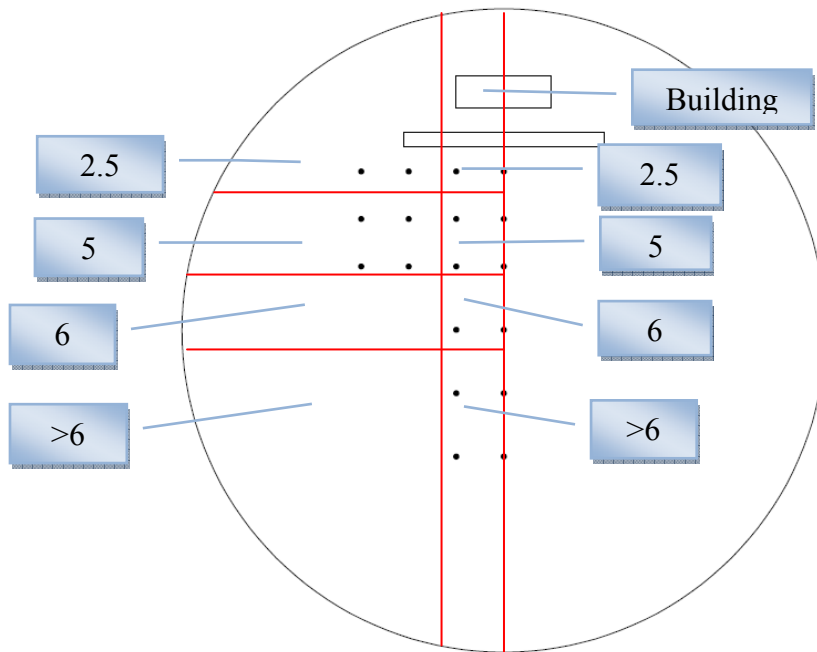
c) PB V's PB with lift-up

Figure 7-5. Concentration distribution for upstream line source for different building configurations with or without lift-up design

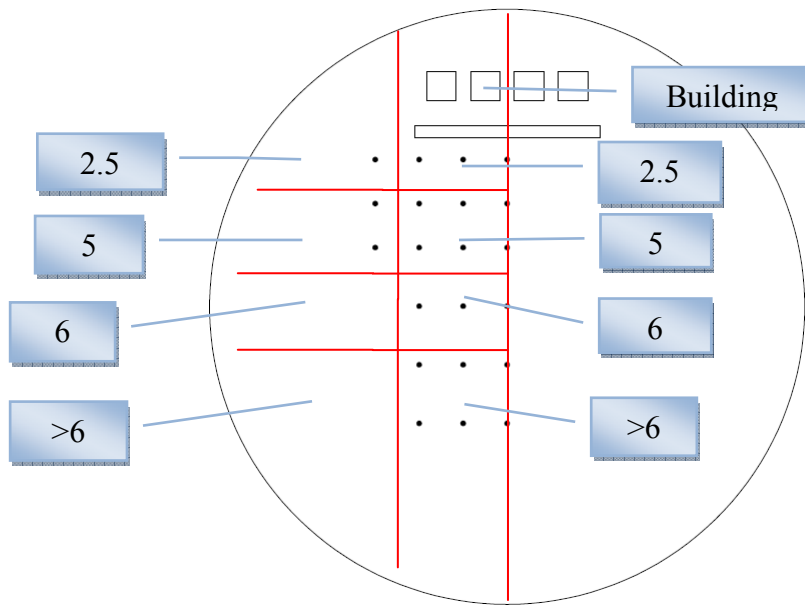
7.3.3 Distribution of pollutant distribution with lift-up design and line source downstream of building

As described in Section 6.3.2 above, for singular building with or without lift-up design, there are only 18 measurement points, whereas 21 measurement points for a row of buildings and podium building with and without lift-up design configurations. Therefore, when analysing mean wind speed distribution and pollutant dispersion for singular building with and without lift-up design, there are no zones with dimensionless length 6 and larger than 6 besides the building when the source line is downstream of the building. Consequently, there are only six zones for the singular building and eight for the other building configurations as indicated in Figure 7-6. For a more direct comparison between the pollutant dispersion with the upstream

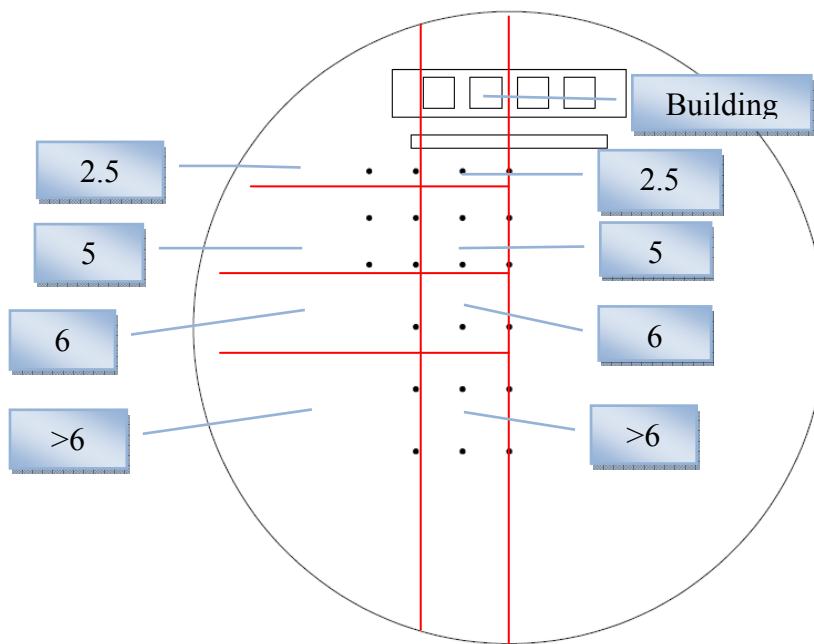
and downstream line source, zone F_1 and F_2 have been added up here for representing the downstream line source location.



a) Singular building



b) A row of buildings



c) Podium building

Figure 7-6. Different zonal distributions for pedestrian pollutant measurement with downstream line source for different building configurations

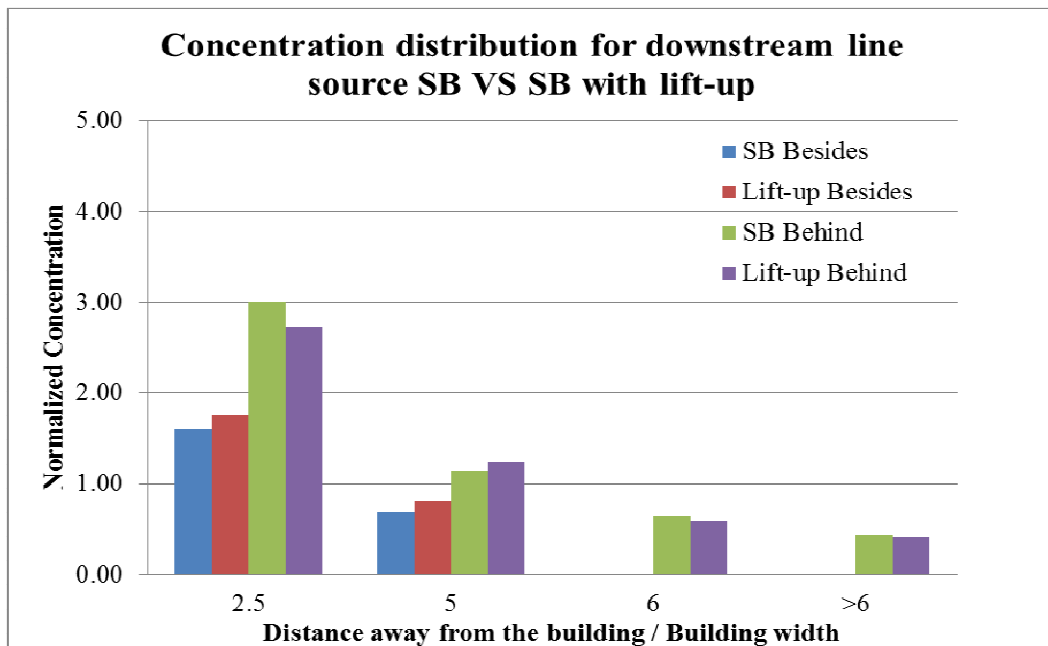
The downstream pollutant concentrations for the various building configurations with and without lift-up design are given in Figure 7-7a) to Figure 7-7c). Generally speaking, the pollutant concentration levels are higher when the pollutant source is released downstream of the building compared to the earlier discussed upstream experiment for all the building configurations whether with or without the lift-up design. This is because the blockage of the pollutant dispersion is much less when the source is emitting from downstream than upstream. When the line source is located at the upstream side of the building, most of the pollutant was dispersed with the flow generated by separation at the building edges. Although there is some recirculation occurring, it is much diluted compared to the major flow stream. Additionally, the phenomena of reattachment length lies at zone with dimensionless length 2.5 behind the building is even more obviously when the pollutant source emitted downstream of building for singular building, a row of buildings and podium building.

For pollutant concentrations results from the downstream releasing line source, the lift-up design increases the normalized concentration level for the side zones which are zone with dimensionless length 2.5 and 5 besides the building. Also this specific design increases the pollutant concentration for the downstream zone with dimensionless length 5 behind the building for singular building. But it helps to reduce the concentration levels for majority of the downstream zones for singular building. Interestingly, from Figure 7-3a), all the downstream zones to have natural ventilation improvement with the lift-up design. Additionally, even when the airflow is higher at the side of the singular building with lift-up design, the pollutant concentration level still increases compared to the non-lift-up design. Therefore, zone with dimensionless length 2.5, 5 and 6 behind the building are the zones that have higher airflow and lower concentration with the lift-up design. These would be the sensible area for locating communal facilities for human activities.

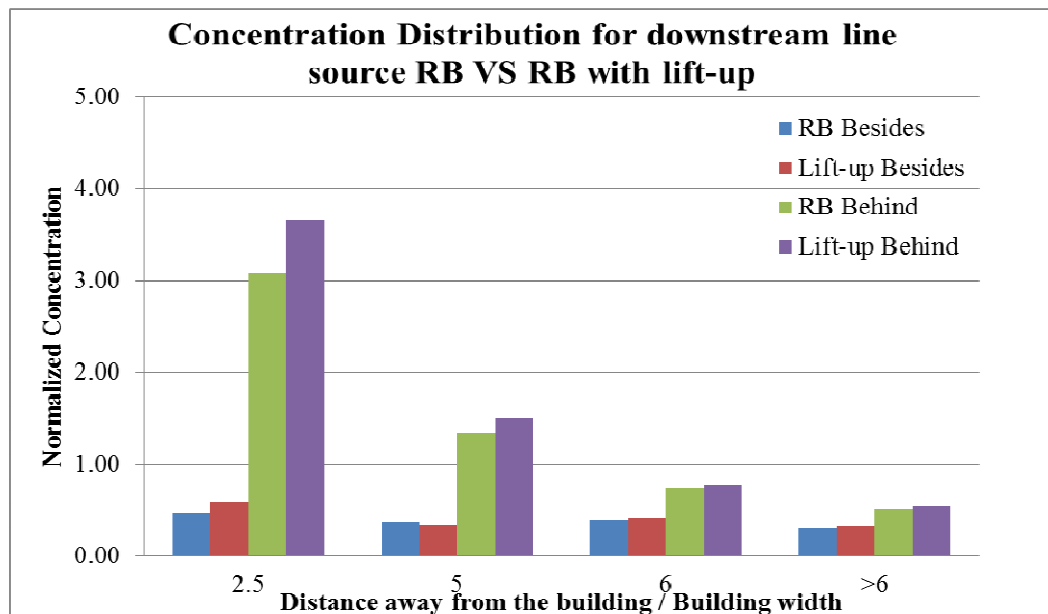
Considering a row of buildings with and without lift-up design where the line pollutant source is emitting from the downstream side, all the zones show increasing pollutant concentration levels apart from zone with dimensionless length 5 besides the building. This is reflected by Figure 7-3b), where mean airflow increases correspond with the pollutant concentration increases. Therefore, for a row of building with the lift-up design, there are some improvements in the natural ventilation environment for the majority of the zones. Similar to the singular building case, the pollutant concentration for a row of buildings is higher for all the zones when the line source is releasing downstream, particularly for the downstream side of the buildings. This can endanger the health of the pedestrians directly. To avoid this public health issue, communal facilities should be situated at zone with dimensionless length 5 besides the building for a row of building with lift-up design when the source is emitted downstream of the building.

The downstream line source pollutant concentration of podium building with lift-up design or non-lift-up design has the most effective findings. With the lift-up design, the pollutant concentration in all zones is reducing gradually compared to the podium building alone. The results show that the podium building with lift-up design is the most effective building design for pollutant concentration reduction for downstream line source situation only. However, as discussed before, it still might not increase the zonal airflow. From Figure 7-3c), the wind speeds at zones with dimensionless length 2.5 besides the building, 5 and 6 behind the building are all decreasing and it maintains the same wind speed for zone with dimensionless length 6 beside the building when lift-up design is implementing for this specific building configuration. Therefore, playgrounds, parks and other communal facilities should be located in zones with dimensionless length 5 besides the building, 2.5 and larger than 6 behind the building for a better wind environment. In order to maximise the benefit of lift-up design on

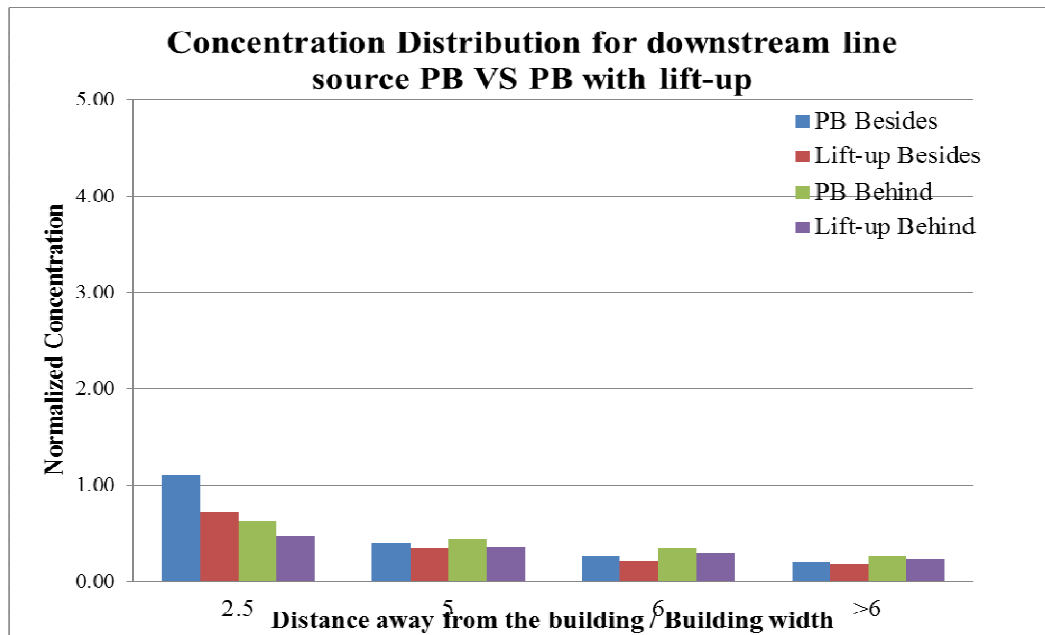
increasing airflow and reducing pollutant when the line source is located downstream of the building, it is recommended to use supplementary mechanical ventilation as well.



a) SB V's SB with lift-up



b) RB V's RB with lift-up



c) PB V's PB with lift-up

Figure 7-7. Concentration distribution for downstream line source for different building configurations with and without lift-up design

7.4 Summary

The general air flow and pollutant dispersion have been studied and compared for singular building, a row of buildings and podium building with and without the lift-up design. The releasing source has been located upstream and downstream of the building. It was found that lift-up design can improve the natural ventilation at the pedestrian level with lift-up design for a singular building and a row of buildings. The majority of the areas benefit with increased mean wind speeds from the lift-up design for the singular building. The lift-up design increases the mean wind speeds for most of the zones apart for zone with dimensionless length -1.5 and 1 for a row of buildings. For the podium building with lift-up design, zone with dimensionless length 1 has the most enhanced wind improvement of 30% compared to podium building alone. Fortunately, there is no LWS for singular building, a row of buildings and podium building with or without the lift-up. Interestingly, no matter

whether the pollutant source is located upstream or downstream of the building for singular building, a row of buildings or podium building, the reattachment length happened at the zone with dimensionless length 2.5.

When the line source is placed upstream of the buildings, the lift-up design will generally result in higher pollutant concentrations compared to the non-lift-up case. The highest concentration normally occurs at upstream of the building for all the cases when the source is releasing at the upstream side. For the singular building with lift-up design, all the zones have higher concentration level than the non-lift-up design, while the wind speed for all the zones are higher as well with the lift-up design. None of zones are suitable for locating communal facilities where public health is susceptible to poor air quality. For a row of buildings with lift-up design, apart from zones with dimensionless length 2.5 behind the buildings and with dimensionless length 5 besides the buildings, the remaining zones all have higher concentration levels than the non-lift-up design as well. As zones with dimensionless length 2.5 behind the buildings and with dimensionless length 5 besides the buildings for a row of buildings with the lift-up design have higher wind speed as well, therefore they are suited to accommodating communal facilities. But the podium building with the lift-up design has higher concentrations in only some of the side and downstream zones. None of the zone has lower concentration level and higher wind speed with lift-up design to place communal facilities. In general, building geometry and sizes could be one of important factors affecting the pollutant dispersion. The smaller the building size generally results in higher pollutant concentrations, and vice versa.

Higher pollutant concentration levels for all the building cases with or without lift-up design can be obtained when the pollutant source is located downstream compared to the situation with the upstream line source. For the singular building with lift-up design, the concentration level is increasing for the side zones which are zone with dimensionless length 2.5 and 5

besides the building, but reducing for most downstream zones apart from zone with dimensionless length 5 behind the building. Also, the higher the airflow downstream of the singular building with lift-up design is, the lower the pollutant concentration level. But the side area is an exception, the normalized concentration increase even when mean wind speed is higher for the building with lift-up design. Therefore, it is suggested to place the communal area in zone with dimensionless length 2.5, 6 and larger than 6 behind the building. For all the zones apart from zone with dimensionless length 5 besides the building, the concentration level is increasing as the airflow is increasing for a row of buildings with the lift-up design. Therefore, the lift-up design for this type of building configuration can directly endanger the health of the pedestrians when the source is located on the downstream side. The lift-up design for the podium building is the most effective building configuration studied to reduce the normalized concentration when the pollutant source is emitting at the downstream side of the building. After considering the effects of pedestrian mean wind speed and concentration level, playgrounds, parks and other communal places should be located in zones with dimensionless length 5 besides the building and with dimensionless length 2.5 and larger than 6 behind the building.

From the pollutant dispersion results, it was found with the upstream line source, pollutant concentrations are generally increasing for all the building types with lift-up design. But the downstream line source decreases pollutant levels when the lift-up design is used. If there is a major source of pollutant such as a chemical plant upstream near to a group of buildings with activities in the open plan area of the lower floor, the lift-up design is not recommended as pollutant level might be even higher. But if the chemical plant is quite far away from this group of buildings and the building is located downstream of the pollutant source, lift-up design might be able to reduce the pollutant levels, but detailed studies needs to be done to validate this. For these pollutant studies, since the measurement equipment took too much

time, therefore, very limited amount of information is generated. Therefore, using CFD to simulate more pollutant measurement points and to measure the pollutant dispersion situation in a real city or street canyon are strongly recommended.

Chapter Eight: Concluding Remarks and Recommendations

In this research, mechanics of the vehicular pollutant dispersion, the distribution of the wind speed and the surface pressure of singular building (SB), a row of buildings (RB) and podium building (PB) were thoroughly identified inside the wind tunnel under the same weather condition first. This was based upon the lowest wind speed cases selected from Tsang et al's (2012) work. With the introduction of lift-up design, the building surface pressure, pedestrian wind speed distribution and pedestrian vehicular pollutant dispersion have been compared and evaluated from those three building types alone and with the lift-up design. Therefore, the effects of implementing the lift-up design for these three building configurations had been assessed. The results for the three aspects demonstrated in this work can lead to the architects, engineers or even policy makers to developing a more targeted and effective urban buildings designs to minimise undesirable living conditions for the occupants or pedestrians.

8.1 Conclusions

8.1.1 Surface pressure distribution and natural ventilation potentials

The experimental results for the surface pressure distribution of lower floors of singular building, a row of buildings and podium building with or without lift-up design had been described. Meanwhile, the ventilation potentials of the various lower floors for these building configurations had also been evaluated. The main findings are summarised below:

- The highest cross ventilation potential for the singular building was found on the first floor, while the smallest cross ventilation was found at fourth floor for singular building. With the lift-up design, seventh floor had the lowest cross ventilation, while third floor had the highest cross ventilation. The lift-up design was helpful for improving the ventilation potential for the occupancies in the lower floors of a cluster

of building or a slab of building. But its effect is less noticeable for the first floor or slightly above. For the higher floors, the ventilation potential decreased instead.

- The pressure pattern for the lower part of the building for RB1 and RB2 were similar. With the lift-up design, it lowered the negative pressures and some positive pressures were generated at the centre of the leeward façade. The ventilation potential for all the lower floors for RB1 and RB2 could be improved by utilising the lift-up design. But the ventilation potential of the central part of RB1 slightly decreased using the lift-up design compared to RB1 alone. RB2 with lift-up increased the pressure differences for the different floors more than RB1 with lift-up. According to the study, it has observed that RB with the lift-up design is the building configuration that can produce more cross ventilation than other building configuration.
- The lift-up design increased the negative pressures at the upper and lower floors near to the centre of the building of the leeward façade. But it decreased the negative pressure at the upper and lower floors near to point C of the leeward façade. Ventilation potential increased more obviously for first to fourth floor when lift-up design was employed for podium building. But ventilation potential changes were less apparent for 5th to 7th floor when lift-up design was used for podium building.

8.1.2 Pedestrian wind environment

The general features of the low and gust wind speed areas around singular building, a row of buildings and podium building with and without lift-up designs by using the weather data from two extreme months (August and December which were the hottest and coldest month of 2013) in Hong Kong were identified from the wind tunnel studies. The key findings are summarised as follows:

- It was found that there is an improvement for the low speed areas at the pedestrian level with lift-up design for singular building and a row of buildings. But for the podium building where wind speeds are generally greater, the lift-up design does not necessarily improve the pedestrian level wind environment.
- In terms of discomfort caused by a strong wind environment, the lift-up design brings a significant increase of the normalized gust wind speed, particularly for the singular building. There are more areas of wind discomfort created by the lift-up design compared to one without. But the downstream low wind speed environment is substantially improved with better natural ventilation. The variations of the normalized gust wind speed between a row of buildings with and without the lift-up design is very minor. With the introduction of the lift-up design in the podium building, there is a significant change in the gust wind speeds adjacent and upstream of the building but downstream is largely very similar.
- Beneath the singular building and podium building with lift-up, there is significant likelihood of discomfort caused by strong winds.
- For a tropical and sub-tropical climate, a lift-up design for a slab building or a cluster of buildings may be considered by architects or urban planners as an effective means to improve air movement for pedestrians. But conversely, excessive air movement due to strong winds would also need to be considered. Central cores of the buildings should not be placed too close to each other to avoid generating discomfort zones due to the channel effect. In a temperate or cold climate, the lift-up design may not be desirable when increased wind speeds coupled with low temperature may cause additional discomfort to pedestrians. A lift-up design for a row of buildings for enhancing pedestrian level wind is not as noticeable as for a singular building; the arising normalized gust wind speed with lift-up design is minor as well. Basically, the

wind environment is fairly unchanged if a 3.5m lift-up design is implemented. The podium building with lift-up design improves air flow in selective areas without causing additional wind discomfort zones to pedestrians.

8.1.3 Pedestrian thermal comfort

The general features of thermal environment around singular building, a row of buildings and podium building with and without lift-up designs were identified from the wind tunnel studies. The key findings are summarised as follows:

- In summer, only positive thermal sensation for all the zones at the pedestrian level for singular building with lift-up or not is discovered. Singular building is the most efficient building configuration among the three to apply lift-up to improve thermal sensation at the pedestrian level. A row of building with the lift-up design is only useful to improve the thermal environment for certain zones at the pedestrian level, particularly for the downstream level. For podium building, lift-up design does not improve the thermal environment for the pedestrians much in summer.
- In winter, generally speaking, all of the zones for singular building with and without lift-up design have negative values for thermal sensation at the pedestrian level. Singular building with or without the lift-up design can provide the most comfort thermal environment among the three building configurations in winter, particularly at the side area of the building. Lift-up design does not benefit so much significantly for singular building or a row of building at the pedestrian level under the winter climatic conditions, but it does benefit for quite reasonable amount of zones at the pedestrian level for podium building under the winter climatic conditions.

8.1.4 Pedestrian pollutant dispersion

The general air flow and pollutant dispersion have been studied and compared for the singular building, a row of buildings and podium building with and without the lift-up design. The releasing pollutant source was located both upstream and downstream of the buildings in the wind tunnel studies.

- Interestingly, no matter whether the pollutant source is located upstream or downstream of the building for singular building, a row of buildings or podium building, the reattachment length happened at the zone with dimensionless length 2.5.
- When the line source is placed upstream of the buildings, the lift-up design will generally result in higher pollutant concentrations compared to the non-lift-up case. None of zones are suitable for locating communal facilities where public health is susceptible to poor air quality for singular building with lift-up design. For a row of buildings with lift-up design, zones with dimensionless length 2.5 behind the buildings and with dimensionless length 5 besides the buildings are suited to accommodating communal facilities. But none of the zones for podium building with lift-up design are suitable for locating communal facilities. In general, building geometry and size is one of the important factors affecting pollutant dispersion. A smaller building size generally results in higher pollutant concentrations .
- Higher pollutant concentration levels for all the building cases with or without lift-up design are obtained when the pollutant source is located downstream compared to the situation with the upstream line source. For the singular building with the lift-up design, it is suggested to place the communal area in zone with dimensionless length 2.5, 6 and larger than 6 behind the building. The lift-up design for a row of buildings can directly endanger the health of the pedestrians when the source is located on the

downstream side. The lift-up design for the podium building is the most effective building configuration studied to reduce the normalized concentration when the pollutant source is emitting at the downstream side of the building. After considering the effects of pedestrian mean wind speed and concentration level, playgrounds, parks and other communal places should be located in zones with dimensionless length 5 besides the building and with dimensionless length 2.5 and larger than 6 behind the building.

8.2 Recommendations for the Further Studies

The present work should be further extended for a better understanding of air flow and pollutants dispersion around SB, RB and PB with and without lift-up design under more complex conditions and investigate more effective strategies on improving pollutant dispersion, more comfortable wind environment and better ventilation potential of different building types. The following recommendations are given.

As the investigations were based on 3.5m lift-up height, additional studies are recommended to further determine the effectiveness of the lift-up design by considering the influence of lift-up height, spacing between cores, interference/shielding by upstream and/or downstream buildings, and angle of wind incidence. These studies can give readers a better insight into how the lift-up design influences different building geometries and configurations. Modelling an actual urban environment is suggested for future studies to understand its effects on real world cases, particularly in known problem areas where the resulting conclusions can possibly provide solutions for implementation.

Furthermore, in terms of thermal comfort evaluation, two predictive formulas were based on experimental data directly under the sun. Cheng et al. (2010) did not carry out any research for the experiments in shade. It is necessary to conduct some surveys and experiments with

shading devices to derive further formulae which should represent the real world situations more precisely.

Extreme weather conditions are recommended to study how the lift-up design behaves under these conditions. Initial studies could be based on the SB, RB and PB then could be expanded to an array of the buildings in various configurations and permutations. These studies are recommended for modelling using the wind tunnel or an accurate CFD model, such as an LES turbulence model with higher order numerical simulations.

On-site physical building model measurement is recommended, such that the accuracy of both methods can be compared and evaluated.

Only some recommendations have been provided as there are limited information. More recommendations will be given after the further CFD simulation results are given.

Appendices

Appendix 1:

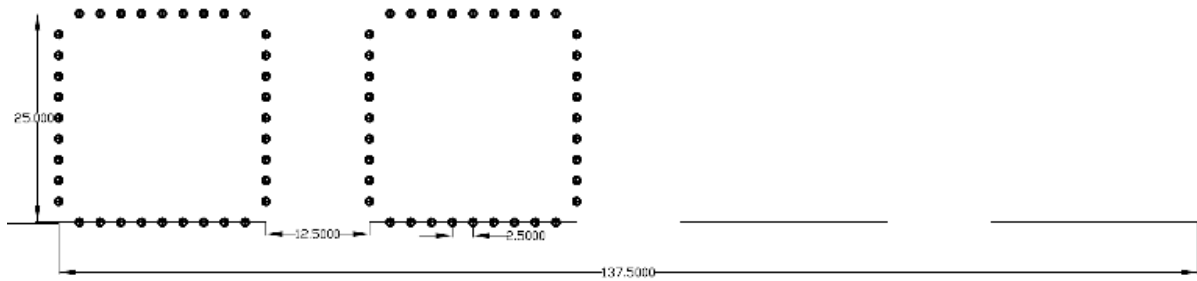


Figure 3-1. Plan view of pressure measurement of a row of buildings

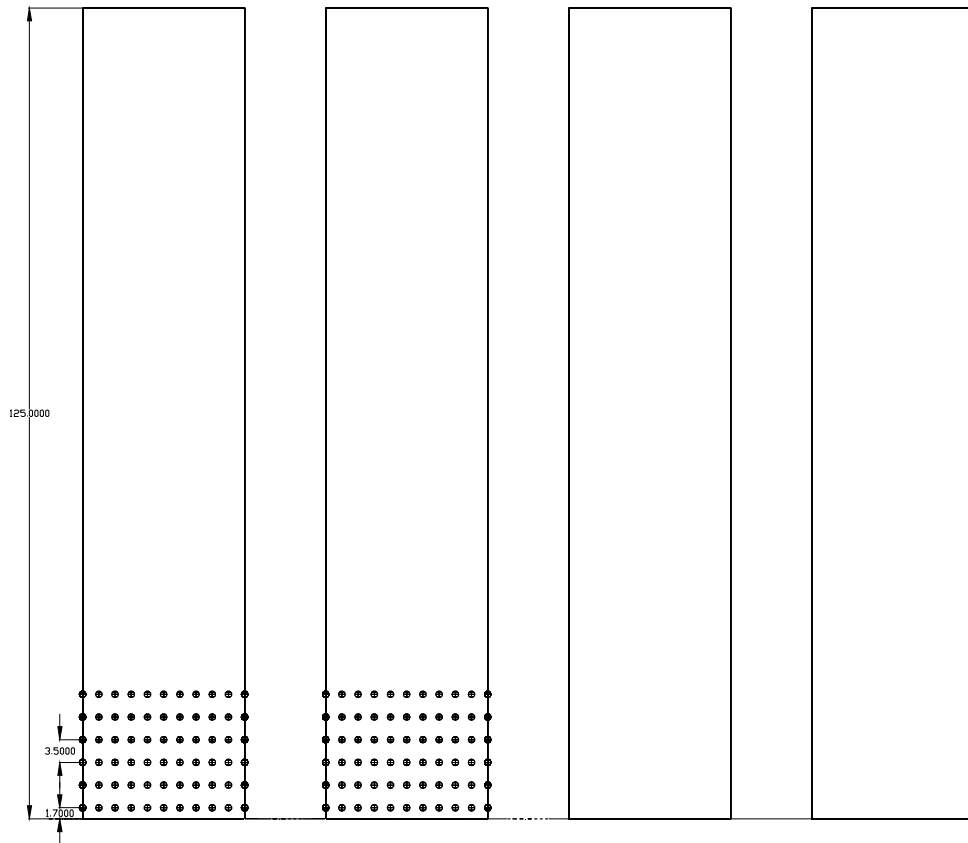


Figure 3-2. Front view of pressure measurement of a row of buildings

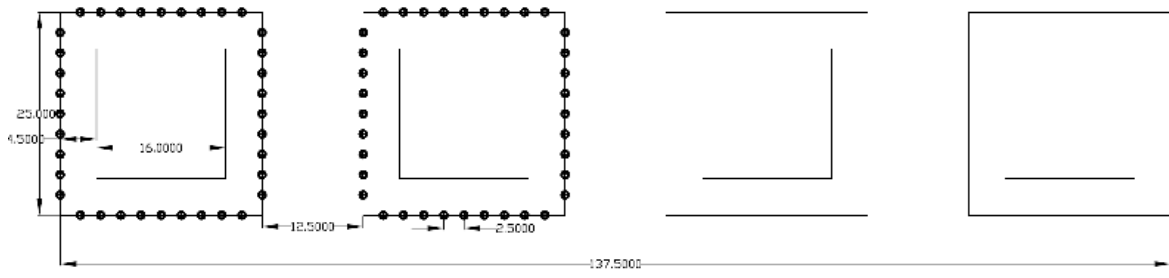


Figure 3-3. Plan view of pressure measurement of a row of buildings with lift-up design

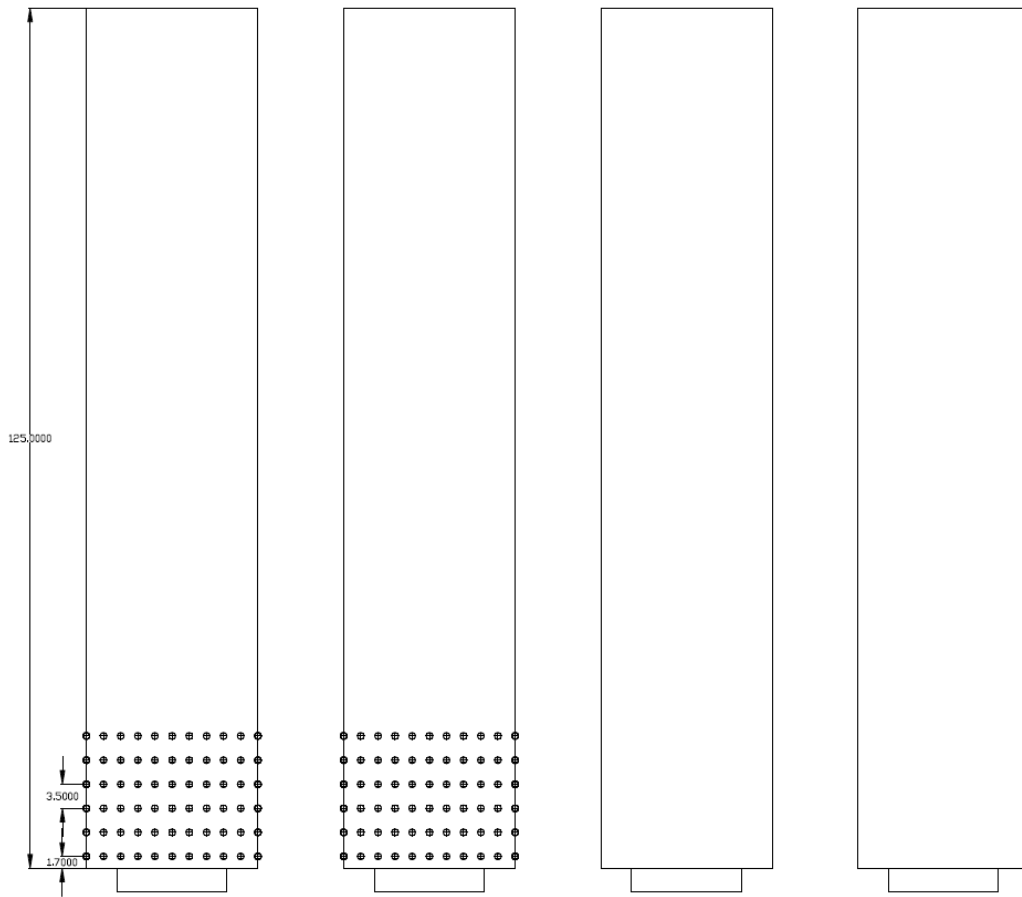


Figure 3-4. Front view of pressure measurement of a row of buildings with lift-up design

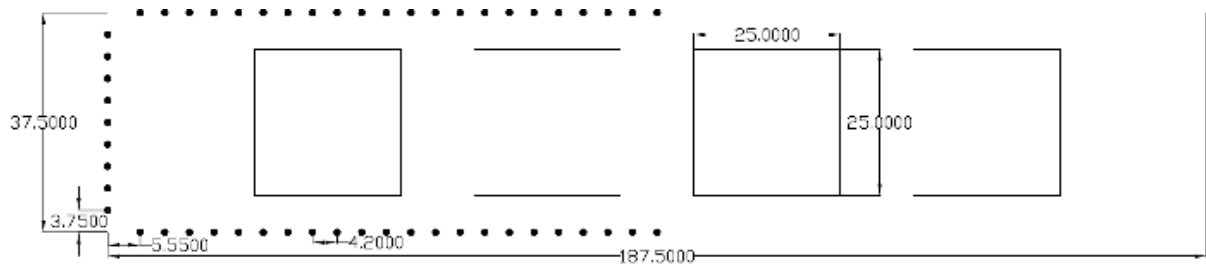


Figure 3-5. Plan view of pressure measurement of a row of buildings with podium

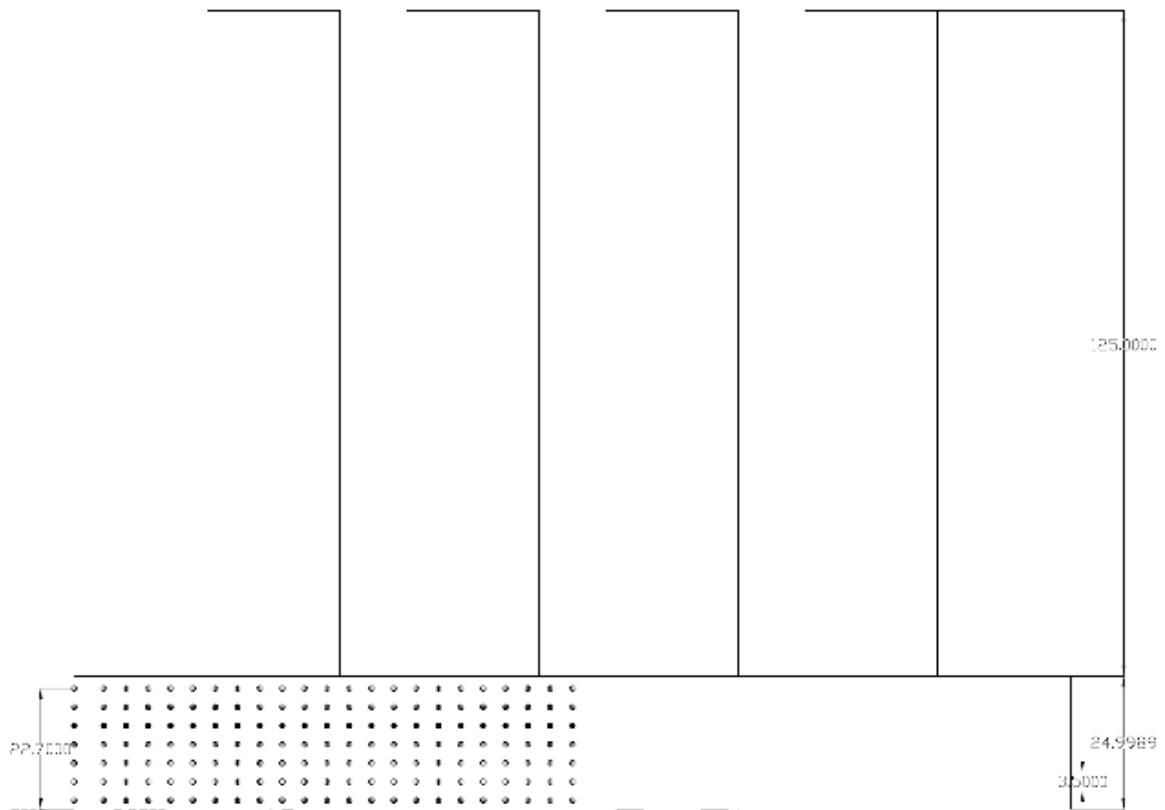


Figure 3-6. Front view of pressure measurement of a row of buildings with podium

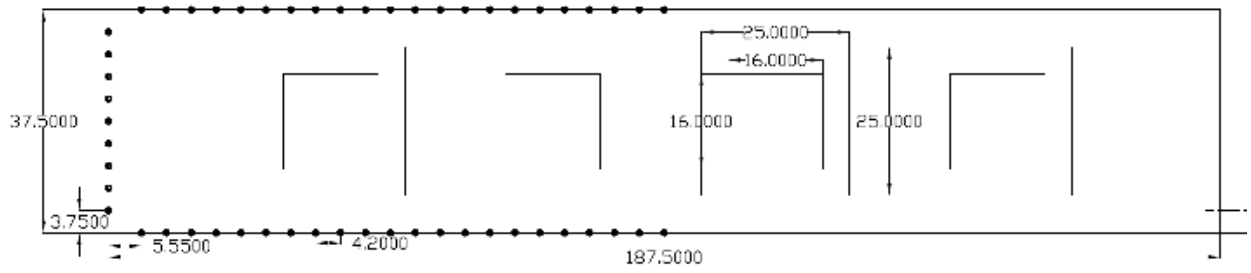


Figure 3-7. Plan view of pressure measurement of a row of buildings with podium and lift-up design

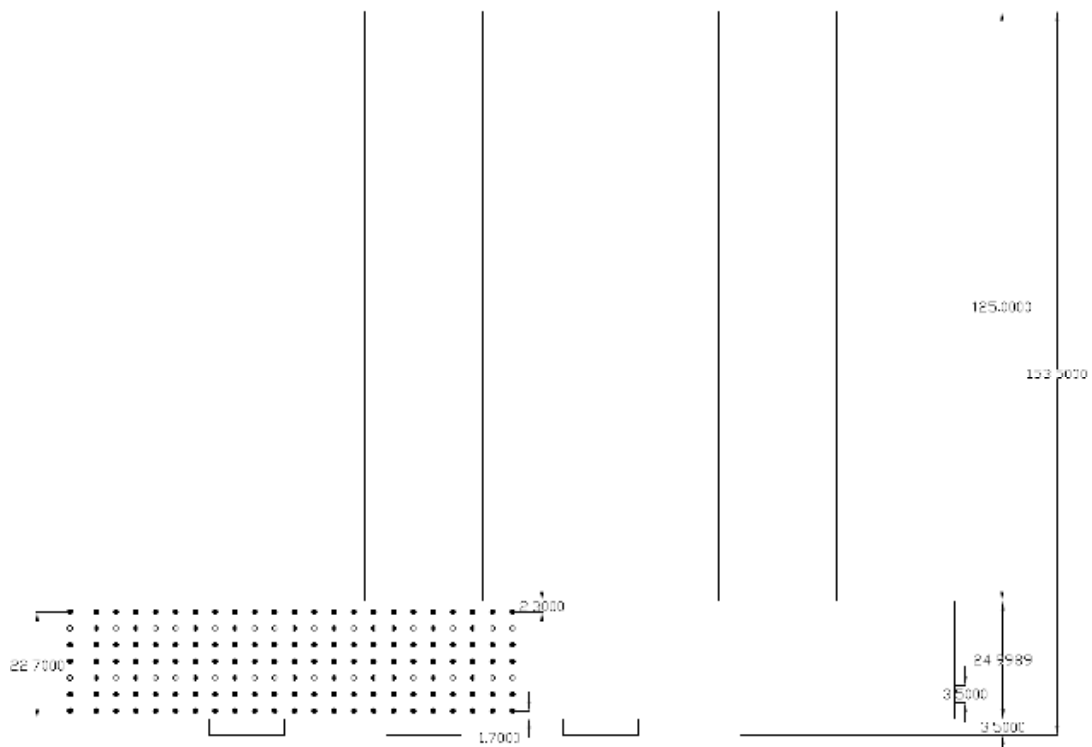


Figure 3-8. Front view of pressure measurement of a row of buildings with podium and lift-up design

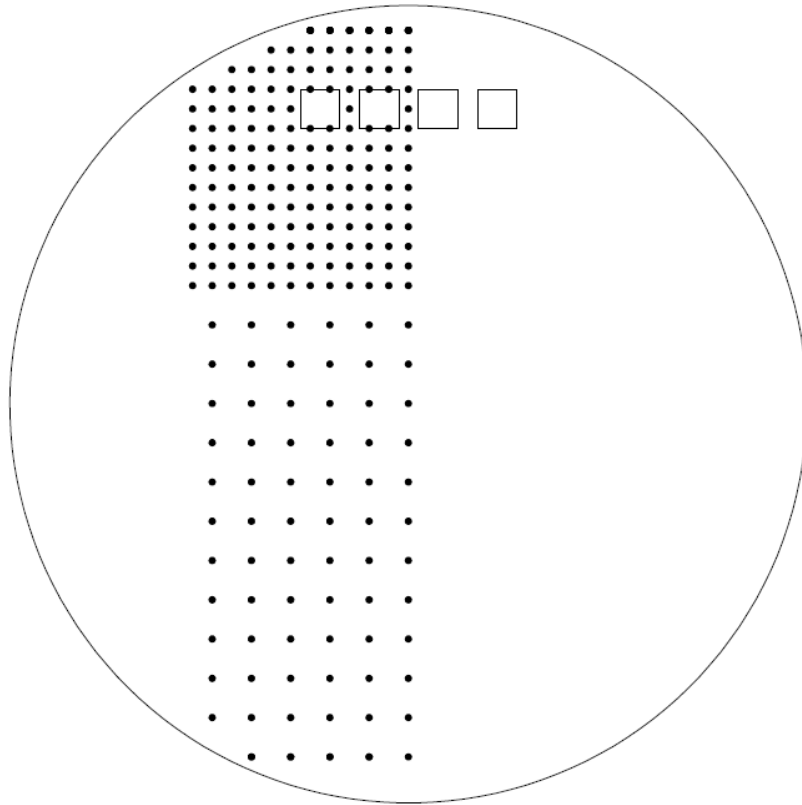


Figure 3-9. Irwin Probes Distribution for a row of buildings with and without lift-up design

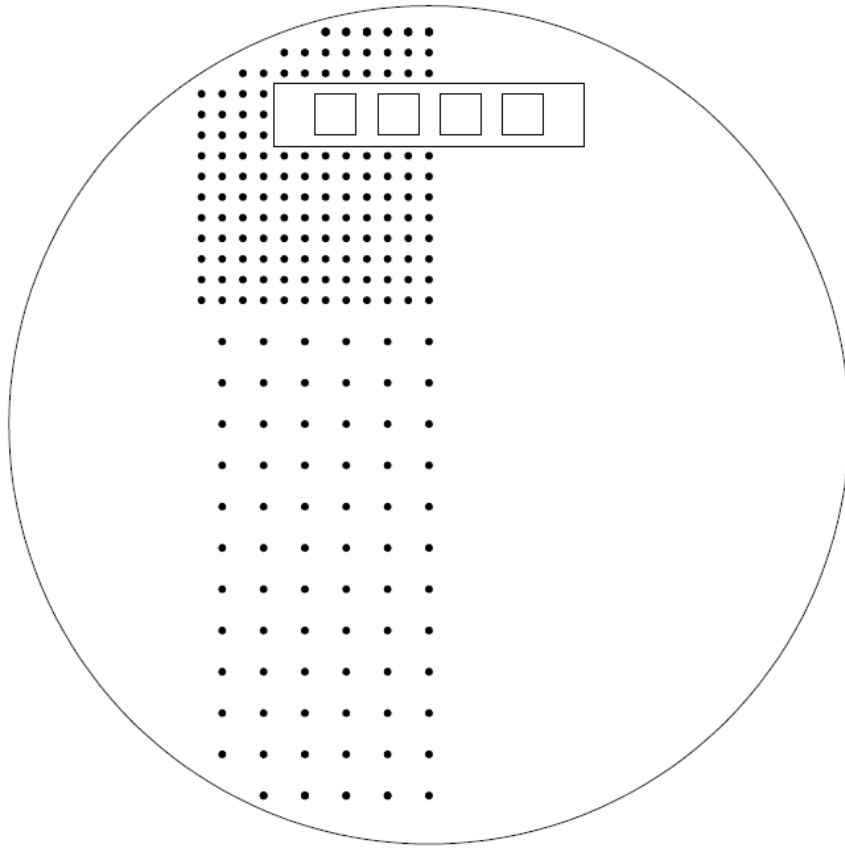


Figure 3-10. Irwin Probes Distribution for podium building with or without lift-up design

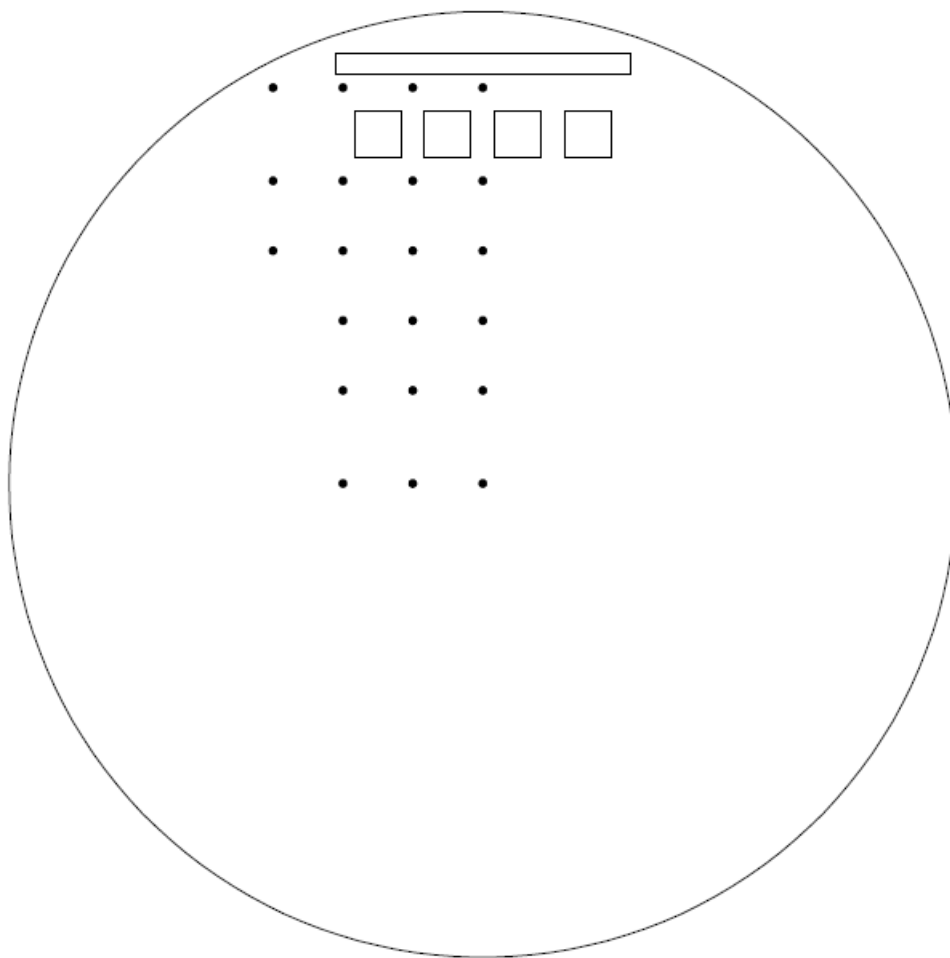


Figure 3-11. Pressure distribution for a row of buildings with or without lift-up design when line source lined upstream

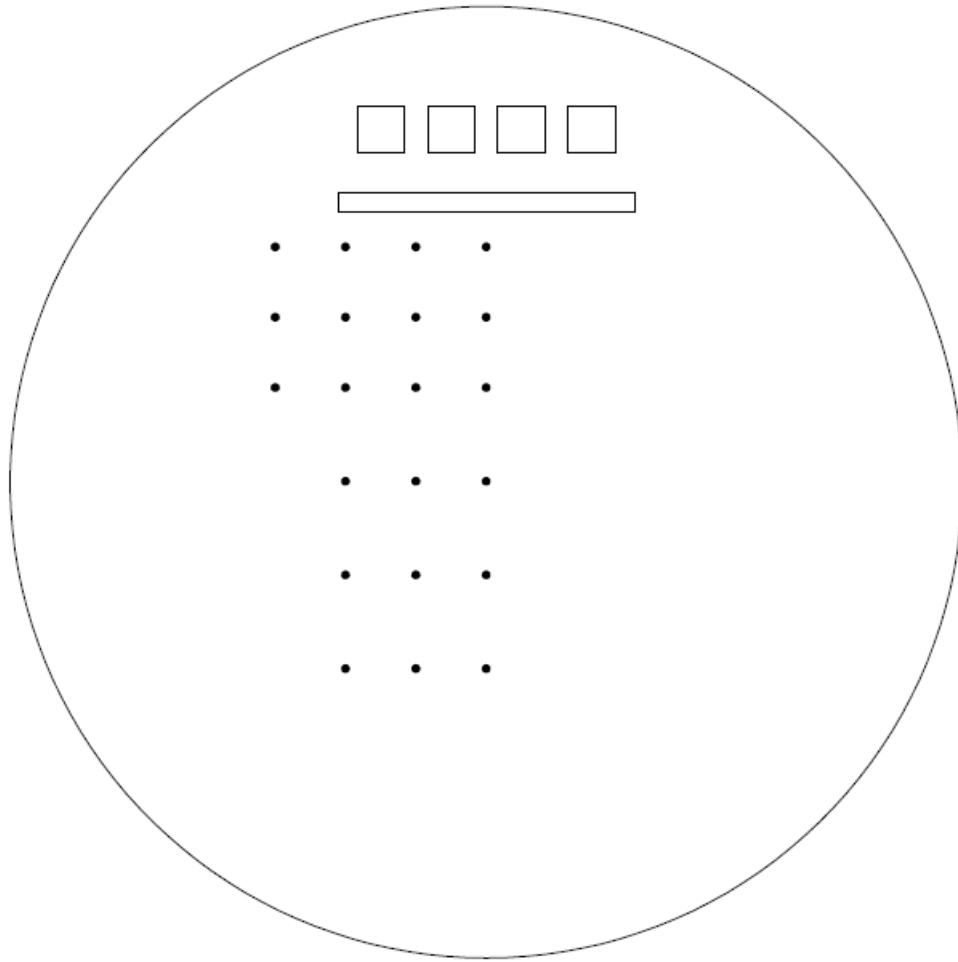


Figure 3-12. Pressure distribution for a row of buildings with or without lift-up design when line source lined downstream

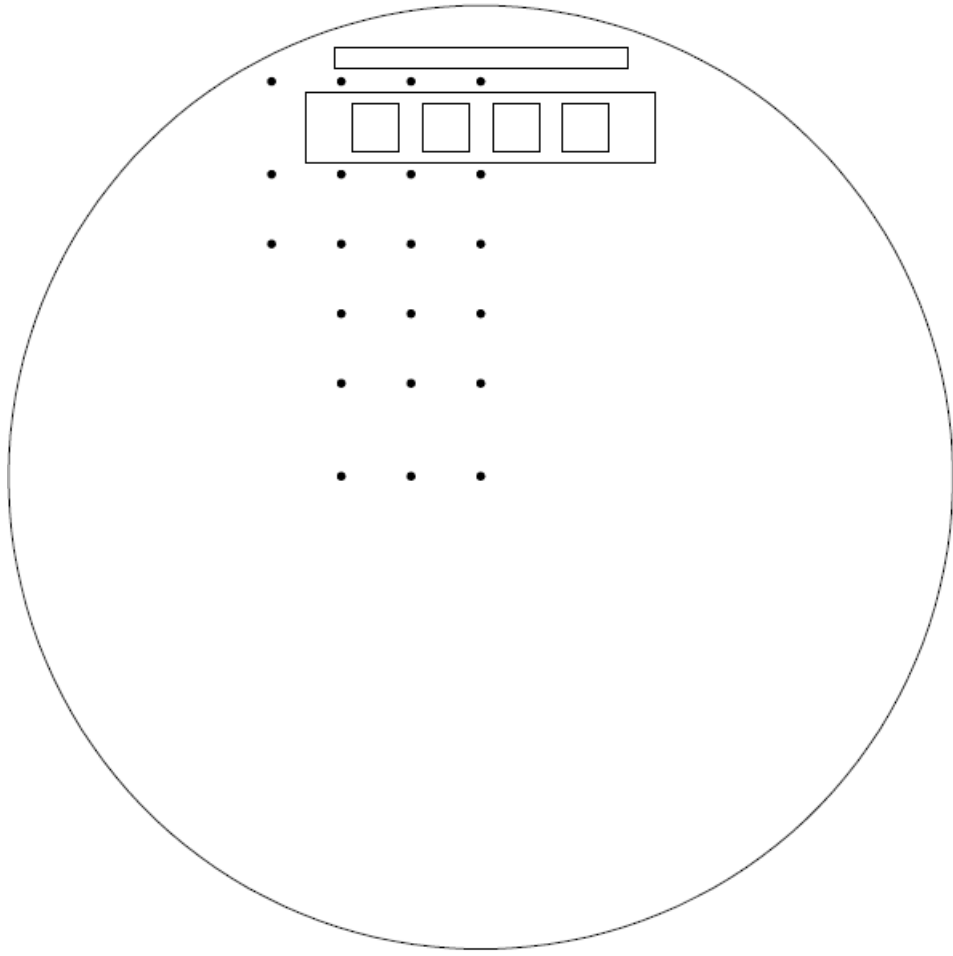


Figure 3-13. Pressure distribution for podium buildings with or without lift-up design when line source lined upstream

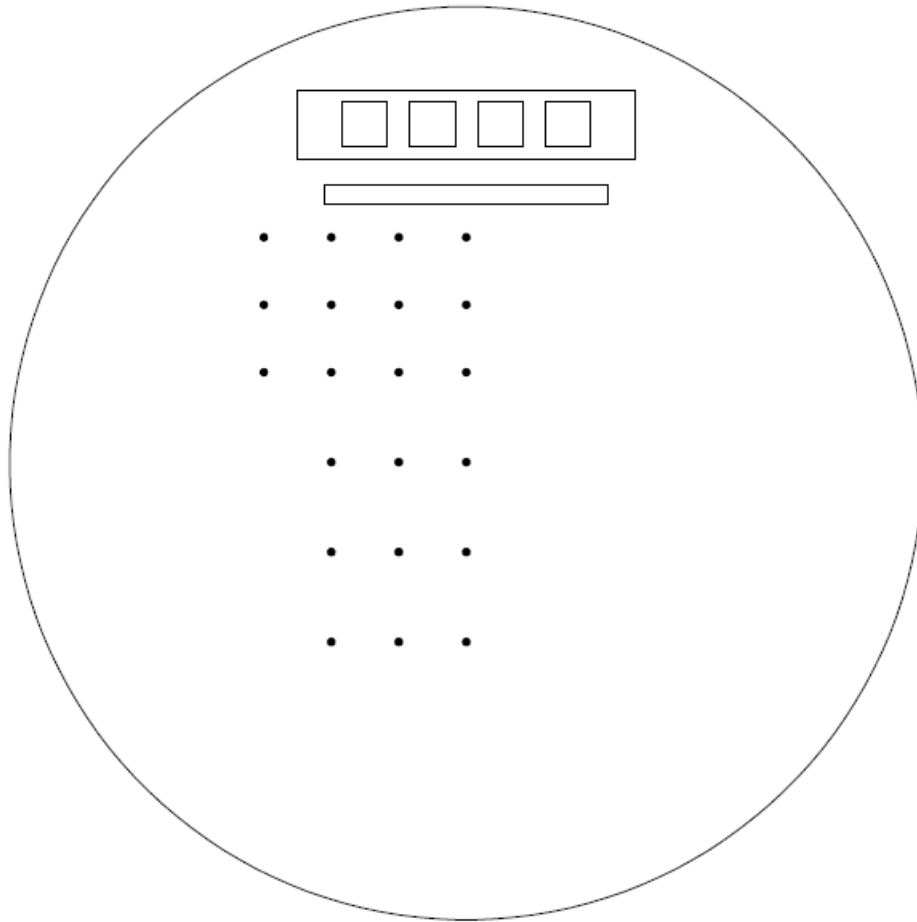


Figure 3-14. Pressure distribution for podium buildings with or without lift-up design when line source lined downstream

References

- Aberdi, J. & Omidyeganeh, M. 2008. Modeling of pollution dispersion around a cubic obstacle. BBAA VI International Colloquium on Bluff Bodies Aerodynamics & Applications Milano, Italy, July, 20-24.
- Air quality guidelines for Europe, 2000, 2nd edition. Copenhagen, World Health Organization Regional Office for Europe.
- ASHRAE. 2004. ASHRAE Standard 55: thermal environmental conditions for human occupancy. American Society of Heating, Refrigerating and Air-Conditioning Engineers, Atlanta.
- American Society of Heating, Refrigerating and Air-Conditioning Engineer. 2009. ASHRAE Handbook - Fundamentals (SI).
- Aubrun, S. & Leitzl, B. 2004. Unsteady characteristics of the dispersion process in the vicinity of a pig barn: Wind tunnel experiments and comparison with field data. Atmospheric Environment, 38(1), 81-93.
- Bachlin, W. Theurer, W. & Plate, E.J. 1991. Wind field and dispersion in a built-up area-A comparison between field measurements and wind tunnel data. Atmospheric Environment, Part A. General Topics 35(7),1135-1142.
- Bady, M. Kato, S. Takahashi, T. & Huang, H. 2011. An experimental investigation of the wind environment and air quality within a densely populated urban street canyon. Journal of Wind Engineering and Industrial Aerodynamics, 99, 857-867.
- Baker, C.J. & Hargreaves, D.M. 2001. Wind tunnel evaluation of a vehicle pollution dispersion model. Journal of Wind Engineering and Industrial Aerodynamics, 89, 187-200.
- Banks, D. Mernoey, R.N. Petersen, R.L. & Carter, J.J. 2003. Evaluation of FLUENT for predicting concentrations on buildings. In: A&WMA Conference, San Diego, CA, Paper #70223.

- Bara, B.M. Wilson, D.J. & Zelt, B.W. 1992. Concentration fluctuation profiles from a water channel simulation of a ground-level release. *Atmospheric Environment, Part A. General Topics* 126 (6), 1053-1062.
- Barynin, J.A.M. & Wilson, M.J.G. 1972. Outdoor experiments on smell. *Atmospheric Environment*, 6, 197-207.
- Blacksmith Institute's World's Worst Polluted Places Report, 2008, WorsePolluted.org. Archived from the original on 11 August 2010. Retrieved 2010-08-29.
- Blocken, B. Janssen, W.D. & Hoff, T.van. 2012. CFD simulation for pedestrian wind comfort and wind safety in urban areas: General decision framework and case study for the Eindhoven University campus. *Environmental Modelling & Software*, 30, 15-34.
- Blocken, B. Roels, S. & Carmeliet, J. 2004. Modification of pedestrian wind comfort in the Silvertop Tower passages by an automatic control system. *Journal of Wind Engineering and Industrial Aerodynamics*, 92, 849-873.
- Blocken, B. Stathopoulos, T. Saathoff, P. & Wang, X. 2008. Numerical evaluation of pollutant dispersion in the built environment. Comparisons between models and experiments: *Journal of Wind Engineering and Industrial Aerodynamics*, 96, 1817-1813.
- Boreham, B.W. 1986. Preliminary wind tunnel: Investigation of the dispersion of pollutant particles in model building wake flows using bipolar space charge. *Atmospheric Environment*, 20(8), 1523-1536.
- Bringfelt, B. 1968. Plume rise measurements at industrial chimney. *Atmospheric Environment*, 2, 575-598.
- Brzoska, M.A. Stock, D. & Lamb, B. 1997. Determination of plume capture by the building wake. *Journal of Wind Engineering and Industrial Aerodynamics*, 67&68, 909-922.
- Buccolieri, R.S.M. & Sabatino, S.D. 2010. City breathability and its link to pollutant concentration distribution within urban-like geometries. *Atmospheric Environment*, 44, 1894-1903.
- Buitijes, P.J.H. 1984. Determination of the flow and concentration-field in street canyon by means of wind tunnel experiments. TNO Report No. 84-02616, Apeldoorn, The Netherlands.

- Bullock, J. & Lewis, W.M. 1968. The influence of traffic on atmospheric pollution: The high street-Warwick. *Atmospheric Environment*, 2, 517-554.
- Burton, A.C. Edholm O.G. 1955. *Man in cold environment: physiological and pathological effects of exposure to low temperatures*. Edward Arnold, London, 273.
- Cai, X.M. 2000. Dispersion of a passive plume in an idealized urban convective boundary layer. A large-eddy simulation. *Atmospheric Environment*, 34, 61-72.
- Cai, X.M. Barlow, J.F. & Belcher, S.E. 2008. Dispersion and transfer of passive scalars in and above street canyons—Large-eddy simulations. *Atmospheric Environment*, 42, 5885-5895.
- Calhoun, R. Gouveia, F. Shinn, J. Chan, S. Stevens, D. Lee, R. & Leone, J. 2004. Flow around a complex building: Experimental and Large-Eddy Simulation comparisons. *Journal of Applied Meteorology*, 44, 571-590.
- Canepa, E. 2004. An overview about the study of downwash effects on dispersion of airborne pollutants. *Environmental Modelling & Software*. 19, 1077-1087.
- Cermak, J.E. 1975. Applications of fluid mechanics to wind engineering-A freeman scholar lecture. *Transaction of the ASME, J. of Fluids Engineering*, 97, 9-38.
- Chan, T.L. Dong, G. Leung, C.W. Cheung, C.S. & Hung, W.T. 2002. Validation of a two-dimensional pollutant dispersion model in an isolated street canyon. *Atmospheric Environment*, 36, 861-872.
- Chang. C.H. & Meroney, R.N. 2003. Concentration and flow distributions in urban street canyons: wind tunnel and computational data. *Journal of Wind Engineering and Industrial Aerodynamics*, 91,1141-1154.
- Chavez, M. Hajra, B. Stathopoulos, T. & Bahloul. A. 2011. Near-field pollutant dispersion in the built environment by CFD and wind tunnel simulations. *Journal of Wind Engineering and Industrial Aerodynamics*, 99, 330-339.
- Cheah, S.C. Cleave,r J.W. & Millward, A. 1983. Water channel simulation of the atmospheric boundary layer. *Atmospheric Environment*, 17(8), 1439-1448.

- Chen, Q.Y. & Srebric, J. 2002. A procedure for verification, validation and reporting of indoor environment CFD analyses. *HVAC&R Research*, 8, 201-216.
- Cheng, V. Ng, E. Chan, C. & Givoni, B. 2010. Outdoor thermal comfort study in sub-tropical climate: a longitudinal study based in Hong Kong. *International Journal of Biometeorology*, 56(1) 43-56.
- Coccal, O. Dobre, A. & Thomas, T.G. 2007. Unsteady dynamics and organized structures from DNS over an idealized building canopy. *International Journal of Climatology*, 27, 1943-1953.
- Coccal, O. Thomas, T.G. Martilli, A. Martin, F. & Pinelli, A. 2006. Mean flow and turbulence statistics over groups urban-like cubical obstacles. *Boundary-Layer Meteorol* 121,491-519.
- Contini, D. & Robins, A. 2004. Experiments on the rise and mixing in neutral crossflow of plumes from two identical sources for different wind directions. *Atmospheric Environment*, 38, 3573-3583.
- Contini, D. & Robins, A. 2001. Water tank measurements of buoyant plume rise and structure in neutral crossflows. *Atmospheric Environment*, 35, 6105-6115.
- Cowan, I.R. Castro, I.P. & Robins, A.G. 1997. Numerical consideration for simulations of flow and dispersion around buildings. *Journal of Wind Engineering and Industrial Aerodynamics*, 67&68, 535-545.
- Davidson, M.J. Mylne, K.R. Jones, C.D. Phillips, J.C. Perkins, R.J. Fung, J.C.H. & Hunt, J.C.R. 1995. Plume dispersion through groups of obstacles — A field investigation. *Atmospheric Environment*, 29(22), 3245-3256.
- Davidson, M.J. Snyder, W.H. Lawson, R.E (Jnr). & Hunt, J.C.R. 1996. Wind tunnel simulations of plume dispersion through groups of obstacles. *Atmospheric Environment*, 30(22), 3715-371.
- Davis, F.K. & Newstein, H. 1968. The meteorology and vertical distribution of pollutants in air pollution episodes in Philadelphia. *Atmospheric Environment*, 2, 559-574.

- Delaunary, D. Lakehal, D. Barre, C. & Sacre, C. 1997. Numerical and wind tunnel simulation of gas dispersion around a rectangular building. *Journal of Wind Engineering and Industrial Aerodynamics*, 67-68, 721-732.
- Drivas, P.J. & Shair, F.H. 1974. Probing the air flow within the wake downwind of a building by means of a tracer technique. *Atmospheric Environment*, 8, 1165-1175.
- Drivas, P.J. & Shair, F.H. 1974. A tracer study of pollutant transport and dispersion in the Los Angeles area. *Atmospheric Environment*, 8, 1155-1163.
- Drivas, P.J. & Shair, F.H. 1974. Dispersion of an instantaneous cross-wind line source of tracer released from an urban highway. *Atmospheric Environment*, 8, 475-485.
- Durgin F.H. 1997. Pedestrian level wind criteria using the equivalent average. *Journal of Wind Engineering and Industrial Aerodynamics*, 66, 215-226.
- Eliasson, I. Offerle, B. Grimmond, C.S.B. & Lindqvist, S. 2006. Wind fields and turbulence statistics in an urban street canyon. *Atmospheric Environment*, 40(1),1-16.
- Fanger, P.O. 1872. *Thermal comfort*. McGraw-Hill, New York, 244.
- Faure, Xavier., Demouge, Francois., 2013. Sensitivity analyses on the definition of wind driven natural ventilation potential. *Proceedings of BS2013: 13th Conference of International Building Performance Simulation Association*, Chambery, France, August 26-28, 2013.
- Gallagher, J. Gill, L.W. & McNabola, A. 2011. Optimizing the use of on-street car parking system as a passive control of air pollution exposure in street canyons by large eddy simulation. *Atmospheric Environment*, 45, 1684-1694.
- Germano, M., Roulet, C. A., 2006. Multicriteria assessment of natural ventilation potential. *Solar Energy*, 80,393-401.
- Gousseau, P. Blocken, B. & Heijst, G.J.F. 2012. Large-Eddy Simulation of pollutant dispersion around a cubical building: Analysis of the turbulent mass transport mechanism by unsteady concentration and velocity statistics. *Environmental Pollution*, 167,47-57.
- Gousseau, P. Blocken, B. & Heijst, G.J.F. 2011. CFD simulation of pollutant dispersion around isolated buildings: On the role of convective and turbulent mass fluxes in the prediction accuracy. *Journal of Hazardous Materials*, 194, 422-434.

- Gousseau, P. Blocken, B. Stathopoulos, T. & Heijst, G.J.F. 2011. CFD simulation of near-field pollutant dispersion on a high-resolution grid: A case study by LES and RANS for a building group in downtown Montreal. *Atmospheric Environment*, 45, 428-438.
- Gosman, A.D. 1999, Developments in CFD for industrial and environmental applications in wind engineering. *Journal of Wind Engineering and Industrial Aerodynamics*, 81,21-39.
- Gromke, C. & Ruck, B. 2007. Influence of trees on the dispersion of pollutants in an urban street canyon: Experimental investigation of the flow and concentration field. *Atmospheric Environment*, 41, 3287-3302.
- Gromke, C. & Ruck, B. 2009. On the impact of trees on dispersion processes of traffic emissions in street canyon. *Boundary Layer Meteorology*, 131, 19-34.
- Gromke, C. Buccolieri, R. Sabatino, S.D. & Ruck, B. 2008. Dispersion study in a street canyon with tree planting by means of wind tunnel and numerical investigations-Evaluation of CFD data with experimental data. *Atmospheric Environment*, 42, 8640-8650.
- Gu, Z.L. Zhang, Y.W. Cheng, Y. & Lee, S.C. 2011. Effect of uneven building layout on air flow and pollutant dispersion in non-uniform street canyons. *Building and Environment*, 46(12)2657-2665.
- Hajra, B. & Stathopoulos, T. 2012. A wind tunnel study of the effect of downstream buildings on near-field pollutant dispersion. *Building and Environment*, 52,19-31.
- Halitsky, J. 1977. Wake and dispersion models for the EBR-II building complex. *Atmospheric Environment*, 11,577-596.
- Hamilton, P.M. 1967. Part III: Plume height measurements at Northfleet and Tilbury Power Station. *Atmospheric Environment*, 1, 379-387.
- Hang, J.L.Y. Sandberg, M. Buccolieri, R. & Sabatino, S.D. 2012. The influence of building height variability on pollutant dispersion and pedestrian ventilation in idealized high-rise urban areas. *Building and Environment*, 56, 346-360.
- He, J.M. & Song C.C.S. 1999. Evaluation of pedestrian winds in urban area by numerical approach. *Journal of Wind Engineering and Industrial Aerodynamics*, 81, 295-309.
- Hefny, M.M. & Ooka, R. 2009. CFD analysis of pollutant dispersion around buildings. Effect of cell geometry. *Building and Environment*, 44, 1699-1706.

- Heschl, C. Sanz, W. Lindmeier, I. & Clauss, G. 2010. Validation of scale adaptive and elliptic relaxation turbulence models applied to flow around buildings. The Fifth International Symposium on Computational Wind Engineering, Chapel Hill, North Carolina, USA.
- Higson, H.L. Griffiths, R.F. Jones, C.D. & Hall, D.J. 1996. Flow and dispersion around an isolated building. *Atmospheric Environment*, 16(30) 2859-2870.
- Hinds, W.T. 1969. Peak-to-mean concentration ratios from ground-level sources in building wakes. *Atmospheric Environment*, 3, 145-156.
- Hino, M. 1968. Maximum ground-level concentration and sampling time. *Atmospheric Environment*, 2, 149-165.
- Hitchcock, P.A. Kwok, K.C.S. & Yu, C.W. 2003. A study of the anemometer measurements at Waglan Island, Hong Kong. Technical Report WWTF002-2003, CLP Power Wind/Wave Tunnel Facility. The Hong Kong University of Science and Technology.
- Hoppe, P. 1999. The physiological equivalent temperature- a universal index for the biometeorological assessment of the thermal environment. *International Journal of Biometeorology*, 43(2) 71-75.
- Hoppe, P. 2002. Different aspects of assessing indoor and outdoor thermal comfort. *Energy Building*, 34(6) 661-665.
- Hu, T.T. & Yoshie, R. 2013. Indices to evaluate ventilation efficiency in newly-built urban area at pedestrian level. *Journal of Wind Engineering and Industrial Aerodynamics*, 112, 39-51.
- Huang, Y.D. Jin, M.X. & Sun, Y.N. 2007. Numerical studies on airflow and pollutant dispersion in urban street canyons formed by slanted roof buildings. *Journal of Hydrodynamics*, 19(1) 100-106.
- Huber, A.H. 1991. Wind tunnel and Gaussian plume modeling of building wake dispersion. *Atmospheric Environment*, 25(7) 1237-1249.
- Huber, A.H. 1989. The influence of building width and orientation of plume dispersion in the wake of a building. *Atmospheric Environment*, 23(10) 2109-2116.

- Huber, A.H. 1988. Video images of smoke dispersion in the near wake of a model building-- Part I: Temporal and spatial scales of vortex shedding. *Journal of Wind Engineering and Industrial Aerodynamics*, 31(2-3) 189-224.
- Hubers, A.H. & Arya, S.P.S. 1989. Video images of smoke dispersion in the near wake of model building. Part II. Cross-stream distribution. *Journal of Wind Engineering and Industrial Aerodynamics*, 32(3) 263-28.
- Irwin, P.A. 1981. A simple omnidirectional probe for the measurement of pedestrian level winds. *Journal of Wind Engineering and Industrial Aerodynamics*, 7(3), 219-239.
- Irwin, H.P.A.H. Cooper, K.R. Girard, R. 1979. Correction of distortion effects caused by tubing systems in measurements of fluctuating pressure. *Journal of Wind Engineering and Industrial Aerodynamics*, 5(1-2), 93-107.
- Johnson, G.T. & Hunter, L.J. 1998. Urban wind flows: wind tunnel and numerical simulations-a preliminary comparison. *Environmental Modelling and Software*, 13(3-4) 279-286.
- Karra, S. Malki-Epshtein, L. & Neophytou, M. 2011. The dispersion of traffic related pollutants across a non-homogeneous street canyon. *Procedia Environmental Sciences*, 4, 25-34.
- Khalighi, B. Zhang, S. Koromilas, C. Balkanyi, S. Bernal, L.P. & Iaccarino, G. 2001. Experimental and computational study of unsteady wake flow behind a bluff body with a drag reduction device. SAE World Congress, Detroit, MI, USA.
- Kim, J.J. & Baik, J.J. 2004. A numerical study of the effects of ambient wind direction on flow and dispersion in urban street canyons using the RNG $k-\epsilon$ turbulence model. *Atmospheric Environment*, 38, 3039-3048.
- Kitabayashi, K. Sugawara, K. & Isomura, S. 1977. A wind tunnel study of automobile exhaust gas diffusion in an urban district. International Clean Air Congress, Tokyo.
- Klein P.K, & Plate E.J. 1999. Wind-tunnel study of concentration fields in street canyons. *Atmospheric Environment*, 33(24-25) 3973-3979.
- Kastner-Klein, P. Plate, E. & Fedorowich, E. 1997. Gaseous pollutant dispersion around urban-canopy elements: wind tunnel case studies. *Int. J. Environment and Pollution*, 8(3-6).

- Koss H.H. 2006. On differences and similarities of applied wind comfort criteria. *Journal of Wind Engineering and Industrial Aerodynamics*, 94, 781-797.
- Krogstad, P.A. & Pettersen, R.M. 1986. Wind tunnel modeling of a release of a heavy gas near a building. *Atmospheric Environment*, 20(5) 867-878.
- Laatar, A.H. Benahmed, M. Belghith, A. & Quere, P.L. 2002. 2D large eddy simulation of pollutant dispersion around a covered roadway. *Journal of Wind Engineering and Industrial Aerodynamics*, 90, 617-637.
- Lakehal, D. & Rodi, W. 1997. Calculation of the flow past a surface-mounted cube with two-layer turbulence models. *Journal of Wind Engineering and Industrial Aerodynamics*, 67-68, 65-78.
- Lateb, M. Masson, C. Stathopoulos, T. & Bedard, C. 2011. Effect of stack height and exhaust velocity on pollutant dispersion in the wake of a building. *Atmospheric Environment*, 45(29), 5150-5163.
- Lateb, M. Masson, C. Stathopoulos, T. & Bedard, C. 2010. Numerical simulation of pollutant dispersion around a building complex. *Building and Environment*, 45(8) 1788-1798.
- Lawson, T.V. & Penwarden, A.D. 1975. The effects of wind on people in the vicinity of buildings. In: *Proceedings 4th International Conference on Wind Effects on Buildings and Structures*, Heathrow: Cambridge University Press, p.605-622.
- Launder, B.E. & Spalding, D.B. 1974. The numerical computation of turbulent flows. *Computer Method in Applied Mechanics and Energy*, 3, 269-289.
- Leitl, B.M. Klein, P.K. Rau, M. & Meroney, R.N. 1997. Concentration and flow distributions in the vicinity of U-shaped buildings. Wind-tunnel and computational data. *Journal of Wind Engineering and Industrial Aerodynamics*, 67-68, 745-755.
- Letzel, M.O. Krane, M. & Raasch, S. 2008. High resolution urban large-eddy simulation studies from street canyon to neighbourhood scale. *Atmospheric Environment*, 42, 8770-8784.
- Leutheusser, H.J. & Motycka, J. 1978. Wind tunnel testing of flue gas dispersion. *Atmospheric Environment*, 12,1313-1318.

- Li, X.X. Liu, C.H. Leung, D.Y.C. & Lam, K.M. 2008. Physical modeling of flow field inside urban street canyons. *Journal Applied Meteorology and Climatology*, 41,2058-2067.
- Li, X.X. Liu, C.H. & Leung, D.Y.C. 2008. Large-eddy simulation of flow and pollutant dispersion in high-aspect-ratio urban street canyons with wall model. *Boundary Layer Meteorology*, 129,249-268.
- Li, Y. Leung, G.M. Tang, J.W. Yang, X. Chao, C.Y.H. Lin, J.Z. Lu, J.W. Nielsen, P.V. Niu, J. Qian, H. Sleigh, A.C. Su, H.J.J. Sundell, J. Wong, T.W. & Yuen, P.L. 2007. Role of ventilation in airborne transmission of infectious agents in the built environment-a multidisciplinary systematic review. *Indoor Air*,17(1) 2-18.
- Li, Y. & Stathopoulos, T. 1997. Numerical evaluation of wind-induced dispersion of pollutants around a building. *Journal of Wind Engineering and Industrial Aerodynamics*, 67&68, 757-766.
- Liu XP, Niu JL, Perino M, Heiselberg P. The airborne transmission of infection between flats in high-rise residential buildings. *Tracer gas simulation: Building and Environment* 2008;43: 1805-1817.
- Liu, X.P. Niu, J.L. Kwok, K.C.S. Wang, J.H. & Li, B.Z. 2010. Investigation of indoor air pollutant dispersion and cross-contamination around a typical high-rise residential building: wind tunnel tests. *Building and Environment*, 45(8) 1-10.
- Lu, W.Z. Lo, S.M. Fang, Z. & Yuen, K.K. 2001. A preliminary investigation of airflow field in designated refuge floor. *Building and Environment*, 36, 219-230.
- Lucas, D.H. James, K.W. & Davies, I. 1967. Paper I: The measurement of plume rise and dispersion at Tilbury Power Station. *Atmospheric Environment*, 1, 389-410.
- Lucas, D.H. 1967. Paper VI: Application and evaluation of results of the Tilbury plume rise and dispersion experiment. *Atmospheric Environment*, 1, 421-424.
- Macdonald, R.W. Griffiths, R.F. & Hall, D.J. 1998. A comparison of results from scaled field and wind tunnel of dispersion in arrays of obstacles. *Atmospheric Environment*, 32(22) 3845-3862.

- Macdonald, R.W. Griffiths, R.F. & Cheah, S.C. 1997. Field experiments of dispersion through regular arrays of cubic structures. *Atmospheric Environment*, 31(6) 783-795.
- Mahjoub, S.N. Mhiri, H. EL, G.S. Le Palec, G. & Bournot, P. 2003. Three-dimensional numerical calculations of a jet in an external cross flow. application of dispersion of pollutants: *Journal of Heat Transfer. Transactions of the ASME*, 125, 510-522.
- Matzarakis, A. Mayer, H. & Iziomon M.G. 1999. Application of a universal thermal index: physiological equivalent temperature. *International Journal of Biometeorology*, 43, 76-84.
- Mavroidis, I. Andronopoulus, S. Bartzis, J.G. & Griffiths, R.F. 2007. Atmospheric dispersion in the presence of a three-dimensional cubical obstacle: Modelling of mean concentration and concentration fluctuations. *Atmospheric Environment* , 41(3)2740-2756.
- Mavroidis, I. Griffiths, R.F. Jones, C.D. & Bilotto, C.A. 1999, Experimental investigation of the residence of contaminants in the wake of an obstacle under different stability conditions. *Atmospheric Environment*, 33, 939-949.
- Mavroidis, I. & Griffiths, R.F.L. 2001. Local characteristics of atmospheric dispersion within building arrays. *Atmospheric Environment*, 35, 2941-2954.
- Mavroidis, I. Griffiths, R.F. & Hall, D.J. 2003. Field and wind tunnel investigations of plume dispersion around single surface obstacles. *Atmospheric Environment* , 37, 2903-2918.
- Mavroidis, I. Griffiths, R.F. & Hall, D.J. 2000. Investigation of building-influenced atmospheric dispersion using a dual source technique. *Environmental Monitoring and Assessment*, 65, 239-247.
- Mayer, H. & Hoppe, P.R. 1987. Thermal comfort of man in different urban environments. *Theor. Appl. Climatol.* 38, 43-49.
- Meroney, R.N. 2004. Wind tunnel and numerical simulation of pollution dispersion: a hybrid approach. Invited Lecture. Croucher Advanced Study Insitute on Wind Tunnel Modeling, Hong Kong University of Science and Technology. 6-10 December, 2004.
- Meng, T. & Hibi, K. 1998. Turbulent measurements of the flow field around a high-rise building. *J. Wind Eng., Jpn.* 76, 55-64.

- Meroney, R.N. Leith, B.M. Rafailidis, S. & Schatzmann, M. 1999, Wind-tunnel and numerical modeling of flow and dispersion about several building shapes. *Journal of Wind Engineering and Industrial Aerodynamics*, 81, 333-345.
- Meroney, R.N. Pavageau, M. Rafailidis, S. & Schatzman M. 1996. Study of line source characteristics for 2-D physical modelling of pollutant dispersion in street canyons. *Journal of Wind Engineering and Industrial Aerodynamics*, 62, 37-56.
- Metje, N. Sterling, M. & Baker, C.J. 2008. Pedestrian comfort using clothing values and body temperature. *Journal of Wind Engineering and Industrial Aerodynamics*, 96, 412-435.
- Mirzai, M.H. Harvey, J.K. & Jones, C.D. 1994. Wind tunnel investigation of dispersion of pollutants due to wind flow around a small building. *Atmospheric Environment*, 28(11)1819-1826.
- Mochida, A. Tabata, Y. Iwata, T. & Yoshino, H. 2008. Examining tree canopy models for CFD prediction of wind environment at pedestrian level. *Journal of Wind Engineering and Industrial Aerodynamics*, 96, 1667-1677.
- Moore, D.J. 1967. Paper IV: SO₂ concentration measurements near Tilbury Power Station. *Atmospheric Environment*, 1, 389-410.
- Moonen, P. Dorer, V. & Carmeliet, J. 2011. Evaluation of the ventilation potential of courtyards and urban street canyons using RANS and LES. *Journal of Wind Engineering and Industrial Aerodynamics*, 99,414-423.
- Murakami, S. 1998. Overview of turbulence models applied in CWE-1997. *Journal of Wind Engineering and Industrial Aerodynamics*, 74-76, 1-24.
- Murphy, C.M. & Davies, A.E. 1998. Wind tunnel modeling of vehicle emissions on roadways as line source. 81st Annual Meeting of APCA, June 19-24, 1998.
- Nakamura, Y. & Oke, T.R. 1988. Wind temperature and stability conditions in an east-west oriented urban canyon. *Atmospheric Environment*, 22, 2691-2700.
- Nikolopoulou M, Baker N, & Steemers K. 2001, Thermal comfort in outdoor urban spaces: understanding the human parameter. *Solar Energy*, 70(3) 227-235.

Niu, J.L. & Tung, T. 2007. Ventilation design in high-rise residential buildings and infectious disease spread. Proceedings of Clima 2007 Wellbeing Indoors.

Niu, J.L. & Tung, T.C.W. 2008. On-site quantification of re-entry ration of ventilation exhausts in multi-family residential buildings and implications. *Indoor Air*, 18, 12-26.

Ogawa, Y. Oikawa, S. & Uehara, K. 1983. Field and wind tunnel study of the flow and diffusion around a model cube—I. Flow measurements. *Atmospheric Environment*, 17(6)1145-1159.

Ogawa, Y. Oikawa, S. & Uehara, K. 1983. Field and wind tunnel study of the flow and diffusion around a model cube--II. Nearfield and cube surface flow and concentration patterns. *Atmospheric Environment*, 17(6) 1161-1171.

Orme, M.m 1999. Applicable models for air infiltration and ventilation calculations. Technical notes. Air infiltration and ventilation centre. Oscar Faber Group Ltd. Document AIC-TN-51-1999. ISBN 1-902177-09-6.

Puttock, J.S. 1979. Turbulent diffusion from sources near obstacles with separated wakes—Part II. Concentration measurements near a circular cylinder in uniform flow. *Atmospheric Environment*, 13, 15-22.

Riley, R.L. & O'Gradt, F. 1961. Airborne infection – transmission and control, New York: The MacMillan Company.

Riley, E.C. Murphy, G. & Riley, R.L. 1978. Air spread of measles in a suburban elementary school. *AM. J. Epidemiology*, 107, 421-432.

Robins, A.G. & Castro, I.P. 1977. A wind tunnel investigation of plume dispersion in the vicinity of a surface mounted cube—I The flow field. *Atmospheric Environment*, 11, 291-297.

Robins, A.G. & Castro, I.P. 1977. A wind tunnel investigation of plume dispersion in the vicinity of a surface mounted cube—II The concentration field. *Atmospheric Environment*, 11, 299-311.

- Robins, A. Castro, I, Hayden, P. Steggel, N. Contini, D. Heist, D. & Taylor, T.J. 2001. A wind tunnel study of dense gas dispersion in a stable boundary layer over a rough surface. *Atmospheric Environment*, 35, 2253-2263.
- Rodi, W. 1997. Comparison of LES and RANS calculations of the flow around bluff bodies. *Journal of Wind Engineering and Industrial Aerodynamics*, 69-71, 55-75.
- Rossi, R. & Iaccarino, G. Numerical simulation of scalar dispersion downstream of a square obstacle. *Annual Research Briefs*. Center for Turbulence Research, Stanford University and NASA-Ames, pp. 287-312.
- Saathoff, P.J. Stathopoulos, T. & Dobrescu, M. 1995. Effects of model scale in estimating pollutant dispersion near buildings. *Journal of Wind Engineering and Industrial Aerodynamics*, 54&55, 549-559.
- Sada, K. & Sato, A. 2000. Numerical simulation of tracer gas concentration fluctuation in atmospheric boundary layer. *Transactions of the Japan Society of Mechanical Engineers*, 66(651) 2800-2806.
- Sada, K. & Sato, A. 2002. Numerical calculation of flow and stack-gas concentration fluctuation around a cubical building. *Atmospheric Environment*, 36, 5527-5534.
- Sagrado, A.P.G. Beeck, J.V. Rambaud, R. & Olivari, D. 2002. Numerical and experimental modeling of pollutant dispersion in a street canyon. *Journal of Wind Engineering and Industrial Aerodynamics*, 90, 321-339.
- Salim, S.M. Buccolieri, R. Chan, A. & Sabatino, S.D. 2011. Numerical simulation of atmospheric pollutant dispersion in an urban street canyon: Comparison between RANS and LES. *Journal of Wind Engineering and Industrial Aerodynamics*, 99(2-3) 103-113.
- Santos, J.M. Griffiths, R.F. Roberts, I.D. & Reis, N.C.Jr. 2005. A field experiment on turbulent concentration fluctuations of an atmospheric tracer gas in the vicinity of a complex-shaped building. *Atmospheric Environment*, 39, 4999-5012.
- Sanz-Andres. & A. Cuerva, A. 2006. Pedestrian wind comfort: Feasibility study of criteria homogenisation. *Journal of Wind Engineering and Industrial Aerodynamics*, 94, 799-813.

- Sasaki, R. Uematsu, Y. Yamada, M. & Saeki, H. 1997. Application of infrared thermography and a knowledge-based system to the evaluation of the pedestrian-level wind environment around buildings. *Journal of Wind Engineering and Industrial Aerodynamics*, 67&68, 873-883.
- Shi, R.F. Cui, G.X. Wang, Z.S. Xu, C.X. & Zhang, Z.S. 2008. Large eddy simulation of wind field and plume dispersion in building array. *Atmospheric Environment*, 42, 1083-1097.
- Snyder, W.H. 1979. Guideline for fluid modeling of atmospheric diffusion. Environmental Protection Agency, Research Triangle Park, NC27711, USA. Technical Report, EPA-450/4-70-016(Draft).
- Soligo, M.J. Irwin, P.A. Williams, C.J. & Schuyler, G.D. 1998. A comprehensive assessment of pedestrian comfort including thermal effects. *Journal of Wind Engineering and Industrial Aerodynamics*, 77&78, 753-766.
- Sommer, H. Hoitz, J. & Haupt, R. 1980. Flue gas dispersion in the vicinity of buildings: Wind tunnel simulation and comparison with field measurements. *Atmospheric Pollution, Proceedings of the 14th International Colloquium, Paris, France, May 5-8, 1980.*
- Spengler, J.D. & Chen, Q. 2000. Indoor air quality factors in designing a healthy building. *Annual Review of Energy and the Environment*, 25, 567-600.
- Standards Australia & Standards New Zealand (2002). AS/NZ 1170.2, Australian/New Zealand Standard, Structural design action Parts 2: wind actions.
- Stathopoulos T. 2006. Pedestrian level winds and outdoor human comfort. *Journal of Wind Engineering and Industrial Aerodynamics*, 94, 769-782.
- Stathopoulos, T. & Baskaran, B.A. 1996. Computer simulation of wind environmental conditions around buildings. *Engineering structures*, 18(11), 876-885.
- Stavrakakis, C.M., Koukou, M.K., Vrachopoulos, M.Gr., Markatos, N.C., 2008. Natural cross-ventilation in buildings: Building-scale experiments, numerical simulation and thermal comfort evaluation. *Energy and Buildings*, 40, 1666-1681.
- Steadman, R.G. 1971. Indices of windchill of clothed person. *J. Appl. Meteorol.* 10, 674-683.
- Sundell, J. 2004. On the history of indoor air quality and health. *Indoor Air*, 14, 51-58.

Surry, D. 1982. Consequence of distortions in the flow including mismatching scales and intensities of turbulence. In *Wind Tunnel Modeling for civil Engineering applications* Cambridge University Press.

Thom, E.C. 1959. The discomfort index. *Weatherwise*. 12, 57-60.

Tihon, J. Legrand, J. & Legentilhomme, P. *Exp Fluids*, 31: 484-493 (2001).

To, A.P. & Lam, K.M. 1995. Evaluation of pedestrian-level wind environment around a row of tall buildings using a quartile-level wind speed descriptor. *Journal of Wind Engineering and Industrial Aerodynamics*, 54-55, 527-541.

Tominaga Y, Mochida A, Murakami S, Sawaki A. Comparison of various revised $k-\varepsilon$ models and LES applied to flow around a high-rise building model with 1:1:2 shape place within the surface boundary layer. *Journal of Wind Engineering and Industrial Aerodynamics* 2008;96: 389-411.

Tominaga, Y. Mochida, A. Yoshie, R. Kataoka, H. Nozu, T. Yoshikawa, M. & Shirasawa, T. 2008. AIJ guidelines for practical applications of CFD to pedestrian wind environment around buildings. *Journal of Wind Engineering and Industrial Aerodynamics*, 96,1749-1761.

Tominaga, Y. & Stathopoulos, T. 2009. Numerical simulation of plume dispersion around an isolated cubic building: Comparison of various types of $k-\varepsilon$ models. *Atmospheric Environment*, 43, 3200-3210.

Tominaga, Y. & Stathopoulos, T. 2010. Numerical simulation of plume dispersion around an isolated cubic building: Model evaluation of RANS and LES. *Building and Environment*, 45(10) 2231-2239.

Tominaga, Y. & Stathopoulos, T. 2009. Numerical simulation of dispersion around an isolated cubic building: Comparison of various types of $k-\varepsilon$ models: *Atmospheric Environment*, 43, 3200-3210.

Tominaga, Y. & Stathopoulos, T. 2011. CFD modeling of pollution dispersion in a street canyon: Comparison between LES and RANS. *Journal of Wind Engineering and Industrial Aerodynamics*, 99(4) 340-348.

- Tsai, M.Y. & Chen, K.S. 2004. Measurements and three-dimensional modeling of air pollutant dispersion in an Urban Street Canyon. *Atmospheric Environment*, 38, 5911-5924.
- Tsang, C.W. Kwok, K.C.S. Hitchcock, P.A. 2012. Wind tunnel study of pedestrian level wind environment around tall buildings: Effect of building dimensions, separation and podium. *Building and Environment*, 49, 167-181.
- Vardoulakis, S. Fisher, B.E.A. Pericleous, K. & Gonzalez-Flesca N. 2003. Modelling air quality in street canyons: A review. *Atmospheric Environment*, 37(2), 155-182.
- Versteeg, H.K. & Malalasekera, W. 2007. *An introduction to computational fluid dynamics—the finite volume method (Second Edition)*. Pearson Education Ltd, Harlow, England.
- Walton, A. Cheng, A.Y.S. & Yeung, W.C. 2002. Large-eddy simulation of pollution dispersion in an urban street canyon—Part I : comparison with field data. *Atmospheric Environment*, 36, 3601-3613.
- Walton, A. & Cheng, A.Y.S. 2002. Large-eddy simulation of pollution dispersion in an urban street canyon—Part II : idealized canyon simulation. *Atmospheric Environment*, 36, 3615-3627.
- Wells, W.F. 1995. *Airborne contagion and air hygiene: an ecological study of droplet infection*. Cambridge, MA, Harvard University Press.
- Wells, W.F. 1934. On airborne infection study. droplets and droplet nuclei. *Am. J. Hyg*, 20, 619-627.
- Willemsen, E. & Wisse, J.A. 2007. Design for wind comfort in The Netherlands: procedures, criteria and open research issues. *Journal of Wind Engineering and Industrial Aerodynamics*, 95,1541-1550.
- Wilson, D.J. & Lamb, B.K. 1994. Dispersion of exhaust gases from roof-level stacks and vents on a laboratory building. *Atmospheric Environment*, 28, 1352-2310.
- Wu, H.Q. & Kriksic, F. 2012. Designing for pedestrian comfort in response to local climate. *Journal of Wind Engineering and Industrial Aerodynamics*, 104-106, 397-407.

- Wu, H. & Stathopoulos, T. 1994. Further experiments on Irwin's surface wind sensor. *Journal of Wind Engineering Industrial Aerodynamics*, 53, 441-445.
- Xie, Z.T. & Castro, I.P. 2009. Large-eddy simulation for flow and dispersion in urban streets. *Atmospheric Environment*, 43, 2174-2185.
- Yakhot, A. Anor, T. Liu, H. & Nikitin, N. 2006. Direct numerical simulation of turbulent flow around a wall-mounted cube. spatio-temporal evolution of large-scale vortices: *Journal Fluid Mechanic*, 556, 1-9.
- Yakhot, V. Orzag, S.A. Thangam, S. Gatski, T.B. & Speziale, C.G. 1992. Development of turbulence models for shear flows by a double expansion technique. *Physics of Fluids A*, 4(7) 1510–1520.
- Yamada, M. Uematsu ,Y. & Sasaki, R. 1996. A visual technique for the evaluation of the pedestrian-level wind environment around buildings by using infrared thermography. *Journal of Wind Engineering and Industrial Aerodynamics*, 65, 261-271.
- Yang, F., Qian, F., Lau, S. S.Y., 2013. Urban form and density as indicators for summertime outdoor ventilation potential: A case study on high-rise housing in Shanghai. *Building and Environment*, 70, 122-137.
- Yang, Y. & Shao, Y. 2008. Numerical simulations of flow and pollutant dispersion in urban atmospheric boundary layers. *Environmental Modeling Assessment*, 23,906-921.
- Yao, R.M., Li, B.Z., Steemers, K., Short, A., 2009. Assessing the natural ventilation cooling potential of office buildings in different climate zones in China. *Renewable Energy*, 64, 2697-2705.
- Yassin, M.F. Kato, S. Ooka, R. Takahashi, T. & Kouno, R. 2005. Field and wind-tunnel study of pollutant dispersion in a built-up area under various meteorological conditions. *Journal of Wind Engineering and Industrial Aerodynamics*, 93(5) 361-382.
- Yee, E. Gailis, R.M. Hill, A. Hilderman, T. & Kiel, D. 2006. Comparison of wind-tunnel and water-channel simulation of plume dispersion through a large array of obstacles with a scaled field experiment. *Boundary-Layer Meteorol*, 121, 389-4 32.

Yoshie, R. Mochida, A. Tominaga, Y. Kataoka, H. Harimoto, K. Nozu, T. & Shirasawa, T. 2007. Cooperative project for CFD prediction of pedestrian wind environment in the Architectural Institute of Japan. *Journal of Wind Engineering and Industrial Aerodynamics*, 95, 1551-1578.

Yu, I.T.S. Li, Y.G. Wong, T.W. Tam, W. Chan, A.T. Lee, W.H.J. Leung, D.Y.C. & Ho, Y. 2004. Evidence of airborne transmission of the severe acute respiratory syndrome virus. *Journal of Medicine*, 350, 1731-1739.

Zhang, Y.W. Gu, Z.L. Lee, S.C. Fu, T.M. & Ho, K.F. 2011. Numerical simulation and in situ investigation of fine particle dispersion in an actual deep street canyon in Hong Kong. *Indoor and Built Environment*, 20(2);206-216.

Zhang, Y.W. Gu, Z.L. Cheng, Y. & Lee, S.C. 2011. Effect of real-time boundary wind conditions on the air flow and pollutant dispersion in an urban street canyon—Large Eddy Simulations. *Atmospheric Environment*, 45(20) 3352-3359.